



The Role of Outer Membrane Vesicles of
Helicobacter pylori in Pathogenesis

Lolwah Mohammad KH E AlSharaf

B.Sc., Medical Laboratory Sciences, Kuwait University

M.Sc., Molecular Microbiology, Nottingham Trent University

A thesis submitted in a partial fulfilment of the requirements
of Nottingham Trent University for the degree of
Doctor of Philosophy

March 2021

Copyright

This work is the intellectual property of the author. You may copy up to 5% of this work for private study, or personal, non-commercial research. Any re-use of the information contained within this document should be fully referenced, quoting the author, title, university, degree level and pagination. Queries or requests for any other use, or if a more substantial copy is required, should be directed in the owner of the Intellectual Property Rights.

Abstract

Background: *H. pylori* continuously produces outer membrane vesicles (OMV) during active growth. These vesicles contain virulence factors and are cytotoxic, but the properties and contents of bacterial OMV can vary depending on the environmental conditions. **Aim:** The study aimed to characterise *H. pylori* OMV isolated from different environmental conditions in terms of their quantity, size, cytotoxicity, and protein contents. **Methods:** OMV were purified from *H. pylori* cultures in BHI broth with 0.2% β -cyclodextrin after 1 or 6 days or blood agar plates after 24 hours. OMV size and quantity were characterised by Zetaview. Their toxicity on human gastric epithelial (AGS) cells was determined by CellTiter, RealTime-Glo assays, IncuCyte and microscopy. Proteins were characterised and quantified by LC-MS/MS and SWATH-MS, label-free, to determine changes in protein expression between growth conditions. A *cagA* mutagenesis plasmid was constructed in the 444A strain background. **Results:** *H. pylori* produced more OMV in broth than on agar plates with differences also observed in average OMV diameter between conditions. OMV isolated from late broth and plate cultures were significantly more toxic to AGS cells than those from early broth ($p < 0.001$). Vacuoles were seen in AGS cells treated with OMV of virulent strains isolated from early broth and plate cultures, indicating VacA activity. Hummingbirds (elongated gastric epithelial cells) were seen in AGS cells treated with OMV from *cag+* strains, indicating CagA activity. There was ~2-fold more VacA protein in OMV from early broth and plate cultures than in OMV from late broth cultures. In contrast, there was more CagA toxin in OMV from early broth than in OMV from late broth and plate cultures. OMV isolated from plate cultures had completely different protein profiles compared with OMV from broth cultures. OMV from *H. pylori* 60190 WT strain were more toxic to AGS cells than those from the $\Delta cagA$ strain. **Conclusions:** In summary, the characteristics of *H. pylori* OMV change dramatically, depending on the environment in which the bacterium is grown. This may influence bacterial virulence.

Declaration

I declare that whilst registered as a candidate for the University's research degree I have not been a registered candidate or enrolled doctoral candidate for any other award of the University or other academic professional institution. I declare that no material contained in the thesis has been used in any other submission for an academic award. Unless otherwise acknowledged, the work presented in this thesis is my own.

Lolwah M AlSharaf

31st March 2021

Acknowledgement

First and foremost, I offer special thanks to Dr Jody Winter, my PhD supervisor and Director of Studies. I do not know how to express my gratitude for her care, support, help, patience and encouragement all the time, especially during my writing-up period. I want to thank her for supervising the project and providing guidance and advice at each stage. Dr Jody Winter is the best supervisor, and I am lucky to be one of her students since my MSc degree. Thank you very much, Dr Jody!

I would also like to thank Dr David Boocock, Clare Coveney, and their team at John van Geest Cancer Research Centre, Nottingham Trent University, to perform the proteomics analysis and their help with data analysis. Also, I would like to show appreciation to Dr Lesley Hoyles for her help with the proteomics data and generating stunning figures. I wish to thank Grace Atobatele at Nottingham Trent University for her help in the Mycoplasma detection test. From the University of Nottingham, I am grateful to Prof John Atherton and his team for providing the clinical strains, Dr Karen Robinson and team for providing the $\Delta cagA$ mutant 60190 strains, and Darren Letley for providing the pBlueKm plasmid. I am tempted to individually thank all the Antimicrobial Resistance, Omics, and Microbiota research group team, all friends and lab mates, all the technicians in the SuperLab (Rosalind Franklin Building) for always being there, providing help and support. Also, I wish to thank all the individuals who participate in the project.

I would like to thank the Government of the State of Kuwait, represented by the Kuwait Cultural Office of the Embassy of the State of Kuwait in London, for the full sponsorship. Also, I would like to thank Nottingham Trent University for the partial sponsorship. Last but not least, I am grateful to my family for their love and support, as well as, I would like to acknowledge all my friends, especially Eman Mohammad, for their strength and support during the hard times. Finally, and most importantly, I offer special thanks from my heart to my mom (Sabeekah AlGhais) and dad (Mohammad AlSharaf) for their love and everything they have done for me. They always believed in me. They are my strength. To them, I dedicate this thesis.

Table of Contents

ABSTRACT	III
DECLARATION	IV
ACKNOWLEDGEMENT	V
PUBLICATIONS	IX
LIST OF TABLES	X
LIST OF FIGURES	XI
LIST OF ABBREVIATIONS	XIII
1. INTRODUCTION.....	2
1.1. <i>HELICOBACTER PYLORI</i> : OVERVIEW	2
1.2. GASTRIC DISEASES AND THEIR HISTOPATHOLOGICAL FEATURES	5
1.2.1. <i>Gastritis</i>	5
1.2.1.1. <i>Acute gastritis</i>	6
1.2.1.2. <i>Chronic gastritis</i>	7
1.2.1.3. <i>Atrophic gastritis</i>	7
1.2.1.4. <i>Intestinal metaplasia</i>	8
1.2.2. <i>Peptic ulcer</i>	10
1.2.3. <i>Gastric Adenocarcinoma</i>	10
1.3. VIRULENCE FACTORS ASSOCIATED WITH PATHOGENICITY.....	11
1.3.1. <i>Urease</i>	12
1.3.2. <i>Adhesins</i>	13
1.3.2.1. <i>Blood group antigen-binding adhesin (BabA)</i>	13
1.3.2.2. <i>Sialic acid-binding adhesin (SabA)</i>	13
1.3.3. <i>Cytotoxin Associated Gene A (CagA)</i>	14
1.3.4. <i>Vacuolating Cytotoxin A (VacA)</i>	16
1.4. <i>H. PYLORI</i> PATHOGENICITY AND SURVIVAL STRATEGIES	18
1.4.1. <i>H. pylori Adherence and Colonisation</i>	18
1.4.2. <i>Biofilm Formation</i>	18
1.4.3. <i>Production of Outer Membrane Vesicles (OMV)</i>	19
1.5. OUTER MEMBRANE VESICLES	19
1.5.1. <i>Roles of outer membrane vesicles</i>	21
1.5.2. <i>Outer Membrane Vesicles in H. pylori</i>	23
1.6. AIM OF THIS THESIS	24
2. MATERIALS AND METHODS	27
2.1. <i>HELICOBACTER PYLORI</i> STRAINS	27
2.2. BACTERIAL STORAGE	29
2.3. GROWING <i>HELICOBACTER PYLORI</i> STRAINS	29
2.3.1. <i>H. pylori growth on solid agar medium</i>	29
2.3.2. <i>H. pylori growth in liquid broth medium</i>	29
2.3.3. <i>Gram's staining</i>	30
2.4. QUANTIFICATION OF OMV FOR VIRULENT AND LESS VIRULENT <i>H. PYLORI</i> STRAINS	30
2.4.1. <i>Miles and Misra method for viable bacterial count</i>	30
2.4.2. <i>BacTiter-Glo Assay</i>	31
2.4.3. <i>OMV isolation and purification</i>	31
2.4.4. <i>OMV quantification</i>	32
2.4.4.1. <i>Pierce BCA- protein assay</i>	32
2.4.4.2. <i>Nanoparticle tracking analysis</i>	33
2.5. EFFECTS OF OMV ON MAMMALIAN CELLS.....	33
2.5.1. <i>Cell culture and media</i>	33
2.5.2. <i>Cytotoxicity</i>	34
2.5.2.1. <i>CellTiter 96 assay</i>	34
2.5.2.2. <i>RealTime-Glo MT cell viability assay</i>	35
2.5.3. <i>Live Cell Analysis (IncuCyte)</i>	36

2.6.	PROTEOMIC ANALYSIS	36
2.6.1.	<i>Sodium dodecyl sulphate - Polyacrylamide gel electrophoresis (SDS-PAGE)</i>	36
2.6.2.	<i>Density gradient centrifugation</i>	37
2.6.3.	<i>OMV proteomics</i>	38
2.6.4.	<i>Cell response proteomics</i>	39
2.7.	MUTAGENESIS OF GENE OF INTEREST	40
2.7.1.	<i>Clone Gene of Interest into pJET cloning vector</i>	40
2.7.1.1.	<i>H. pylori genomic DNA extraction</i>	40
2.7.1.2.	<i>Polymerase chain reaction (PCR)</i>	43
2.7.1.3.	<i>Agarose gel</i>	45
2.7.1.4.	<i>Gel extraction for PCR product</i>	45
2.7.1.5.	<i>Ligation (to clone the gene of interest into pJET cloning vector)</i>	46
2.7.1.6.	<i>Colony screening</i>	46
2.7.1.7.	<i>Plasmid purification</i>	47
2.7.1.8.	<i>Sanger DNA Sequencing</i>	47
2.7.2.	<i>Inverse PCR and construction of mutation plasmid</i>	47
2.7.2.1.	<i>Inverse PCR</i>	47
2.7.2.2.	<i>Purification of pBlueKm plasmid</i>	48
2.7.2.3.	<i>Restriction digest</i>	48
2.7.2.4.	<i>Dephosphorylation reaction</i>	49
2.7.2.5.	<i>Ligation pJET-cagA flanks to KanR cassette</i>	49
2.7.2.6.	<i>Colony screening</i>	50
2.7.2.7.	<i>Transformation of H. pylori</i>	50
2.8.	STATISTICAL ANALYSIS (OVERVIEW)	51
3.	<i>H. PYLORI OMV PRODUCTION AND CHARACTERISTICS</i>	54
3.1.	INTRODUCTION	54
3.2.	AIM OF THIS STUDY	57
3.3.	RESULTS	58
3.3.1.	<i>Characterisation of OMV from H. pylori with High or Low Virulence</i>	58
3.3.1.1.	<i>Quantification of H. pylori OMV</i>	58
3.3.1.1.1.	<i>Correlation between BacTiter-Glo assay and Miles and Misra method</i>	62
	62
3.3.1.2.	<i>Size of H. pylori OMV</i>	63
3.3.2.	<i>Correlation Between Pierce BCA- Protein Assay and Zetaview</i>	66
3.3.3.	<i>Association Between the Quantity of OMV Produced and Bacterial Virulence</i>	67
3.4.	DISCUSSION	69
3.4.1.	<i>Characterisation of OMV from H. pylori Strains</i>	69
3.4.2.	<i>Correlation Between Pierce BCA- Protein Assay and Zetaview</i>	74
3.4.3.	<i>Association Between the Quantity of Isolated OMV and Bacterial Virulence</i>	74
3.5.	CHAPTER SUMMERY	75
4.	EFFECTS OF OMV ON MAMMALIAN CELLS	77
4.1.	INTRODUCTION	77
4.2.	AIM OF THIS STUDY	79
4.3.	MATERIAL AND METHODS	81
4.3.1.	<i>H. pylori OMV</i>	81
4.3.2.	<i>Cell Culture</i>	81
4.3.3.	<i>OMV cytotoxicity</i>	81
4.3.4.	<i>Mycoplasma Detection Test</i>	81
4.3.5.	<i>Statistical Analysis</i>	82
4.4.	RESULTS	83
4.4.1.	<i>Mycoplasma detection</i>	83
4.4.2.	<i>OMV cytotoxicity</i>	84
4.4.2.1.	<i>Effect of OMV on AGS cells after 24 hours (CellTiter assay)</i>	84
4.4.2.2.	<i>Effects of OMV on AGS cell viability over 24 hours (Realtime Glo assay)</i>	87
4.4.3.	<i>Live OMV-AGS cells image-based (Incucyte) analysis</i>	89
4.4.3.1.	<i>Cell viability (% confluence)</i>	89
4.4.3.2.	<i>Cell death</i>	93

4.4.3.3.	<i>Microscopy analysis of OMV treated cells</i>	95
4.5.	DISCUSSION	99
4.5.1.	<i>OMV cytotoxicity</i>	99
4.5.1.1.	<i>Effect of OMV on AGS cells after 24 hours (CellTiter assay)</i>	99
4.5.1.2.	<i>Effect of OMV on AGS cells over 24 hours (Realtime Glo assay)</i>	101
4.5.2.	<i>Microscopy analysis of OMV treated cell</i>	103
5.	PROTEOMIC STUDY	108
5.1.	INTRODUCTION	108
5.2.	AIM OF THIS STUDY	110
5.3.	RESULTS	112
5.3.1.	<i>OMV-associated protein analysis by SDS-PAGE</i>	112
5.3.2.	<i>OMV associated protein analysis by LC-MS/MS</i>	115
5.3.3.	<i>Analysis of proteins associated with AGS cell response to OMV treatment</i>	126
5.3.4.	<i>Correlation between VacA and CagA quantities and OMV cytotoxicity effect</i>	130
5.4.	DISCUSSION	131
5.4.1.	<i>SDS-PAGE</i>	131
5.4.2.	<i>Analysis of OMV associated proteins</i>	132
5.4.3.	<i>Analysis of proteins associated with cell response</i>	137
5.4.4.	<i>Correlation between VacA and CagA quantities and OMV cytotoxicity effect</i>	138
5.5.	CHAPTER SUMMARY	140
6.	MUTAGENESIS OF KEY GENE	143
6.1.	INTRODUCTION	143
6.2.	AIM OF THE STUDY	145
6.3.	MATERIALS AND METHODS	147
6.3.1.	<i>H. pylori Strain</i>	147
6.3.2.	<i>Selection of Gene of Interest (GOI)</i>	147
6.3.3.	<i>Cloning Gene of Interest into pJET Cloning Vector</i>	147
6.3.4.	<i>Inverse PCR and Construction of Mutation Plasmid</i>	150
6.3.5.	<i>Transformation of H. pylori</i>	153
6.3.6.	<i>Cytotoxicity of ΔcagA H. pylori 60190 OMV</i>	155
6.3.6.1.	<i>Cell culture</i>	155
6.3.6.2.	<i>H. pylori strain</i>	155
6.3.6.3.	<i>OMV isolation</i>	155
6.3.6.4.	<i>OMV cytotoxicity</i>	155
6.3.7.	<i>Statistical Analysis</i>	156
6.4.	RESULTS	157
6.4.1.	SELECTION OF GENE OF INTEREST	157
6.4.2.	<i>Clone Gene of Interest into pJET Cloning Vector</i>	157
6.4.3.	<i>Inverse PCR and Construction of Mutation Plasmid</i>	160
6.4.4.	<i>Transformation of H. pylori</i>	161
6.4.5.	<i>Effect of WT and ΔcagA H. pylori 60190 OMV on AGS cells</i>	161
6.5.	DISCUSSION	163
6.5.1.	<i>Mutagenesis of cagA gene</i>	163
6.5.2.	<i>Effect of WT and ΔcagA H. pylori 60190 OMV on AGS cells</i>	163
6.6.	CHAPTER SUMMARY	166
7.	DISCUSSION	168

Publications

Murray, B., Dawson, R., AlSharaf, L. and Winter, J., 2020. Protective effects of *Helicobacter pylori* membrane vesicles against stress and antimicrobial agents. *Microbiology*, 166(8), pp.751-758.

List of Tables

Table 2.1: <i>H. pylori</i> strains used in the study.	28
Table 2.2: PCR Primers and Cycling Condition of <i>cagA</i> mutation used in the study.	44
Table 2.3: Plasmids.....	47
Table 2.4: Restriction digest	49
Table 4.1: Vacuolation grading score.	97
Table 4.2: Images of untreated AGS cells at time points 0, 6, 12, and 18 hours.....	98
Table 4.3: Images of AGS cells treated with OMV of <i>H. pylori</i> 444A strain at time points 6 and 18 hours.....	99
Table 4.4: Images of AGS cells treated with OMV of <i>H. pylori</i> 221A strain at time points 0, 6, 12, and 18 hours.	100
Table 4.5: Images of AGS cells treated with OMV of <i>H. pylori</i> 60190 strain at time points 6 and 18 hours.	101
Table 4.6: Images of AGS cells treated with OMV of <i>H. pylori</i> Tx30a strain at time points 0, 6, 12, and 18 hours.	102
Table 4.7: Effects of OMV on AGS cells.	104
Table 5.1: Common identified proteins of <i>H. pylori</i> 444A OMV in all data sets.....	122
Table 5.2: Differentially expressed proteins from AGS cells treated with <i>H. pylori</i> 444A OMV isolated from early broth cultures compared to untreated control cells identified by LC-MS/MS.....	127
Table 5.3: Differentially expressed proteins from AGS cells treated with <i>H. pylori</i> 444A OMV isolated from late broth cultures compared to control cells identified by LC-MS/MS.	128
Table 5.4: Quantity of toxins within <i>H. pylori</i> 444A OMV and their activities on OMV-treated AGS cells.....	129

List of Figures

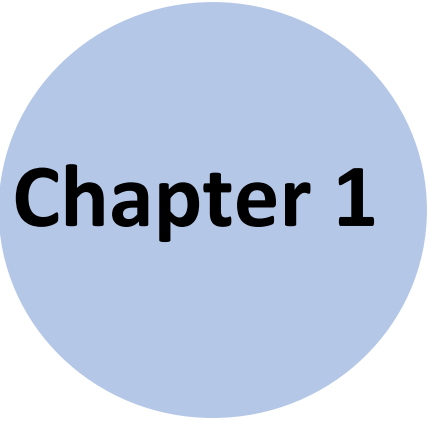
Figure 1.1: Patterns of gastritis.....	6
Figure 1.2: Sydney score of gastritis grading and histopathological changes.....	9
Figure 1.3: Main virulence factors of <i>H. pylori</i> and their cytotoxicity.....	12
Figure 1.4: Effects of CagA toxin on host cells.....	15
Figure 1.5: <i>H. pylori</i> VacA toxin.....	17
Figure 1.6: Model of outer membrane vesicle biogenesis.....	20
Figure 2.1: Cloning strategy overview.....	42
Figure 3.1: Quantity of OMV produced by different <i>H. pylori</i> strains on agar plates and in early broth cultures.....	60
Figure 3.2: Quantity of OMV produced by different <i>H. pylori</i> strains in late broth culture.....	61
Figure 3.3: Comparison of BacTiter-Glo and Miles and Misra methods for quantification of viable bacteria.....	62
Figure 3.4: The size of <i>H. pylori</i> OMV.....	64
Figure 3.5: OMV size distribution.....	65
Figure 3.6: Correlation between Pierce BCA- protein assay and Zetaview.	66
Figure 3.7: Association between OMV quantity and bacterial virulence.	68
Figure 3.8: Gram stain of 60190 strain.....	73
Figure 4.1: Detection of <i>Mycoplasma</i> in AGS cells.	84
Figure 4.2: Effects of high dose of OMV on human gastric epithelial cells.	85
Figure 4.3: Effects of a range of doses of OMV on human gastric epithelial cells....	86
Figure 4.4: Real-time effects of OMV on human gastric epithelial cells.....	88
Figure 4.5: Confluence of human gastric epithelial cells treated with <i>H. pylori</i> OMV.....	91
Figure 4.6: Effect of each OMV treatment on % confluence of human gastric epithelial cells.....	92
Figure 4.7: Cell death of human gastric epithelial cells treated with <i>H. pylori</i> OMV.	94
Figure 4.8: Hummingbird phenotype.	103
Figure 5.1: SDS-PAGE analysis of 444A and 221A OMV isolated from three growth conditions.....	112
Figure 5.2: SDS-PAGE analysis of 60190 and Tx30a OMV isolated from three growth conditions.	113
Figure 5.3: Comparison of early and late broth OMV proteins level.	116
Figure 5.4: Comparison of early broth and plate OMV proteins level.	117
Figure 5.5: Comparison of late broth and plate OMV proteins level.	118
Figure 5.6: Correlation heatmap of proteins detected within <i>H. pylori</i> 444A OMV isolated from early broth (EB), late broth (LB), and plate (P) cultures...	119
Figure 5.7: Venn diagram of detected differentially expressed <i>H. pylori</i> 444A OMV proteins.....	121
Figure 5.8: Relative quantities of <i>H. pylori</i> 444A proteins that were detected in OMV from all three growth conditions.	123
Figure 5.9: Relative quantities of <i>H. pylori</i> 444A proteins that were detected in OMV from all three growth conditions.	124
Figure 5.10: Venn diagram of treated and untreated AGS cells detected Proteins.....	126
Figure 6.1: Polymorphism of <i>cagA</i> in EPIYA-repeated region.....	143
Figure 6.2: The map of pJET 1.2/blunt plasmid.....	147
Figure 6.3: Ligation of <i>cagA</i> into pJET plasmid.....	148

Figure 6.4: Colony PCR screening of <i>cagA</i> insert.....	148
Figure 6.5: Inverse PCR of pJET- <i>cagA</i> plasmid.....	149
Figure 6.6: The extracted pBlueKm plasmid.....	150
Figure 6.7: Digested pBlueKm plasmid.....	151
Figure 6.8: Digested pJET- <i>cagA</i> flanks plasmid (inverse PCR product)	151
Figure 6.9: Constructed pJET- <i>cagA</i> flanks-KanR plasmid.....	152
Figure 6.10: <i>H. pylori</i> DNA Recombination.	153
Figure 6.11: Gel electrophoresis of gradient PCR amplification of <i>cagA</i> gene.	157
Figure 6.12: Gel electrophoresis of PCR amplification of <i>cagA</i> gene.....	157
Figure 6.13: Colony screening of <i>E. coli</i> carrying <i>cagA</i> -pJET plasmid.	158
Figure 6.14: Gel electrophoresis of PCR colony screening of <i>cagA</i> insert.....	158
Figure 6.15: Gel electrophoresis of gradient inverse PCR of pJET- <i>cagA</i> plasmid.....	159
Figure 6.16: Gel electrophoresis of restriction digest.	160
Figure 6.17: Effects of high dose of OMV on human gastric epithelial cells.	161

List of Abbreviations

<i>H. pylori</i>	<i>Helicobacter pylori</i>	2
VBNC	Viable but non-culturable	2
MALT	Mucosa-associated lymphoid tissue	3
Ig	Immunoglobulin	4
PCR	Polymerase chain reaction	4
CagA	Cytotoxin associated gene A	4
VacA	Vacuolating cytotoxin A	4
IL	Interleukin	6
SabA	Sialic acid-binding	13
BabA	Blood group antigen-binding	13
PAI	Pathogenicity island	14
T4SS	Type IV secretion system	14
OMV	Outer membrane vesicles	18
LPS	Lipopolysaccharides	20
OMPs	Outer membrane proteins	21
I-OMV	Inner-outer membrane vesicles	21
NAP	Neutrophil-activating protein	23
Oip	Outer inflammatory protein	23
Alp	Adherence-associated protein	24
BHI	Brain heart infusion	29
OD	Optical density	29
D-PBS	Dulbecco's phosphate buffer saline	30
CFU	Colony-forming units	30
NTA	Nanoparticle tracking analysis	32
AGS	Human gastric epithelial cells	32
HI-FCS	Heat-inactivated foetal calf serum	33
UV	Ultraviolet	33
SDS-PAGE	Sodium Dodecyl Sulphate - Polyacrylamide Gel Electrophoresis	35
TEMED	Tetramethylethylenediamine	35
RSB	Reduced sample buffer	35
DTT	DL-dithiothreitol	35
LC-MS	Liquid chromatography-mass spectrometry	37
LC-MS/MS	Liquid chromatography-tandem mass spectrometry	37
IDA	Information-dependent acquisition	37
FDR	False discovery rate	38
RIPA	Radioimmunoprecipitation assay	38
GOI	Gene of interest	38
KanR	Kanamycin resistance	47
$\Delta cagA$	<i>cagA</i> mutant	50
<i>E. coli</i>	<i>Escherichia coli</i>	53
<i>hns</i>	Histone-like nucleoid-structuring	53
SD	Standard deviations	57
<i>C. jejuni</i>	<i>Campylobacter jejuni</i>	71
EHEC	<i>Enterohemorrhagic E. Coli</i>	77
HlyA	Hemolysin A	77
ELISA	Enzyme-linked immunosorbent assay	137

PTBP1	polypyrimidine tract-binding protein 1	140
SHP2	Src homology 2-containing phosphatase 2	146
WT	wild type	160



Chapter 1

INTRODUCTION

1. INTRODUCTION

1.1. *Helicobacter pylori*: Overview

Helicobacter pylori (*H. pylori*) is a Gram-negative, microaerophilic bacterium, which requires nitrogen, carbon dioxide (10%), a low level of oxygen (5%) and high humidity to grow. It has four to six unipolar sheathed flagella. *H. pylori* was initially known as *Campylobacter pyloridis* and was classified under the *Campylobacter* genus. That was due to its similarities to the other *Campylobacter* species as both have curved shape, are highly motile, and oxidase-, urease- and catalase-positive (Andersen and Wadtröm 2001; Owen 1998). The name was then grammatically corrected to *Campylobacter pylori*. The term pylori refers to the pyloric sphincter valve located between the stomach and the duodenum (pylorus region). In 1989, differences in flagella characteristics, major proteins, and the genome between *Campylobacter pylori* and other *Campylobacter* species were observed. Therefore, its name was changed afterwards to *Helicobacter pylori*, and a new genus was created (*Helicobacter* genus) (Marshall and Warren 2001; Owen 1998). The “*helicobacter*” taxonomy refers to the helical or spiral rod shape of the bacterium.

There are two cell shapes of *H. pylori*. The most well-known is the spiral shape, which is the culturable shape (Cammarota *et al.* 2012). *H. pylori* can transform into a coccoid form in stressful environments to survive, as well as after prolonged incubation periods (Owen 1998; Ketley 2007; Cellini *et al.* 2008; Andersen and Rasmussen 2009; Yonezawa *et al.* 2015; Grande *et al.* 2012; Loke *et al.* 2016). The transition to coccoid form begins with bending into U and doughnut shapes (Cammarota *et al.* 2012; Rudnicka *et al.* 2014). The coccoid shape is considered to be a viable but non-culturable (VBNC) form (Cellini *et al.* 2008; Andersen and Rasmussen 2009). The VBNC form has been reported as a carcinogenic form as it has more carcinogenic proteins comparing to the spiral form (Loke *et al.* 2016). Moreover, a third form of *H. pylori* has been reported, which is also a coccoid shape; however, unviable and non-culturable. Due to lacking DNA, RNA, and the membrane potential in this shape, it is thought to represent the death stage of *H. pylori* (Kusters *et al.* 1997).

H. pylori targets the human gastrointestinal tract, mainly the stomach and in some cases, it targets the duodenum. The gastrointestinal tract gets infected with *H. pylori*

due to consumption of contaminated water or foods, or via direct contact either faecal-oral or oral-oral routes as *H. pylori* has been found in dental plaque, saliva and faeces of infected patients (Blaser and Atherton 2004; Perry *et al.* 2006; Lehours and Yilmaz 2007). The infection can also be transmitted within a family either directly from parent to child (from the mother more than from the father) or between young siblings (Stark *et al.* 1999; Han *et al.* 2000; Nguyen *et al.* 2006). Transmission within the family is thought to involve more vertical transmissions than horizontal.

H. pylori colonises more than half of the world's population. Although *H. pylori* infection is widespread, the rate of infection varies between countries. That depends on the country's geographic area and its socio-economic status (Brown 2000; Cover *et al.* 2001). Developed countries show lower *H. pylori* prevalence than developing countries, 30-50% and 85-95%, respectively (Brown 2000; Zamani *et al.* 2018; Khoder *et al.* 2019). The infection prevalence rate and the risk of carcinoma development might also be affected by the age and gender demographics of the population. Although *H. pylori* colonisation is thought to be initiated early in childhood in all populations, mostly due to transmission from parents to their children and between young siblings, the prevalence among children in developed countries seems to be lower than in developing ones (Brown 2000; Cover *et al.* 2001). That might be related to improved socio-economic and sanitation levels with improved hygienic practices in the developed countries. Also, colonisation in early childhood appears to raise the risk of developing gastric cancer (Blaster *et al.* 2007). Additionally, a higher prevalence rate of *H. pylori* infection was reported in males than in females (Chen *et al.* 2016).

Infections with *H. pylori* causes gastritis, which is an inflammation of the stomach lining that might cause damage to epithelial cells if it persists. Over a lifetime, about 10% of *H. pylori* infection will progress to life-threatening diseases like peptic or duodenal ulcers (Wroblewski *et al.* 2010). Also, between 1 to 3% will lead to gastric adenocarcinoma and less than 0.1% will lead to mucosa-associated lymphoid tissue (MALT) lymphoma (Wroblewski *et al.* 2010). The conditions are mostly asymptomatic, which means that infected patients might not be aware of getting *H. pylori* infection. However, in other cases, patients might show some symptoms.

These include upper abdominal pain, nausea and vomiting, bloating, and diarrhoea, in addition to bad breath.

Since the diseases are mostly asymptomatic, non-invasive tests are performed to diagnose *H. pylori* infections. For example, serology tests, which detect anti-*H. pylori* immunoglobulin (Ig) antibodies in patients' serum such as IgG, IgM, and IgA, and *H. pylori* antigens. Moreover, the urea breath test measures the amount of generated carbon dioxide in the stomach (Brown 2000; Ketley 2007). In some cases, polymerase chain reaction (PCR) and faecal antigen test may also be performed to identify *H. pylori* (Ketley 2007). Patients may also undergo endoscopy, which is an invasive test, to collect biopsies from their stomach lining for microscopic and histopathological examinations, bacterial isolation and biopsy urease test (Brown 2000; Ketley 2007). Once these tests confirm the presence of *H. pylori*, a course of combined antibiotics should be started to eradicate *H. pylori* and prevent disease progression.

Moreover, some factors might increase the susceptibility of developing gastric inflammation or other gastric diseases. These include host and environmental factors. For instance, the individual behaviours of infected people such as smoking, alcohol consumption, and their diet might increase the risk of developing gastric cancer due to *H. pylori* infection (Brown 2000; Ordonez-Mena *et al.* 2016; Fang *et al.* 2015). Besides, the individuals' general health and wealth, hygiene practices, and their family history of gastroduodenal diseases may contribute to their disease risk (Brown 2000). Furthermore, the host immune system and genetic traits also influence disease progression.

Some bacterial factors also increase the risk of ulcers and cancer developing after infection, for example, the virulence level of the infected strain. Type I *H. pylori* strains have high virulence, including the production of the cytotoxin associated gene A (CagA) toxin and the more virulent alleles type 1 in all polymorphic regions (signal (s), intermediate (i), and mid-region (m)) of the vacuolating cytotoxin A (VacA). They are associated with more severe disease (see also Sections 1.3.3. and 1.3.4.). Infection with type I strains, in particular, increases the risk of severe histopathological changes such as intestinal metaplasia and atrophy, which might cause progression to gastric adenocarcinoma (Amieva and Peek 2016; Correa and

Houghton 2007; Atherton and Blaser 2009; Winter *et al.* 2014). Studies showed that *H. pylori* infections in the stomach's corpus portion causes atrophic gastritis (see Section 1.2.1.3.) due to damaging the acid producing cells causing hypochlorhydria (Ubukata *et al.* 2011; Konturek *et al.* 2006). Thus, infected patients might be at a high risk of developing gastric cancer, if infection persists.

1.2. Gastric Diseases and Their Histopathological Features

1.2.1. Gastritis

Gastritis is an inflammation of gastric epithelium lining that mainly occurs due to *H. pylori* colonisation (NIDDK 2013). There are other causes of gastritis, such as autoimmune diseases; however, this section will focus on gastritis that is caused by *H. pylori*. Gastritis has different patterns representing the infected region, including antral- or corporal-gastritis and pan-gastritis, representing the infection of both regions (Waters and Voltaggio 2017). Gastritis severity is classified based on the histological changes to the gastric mucosa. Indeed, histopathological changes are not similar in all patients with gastritis because it depends on the different factors, as stated earlier. However, this section will explain the gastritis types caused by *H. pylori* and their main histological characteristics.

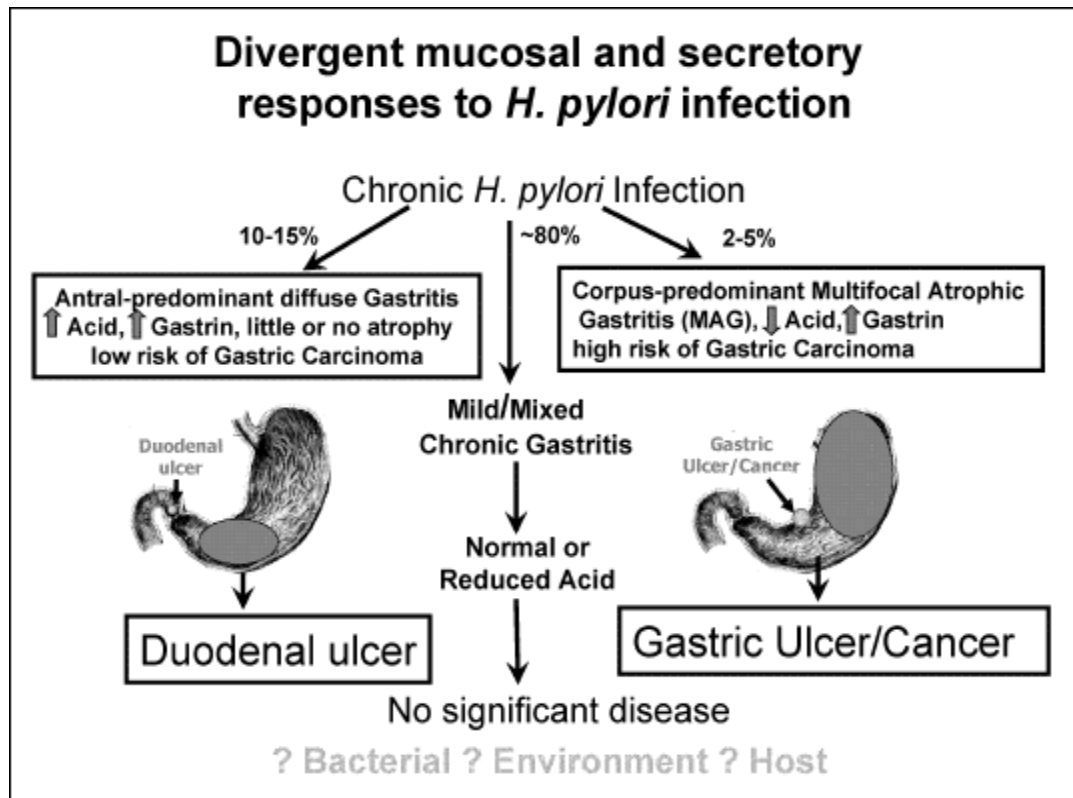


Figure 1.1: Patterns of gastritis. Antral-gastritis (left) and corpral-gastritis (right) (Konturek *et al.* 2006).

1.2.1.1. Acute gastritis

Acute gastritis is the major type, and it is inflammation with few histological changes. Once the stomach is infected, *H. pylori* produces some virulence factors (see Section 1.3.) to protect itself and colonise the stomach lining. These factors stimulate the secretion of interleukin (IL) 8 and other chemokines and cytokines (Cammarota *et al.* 2012; Kim *et al.* 2006; Winter *et al.* 2014; Cook *et al.* 2014). That causes acute inflammation and triggers the host immune system. Neutrophils, lymphocytes, macrophages, and other inflammatory cells then migrate to the inflammation site to provide defence against the bacteria (Figure 1.4) (Sobala *et al.* 1991; Atherton 2006; Brandt *et al.* 2005; Atherton and Blaser 2009). Exfoliation and regeneration of epithelial cells, in addition to a reduction in mucin synthesis, occur as a cellular response (Oohara *et al.* 1983).

Moreover, the infection reduces gastric acidity (hypochlorhydria) (Sobala *et al.* 1993). Acute gastritis is a superficial, short-term inflammation, which means that the

infection might be eradicated in 2 to 3 weeks, and the epithelium lining and stomach acidity would be recovered. However, typically the immune system fails to eliminate *H. pylori*, leading to chronic gastritis.

1.2.1.2. Chronic gastritis

A prolonged period of hypochlorhydria indicates *H. pylori* persistence. In such a case, more neutrophils migrate to the infection with the help of the lymphocytes (T and B cells) and plasma cells. Based on the Sydney scoring system, the high accumulation of plasma cells and lymphocytes in the lamina propria indicates chronic inflammation (Dixon *et al.* 1996). This inflammation ranges from mild to severe grade, depending on the density of lymphocyte and plasma cells (Figure 1.4). Lymphoid follicles might also be seen in gastric biopsies of patients with chronic gastritis (Genta *et al.* 1993; Enno *et al.* 1995).

Moreover, neutrophilic infiltration at the infected lining indicates the activity of chronic gastritis (Figure 1.4) (Brandt *et al.* 2005; Tham *et al.* 2001). The infiltrated portion size indicates the activity grading level (Dixon *et al.* 1996). These abnormalities characterise the histopathological picture of chronic gastritis. If the bacteria are eradicated using antibiotic therapy, histological abnormalities will revert, and neutrophilic infiltrates will disappear. However, this might take years. On the other hand, reinfection or failure of *H. pylori* eradication might progress to ulceration and adenocarcinoma.

1.2.1.3. Atrophic gastritis

Atrophic gastritis is a prolonged (several decades) severe inflammation characterised by gradual loss of glandular layers from either corpus or antrum (Figure 1.4). In the Sydney scoring system, the percentage of glandular loss shows the severity level of gastritis (Dixon *et al.* 1996). Atrophic gastritis is also characterised by progressive cellular damage and loss. Loss of mucosal cells responsible for acid production and secretion, such as parietal cells, might result in reduced pepsin production (Atherton 2006; Asaka *et al.* 1997). That increases the risk of developing gastric ulcers and progression to gastric adenocarcinoma. On the other hand, low stomach acid production would lower the risk of developing duodenal ulcers (Atherton 2006).

1.2.1.4. Intestinal metaplasia

Intestinal metaplasia is a type of cellular transformation that occurs to replace severely damaged gastric epithelial cells with intestinal-type epithelium lining (Figure 1.4). In response to prolonged chronic gastritis, gastric cells excessively regenerate, which might cause abnormal growth stimulation. That results in intestinal metaplasia changes after years or decades of chronic persistent infection (Mukawa *et al.* 1987; Fikret *et al.* 2001; Ogata 1995). *H. pylori* colonisation might also stimulate the G cells, which are located at the pyloric region and are responsible for inducing gastric acid production (McColl *et al.* 1997; Ilver *et al.* 1997). High acid production might damage the stomach (especially the antrum region) as well as the duodenum, causing gastric intestinal metaplasia and duodenal ulceration (McColl *et al.* 1997; Ilver *et al.* 1997). Moreover, intestinal metaplasia is observed in the antrum region more than in the corpus (Eidt and Stolte 1994). The presence of goblet cells in the gastric mucosa is an indication of intestinal metaplasia.

Additionally, the percentage of transformed cells in the mucosa indicates the severity of intestinal metaplasia (Dixon *et al.* 1996). Both atrophy and intestinal metaplasia are considered precancerous changes. Patients with intestinal metaplasia are at high risk of duodenal ulcers and gastric adenocarcinoma.

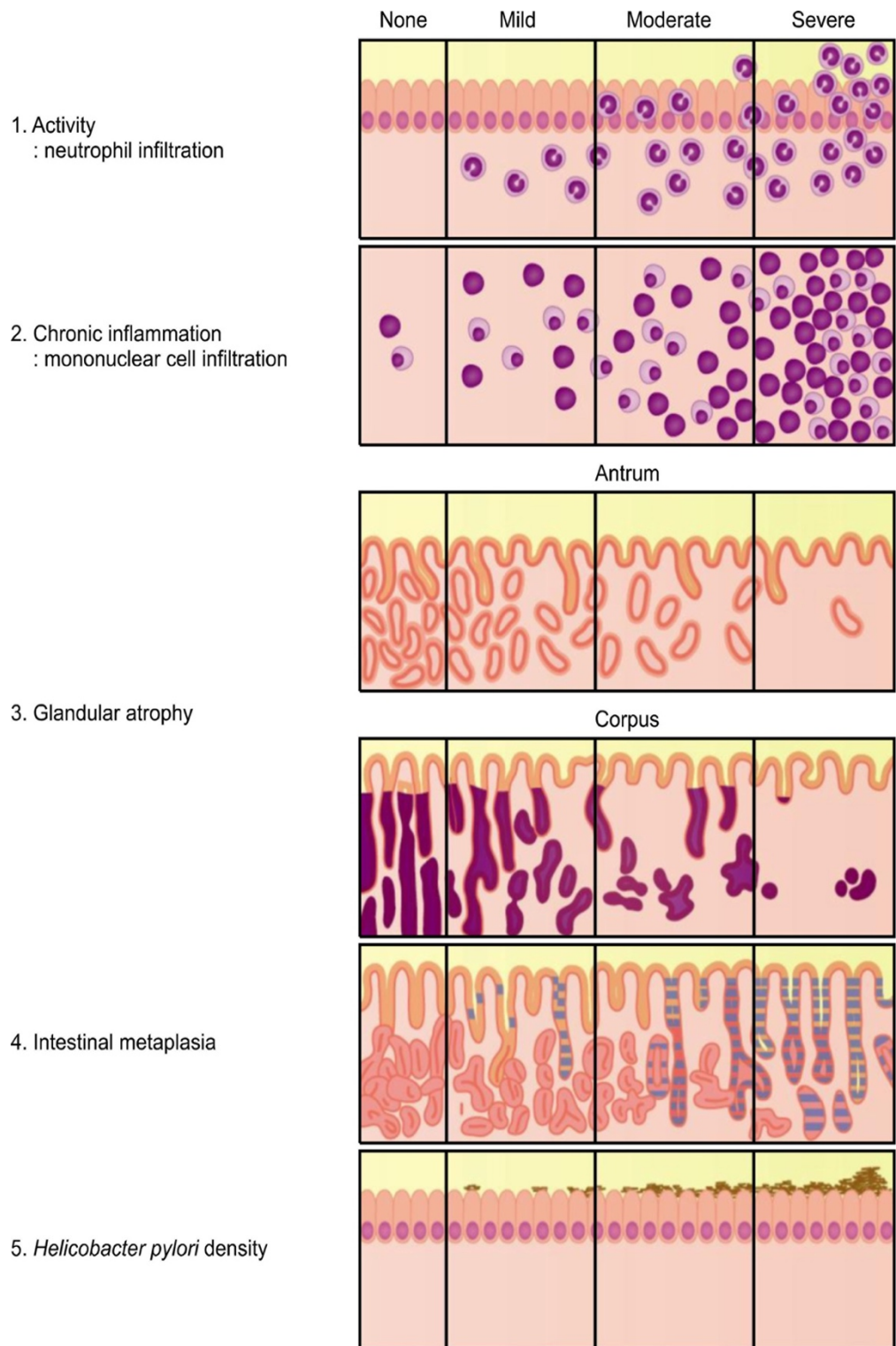


Figure 1.2: Sydney score of gastritis grading and histopathological changes. (Dixon *et al.* 2015; see Park and Kim 2015).

1.2.2. Peptic ulcer

Peptic ulcers occur due to the death and breakage of the epithelial lining in prolonged *H. pylori* infection, especially with high virulence strains (Najm 2011). About 10% of *H. pylori* infections will lead to peptic ulcers (Wroblewski *et al.* 2010). Ulcers can occur either in the stomach (gastric ulcer) or in the duodenum (duodenal ulcer), depending on the colonisation location and stomach acidity level. The antral-corporal transitional area has a gradient pH; therefore, gastric ulcers mainly develop in this area in individuals with low to normal acid secretion (Atherton 2006, Dixon 2001). Nevertheless, ulcers can also occur in the antrum or the corpus regions depending on their acidity level. Although *H. pylori* cannot withstand extremely low pH, it can colonise the corpus and cause diseases in patients with normal to high acid secretion (Dixon 2001). That occurs when the stomach acidity in these people reduced for a short time, such as after having meals.

As previously mentioned, *H. pylori* colonisation in the antrum might induce acid secretion by stimulating the G cells as an inflammatory response. G cells are responsible for secreting gastrin hormone (McCull *et al.* 1997). This hormone stimulates acid-secreting cells like the parietal cells to increase acid secretion. High acid secretion might damage gastric cells; therefore, gastric cells migrate to the duodenum as a protection mechanism (Fikret *et al.* 2001). This migration damages the duodenum and causes gastric metaplasia, which is transforming the intestinal lining into the gastric lining (Walker and Dixon 1996). Consequently, *H. pylori* colonisation occurs in the duodenum, causing inflammation there and progression to duodenal ulcers.

1.2.3. Gastric Adenocarcinoma

Gastric adenocarcinoma is a malignant tumour of the stomach lining. After decades of gastric atrophy and intestinal metaplasia, gastric cancer might develop. Globally, more than one million new cases diagnosed with gastric cancer are recorded each year (Rawla and Barsouk 2019). *H. pylori* is the leading cause of around 70% of gastric cancers cases worldwide (Muzahed 2020). Between 1 to 3% of *H. pylori* infections

will lead to gastric adenocarcinoma (Wroblewski *et al.* 2010). This depends on several factors, as mentioned in Section 1.1. It should also be pointed out that *H. pylori* is classified as a class I carcinogenic pathogen (IARC 1994) that increases the risk of developing carcinoma. There are two types of gastric carcinoma classified based on their stomach location; distal (gastroduodenal region) and proximal (gastroesophageal) cancers. Distal gastric cancer is known as non-cardia, mainly caused by *H. pylori* infection (Plummer *et al.* 2014). Gastric cancer is one of the most common cancers globally and is the third common cause of cancer-related deaths (Rawla and Barsouk 2019; Herrero *et al.* 2014). Based on GLOBOCAN 2020 data, there were approximately 768,793 deaths due to gastric cancer were recorded in 2020 (GLOBOCAN). Although the long-term infection can progress to carcinoma, eradication of *H. pylori* before the occurrence of precancerous changes might reduce gastric cancer development.

1.3. Virulence Factors Associated with Pathogenicity

There are many different virulence factors expressed by *H. pylori* that might contribute to causing the disease states outlined above (Figure 1.3). However, the expression of these virulence factors depends on the virulence type and level of the *H. pylori* strain. *H. pylori* is a polymorphic and highly variable pathogen. It can be easily mutated during replication and evolution, which might cause switching genes on and off (Chen *et al.* 2016). Moreover, high rates of mutations and recombinations might occur during adaptation to the stomach environment (Chen *et al.* 2016). Studies also found that biofilm formation (see Section 1.4.2.) can alter *H. pylori* genetics and physiological traits (Attaran *et al.* 2016; Cammarota *et al.* 2010; Donlan and Costerton 2002; Mah and O'Toole 2001). These mutations and alterations might occur in virulence genes, affecting the virulence of each strain. Thus, the *H. pylori* genome's variation and the diversity between different strains would consequently affect disease outcome. In this section, some significant virulence factors associated with *H. pylori* pathogenicity will be described, such as urease enzyme, adhesins, CagA, and VacA.

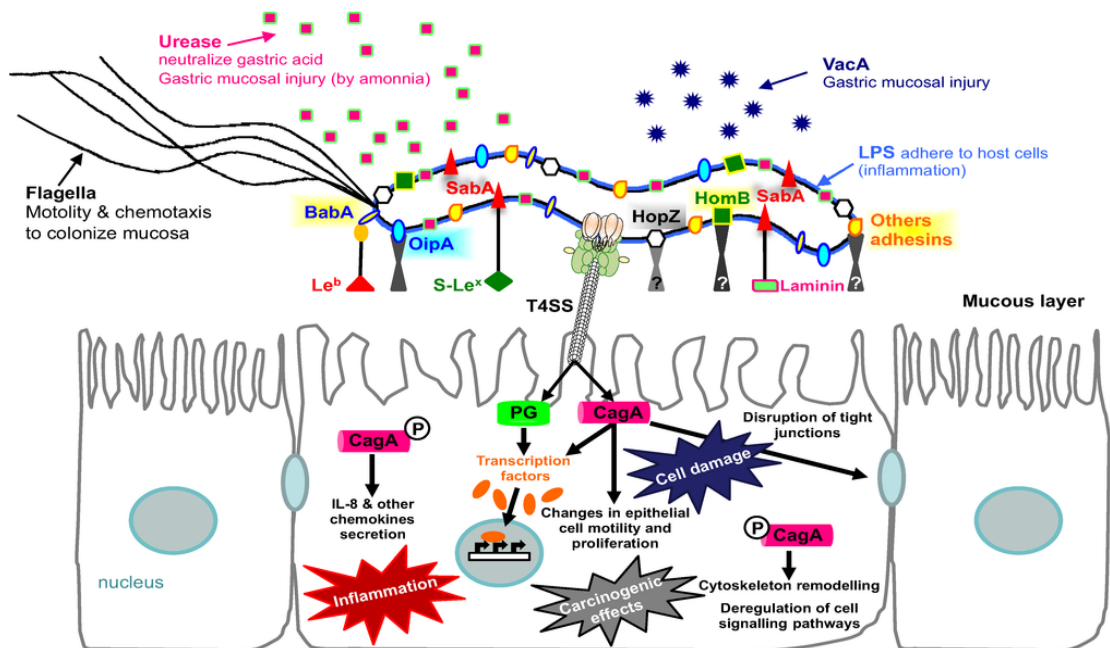


Figure 1.3: Main virulence factors of *H. pylori* and their cytotoxicity. (Oleastro and Ménard 2013).

1.3.1. Urease

Urease is a protein that is made up of multiple subunits and a range of bacteria produce it. The main two subunits are UreA and UreB, encoded by the *ureA* and *ureB* genes, respectively. The UreB hydrolyses the gastric urea, which generates ammonium and carbon dioxide (Figure 1.3). The generated ammonium, which is a basic compound, helps to neutralise stomach acidity. Since *H. pylori* is sensitive to extremely low pH, this creates a more favourable environment for the bacteria, promoting their attachment to epithelial cells (Stark *et al.* 1999; Ketley 2007; Cammarota *et al.* 2012; Garcia *et al.* 2014; Yonezawa *et al.* 2015; Cole *et al.* 2004).

Moreover, ammonium might be severely toxic to the epithelial lining and might cause disturbance to the tight junctions (Segal *et al.* 1992; Mobley *et al.* 2009). Similarly, UreA can also damage the gastric epithelial cells (Mullaney *et al.* 2009). That might provoke the host immune response. Studies on urease mutant *H. pylori* showed that urease mutant strains could not colonise piglets and, *in vitro*, they did not show any cytotoxic effects on human adenocarcinoma gastric (AGS) cell line. In contrast, urease-positive strains were successful colonisers in the piglet model and were cytotoxic (Eaton *et al.* 1991; Segal *et al.* 1992). Thus, the urease enzyme has an essential role in *H. pylori* colonisation.

1.3.2. Adhesins

Adhesins are either protein, lipids, or glycoconjugates that are expressed by bacteria on their outer surface. They are responsible for bacterial-host interactions. *H. pylori* expresses several adhesins, including sialic acid-binding (SabA), and blood group antigen-binding (BabA). These are used by the bacteria to attach to host epithelial cells, promoting the secretion of toxins and other virulence factors (Figure 1.3). BabA and SabA are the most common outer membrane proteins of *H. pylori* that belong to the Hop family. They are also known as HopP and HopS, respectively. The expression of these adhesins is regulated by a slipped-strand mispairing mechanism (phase variation) (Harvey *et al.* 2014; Bäckström *et al.* 2004; Nell *et al.* 2014).

1.3.2.1. Blood group antigen-binding adhesin (BabA)

BabA adhesin is encoded on two genes, silent gene (*babA1*) and active gene (*babA2*). It binds to difucosylated Lewis b histo-blood group antigen on gastric cells (Figure 1.3), which is expressed by healthy gastric epithelial cells and enhances *H. pylori* colonisation of gastric lining and increases gastritis severity (Boren *et al.* 1993; Ilver 1998; Rad *et al.* 2002). Weak to no cell binding were observed in BabA mutant stains, which means that BabA has an essential role in adherence and colonisation (Quintana-Hayashi *et al.* 2018). Also, active BabA has a relationship with other virulence factors, mainly, VacA and CagA as it helps in their entry into gastric cells and might enhance their toxic effect (Yu *et al.* 2002; Ishijima *et al.* 2011). Thus, BabA can increase the severity of inflammation by stimulating an inflammatory response and might lead to ulceration and carcinoma.

1.3.2.2. Sialic acid-binding adhesin (SabA)

SabA adhesin is encoded by the *sabA* gene that expressed in response to the stomach environment and acidity as SabA is indirectly related to the stomach pH (Yamaoka *et al.* 2006; Yamaoka 2008; Michael *et al.* 2004; Loh *et al.* 2010). Low pH (high acidity) inhibits the expression of *sabA* and vice versa. SabA binds to sialylated Lewis (x and a) antigens that are expressed by gastric epithelium during infection (Figure 1.3), promoting *H. pylori* adherence and colonisation of the gastric mucosa (Marcos *et al.* 2008; Alm *et al.* 2000; Mahdavi *et al.* 2002). Some studies reported that SabA

expression could increase the risk of developing precancerous histopathological changes, as well as gastric cancer (Sakamoto 1989; Yamaoka *et al.* 2006). In contrast, another study found no association between *sabA* expression and the progression of *H. pylori* infection into gastric cancer (Yanai *et al.* 2007). The relationship between SabA and other virulence factors is still debatable.

1.3.3. Cytotoxin Associated Gene A (CagA)

CagA is a significant virulence factor of *H. pylori*. It is an immunogenic protein encoded on the *cagA* gene, which is a major gene within the *cag* pathogenicity island (PAI). The *cag* PAI encodes for several other *cag* genes as well as the *cag* type IV secretion system (T4SS). Once *H. pylori* colonises the gastric lining, it injects the CagA protein directly into the gastric epithelial cells via the *cag* type IV secretion system (Kim *et al.* 2006) (Figures 1.3 and 1.4). This injection is supported by *H. pylori* adhesin proteins such as BabA and SabA (Jiménez-Soto *et al.* 2009; Kwok *et al.* 2007). The gene has different polymorphisms in the EPIYA region, which is responsible for CagA phosphorylation once injected into host cells (Figure 1.4) (Hatakeyama 2017) (see also Section 6.1). This has a crucial role in *H. pylori* pathogenicity as it causes alteration in the signalling pathways, inducing the expression of IL-8 by gastric cells (Hatakeyama 2017; Cammarota *et al.* 2012; Kim *et al.* 2006; Winter *et al.* 2014) (see also Section 6.1). This cytokine attracts immune cells, mainly neutrophils, driving gastritis (Cammarota *et al.* 2012). AGS cells infected with *H. pylori cagA* positive strains increased the expression of IL-8 protein in epithelial cells (Crabtree *et al.* 1995).

The CagA toxin also interacts with host cellular factors disrupting normal proliferation and differentiation of gastric cells and might damage the tight junctions between them, which in turn might cause abnormal histopathological changes (Figure 1.4) (Saadat *et al.* 2007; Backert *et al.* 2010). It also causes elongation in gastric cells, known as the hummingbird phenotype (Kurashima *et al.* 2008). Multiple studies have reported that *H. pylori* strains with the *cagA* gene are significantly associated with increasing risk of intestinal metaplasia and atrophic gastritis. CagA is also associated with disease progression into ulcerations and gastric carcinomas (Peek *et al.* 1997; Atherton 1999; Atherton 1998; Atherton 2000; Rokkas *et al.* 1999). Most *H. pylori*

strains isolated from patients with duodenal ulcers were *cagA* positive (around 80%) (Covacci *et al.* 1993; Crabtree *et al.* 1991). The amount of expressed CagA also plays a crucial role in *H. pylori* pathogenicity (Jiménez-Soto and Haas 2016). High expression of CagA appears to induce carcinogenesis more readily. Therefore, it has been classified as an oncogenic protein (Ohnishi *et al.* 2008; Neal *et al.* 2013). CagA polymorphisms and toxicity are discussed further in Chapter 6 (see Section 6.1).

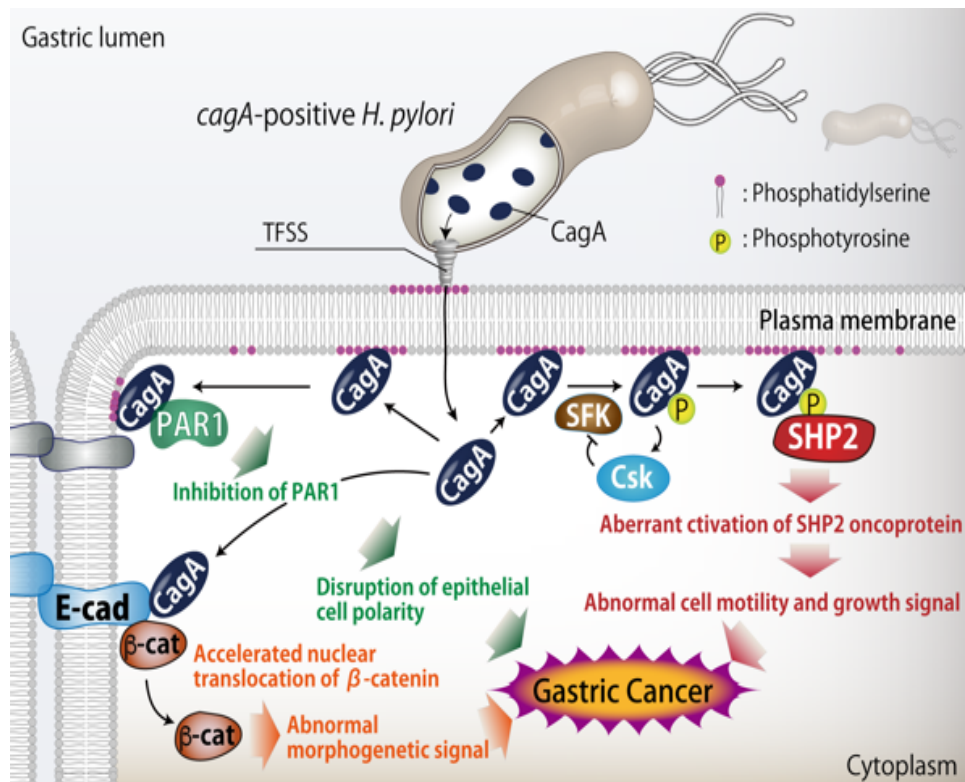


Figure 1.4: Effects of CagA toxin on host cells. (Hatakeyama 2016).

1.3.4. Vacuolating Cytotoxin A (VacA)

VacA is another significant virulence factor. The *vacA* gene encodes for VacA toxin. The release of this toxin induces disease manifestations and autophagy and mediates cellular degradation (apoptosis and necrosis). It also induces gastric epithelial cell vacuolisation (Figure 1.5 b); therefore, it is known as a pore-forming toxin. Moreover, VacA alters the host immune response and inhibits the parietal cells, which produce and secrete stomach acid (Wang *et al.* 2008; Sundrud *et al.* 2004). All *H. pylori* strains have the *vacA* gene; however, this gene is highly polymorphic. Therefore, VacA toxicity on host cells varies between strains. The gene has three main polymorphic regions, each with two allelic variants (alleles type 1 and type 2) (Figure 1.5 a). These regions are signal (s) and intermediate (i) regions, which are responsible for the vacuolating activity, in addition to the mid-region (m), which is responsible for cellular binding.

Allele 1 of each region is more toxic than allele 2. For example, s1 i1 m1 type induces high vacuolating activity and can bind to a variety of cells. Whereas, the s2 i2 m2 type of *vacA* has little to no toxic effect on host cells and can bind to fewer cell types. Nevertheless, some strains express a mosaic type of *vacA* such as s1 i2 m2, which have mild to moderate toxicity to the host cells. *In vitro*, that might depend on the cell line used because, in contrast to the m1 type, m2 cannot bind to a wide range of cell lines. Strains with s1 i1 m1 type *vacA* are significantly associated with peptic ulcer and gastric cancer pathogenesis (Rhead *et al.* 2007; Cover 2016).

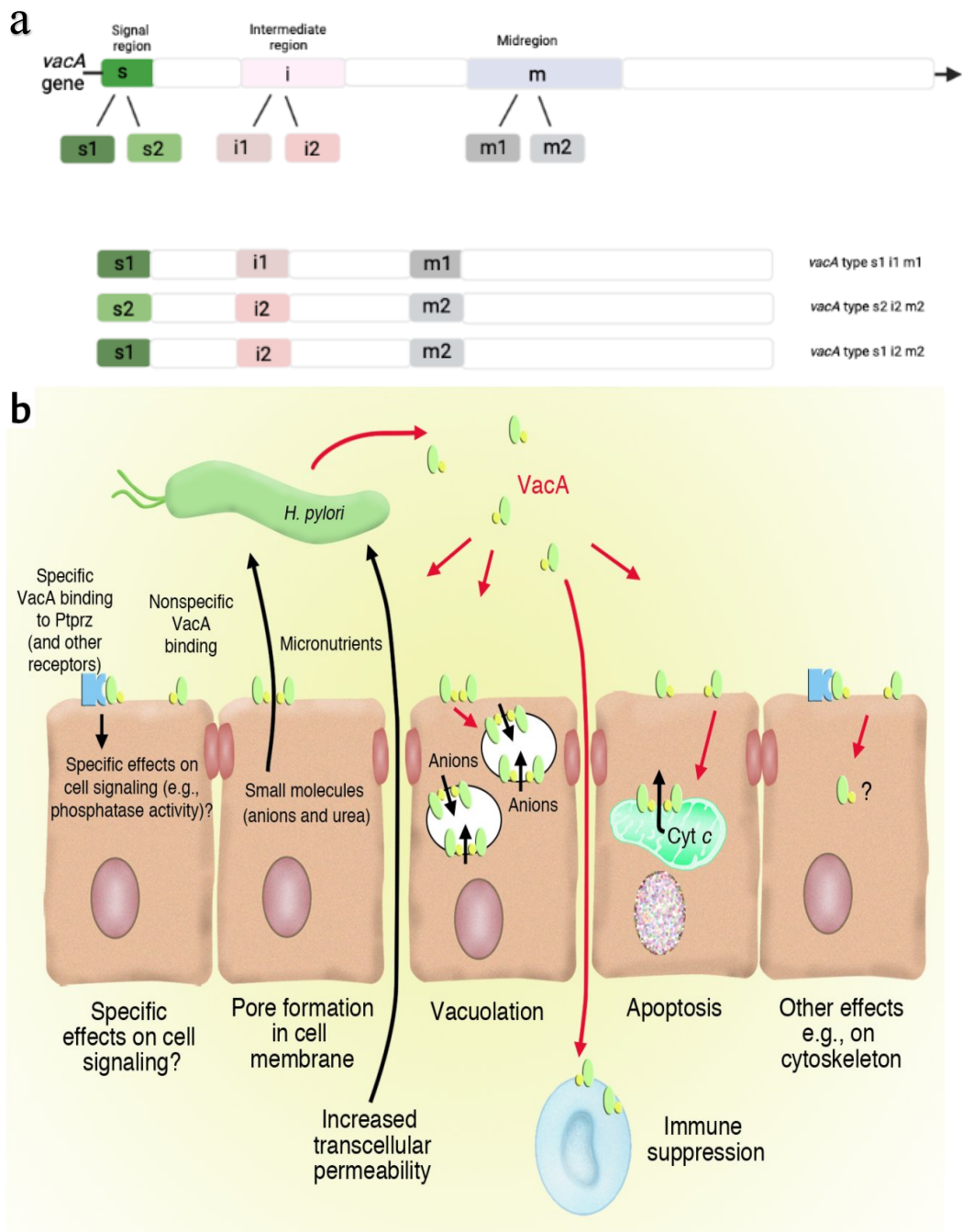


Figure 1.5: *H. pylori* VacA toxin. (a) Polymorphisms of *vacA* gene (created by Biorender). (b) Effects of VacA toxin on host cells (Blaser and Atherton 2004).

1.4. *H. pylori* Pathogenicity and Survival Strategies

Helicobacter pylori has different strategies to ensure its survival and persistence in the human stomach environment. These also might contribute to its pathogenicity. These strategies include bacterial adherence and colonisation, biofilm formation, and production of outer membrane vesicles (OMV).

1.4.1. *H. pylori* Adherence and Colonisation

Within the stomach, *H. pylori* swims toward the gastric epithelial cells underlying the thick mucus layer (where there is a more neutral pH) to protect itself from stomach acidity, and from gastric emptying. Simultaneously, *H. pylori* produces urease enzyme to neutralise stomach acidity (Section 1.3.1.). That protects *H. pylori* and promotes environmental adaptation to establish stomach colonisation. *H. pylori* colonisation mainly occurs at the antrum portion of the stomach, and in some cases, it occurs at the corpus region.

Once *H. pylori* reaches the gastric lining, it associates closely with the epithelial cells and uses adhesins such as BabA and SabA to attach to specific receptors on gastric epithelial cells, initiating colonisation (Section 1.3.2.). The bacteria secretes several virulence factors before and after attachment, including CagA, VacA, and other cytotoxins. The effects of each virulence factor differ between strains and from one patient to another (Section 1.3.). Bacterial colonisation stimulates the expression of cytokines and chemokines by host cells that trigger the host immune system. Together, virulence factors from the bacteria and the host immune response cause cellular damage and might lead to histopathological abnormalities, initiating precancerous indications (Section 1.2.). Therefore, patients start suffering from gastritis and this might progress to ulceration and other stomach diseases if not treated.

1.4.2. Biofilm Formation

Bacterial biofilm is an aggregation of bacteria on a surface attached by self-extracellular matrix. *H. pylori* proliferates and undergoes biofilm formation to protect itself from the host immune response and undesirable harsh environment. The

bacterial biofilm contains an extracellular polymeric matrix that inhibits antibiotics penetration, facilitating bacterial resistance to antibiotics (Mah and O'Toole 2001; Donlan and Costerton 2002). *H. pylori* can form biofilm *in vitro*, as well as *in vivo*. A range of *H. pylori* clinical isolates from patients with and without disease were able to form biofilms *in vitro* to varying extents (AlSharaf and Winter, unpublished data; Cammarota *et al.* 2012). *H. pylori* biofilm was also observed in gastric biopsies of infected patients, using scanning electronic microscopy (Garcia *et al.* 2014). Moreover, both the spiral and coccoid shapes of *H. pylori* were able to form biofilms (Cammarota *et al.* 2012; Grande *et al.* 2012). Another study also reported that *H. pylori* biofilms could consist of different *H. pylori* strains (Yonezawa *et al.* 2013). The significance of this is that the biofilm complexity and diversity might promote *H. pylori* persistence and eradication failure, increasing the severity of the disease.

1.4.3. Production of Outer Membrane Vesicles (OMV)

Similar to other Gram-negative bacteria, *H. pylori* can package and deliver virulence factors and other bacterial products in the form of outer membrane vesicles. The production of OMV is also considered one of the persistence strategies. OMV were reported for their ability to bind to and invade the gastric and intestinal epithelial cells (Keenan 2000). Some studies claimed that OMV could also fuse with the membrane of target cells (Kuehn and Kesty 2005; Ellis and Kuehn 2010). Other studies showed disruption of lipids on the cell membrane influenced OMV uptake into cells. Also, they might be taken up into gastric epithelial cells either via phagocytosis or due to the presence and allocation of the cellular membrane lipids (O'Donoghue and Karchler 2016). Moreover, OMV were observed within bacterial biofilms (Keenan 2000; Yonezawa *et al.* 2009). It seems that OMV might promote disease progression, as well as bacterial survival and pathogenesis.

1.5. Outer Membrane Vesicles

Outer membrane vesicles are small, spherical bleb-like structures that vary in size, between 20 to 300 nm (Perez-Cruz *et al.* 2013). Some studies reported OMV size up to 400 nm or 500 nm (Zavan *et al.* 2018; Turner *et al.* 2015). OMV are normally liberated from the outer membrane of Gram-negative bacteria (Kuehn 2005) (Figure

1.6). The distribution of outer membrane lipids, proteins, and lipopolysaccharides (LPS) can affect the biogenesis of OMV. The significance of this is that any disruption of their allocation might result in increasing or decreasing the amount of OMV produced. A mutation in the *tolA* gene of *E. coli* Tol-Pal complex (responsible for outer membrane maintenance) increased the production of OMV (Bernadac *et al.* 1998). Another study found that *tolB* mutation in *H. pylori* increased OMV production (Turner *et al.* 2015). It is worth mentioning that Gram-positive bacteria, as well as eukaryotic cells, also produce vesicles, known as membrane vesicles and exosomes, respectively (Deatherage and Cookson 2012; Schwechheimer and Kuehn 2015).

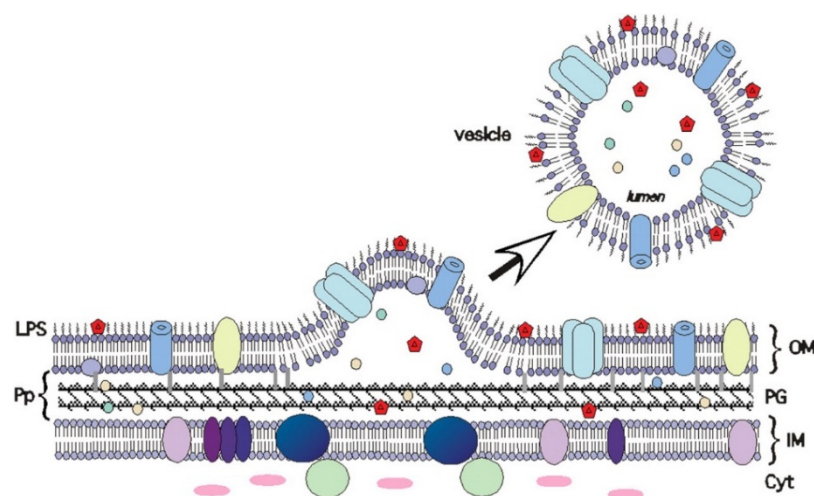


Figure 1.6: Model of outer membrane vesicle biogenesis (Kuehn 2005).

In the early 1960s, the formation of OMV was visualised first in *Vibrio cholera* under normal growth condition, using electron microscopy (Chatterjee and Das 1966; Knox *et al.* 1966). The production of OMV was then considered as a novel secretion process (Chatterjee and Das 1966). The production of OMV was then observed in many other bacterial species as research progressed, such as *Escherichia coli*, *Salmonella enterica*, and *Neisseria meningitidis* (DeVoe and Gilchrist 1973; Rothfield and Pearlman-Kothencz 1969). Moreover, a variation in OMV formation process was observed between different growth phases, as no formation was observed in the stationary and cell lysis phases of *V. cholera* and *N. meningitidis* (Chatterjee and Das 1967; DeVoe and Gilchrist 1973; Rothfield and Pearlman-Kothencz 1969). In the early 1970s, OMV were observed in the spinal fluid of patients suffering from meningococcal disease (Avakian *et al.* 1972; DeVoe and Gilchrist 1975). Researchers also found that OMV formation increases in stressful environments such as inhibition

of bacterial proteins and exposure to antibiotic treatment or bacteriophage (Rothfield and Pearlman-Kothencz 1969; Leive *et al.* 1968; Loeb 1974). Thus, researchers suggested that OMV are produced for pathogenic purposes or in response to a stressor.

Since OMV are originated from the bacterial membrane, they are composed of some bacterial membrane components (Perez-Cruz *et al.* 2013; Kuehn 2005; Chatterjee and Chaudhuri 2012). These include outer membrane proteins (OMPs), LPS, lipoproteins, periplasmic proteins, peptidoglycan, and porins. Moreover, OMV contain some bacterial virulence factors, antigens and other proteins and lipids (Perez-Cruz *et al.* 2013; Kuehn 2005; Chatterjee and Chaudhuri 2012; Parker and Keenan 2012; Winter *et al.* 2014). Recent studies reported that some OMV could also pack nucleic acids (DNA and RNA) and other cytoplasmic components from the parent bacterium (Perez-Cruz *et al.* 2015; Bitto *et al.* 2017; Sjostrom *et al.* 2015). Some OMV might contain some of the bacterial inner membrane structure as they are bounded with a double membrane similar to their parent bacterium (Perez-Cruz *et al.* 2013). This type of OMV is hypothesised to be generated from the bacterial inner and outer membranes; therefore, they are called inner-outer membrane vesicles (I-OMV) (Perez-Cruz *et al.* 2013). The packaging of these components is hypothesised to be a selective process as bacteria might purposely select and pack their cargo.

A study on OMV isolated from *Porphyromonas gingivalis* showed that OMV contain numerous virulence factors compared to the bacterial outer membrane proteins, which were much less (Haurat *et al.* 2011). Although it is generally accepted that different factors affect the production of OMV such as bacterial growth phase, the process of determination of bacterial cargo in the OMV is still controversial. The mechanisms of OMV synthesis and cargo packing are not fully understood yet, and further studies and investigations are needed.

1.5.1. Roles of outer membrane vesicles

OMV appear to have essential roles in bacterial communications and pathogenesis. They enable bacterial cell-cell interactions (quorum sensing) and bacterial-host

interactions (Kuehn 2005; Chatterjee and Chaudhuri 2012; Kuehn 2005). They also help in protecting their parent bacteria. For instance, OMV isolated from *Pseudomonas aeruginosa* can kill competing bacteria and lyse any neighbouring bacteria within the environment, promoting the survival of their parent bacteria (MacDonald and Beveridge 2002; Kadurugamuka and Beveridge 1996). OMV can also enhance the growth of parent bacteria in the presence of a stressor (Kulp and Kuehn 2010; Murray *et al.* 2020). Bacterial OMV also have a role in inducing the immune response due to their cellular interactions with the host (Kuehn 2005; Winter *et al.* 2014). For instance, the interactions of *Pseudomonas aeruginosa* and *H. pylori* OMV with host epithelial cells can alter IL-8 expression, causing inflammation (Bauman and Kuehn 2006; Ismail *et al.* 2003).

OMV can also cross the gastric epithelial barrier and induce the immune response, stimulating the secretion of cytokines and chemokines of host cells (Allison *et al.* 2009; Kaparakis *et al.* 2010). On the other hand, recent research showed that commensal bacteria could also produce OMV that could contribute to a protective response against infectious pathogens if engineered to form the basis of vaccines. These OMV could travel between and interact with host cells, initiating immune responses (Carvalho *et al.* 2019). Thus, OMV produced by engineered commensal bacteria can promote pathogen eradication by inducing an early inflammatory response. OMV from natural commensal bacteria (non-engineered) tend to play an immunoregulatory role (Gul *et al.* 2021; Hiippala *et al.* 2020).

Bacterial OMV can also assist in the formation of biofilm. A study on *H. pylori* TK1402 strain showed that OMV could enhance *H. pylori* biofilm formation (Yonezawa *et al.* 2009). Other studies on *Porphyromonas gingivalis* also showed that biofilm formation was enhanced in the presence of OMV (Unal *et al.* 2010; Ellis and Kuehn 2010). Furthermore, these studies showed that OMV could aid in bacteria aggregation and colonisation, causing oral diseases (Mayrand and Ginier 1989; Ellis and Kuehn 2010). It seems that OMV can promote bacterial persistence within the host, causing severe diseases.

1.5.2. Outer Membrane Vesicles in *H. pylori*

H. pylori OMV are like other bacterial OMV as they bleb and release from the bacterial surface, containing some of the outer membrane and bacterial structures. Several proteomics studies have been conducted to identify the content of *H. pylori* OMV. These studies revealed that *H. pylori* OMV contain a variety of proteins (including virulence factors), and more than 500 proteins were identified to date. Some of these proteins are associated with bacterial motility and toxicity like flagellar proteins, VacA, and CagA (Mullaney *et al.* 2009; Zavan *et al.* 2018; Turner *et al.* 2018; Olofsson *et al.* 2010; Turner *et al.* 2015; Lui *et al.* 2019; Winter *et al.* 2014; Ayala *et al.* 2006). Although some studies reported the presence of CagA toxin within *H. pylori* OMV, other proteomic studies did not detect any CagA within OMV isolated from *cagA*-positive strains (Parker and Keenan 2012; Keenan 2000).

Several adhesins were also identified within *H. pylori* OMV, including SabA, BabA, Alp, lipoprotein 21, *H. pylori* adhesin A, and outer membrane proteins (HopZ and HopB) (Mullaney *et al.* 2009; Zavan *et al.* 2018; Turner *et al.* 2018; Olofsson *et al.* 2010; Turner *et al.* 2015; Lui *et al.* 2019). Moreover, proteins that are responsible for host immunity alteration were identified, including LPS-Lewis antigens, Neutrophil-activating protein (NAP), and outer inflammatory protein (Oip) (Mullaney *et al.* 2009; Zavan *et al.* 2018; Turner *et al.* 2018; Olofsson *et al.* 2010; Turner *et al.* 2015). *H. pylori* OMV also contain proteins that are implicated in secretion systems, such as Cag PAI type IV secretion system proteins, in addition to acid resistance proteins like urease (Mullaney *et al.* 2009; Zavan *et al.* 2018; Olofsson *et al.* 2010; Turner *et al.* 2015; Lui *et al.* 2019; Kaparakis *et al.* 2010; Choi *et al.* 2017). Furthermore, differences in protein content of *H. pylori* OMV between strains have been reported, as well as changes in protein content between different growth conditions and phases (Parker and Keenan 2012; Zavan *et al.* 2018).

OMV of *H. pylori* not only contain proteins but also contain a broad set of LPS and peptidoglycan, which also varied between different growth conditions (Keenan *et al.* 2008). Additionally, recent studies showed that DNA and microRNA are enclosed within *H. pylori* OMV (Koeppen *et al.* 2016; Zhang *et al.* 2020; Polakovicova *et al.*

2018). It has been suggested that microRNAs contribute to human IL-8 induction, which subsequently induces an inflammatory response (Zhang *et al.* 2020).

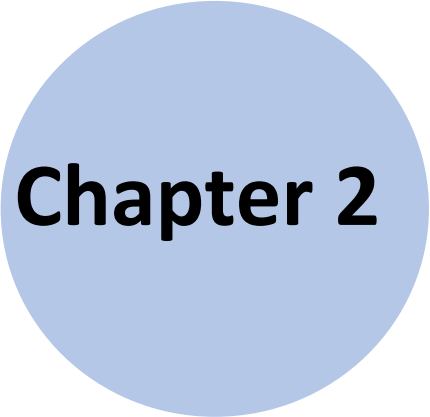
H. pylori OMV have potential roles in bacterial survival and pathogenesis. As mentioned in Section 1.4.2., *H. pylori* OMV were observed within biofilms and were reported to enhance biofilm formation of TK1402 strain (Yonezawa *et al.* 2009; Yonezawa *et al.* 2011). Moreover, proteomic studies on *H. pylori* OMV isolated from biofilms showed that OMV contain some essential factors that are required for forming a biofilm, such as adherence-associated protein (Alp), which is also known as outer membrane protein 20 (Yonezawa *et al.* 2016). Thus, OMV seem to enhance biofilm development, promoting *H. pylori* survival and persistence in the stomach. *H. pylori* OMV have also been observed in the antral biopsies of infected patients (Keenan 2000). Besides, most *H. pylori* cells remain in the mucus layer, closely associated with the epithelial cells, but do not invade the gastric mucosa. Their OMV, however, are readily taken up and across the epithelial barrier (Parker and Keenan 2012; Ayala *et al.* 2006). Consequently, *H. pylori* virulence factors and other toxins will be delivered to the epithelial cells and beyond, by OMV. Although several potential roles of *H. pylori* OMV have been identified, the exact role of these OMV in the pathogenesis of stomach disease is not yet fully understood and further investigation is needed.

1.6. AIM OF THIS THESIS

Helicobacter pylori infection is a significant cause of disease worldwide. *H. pylori* has different mechanisms that contribute to causing gastric diseases that might last for a lifetime. Numerous studies have been conducted to identify and understand these mechanisms and their role in pathogenesis. However, the production of OMV and its role in causing disease is still not fully understood. Therefore, this thesis aimed to:

- characterise the OMV of *H. pylori* clinical strains with high and low virulence under different growth conditions.
- determine whether the virulence of *H. pylori* strains and the bacterial growth conditions affect the production and characteristics of OMV.

- characterise the cytotoxicity of these OMV on mammalian cells, to determine whether *H. pylori* virulence and bacterial growth conditions influence the toxicity of *H. pylori* OMV.
- identify the protein contents and measure the cytotoxicity of OMV isolated from a virulent *H. pylori* strain that was grown in different growth conditions.
- mutate a critical virulence factor in *H. pylori* OMV and measure the cytotoxicity of OMV produced by wild type and mutant *H. pylori* strains, to improve understanding of the roles of *H. pylori* OMV in pathogenesis.



Chapter 2

MATERIALS AND METHODS

2. MATERIALS AND METHODS

2.1. *Helicobacter pylori* Strains

Six clinical strains of *H. pylori*, including 444A, 221A, 606C, 109A, 223C, 121A, and two lab strains (60190 and Tx30a), were used in this study (Table 1). All clinical strains were provided by Prof John Atherton and his team at The University of Nottingham. These strains were isolated from corporal and antral biopsies of patients attending routine endoscopy at the Queen's Medical Centre, Nottingham, United Kingdom. These patients each had different degrees of inflammation and precancerous changes in their stomach and duodenum, as determined by Sydney scoring (Dixon *et al.* 1996; Hassan *et al.* 2016). Some patients did, and others did not have ulcer disease at the time of sampling. Ethical approval for the use of *H. pylori* clinical isolates was granted by the NHS National Research Ethics Service, Nottingham Research Ethics Committee (Ref: 08/H0408/195) 27th January 2009. All patients gave their informed consent prior to participating in this study to the collection and storage of the stomach biopsies and isolation of *H. pylori* for further study for research purposes.

In this study, each of the *H. pylori* strains was classified according to its virulence level as a "high" or "low" virulence strain. This classification was based on the presence of the *cagA* gene and *vacA* genotype. For example, as shown in Table 1 below, strain 444A is a high virulence strain as it has *vacA* s1 i1 m1 genotype and is positive for the *cagA* gene. Strain 221A is a low virulence strain as it has *vacA* s1 i2 m2 and is negative for the *cagA* gene. Strain with *vacA* s1 i1 m1 and negative *cagA* would consider as an intermediate virulence. However, this strain is not included in this study.

Table 2.1: *H. pylori* strains used in the study.

<i>H. pylori</i> Strain	Type of Strain	Virulent Type				Sydney Score				Disease Association
		<i>vacA</i> s Type	<i>vacA</i> i Type	<i>vacA</i> m Type	<i>cagA</i>	Inflammation	Activity	Atrophy	Intestinal Metaplasia	
221A	Clinical	s1	i2	m2	-	1	0	1	0	None
109A	Clinical	s2	i2	m2	-	2	2	0	0	None
223C*	Clinical	s2	i2	m2	-	n/a	n/a	n/a	n/a	None
444A	Clinical	s1	i1	m1	+	2	2	1	2	GUD
121A	Clinical	s1	i1	m1	+	3	2	1	0	DUD
606C	Clinical	s1	i1	m1	+	2	2	0	0	GUD
60190	Lab	s1	i1	m1	+	n/a	n/a	n/a	n/a	n/a
Tx30a	Lab	s2	i2	m2	-	n/a	n/a	n/a	n/a	n/a

s1 = more toxic allele; s2 = less toxic allele; i1 = more toxic allele; i2 = less toxic allele; m1 = more toxic allele; m2 = less toxic allele; 0 = absent; 1 = low; 2 = intermediate; 3 = high; GUD = gastric ulceration disease;

DUD = duodenal ulceration disease; A = antral; C = corpus; light blue shade = high virulence strains; dark blue shade = low virulence strains

*Patient refused to complete the procedure

2.2. Bacterial Storage

All *H. pylori* strains used in this study were grown on blood agar plates for 24-48 hours and inoculated in 5 ml sterile isosensitest broth (Oxoid) with 10% glycerol (Sigma-Aldrich; Merck). Each 0.5 ml of the suspension were aliquoted into a cryovial and stored at -80 °C for long term storage.

E. coli carrying pBlueKm plasmid was inoculated into 5 ml LB broth supplemented with 10 µg/ml kanamycin and incubated at 37 °C overnight. After overnight incubation, 500 µl of the culture was added to 500 µl of 50% sterile glycerol (Sigma-Aldrich; Merck) in 1ml sterile tube and placed at -80 °C for long term storage.

2.3. Growing *Helicobacter pylori* Strains

All *H. pylori* strains used in this study were grown in different *in vitro* environments, including solid and liquid growth medium.

2.3.1. *H. pylori* growth on solid agar medium

All *H. pylori* strains were grown from frozen stocks onto blood agar base no. 2 (Oxoid) containing 7.5% (v/v) of defibrinated horse blood (TCS Biosciences). Cultures plated were incubated in microaerophilic (85% N₂, 10% CO₂, and 5% O₂) condition for 24 to 72 hours at 37 °C with high humidity. All strains were then passaged onto fresh blood agar plates and incubated for 48 hours in the microaerobic cabinet (85% N₂, 10% CO₂, 5% O₂) at 37 °C with 80% humidity. The passaging process was continued three times a week. Aseptic techniques and a Bunsen burner were used to avoid contamination during all experiments and processes.

2.3.2. *H. pylori* growth in liquid broth medium

Each *H. pylori* strain was passaged onto a fresh blood agar plate and incubated for 20 to 24 hours in the microaerobic cabinet at 37 °C. The bacterial growth from the edge of the plate was then inoculated into 5 to 10 ml of brain heart infusion (BHI) broth (Oxoid) supplemented with 0.2% of β-cyclodextrin (Sigma-Aldrich; Merck) to high density. Then diluted into 100 to 200 ml of supplemented BHI broth in a vented cap

tissue culture flask to 0.1 optical density (OD) at 600 nm and incubated in the microaerobic cabinet with shaking at 100 rpm for 1 day (early broth) and 6 days (late broth) at 37 °C. Broths were incubated for different lengths of time to determine the effect of incubation time (bacterial growth phase) on OMV characterisation. The purity of *H. pylori* cultures was confirmed by Gram's staining and microscopy.

2.3.3. Gram's staining

A smear was prepared on a microscopy slide from the bacterial pellet and let to dry. It was then fixed by flame. Crystal violet was applied for 2 minutes and washed with distilled water. Iodine was then applied for 2 minutes and washed with distilled water. The smear was then decolourised with alcohol for 10 seconds and washed. Finally, safranin (counterstain) was applied for 10 seconds and washed. The slide was allowed to air dry before the examination.

2.4. Quantification of OMV for Virulent and Less Virulent *H. pylori* Strains

2.4.1. Miles and Misra method for viable bacterial count

Miles and Misra method (Miles, Misra and Irwin 1938) was used to measure the viable bacterial count of all strains grown on the plate and in early broth cultures. All grown bacteria on blood agar (full plate) of each strain was suspended in 20 ml Dulbecco's phosphate buffer saline (D-PBS) (Sigma-Aldrich; Merck). The D-PBS (catalogue number is D8537) is particle and endotoxin free that specifically used in the study. Each sample was then serially diluted to 10^{-9} in D-PBS in a sterile 96-well plate. Samples from broth cultures were also serially diluted to 10^{-9} in D-PBS in a sterile 96-well plate. A fresh blood agar plate was used for plating out the dilution series of each sample. All plates were divided into 10 equal sectors and labelled with the dilutions from neat to 10^{-9} . Triplicate 10 µl drops of each dilution were pipetted onto the blood agar plate, which was left upright for a few minutes allowing drops to be absorbed, and then inverted and incubated at 37 °C in the microaerobic cabinet for 24 to 48 hours. After that, the sector with 3-30 colonies was used to count the colonies and calculate the colony-forming units per ml (CFU/ml) of the original sample.

2.4.2. BacTiter-Glo Assay

BacTiter-Glo assay was used to measure the viable bacterial count of all strains grown in late broth cultures only. BacTiter-Glo reagent (Promega) was prepared following the manufacturer's instructions and left for 15 minutes to equilibrate. After incubation, 40 μ l of each late broth culture were transferred separately into an opaque (white) 96-well plate. Then 40 μ l of the BacTiter-Glo reagent was added to each well. The opaque 96-well plate was then placed on a flat shaker for 5 minutes of gentle shaking. After that, the plate was read by a luminometer. The Promega BacTiter-Glo reagent lyses the non-killed bacteria, releasing ATP. This ATP is then measured by the luminometer. As the luminescent signal is proportional to the ATP, the higher luminescent signal indicates high bacterial survival. These results were compared to the control (broth with no bacteria) and expressed in units of luminescence.

2.4.3. OMV isolation and purification

Broth cultures and bacterial suspensions from plate cultures were transferred to sterile 50 ml falcon tubes and centrifuged at 4,000 xg for 10 minutes at 4 °C to pellet down and remove the bacteria. Supernatants were then transferred to fresh 50 ml sterile falcon tubes and centrifuged again to ensure that any remaining bacteria were removed. Samples from the bacterial pellets were Gram-stained and examined under the microscope to confirm the purity of *H. pylori*.

Ammonium sulfate precipitation (40%) concentration of OMV was performed on supernatants from broth cultures only to precipitate all proteins, including OMV. 24 g of ammonium sulfate (Fisher Scientific) was added per 100 ml of the supernatant of each strain in a fresh flask and left on a shaker to rock gently for 30 to 60 minutes at room temperature. After precipitation, the suspensions were transferred to Nalgene centrifuge tubes (Thermo Scientific) and centrifuged at 10,000 xg for 15 minutes at 4 °C, using Heraeus Megafuge 16R centrifuge (Thermo Scientific) (F15-6x100y Bio-Seal rotor). Supernatants were discarded, and pellets (containing precipitated OMV) were suspended completely in 20 ml D-PBS. The OMV-containing

fractions from broth and plate cultures were then filtered twice using 0.45 µm and 0.20 µm syringe filters and stored in the fridge overnight.

All OMV-containing fractions were then transferred into 26.3 ml polycarbonate centrifuge bottles (Beckman Coulter) for ultracentrifugation at 100,000 xg for 2 hours at 4 °C, using an Optima L-100XP ultracentrifuge (Type 70. Ti rotor) (Beckman Coulter) to purify OMV and wash away the ammonium sulfate salt and any contaminating substances from the blood agar plates. Pellets from ultracentrifugation were resuspended in 20 ml of D-PBS and ultracentrifuged again to wash away any remaining ammonium sulfate and other contaminants. After the second wash, pellets were resuspended in 500 µl of D-PBS and stored at -20 °C until use.

2.4.4. OMV quantification

Two different methods were used to quantify the OMV generated by *H. pylori* strains. The first method was the BCA- protein assay used to quantify OMV based on their protein concentration. The second method, nanoparticle tracking analysis, Zetaview, was used to quantify OMV based on particle number and measure and compare their size.

2.4.4.1. Pierce BCA- protein assay

A Pierce BCA- protein assay kit (Thermo Scientific) was used for this assay, following the manufacturer's instructions. The working reagent was prepared at a ratio of 1:50. Twenty-five microliters of all OMV samples were pipetted in triplicate into a 96-well plate. Then 200 µl of the working reagent were added to each well and mixed (sample to working reagent ratio = 1:8). The plate was then placed on a shaker to mix. After 30 seconds, the plate was covered and incubated for 30 minutes at 37 °C. A plate reader was then used to measure the absorbance at 562 nm. The working reagent colour changes from green to purple based on protein in each sample and its concentration. The higher absorbance indicates high protein concentration. Serially diluted albumin with known concentrations was used to construct a standard curve. D-PBS, with no OMV or protein, was used as a negative control. The absorbance of each sample was converted to µg per ml by interpolation from the standard curve. In

this assay, the OMV number was represented by the amount of proteins within OMVs (μg per ml).

2.4.4.2. Nanoparticle tracking analysis

Nanoparticle tracking analysis (NTA) was performed using Zetaview PMX 110 instrument (Particle Metrix GmbH). The Zetaview scans biological nanoparticles, including exosomes, extracellular vesicles, or viruses. It measures particle size, count, and concentration at 11 different positions within less than 90 seconds. All measurements are based on capturing the Brownian motion of each particle (Particle Metrix 2020).

The Zetaview was calibrated with polymer microspheres (PS100) nanoparticles (Applied Microspheres BV) of known concentration and diameter (100 nm diameter; 1:266000 dilution in Milli-Q water; particle-free water), and all the parameters were set for the analysis using the Zetaview software. All OMV samples were diluted to 1:10,000 dilution using particle-free D-PBS. About 1 ml of each sample was loaded and analysed in two cycles of 11 chambers per cycle, and a flow cell sensitivity of 80% and D-PBS was used as blank. The Zetaview was washed after each sample by flushing the chamber with 2 to 5 ml of D-PBS. At the end of the analysis, 70% of ethanol and Milli-Q water were used to disinfect and clean the instrument.

2.5. Effects of OMV on Mammalian Cells

2.5.1. Cell culture and media

Human gastric epithelial (AGS) cells (ATCC CRL-1739) were used in this study. Cells were purchased directly from ATCC, especially for this study, and were minimally passaged before used. Cells were maintained in Kaighn's Modification of Ham's F-12 (F-12K) medium (ATCC) supplemented with 10% heat-inactivated foetal calf serum (HI-FCS) (Sigma-Aldrich; Merck) in T25 (8 ml) tissue culture flasks horizontally as monolayers and incubated in 5% CO₂ humidified atmosphere at 37 °C until they reached the confluence of 60 to 80%. Cells were regularly passage once they reached the confluence of 75%. The media was discarded and replaced with fresh media three times a week. All experiments and processes were conducted in the Laminar flow cabinet using aseptic techniques to avoid contamination. Ultraviolet (UV) light and

70% Industrial methylated spirit (Fisher Scientific) were used in the cabinet to maintain sterility.

2.5.2. Cytotoxicity

The cytotoxic effects of OMV on mammalian cells were determined using two different methods. The first was the CellTiter 96 assay, which was used to measure the toxicity of OMV on gastric epithelial cells after 24 hours (endpoint assay). The second was the RealTime-Glo MT cell viability assay used to determine the toxicity effect of OMV on gastric epithelial cells at regular time points over 24 hours (Kinetic assay).

2.5.2.1. CellTiter 96 assay

An AGS cell suspension was prepared to a concentration of 1×10^5 cells per ml in the usual cell culture media (see section 2.4.1). The media was discarded and cells were washed with 5 ml of D-PBS first, then cells were trypsinised to detach from the bottom of the flask, using 2 ml of trypsin- EDTA (Sigma-Aldrich; Merck). Cells were then washed twice by adding F-12K media supplemented with 10% HI-FCS up to 10 ml and centrifuged at 500 rpm for 3 minutes. The supernatant was discarded, and the pellet was resuspended in 5 ml of fresh culture media. 10 μ l of the suspension was mixed with 10 μ l of trypan blue stain (Sigma-Aldrich; Merck) to check for cells viability. Blue stained cells indicate dead cells, and white cells indicate viable cells. Cells were counted using a haemocytometer. Cells were only included in experiments if their viability was more than 95%. The 1:2 dilution of cells with trypan blue was corrected by multiplying cells count by 2. The number of cells was then multiplied by 10^4 to find the number of cells per ml, and the concentration was adjusted to 1×10^5 cells/ml.

After that, 100 μ l of this cell suspension was added to each well of a 96-well flat-bottom tissue culture treated plate (Greiner bio-one CELLSTAR) in triplicate and incubated in 5% CO₂ humidified condition at 37 °C overnight to allow the cells to adhere. Cells were then treated with a range of OMV with protein concentrations from 0-50 μ g/ml (adjusted using Pierce BCA-protein assay) to study the dose-dependent effect and incubated in a 5% CO₂ humidified atmosphere at 37 °C for 24

hours in the presence of the OMV. Untreated cells and media with and without OMV were used as controls. To determine the IL-8 induction, after incubation, 50 µl of media from each triplicate was transferred into an Eppendorf tube and centrifuged at 13,000 for a minute using a microfuge to remove the cells. Supernatants were stored at -80 °C until use. However, this assay failed twice and due to shortage of time and other circumstances it was excluded from the study. Cell viability was determined by adding 10 µl of CellTiter 96 reagent (Promega) to the cells in the 96-well plate. The plate was wrapped in foil and incubated at 37 °C for 1 hour. The absorbance of each well was then measured at 490 nm using a plate reader. The higher absorbance indicates a high viable cell count. These results were compared to untreated controls and expressed as percentage (%) survival.

2.5.2.2. RealTime-Glo MT cell viability assay

An AGS cell suspension was prepared to a concentration of 1×10^5 cells per ml in the usual cell culture media. A 100 µl of cell suspension was added to each well of a 96-well opaque-walled assay plate (Greiner bio-one CELLSTAR) in triplicate and incubated in 5% CO₂ humidified condition at 37 °C overnight. RealTime-Glo MT reagents (Promega), MT cell viability substrate and NanoLuc enzyme, and *H. pylori* OMV samples were equilibrated to 37 °C. The MT cell viability substrate and NanoLuc enzyme were then added to 50 µg/ml of OMV of each *H. pylori* strain to a concentration of 2X each reagent and mixed well by vortex mixer. An equal volume of the mixture (100 µl) was added to the cells. Final concentrations were 25 µg/ml of OMV, 1X of MT substrate, and 1X of NanoLuc enzyme. The plate was then placed into an incubator in 5% CO₂ humidified condition at 37 °C. Luminescence was measured every 1 hour for 24 hours using a plate reader. The MT cell viability substrate enters the cell, and a viable active cell reduces the substrate. Reduced substrate exits the cell and binds to the NanoLuc enzyme-producing luminescence. The luminescence is measured by the luminometer. As the luminescent signal is proportional to cell viability, the higher luminescent signal indicates high cell viability. These results were compared to the control (untreated cells) and expressed as a luminescent unit.

2.5.3. Live Cell Analysis (IncuCyte)

The interaction between *H. pylori* OMV and human gastric epithelial cells over 24 hours was determined and visualised on an hourly basis using the live-cell analysis, IncuCyte S3 system (Sartorius). An AGS cells suspension was prepared to a concentration of 1×10^5 cells per ml. 100 μ l of cell suspension was added to each well of a 96-well flat-bottom tissue culture treated plate (Greiner bio-one CELLSTAR) in triplicate and incubated under 5% CO₂ condition at 37°C for overnight. Media was discarded and cells were then treated in triplicate with 50 μ g/ml of OMV of four *H. pylori* strains isolated from the early broth, late broth, and plate cultures, final volume 100 μ l. The tissue culture plate was then incubated in the IncuCyte under 5% CO₂ condition at 37 °C for 24 hours. Four images per well were captured every hour, from 0 to 24 hours. In total, 12 images per hour were taken for each analysis condition. Cell viability was also quantified based on two measures. The first was phase confluence, which is a label-free measure of the percentage of viable cells over time based on the area of each well covered by cells (% confluence). The second measure is the red area, which quantifies cell death in real time using IncuCyte Cytotox Red Reagent (Sartorius) (0.2 μ l per 300 μ l) to detect cell death. Untreated cells were used as controls.

2.6. Proteomic Analysis

2.6.1. Sodium dodecyl sulphate - Polyacrylamide gel electrophoresis (SDS-PAGE)

SDS-PAGE was conducted to compare the protein profiles between isolated OMV of each *H. pylori* strain and compare isolated OMV from the different growth conditions. A 12% Tris-Glycine SDS-PAGE resolving gel was prepared by mixing 2.4 ml of 30% acrylamide (Sigma-Aldrich; Merck), 1.5 ml resolving buffer (1.5 M Tris-HCl, pH 8.8), and 2.1 ml of distilled water with 30 μ l of 20% sodium dodecyl sulphate (SDS) (Sigma-Aldrich; Merck), 120 μ l of Ammonium persulfate (APS) (Sigma-Aldrich; Merck), and 6 μ l of Tetramethylethylenediamine (TEMED) (Sigma-Aldrich; Merck). The resolving gel was poured into the gel casting apparatus to $\frac{3}{4}$ full. Around 100 μ l of distilled water was added onto the gel surface by gentle pipetting, and the gel was left to sit for 30 minutes. The stacking gel was prepared by mixing 3 ml of a stacking gel mixture (510 μ l 30% acrylamide, 750 μ l stacking buffer (0.5 M Tris-HCl, pH 6.8), and 1.74 ml distilled

water) with 15 μ l of 20% SDS, 60 μ l of APS, and 3 μ l of TEMED. The distilled water in the gel casting apparatus was discarded, and the stacking gel was poured onto the resolving gel until the casting apparatus was full. The plastic comb was then placed into the stacking gel, and it was left to sit for another 30 minutes.

All OMV samples were adjusted to a concentration of 100 μ g/ml as determined by Pierce BCA- protein assay. Samples were then diluted with distilled water to 1:10 dilution to reduce the D-PBS salt concentration. StrataClean resin (Agilent Technologies) was mixed very well. Then, 5 μ l resin suspension was added to each sample and vortexed to concentrate all of the proteins within each sample by binding proteins to the resin. All samples were then centrifuged at 13,000 rpm for 1 minute to pellet the resin + proteins. Supernatants were discarded, and pellets were resuspended in 15 μ l distilled water and 5 μ l 4x reduced sample buffer (RSB) and mixed well. The 4x RSB was prepared by mixing 2 ml of 0.5nM Tris (Fisher Scientific) (pH 6.8), 4 ml of 80% glycerol (Sigma-Aldrich; Merck), and 4 ml of 20% SDS with 0.31g of DL-Dithiothreitol (DTT) (Sigma-Aldrich; Merck) and a minimal quantity of bromophenol blue. Samples were then heated at 99 $^{\circ}$ C for 2 to 3 minutes. All samples were centrifuged for 3 seconds after heating and cooling to bring the condensed water back to the bottom of the tube. Fifteen microliters of each sample were mixed and loaded into the gel. A mixture of 5 μ l resin, 10 μ l distilled water, and 5 μ l 4xRSB was used as a negative control. PageRuler pre-stained protein ladder 10 to 250 kDa (Thermo Scientific) was used for protein standards. The gel casting apparatus was placed into a gel tank filled with 1X SDS running buffer and covered with a lid. The 1X SDS running buffer was prepared by diluting 5X SDS running buffer (15 g Trisma base (Fisher Scientific), 72 g Glycine (Fisher Scientific), 12.5 ml 20% SDS, and up to 1 litre of distilled water). The gel was run at 40 mA with a voltage of 250 V for 80 minutes to separate proteins. PageBlue protein stain (Thermo Scientific) was then used to stain the gel following the manufacturer's instructions. After staining, the gel was rocked in water at room temperature for a few days to de-stain.

2.6.2. Density gradient centrifugation

To further purify OMV for proteomics, OMV preparations were pelleted by ultracentrifugation (as in section 2.3.2 above), resuspended in 100 μ l D-PBS and

mixed with 150 μ l of 45% OptiPrep™ density medium (Sigma-Aldrich; Merck). The mixture was added to the bottom of a 1 ml ultracentrifuge tube (Beckman Coulter). Then 150 μ l of each other density fraction (40, 35, 30, 25, 20%) were carefully added from high to low. Samples were then ultracentrifuged at 292,700 xg for 6 hours at 4 °C using benchtop optima TLX ultracentrifuge (Type 120.1 rotor) (Beckman Coulter). Each 150 μ l fraction was then collected carefully from the top and diluted separately in 1 ml D-PBS. Fractions were ultracentrifuged at 120,000 xg for 90 min to wash out the density medium and recover the OMV pellet. Supernatants were discarded, and pellets were resuspended in 100 μ l D-PBS and stored at -80 °C until used.

2.6.3. OMV proteomics

Proteomic analysis was conducted to identify and compare the protein content of isolated OMV of *H. pylori* 444A strain from different conditions (6 samples per condition). Highly purified OMV were prepared for this analysis by density gradient ultracentrifugation (section 2.6.2). The concentration of *H. pylori* 444A strain OMV was adjusted to 50 μ g/ml using the Pierce BCA- protein assay. One millilitre of OMV at 50 μ g/ml was pelleted using ultracentrifugation (100,000 xg for 2 hours at 4 °C). Each OMV pellet containing 50 μ g OMV was then completely resuspended in 50 μ l of lysis buffer (8 M urea (Sigma-Aldrich; Merck), 50 mM Tris (Fisher Scientific), and 0.1% ProteaseMax (Promega)) and vortexed. Samples were reduced, digested, and analysed by David Boocock, Clare Coveney, and their team at John van Geest Cancer Research Centre, Nottingham Trent University. A 1 μ l of 0.5 M DTT was added to each sample to reduce disulfides. Samples were incubated in a shaking thermomixer at 56 °C for 20 minutes then cooled down to room temperature. 2 μ l of 0.5 M iodoacetamide was added to each sample and incubated at room temperature for 15 minutes in the dark.

Samples were then centrifuged at 13,000 xg for 8 minutes to remove undissolved matter. Around 12% of aqueous phosphoric acid were added at 1:10 concentration. Then, 185 μ l of S-Trap buffer was added to 30.8 μ l of acidified sample and then added to the S-Trap micro column and centrifuged at 4,000 xg to around 45 seconds until all the mixture has passed through the column. The protein-trapping matrix has trapped the proteins, and 150 μ l of S-Trip buffer were added to the column

to wash captured proteins three times. The column was then transferred to a clean 1.7 Eppendorf protein lo-bind sample tube. Sample digestion was carried out by adding digestion buffer (50 mM TEAB pH 7.5-8) to each 20 µg vial of trypsin and mixed. Then, 25 µl of digestive buffer with Protease were added to the column. The column was loosely capped and incubated at 45 °C for 1.5 hours. The peptides were then eluted by adding digestion buffer and 0.2% aqueous formic acid and centrifuged at 4,000 *xg*. Peptides were then dried out at 60°C for 4 hours and stored at -80°C (following a previously described method by Aldis *et al.* (2020)).

For further analysis, samples were resuspended in liquid chromatography-mass spectrometry (LC-MS) grade solvent (5% acetonitrile in 0.1% formic acid). All samples were analysed by liquid chromatography-tandem mass spectrometry (LC-MS/MS), using the SCIEX TripleTOF 6600 instrument (following a method that was previously described by Aldis *et al.* (2020)). Protein identifications, quantifications, and expression changes were analysed using information-dependent acquisition (IDA) and data-independent acquisition (SWATH-MS) modes, label-free. Raw IDA data were processed using ProteinPilot 5.0.2 and searched against *Helicobacter* filtered FASTA protein file from UniProt using Sciex OneOmics software. Data sets of identified OMV proteins were compared against each other. Reported proteins were identified with a 1% false discovery rate (FDR).

2.6.4. Cell response proteomics

Proteomic analysis was conducted to identify and compare proteins produced from gastric epithelial cells as a cellular response to *H. pylori* 444A strain OMV. AGS cell suspensions were prepared to a concentration of 3 to 5x10⁶ cells per ml in tissue culture flasks and incubated in 5% CO₂ condition at 37 °C overnight. Cells were then treated with 6 µg/ ml of OMV isolated from early and late broth cultures and incubated in 5% CO₂ incubator at 37 °C for 24 hours. Untreated AGS cells were used as control. After incubation, the media containing OMV was removed, and cells were washed with D-PBS and then trypsinised to release them from the tissue culture flasks. Cells were then transferred to 1.5 ml Eppendorf tubes and pelleted by centrifugation at 2,500 *xg* for 5 minutes; then, the supernatants were discarded. Cells were washed in cold D-PBS twice and pelleted by centrifugation at 2,500 *xg* for 5

minutes. 80 µl of Protease and phosphatase inhibitor (Sigma-Aldrich; Merck) was added to 1 ml of Radioimmunoprecipitation assay (RIPA) buffer (Thermo Scientific) and immediately added to the AGS cells pellet and gently mixed. The mixtures were placed on ice with gentle shaking for 15 minutes to lyse the cells and release the proteins. The mixtures were centrifuged at 14,000 *xg* for 15 minutes to pellet the cell debris.

The supernatants were transferred to a new tube for protein assay. Pierce BCA-protein assay was used to measure the protein concentration in each sample. 50 µg volume of each sample was transferred to a new tube for proteomics analysis. David Boocock, Clare Coveney, and their team at John van Geest Cancer Research Centre at Nottingham Trent University reduced, digested, and analyse all samples as described above (see Section 2.6.3.).

2.7. Mutagenesis of Gene of Interest

Mutagenesis was conducted to knock out the gene of interest (GOI) from *H. pylori* 444A and 60190 strains. There are different stages of mutagenesis (Figure 2.1). These include the selection of GOI, clone GOI into pJET cloning vector, inverse PCR and construction of mutation plasmid, and transformation of *H. pylori*. Each stage and its procedures will be discussed below.

2.7.1. Clone Gene of Interest into pJET cloning vector

2.7.1.1. *H. pylori* genomic DNA extraction

GenElute bacterial genomic DNA kit (Sigma-Aldrich; Merck) was used to extract *H. pylori* DNA following the manufacturer's instructions (Figure 2.1; step 1). *H. pylori* 444A and 60190 strains were grown on a blood agar plate for 24 hours. Grown bacteria were then suspended in 1.5 ml D-PBS and centrifuged at 16,000 *xg* for 2 minutes. The supernatant was discarded, and the pellet resuspended in 180 µl of lysis solution T/ buffer STL. A 20 µl of protease K solution was added to the pellet, mixed and incubated at 55 °C for 30 minutes. A 200 µl of lysis solution C was added, vigorously agitated for a few seconds and incubated for 10 minutes at 55 °C. A binding column was assembled with a 2 ml collection tube, and 500 µl of column preparation solution was added to the column to maximise DNA binding to the membrane. The

column was then centrifuged for 1 minute at 12,000 *xg*. The flow-through liquid was discarded, and the collection tube was retained. 100% ethanol was added (200 μ l) to the lysate and vortexed for a few seconds.

The homogeneous mixture was then transferred into a binding column and centrifuged at 6,500 *xg* for 1 minute. The collection tube with flow-through liquid was discarded, and the column was placed in a new collection tube. To wash extracted DNA, 500 μ l of washing solution 1 was added to the column and centrifuged at 6,500 *xg* for 1 minute. The flow-through liquid was discarded, and the collection tube was retained, and a second wash was performed, however, with a diluted washing solution with ethanol. The column was then centrifuged at 16,000 *xg* for 3 minutes to dry the column. The collection tube was emptied, and the column was recentrifuged for 1 minute at 16,000 *xg*. The collection tube was discarded, and the binding column was placed in a new collection tube. Elution solution was added (200 μ l) onto the centre of the column, incubated for 5 minutes at room temperature, and centrifuged at 6,500 *xg* for 1 minute to elute the DNA. A second elution process was performed. Pure bacterial genomic DNA was stored at -20 °C until use.

Cloning strategy overview diagram

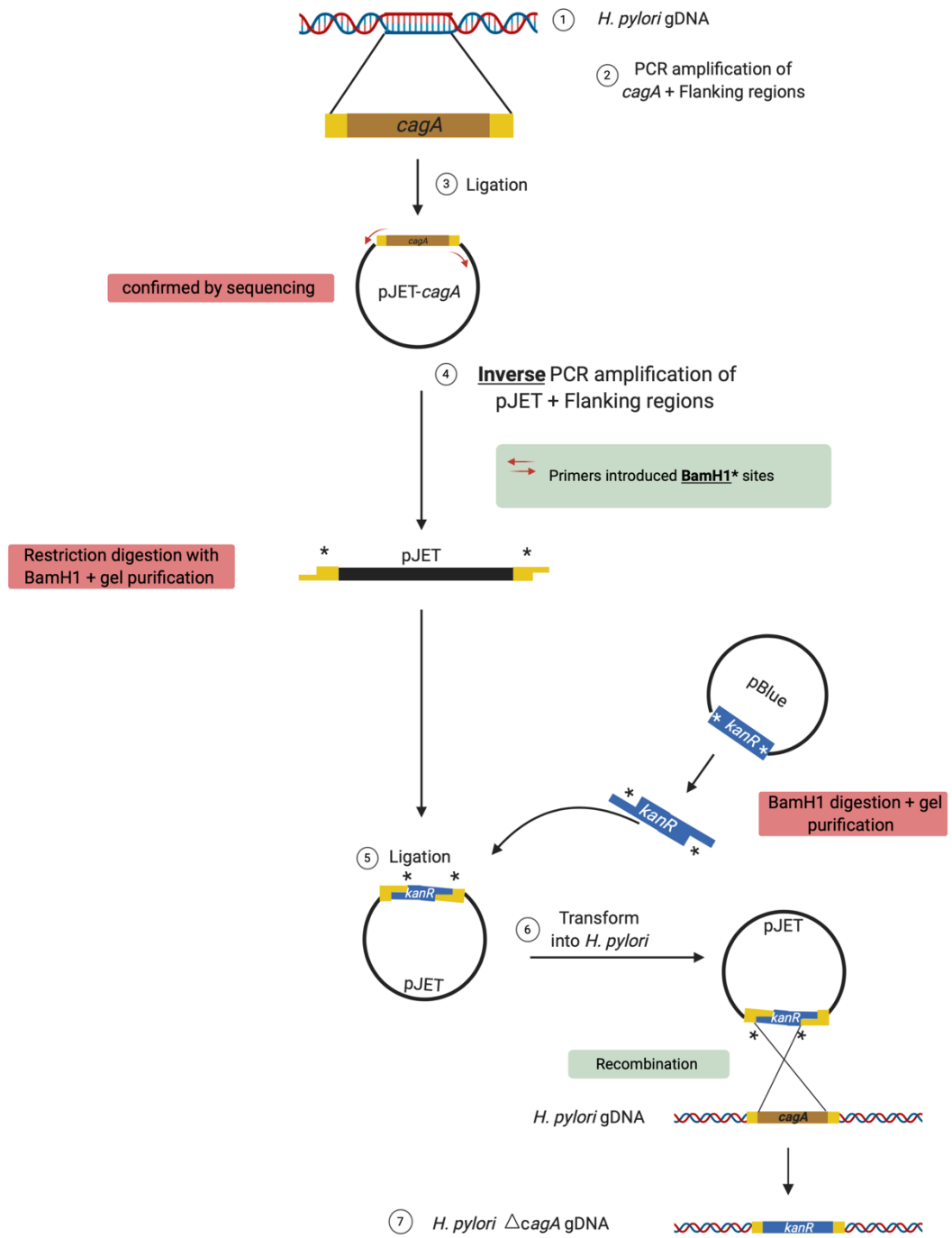


Figure 2.1: Cloning strategy overview (Created by Biorender.com).

2.7.1.2. Polymerase chain reaction (PCR)

The *cagA* plus flanking regions was amplified in this study to be used for cloning into a pJET vector (ThermoFisher 2019; URL) (Figure 2.1; step 2). A set of primers (forward and reverse) specific for the *cagA* gene was used (Table 2.2). In this study the Phusion high fidelity PCR kit (Thermo Scientific) should be used, however, the kit did not work well at this stage. Therefore, the MangoMix™ (Bioline) was used instead to amplify the *cagA* gene. The reaction was carried out in 20 µl final volume containing 2 µl (~50-100 ng) of genomic DNA as a template, 50 µM of the relevant sense and antisense primers, 10 µl of MangoMix™ (Bioline), and PCR grade water. Reaction with no template was used as a negative control. The reactions were mixed, and then the samples were subjected to an initial denaturation and enzyme activation cycle of 95 °C for 30 seconds followed by 30 cycles of denaturation at 95 °C for 10 seconds, gradient annealing temperature from 50 to 64 °C each for 30 second and extension at 72 °C for 1 minute followed by a final extension step at 72 °C for 10 minutes and hold at 4 °C, using a Master Cycler Nexus Gradient PCR machine (Eppendorf). PCR products were checked by gel electrophoresis on 1% agarose gel to determine the optimum annealing temperature. The PCR reaction was then repeated with the most appropriate annealing temperature (57.9 °C) and electrophoresed on 1% agarose gel (Table 2.2).

Table 2.2: PCR Primers and Cycling Condition of *cagA* mutation used in the study.

No.	Purpose	Primer name	Sequence	Annealing T _m	Cycle #	Extension time	Product Size
1	<i>cagA</i> amplification for cloning into pJET1.2	cagmutF	5' -CAACTCCATAGACCACTAAAG- 3'	57.9 °C	30	1 min	~2000 bp
		cagmutR	5' -GGCTACCTTGGAGAGTAAC- 3'				
2	Sequencing pJET1.2- <i>cagA</i> clones	pJET1.2f	5'- CGACTCACTATAGGGAGAGCGGC- 3'	60 °C	25	1 min	~2000 bp
		pJET1.2r	5'- AAGAACATCGATTTTCCATGGCAG- 3'				
3	Inverse PCR using pJET- <i>cagA</i> as a template	cagINV-f	5' -ACTGCGGATCCAAGCACGATTGGAAC- 3'	64.4 °C	30	1 min	~4000 bp
		cagINV-r	5' -ACTGCGGATCCGTTTCGTTAGTCATTG - 3'				

2.7.1.3. Agarose gel

One per cent agarose gel was prepared by dissolving 0.5 g agarose (Sigma-Aldrich; Merck) in 50 ml 1X TAE buffer (Sigma-Aldrich; Merck). The mixture was melted, cooled down to 55 °C, then 10 µl Sybr safe DNA gel stain (Invitrogen) was added and swirled to mix. The gel was poured into the gel casting tray, sample comb was added and allowed to set. The gel tray was placed into the gel tank and covered with 1X TAE buffer. Samples were mixed with 1/5 volume of loading dye, loaded on the gel alongside 10 µl of 1 Kb DNA ladder (Sigma-Aldrich; Merck) and electrophoresed at 100 V constant voltage for 30 to 45 minutes or until the loading dye migrated two-thirds of the distance of the gel. The DNA was then visualised with a UV light transilluminator and photographed.

2.7.1.4. Gel extraction for PCR product

GeneJET gel extraction kit (Thermo Scientific) was used to purify the PCR product (*cagA* plus flanking regions). After running the agarose gel, the gel was placed in a blue lightbox, and the gel slice that contained the desired DNA fragment was excised using a scalpel. The gel slice was added into a 1.5 ml sterile Eppendorf tube. This Eppendorf tube was weighed before and after adding the gel slice, and the gel slice weight was recorded. The binding buffer was then added following the manufacturer's instructions (1:1 volume). The tube was incubated at 55 °C until the gel was completely dissolved. The solution colour was yellow, which indicated an optimal pH for DNA binding. This solution was then transferred to the GeneJET purification column and centrifuged for 1 minute. The flow-through was discarded, and the column placed back into the collection tube. The diluted wash buffer with ethanol was added (700 µl) to the column and centrifuged for 1 minute. The flow-through was discarded, and the column placed back into the collection tube. The empty column was centrifuged for a further 1 minute to remove residual ethanol in the wash buffer completely. The GeneJET purification column was then transferred into a new sterile 1.5 ml Eppendorf tube. The elution buffer was added (30 µl) to the centre of the column and centrifuged for 1 minute. The column was discarded, and the purified DNA was stored at -20 °C until used. All purification steps were carried out at room temperature.

2.7.1.5. Ligation (to clone the gene of interest into pJET cloning vector)

The pJET cloning kit (Thermo Scientific) was used to ligate the *cagA* plus flanking regions into the pJET vector (Table 2.3), following the manufacturer's instructions (Figure 2.1; step 3). A blunt-ended ligation reaction was set up on the ice. Into a PCR tube, 10 μ l of 2X ligation buffer, 1 μ l (0.05 pmol ends) pJET 1.2/blunt plasmid, 8 μ l gel extracted PCR product (*cagA* plus flanking regions) and 1 μ l T4 DNA ligase were added, vortex and centrifuged for 3 to 5 seconds. A ligation reaction with no PCR product was used as a negative control. Ligation mixtures were then incubated at room temperature (\sim 22 $^{\circ}$ C) for 5 minutes and used directly for transformation. Two aliquots of NEB 5 alpha competent cells (50 μ l each) (New England BioLab) were thawed on ice. The pJET-*cagA* ligation (5 μ l) was added to one aliquot of cells, and 5 μ l of the negative control was added to the second aliquot. Both were gently mixed and kept on ice for 30 minutes. The tubes were then heat shocked by placing them at 42 $^{\circ}$ C for 45 seconds, then immediately back on the ice for 2 minutes, and then 750 ml of warm LB broth was immediately added and incubated at 37 $^{\circ}$ C for 45 minutes. A sample of 200 μ l of each tube was plated out separately onto LB agar plates supplemented with ampicillin (100 μ g/ml) (Sigma-Aldrich; Merck), and 20 μ l of each tube were also plated out individually onto other LB ampicillin agar plates and incubated at 37 $^{\circ}$ C overnight.

2.7.1.6. Colony screening

After ligation, colonies on the LB ampicillin agar plates were streaked out onto fresh LB ampicillin agar plates to purify and identify colonies that contained the pJET-*cagA* plasmid with the appropriate PCR insert. Purified colonies were then used for PCR screening. A 20 μ l PCR reaction was prepared on ice by adding 10 μ M of pJET1.2 sequencing primers (forward and reverse) (Table 2.2), 9.2 μ l nuclease-free water, and 10 μ l 2X DreamTaq Green PCR master mix into PCR tube and mixed well. A small amount of purified colony was resuspended in the PCR master mix. The reaction was then subjected to an initial denaturation and enzyme activation cycle of 95 $^{\circ}$ C for 3 minutes, followed by 25 cycles of denaturation at 94 $^{\circ}$ C for 30 seconds, annealing at 60 $^{\circ}$ C for 30 second and extension at 72 $^{\circ}$ C for 1 minute. Colony PCR was checked by gel electrophoresis on 1% agarose gel.

2.7.1.7. Plasmid purification

An identified colony containing pJET-*cagA* (as determined by colony PCR screening) was subcultured in 5 ml LB broth supplemented with ampicillin (100 µg/ml) and incubated at 37 °C. After overnight incubation, 500 µl of the culture was added to 500 µl of 50% sterile glycerol (Sigma-Aldrich; Merck) in 1ml sterile tube and placed at -80 °C for long term storage. A GeneJET plasmid miniprep kit (Thermo Scientific) was used to purify the plasmid from the overnight culture, following the manufacturer's instructions. The eluted pJET-*cagA* plasmid was collected and stored at -20 °C until used.

Table 2.3: Plasmids

No.	plasmid name	DNA Size	Reference
1	pJET	2974 bp	(ThermoFisher 2019; URL)
2	pBluescript	2998 bp	(Alting-Mees, Sorge and Short 1995)

2.7.1.8. Sanger DNA Sequencing

Purified pJET-*cagA* plasmid concentration was adjusted to 50-100 ng/µl using the nanodrop. Two samples were prepared for Sanger sequencing. The first was a mixture of 15 µl of purified plasmid DNA with 2 µl pf pJET forward primer (10 pmol/µl). The second sample was a mixture of 15 µl of purified plasmid DNA with 2 µl of pJET reverse primer (10 pmol/µl). Both samples were labelled and sent to Eurofins Genomics for DNA sequencing to confirm that the *cagA* gene had been successfully cloned into the pJET plasmid.

2.7.2. Inverse PCR and construction of mutation plasmid

2.7.2.1. Inverse PCR

Phusion high fidelity PCR kit (Thermo Scientific) was used in this part of the study. A set of primers (forward and reverse) specific for pJET-*cagA* flanking regions plasmid was also used in the inverse PCR to amplify the ends of the pJET-*cagA* flanking regions (without the *cagA* gene) (Figure 2.1; step 4) (Table 2.2). The reaction was carried out in 20 µl final volume containing 2 µl (~50-100 ng) of pJET-*cagA* plasmid as a template, 50 µM of the relevant sense and antisense primers, 40 µl of 5X Phusion GC buffer (Thermo Scientific), 1 µl MgCl, 10 mM dNTPs, 2 µl Phusion DNA polymerase, and PCR

grade water. Reaction with no template was used as a negative control. The reactions were mixed, and the samples were then subjected to an initial denaturation and enzyme activation cycle of 98 °C for 30 seconds followed by 30 cycles of denaturation at 98 °C for 10 seconds, gradient annealing temperature from 60 to 74 °C each for 30 second and extension at 72 °C for 1 minute followed by a final extension step at 72 °C for 10 minutes and hold at 4 °C using a Master Cycler Nexus Gradient PCR machine (Eppendorf). PCR products were checked by gel electrophoresis on 1% agarose gel to determine the optimum annealing temperature. The PCR reaction was then repeated with the optimum annealing temperature (67 °C) and electrophoresed on a 1% agarose gel (see Section 2.7.2.3.). The inverse PCR product (pJET-*cagA* flanking regions) was then gel extracted using the GeneJET gel extraction kit, as described previously (see Section 2.7.2.4.). The pJET-*cagA* flanking regions plasmid was purified using the GeneJET plasmid miniprep kit (Thermo Scientific), as described previously (see Section 2.7.2.7.).

2.7.2.2. Purification of pBlueKm plasmid

In this study, a Kanamycin resistance (*KanR*) cassette was used to construct a mutant plasmid (Figure 2.1). The cassette was cloned into pBluescript plasmid (Alting-Mees, Sorge and Short 1995) (Table 2.3) by Darren Letley at the University of Nottingham. The NovaBlue pBlueKm plasmid used in this study was provided by Darren. *E. coli* carrying pBlueKm plasmid was streaked out from glycerol stock on an LB agar plate containing 10 µg/ml kanamycin and incubated at 37 °C overnight. Single colony was inoculated into 5 ml LB broth supplemented with 10 µg/ml kanamycin and incubated at 37 °C overnight. The pBlueKm plasmid was purified using the GeneJET plasmid miniprep kit (Thermo Scientific), following the manufacturer's instructions (see Section 2.7.2.7.).

2.7.2.3. Restriction digest

Plasmids were digested for further construction and to cut out the *KanR* cassette from pBlueKm plasmid. Two sets of digests were set; 1 for pJET-*cagA* flanks plasmid (inverse PCR product) and 1 for pBlueKm plasmid. The digestion was carried out in 20 µl final volume containing 2 µl of 10X cutsmart buffer (New England BioLab), 1 µl of

*Bam*HI enzyme (New England BioLab), and 17 µl of plasmid DNA. Digests with no enzyme were used as negative controls. All tubes were incubated at 37 °C for 1 hour and then run on a 1% agarose gel. The appropriate sized bands of *KanR* cassette and pJET-*cagA* flanks plasmid (Table 2.4) were gel extracted using the GeneJET gel extraction kit, following the manufacturer's instructions (see Section 2.7.2.4). The DNA concentration of pJET-*cagA* flanks plasmid (vector) and *KanR* cassette (insert) was measured using nanodrop.

Table 2.4: Restriction digest

No.	plasmid name	DNA Size
1	pJET- <i>cagA</i> flanks	~4000 bp
2	pBlueKm	~4000 bp
3	pBluescript	~3000 bp
4	KanR cassette	~1000 bp

2.7.2.4. Dephosphorylation reaction

A Quick CIP enzyme (New England Biolab) was added to pJET-*cagA* flanks (vector) after restriction digestion to dephosphorylate the 5' ends and promote insert ligation. The ligation was carried out in 20 µl final volume containing 17 µl of vector DNA (pJET-*cagA* flanks), 2 µl 10X cutsmart buffer, and 1 µl Quick CIP enzyme. The reaction was incubated at 37 °C for 10 minutes. The reaction was then incubated at 80 °C for 2 minutes to inactivate the Quick CIP enzyme.

2.7.2.5. Ligation pJET-*cagA* flanks to KanR cassette

The purified Kanamycin resistance cassette was ligated into the pJET-*cagA* flanks vector (Figure 2.1; step 5). The reaction was carried out in 20 µl final volume containing 2 µl of 10X T4 DNA ligase buffer (New England BioLab), 0.02 pmol dephosphorylated vector DNA, 0.06 pmol of insert DNA, 19 µl nuclease-free water, and 1 µl T4 DNA ligase. The reaction was gently mixed and incubated at room temperature for 10 minutes, followed by another 10 minutes at 65 °C to inactivate

the enzyme. The ligation reaction was then kept on ice. A ligation reaction with no KanR cassette was used as a negative control.

Two aliquots of NEB 5 alpha competent cells (50 µl each) (New England BioLab) were thawed on ice. A 5 µl of the ligation mixture was added to one aliquot of cells, and 5 µl of the negative control was added to the second aliquot. Both were gently mixed and kept on ice for 30 minutes. The tubes were then heat shocked by placing them at 42 °C for 45 seconds, then immediately back on the ice for 2 minutes, and then 750 ml of warm LB broth was immediately added and incubated at 37 °C for 45 minutes. A sample of 200 µl of each tube was plated out separately onto LB agar plates supplemented with kanamycin (10 µg/ml), and 20 µl each tube were also plated out individually onto other LB kanamycin agar plates and incubated at 37 °C overnight.

2.7.2.6. Colony screening

After ligation, colonies on the LB kanamycin agar plates were streaked out onto fresh LB kanamycin agar plates to purify and identify colonies that contained the pJET-*cagA* flanks plasmid with the appropriate KanR cassette insert. After overnight incubation, 500 µl of the culture was added to 500 µl of 50% sterile glycerol (Sigma-Aldrich; Merck) in 1ml sterile tube and placed at -80 °C for long term storage. Colony PCR screening was not conducted at this stage of the study due to the COVID-19 Pandemic circumstances. Instead, an analytical restriction digest was carried out as previously described (see Section 2.7.2.3.). Successfully constructed mutation plasmid was purified using the GeneJET plasmid miniprep kit (Thermo Scientific), following the manufacturer's instructions (see Section 2.7.1.7.).

2.7.2.7. Transformation of *H. pylori*

At this stage, the purified constructed mutation plasmid transformation into *H. pylori* was conducted (Figure 2.3; step 6). *H. pylori* 444A strain was grown on blood agar plates for 24 hours. Grown bacteria on 2 blood agar plates were suspended using a loop in 1 ml isosensitest broth containing 10% foetal calf serum on ice (see Section 2.7.3.5.). Bacteria were pelleted by centrifugation at 4,000 *xg* for 10 minutes. The supernatant was carefully discarded, and the pellet of bacteria was resuspended in

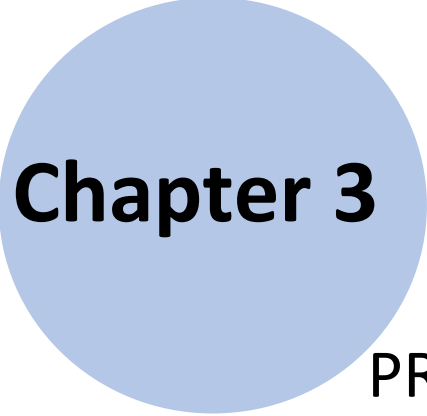
100 µl of isosensitest broth with 10% glycerol. 30 µl was then spotted onto a blood agar plate. The plate was kept upside down for 5 hours in the microaerobic cabinet to allow bacteria to adhere to the plate. 5 µl of the constructed mutation plasmid DNA (pJET-*cagA* flanks-KanR) was added to the centre of the spot and incubated in the microaerobic cabinet for 24 hours. Spotted bacteria were then spread over the plate's surface, using a swab, and incubated in the microaerobic cabinet for another 24 hours. Grown bacteria were streaked out on a fresh kanamycin blood agar plate and incubated for 4 days to check *H. pylori* transformation (see Section 2.7.3.5.). Transformant *H. pylori* will grow on the blood kanamycin agar plate however, these grown bacteria would have both the *cagA* and *KanR* cassette (intermediate strain). Therefore, a second recombination will be performed to knock-out the *cagA* gene (Figure 2.3; step 7). DNA sequencing will be performed in both recombination to confirm *H. pylori* transformation ($\Delta cagA$).

2.8. Statistical analysis (Overview)

All data were analysed using GraphPad Prism software version 8 for Mac IOS. In the quantification study, all the statistical analysis were carried out using one-way, or two-way ANOVA of variance with multiple comparisons. The correlation between Pierce BCA- protein assay and Zetaview, and the correlation between BacTiter-Glo assay and Miles and Misra quantification method were analysed using simple linear regression. The association between the quantity of produced OMV and the virulence of bacterial strain was analysed using unpaired t-test. After performing the cytotoxicity study, statistical analysis was carried out using two-way ANOVA of variance with multiple comparisons to investigate the effect of OMV on the human gastric epithelial cells. No statistical analysis was performed for the live cell analysis.

OMV proteins were clustered with confidence scores ≥ 0.75 . Kendall correlation was performed to test differences between conditions using R software. Bar graphs, heatmap with bidirectional clustering, Venn diagram, Sankey plot, and box plot were generated by Lesley Hoyles at the Department of Biosciences, Nottingham Trent University using R software. Probability (p) value <0.05 (*), <0.01 (**), <0.001 (***), and <0.0001 (****) were considered statistically significant. Error bars on graphs

indicate the standard deviations (SD) around the mean of three independent repeats of experiments that were performed in triplicate.



Chapter 3

H. PYLORI OMV
PRODUCTION
AND
CHARACTERISTICS

3. *H. PYLORI* OMV PRODUCTION AND CHARACTERISTICS

3.1. INTRODUCTION

Outer membrane vesicles are typically formed and released from pathogenic and non-pathogenic Gram-negative bacteria during active growth (Chatterjee and Das 1967; McBroom *et al.* 2006), and no production of OMV was observed during bacterial cell death (Chatterjee and Das 1967). OMVs are produced for different roles and purposes. For example, bacteria may release OMV to promote their survival, and for bacterial-bacterial or bacterial-host cell interactions. Several studies reported that bacteria could produce and release OMV under different growth conditions, including liquid and solid culturing medium, within bacterial biofilms, in intracellular infections, and within the infected host (Chatterjee and Das 1967; Unal *et al.* 2010; Yonezawa *et al.* 2009; Unal *et al.* 2010; Galka *et al.* 2008; Fiocca *et al.* 1999; Ellis and Kuehn 2010). However, not all conditions are equally favourable for the bacteria to generate OMV.

These conditions, in addition to the bacterial growth phases, can affect the production of OMV. It has been reported that more OMV are produced during the exponential growth phase, while the bacteria are actively dividing and growing, than the stationary phase where minimal to no OMV are produced (Kuehn and Kesty 2005; Bauman and Kuehn 2006; Chatterjee and Das 1967). Moreover, differences in vesicles component between those isolated from exponential and stationary phases were observed (Tashiro *et al.* 2010; McCaig *et al.* 2013). The environmental features of each growth condition, for instance, the type of medium used for *in vitro* growth conditions and the nutrients or supplements used and other variables might alter the amount of produced OMV (Hazlett *et al.* 2008; Zarrella *et al.* 2011; McCaig *et al.* 2013). This means that although bacteria produce OMV constitutively, the amount of produced OMV is regulated by bacterial growth and environmental triggers.

Indeed, the *in vivo* environment would alter vesicles production and composition as well. For example, *H. pylori* produced more OMV *in vitro* than *in vivo* (Kuehn 2005). This was thought to be due to different variables within the host such as the availability of iron, oxygen level (Kuehn and Kesty 2005), and whether the host smokes or undergoes antibiotic treatment, the host lifestyle and dietary habits, and

others. Several studies reported that the presence of iron and its level could alter OMV composition. For instance, *H. pylori* grown in low iron conditions produced OMV with less VacA than those from higher iron levels (Keenan *et al.* 2000; Keenan and Allardyce 2000; Fiocca *et al.* 1999). In contrast, vesicles isolated from low iron conditions had higher protease concentration than the others (Keenan and Allardyce 2000). Moreover, iron depletion causes changes in LPS (Keenan *et al.* 2008). Thus, the growth conditions might alter the physiological trait of bacteria, which in turn changes the formation of membrane vesicles and their structure and components as these vesicles bleb and shed from the bacterial outer membrane.

The structure of the bacterial outer membrane impacts bacterial vesiculation. Generally, Gram-negative bacteria can change their membrane structure to protect themselves from the host immune response (Pier 2000). As described previously, OMV bud from the bacterial membrane, packing some of the membrane components such as LPS, OMPs, and Lipoproteins (Perez-Cruz *et al.* 2013; Kuehn 2005). Alteration of these membrane components might affect the budding and formation of OMV and their composition. For instance, a mutation in LPS increased the vesiculation of *Salmonella* strains (Smit *et al.* 1975). Where the growth environment has an impact on bacterial physiology, this will consequently impact their vesiculation.

Other factors also affect the production of OMV. As stated earlier, both pathogenic and non-pathogenic bacteria can produce OMV. However, some studies showed that pathogenicity could affect bacterial OMV production (Lai *et al.* 1981; Wai *et al.* 1995) as pathogenic bacteria can produce more OMV than their non-pathogenic equivalents. A study on *Escherichia coli* (*E. coli*) showed that Enterotoxigenic *E. coli* produced ten-times more OMV than the non-pathogenic *E. coli* (Horstman and Kuehn 2002). Moreover, the study also showed that the non-pathogenic *E. coli* K-12 strain with histone-like nucleoid-structuring (*hns*) mutation, which is a virulence regulatory factor, produced more OMV than the other K-12 strains used in the study (Horstman and Kuehn 2002). Bacteria may produce OMV for a protective purpose as they pack their toxins and virulence factors in these vesicles to protect and deliver them to cellular targets. Thus, pathogenic or virulent bacteria may have upregulated the constitutive process of OMV production and added virulence factors to the OMV cargo as they evolved pathogenicity.

Additionally, the presence of antibiotics can increase bacterial vesiculation. A study on *Pseudomonas aeruginosa* showed that bacteria exposed to antimicrobial treatment produced a higher amount of membrane vesicles than those without treatment, and the diameter of the vesicles was larger as well (Dutta *et al.* 2004; Kadurugamuwa and Beveridge 1998). There are different types of antibiotics, and some of them target the bacterial cell wall. That would cause the bacteria to change their cell wall structure for protection, which might cause alteration of OMV structure and formation. Studies showed that the effect of antibiotics on bacterial vesiculation and toxicity depends on the type of antibiotic used for treatment as some antibiotics did not have any impact on OMV production or composition (Dutta *et al.* 2004; Kuehn and Kesty 2005).

Production of OMV can also protect the parent bacterial cells against antibiotics and environmental stressors. For example, *H. pylori* OMV protect *H. pylori* in the presence of levofloxacin and clarithromycin (Murray *et al.* 2020). However, they could not protect *H. pylori* in metronidazole and amoxicillin (Murray *et al.* 2020). Other studies showed that membrane vesicles could protect their parental bacteria in an environment with antibiotics, promoting bacterial survival (Allan and Beveridge 2003). Therefore, antimicrobial treatment would alter the bacterial cell wall, which will alter the formation and structure of OMV, as describes previously. Also, it would increase vesiculation as a defense mechanism to survive and persist.

Moreover, stressful environments can influence bacterial vesiculation. Bacterial vesiculation increases during the activation of the stress response, which helps in eliminating accumulated misfolded proteins (McBroom and Kuehn 2007). Other stressors can also induce increased vesicle production, such as temperature stress and oxidative stress. An increase in OMV production was observed in *Pseudomonas putida* after a heat shock at 55 °C (Baumgarten *et al.* 2012). Whereas no significant differences were seen in *Pseudomonas aeruginosa* after exposure to heat shock (MacDonald and Kuehn 2013). In terms of oxidative stress, a higher yield of OMV was observed in *Pseudomonas aeruginosa* in an oxidative stressed environment (MacDonald and Kuehn 2013). Also, recent studies showed that OMV protect *H. pylori* against hydrogen peroxide (Lekmeechai *et al.* 2018; Murray *et al.* 2020). This is consistent with the idea that the growth environment can have a dramatic impact on

bacterial physiology, causing alterations in OMV production, composition, and toxicity.

3.2. AIM OF THIS STUDY

The biogenesis of membrane vesicles, their compositions and toxicity are not fully understood yet. Also, there are several variables that might influence OMV production and characteristics.

This chapter aimed to characterise OMV produced by *H. pylori* strains with high and low virulence, under different growth conditions. The research questions were:

- Do more virulent *H. pylori* strains produce more OMV compared with less virulent *H. pylori* strains?
- Do the bacterial growth conditions influence the quantity and cytotoxicity of the OMV produced by *H. pylori*?

3.3. RESULTS

Eight strains of *H. pylori* (2 control strains and 6 clinical isolates) were used in this study (Table 2.1). Three of the clinical isolates were isolated from patients suffering gastric ulcer disease, and duodenal ulcer disease and all of them had different degrees of inflammation in their stomach lining. The other 3 clinical isolates were isolated from patients not suffering such ulcer disease, however, also having different degrees of inflammation (Table 2.1). The virulence classification was based on the presence of the *cagA* gene and *vacA* genotype as described in Chapter 2 (Section 2.1.). Outer membrane vesicles from these *H. pylori* strains were produced *in vitro* in different environments; BHI broth supplemented with 0.2% β -cyclodextrin and on blood agar plates for 24 hours as described previously (see Section 2.2.; 2.2.1. and 2.2.2.). The OMV were then purified by syringe filtration and ultracentrifugation as described previously (see Section 2.3.2.). The quantities of OMV produced by strains with high and low virulence were determined using Pierce BCA- protein assay (Sections 2.3.3.1.), which measures protein concentration per ml, and Zetaview (Section 2.3.3.2.), which measures particles number per ml and their diameter. All data were normalised to the viable bacterial count to determine the amount of OMV and OMV-associated proteins generated per bacterial cell.

3.3.1. Characterisation of OMV from *H. pylori* with High or Low Virulence

3.3.1.1. Quantification of *H. pylori* OMV

All *H. pylori* strains used in this study (Table 2.1) were analysed *in vitro* for OMV production in early (1 day) and late (6 days) broth and on plate (1 day) cultures. All strains were able to produce OMV in all growth conditions with variations in OMV quantity (Figures 3.1 and 3.2). Strain 121A produced very few OMV per CFU when grown on plates, when the OMV were quantified by Zetaview, but a similar quantity of OMV per CFU as determined by BCA assay (Figure 3.1 A and B). The quantity of isolated OMV from different culture methods were compared using two-way ANOVA of variance with multiple comparisons. However, the differences between the quantity of isolated OMV from late broth cultures of each strain (Figure 3.2) were

compared using one-way ANOVA of variance with multiple comparisons. All strains showed better OMV production in broth cultures than on plates, except strain 109A; however, the difference between both culture methods was not statistically significant ($p > 0.05$) (Figures 3.1).

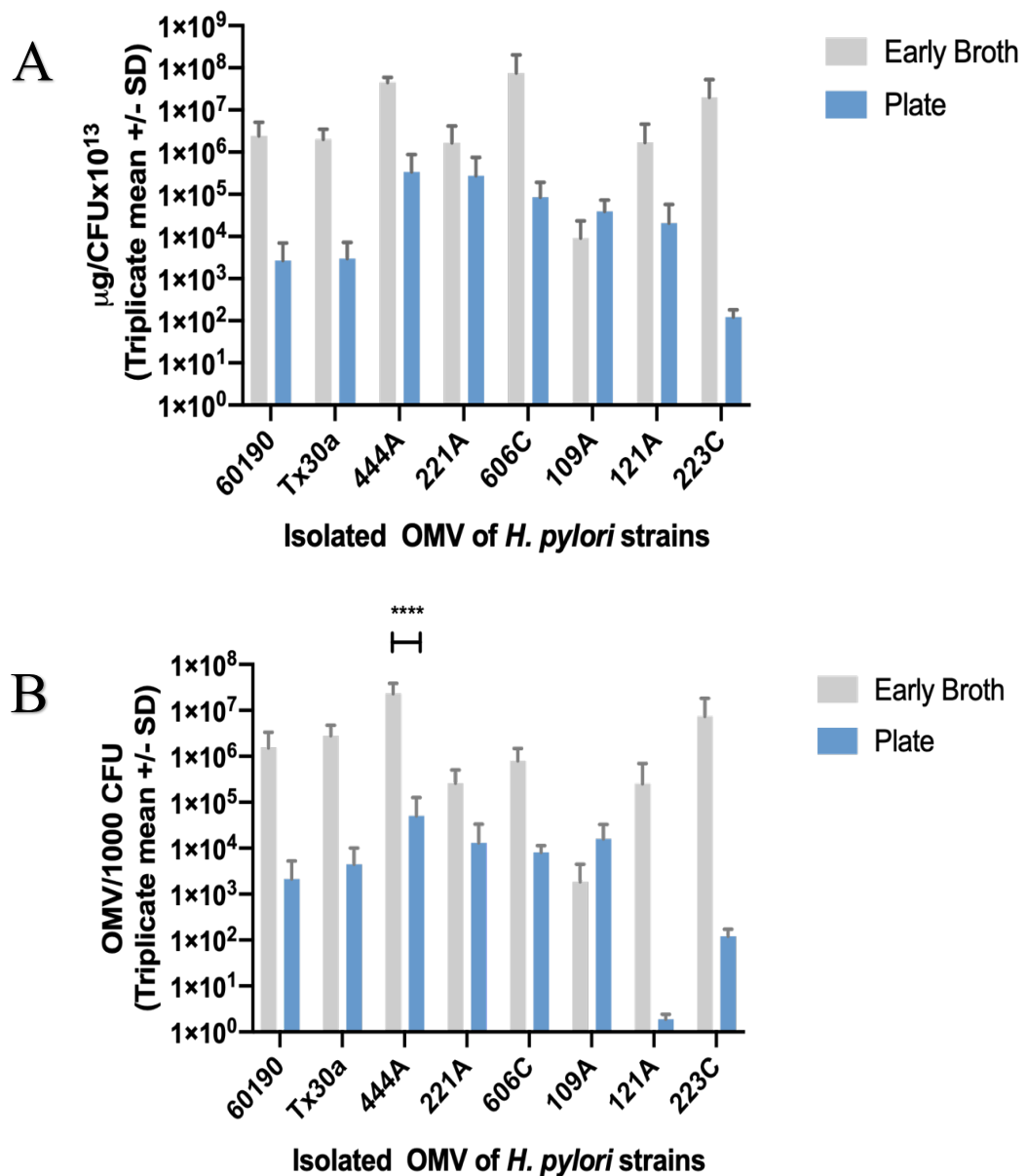


Figure 3.1: Quantity of OMV produced by different *H. pylori* strains on agar plates and in early broth cultures. Isolated OMV from early broth and plate cultures of each strain were quantified using (A) Pierce BCA- protein assay and (B) Zetaview. (A) OMV were added to BCA assay working reagent in triplicate, mixed well, and incubated for 30 minutes at 37 °C. The absorbance was read at 594 nm by plate reader. Two-way ANOVA test was performed to compare OMV quantity in μg per CFU $\times 10^{13}$ per ml of each strain. (B) OMV were diluted to 1:10,000 dilution and analysed using Zetaview; nanoparticle tracking analysis. Two-way ANOVA test was performed to compare OMV quantity in particles per 1000 CFU per ml of each strain. Error bars show the mean of blank corrected values of three independent replicates (\pm SD). **** indicates $p < 0.0001$.

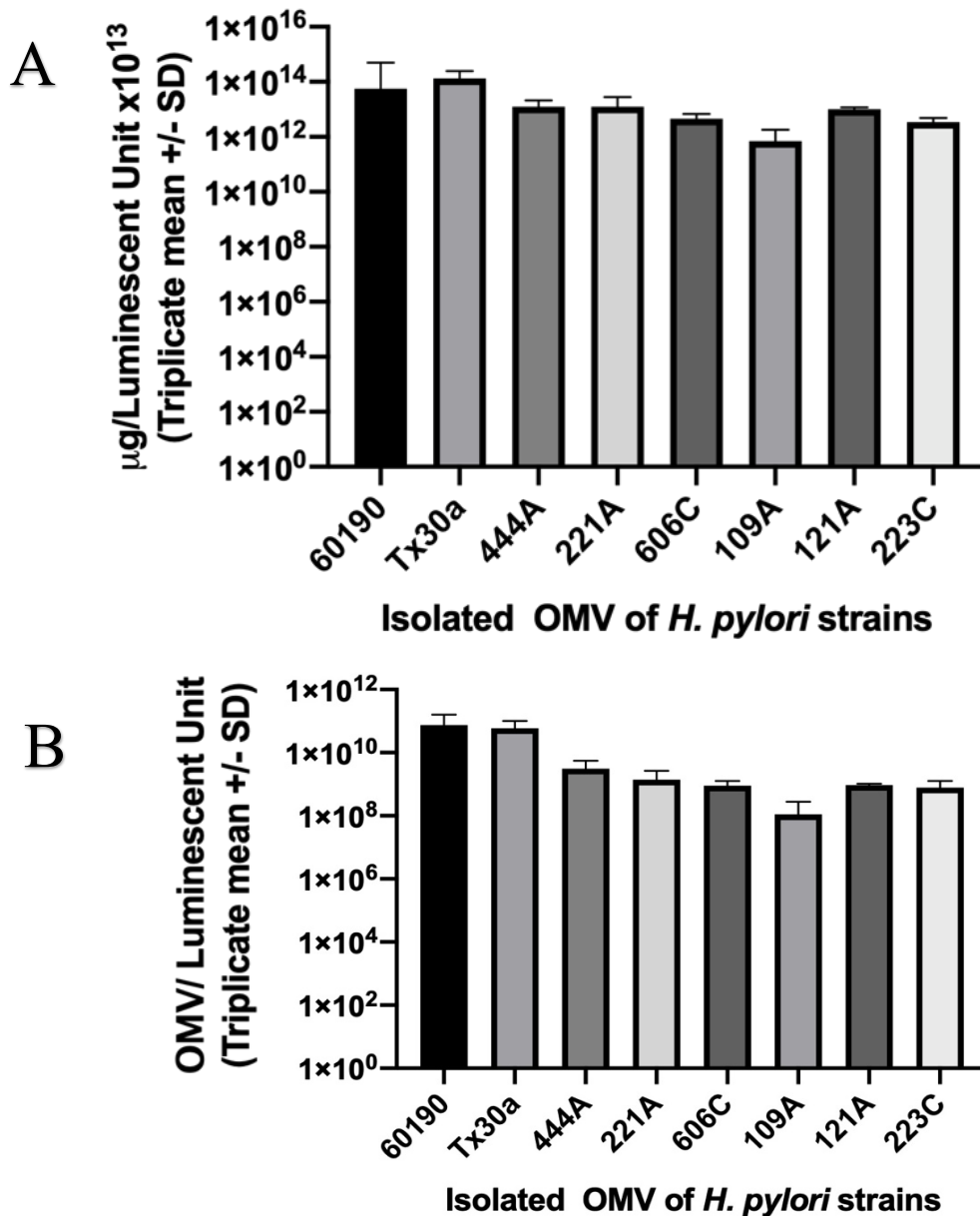


Figure 3.2: Quantity of OMV produced by different *H. pylori* strains in late broth culture. Isolated OMV from late broth cultures of each strain were quantified using (A) Pierce BCA- protein assay and (B) Zetaview. (A) OMV were added to BCA assay working reagent in triplicate, mixed well, and incubated for 30 minutes at 37 °C. The absorbance was read at 594 nm by plate reader. One-way ANOVA test was performed to compare OMV quantity in μg per luminescent unit $\times 10^{13}$ of each strain. (B) OMV were diluted to 1:10,000 dilution and analysed using Zetaview; nanoparticle tracking analysis. One-way ANOVA test was performed to compare OMV quantity in OMV per luminescent unit of each strain. Error bars show the mean of blank corrected values of independent replicates (\pm SD). No statistically significant differences in OMV production between strains were detected using either method.

3.3.1.1.1. Correlation between BacTiter-Glo assay and Miles and Misra method

The correlation between the BacTiter-Glo assay and Miles and Misra quantification of isolate OMV from early broth culture of 60190 strain was statistically analysed using simple linear regression to determine the extent of agreement of both methods with each other (Figure 3.3). This analysis showed a strong positive correlation between the two techniques as the correlation coefficient (r value) is 0.8922 (Figure 3.3). This correlation was statistically significant ($p < 0.005$).

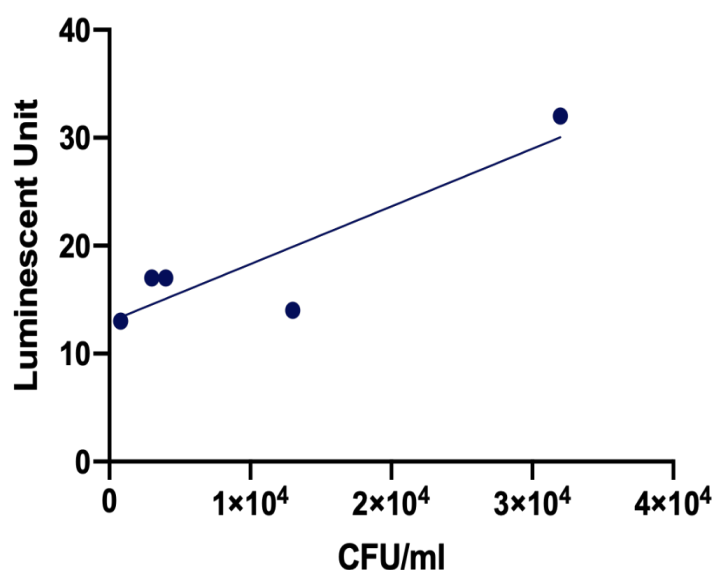


Figure 3.3: Comparison of BacTiter-Glo and Miles and Misra methods for quantification of viable bacteria. The number of viable bacterial cells of strain 60190 in a dilution series from early broth culture was quantified using BacTiter-Glo assay and Miles and Misra quantification method. Simple linear regression ($Y = 0.001096 * X + 0.000$) and two-tailed Pearson correlation coefficient analyses were performed to assess how well the BacTiter-Glo assay and Miles and Misra quantification method correlated with each other. The mean of blank corrected values of three independent replicates is shown (+/-SD). $r = 0.8922$ and $p < 0.005$.

3.3.1.2. Size of *H. pylori* OMV

The size of the produced OMV was determined using the Zetaview. Isolated OMV from all growth conditions and all strains were approximately similar in size, with mean diameters that ranged from 100 to 130 nm (Figures 3.4 and 3.5). However, OMV of strain Tx30a isolated from late broth showed statistically larger OMV size than those isolated from plate cultures (** $p < 0.01$). OMV of strains 606C and 223C isolated from early and late broth cultures showed larger OMV size compared to those isolated from the plate cultures (* $p < 0.05$) (Figure 3.4). OMV sizes in each condition were compared against each other using two-way ANOVA of variance with multiple comparisons. The comparison showed that late broth OMVs were statistically larger than early broth OMV (* $p < 0.05$) (Figure 3.4). Plate OMV were statistically smaller than early and late broth OMV (* $p < 0.05$ and ** $p < 0.01$, respectively), except strain 444A which showed larger plate OMV compared to early and late broth (Figure 3.4).

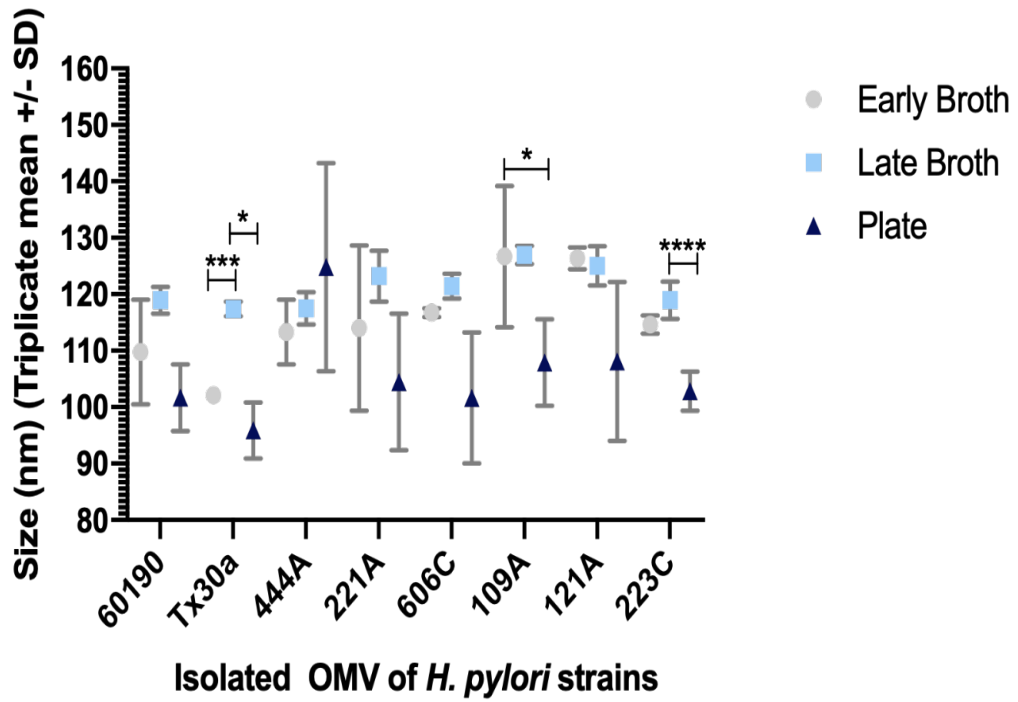


Figure 3.4: The size of *H. pylori* OMV. Isolated OMV from early, late broth and plate cultures of each strain were diluted to 1:10,000 dilution and analysed using Zetaview; nanoparticle tracking analysis. Two-way ANOVA test was performed to compare OMV size in nm of each strain. Error bars show the mean of blank corrected values of three independent replicates (+/- SD).

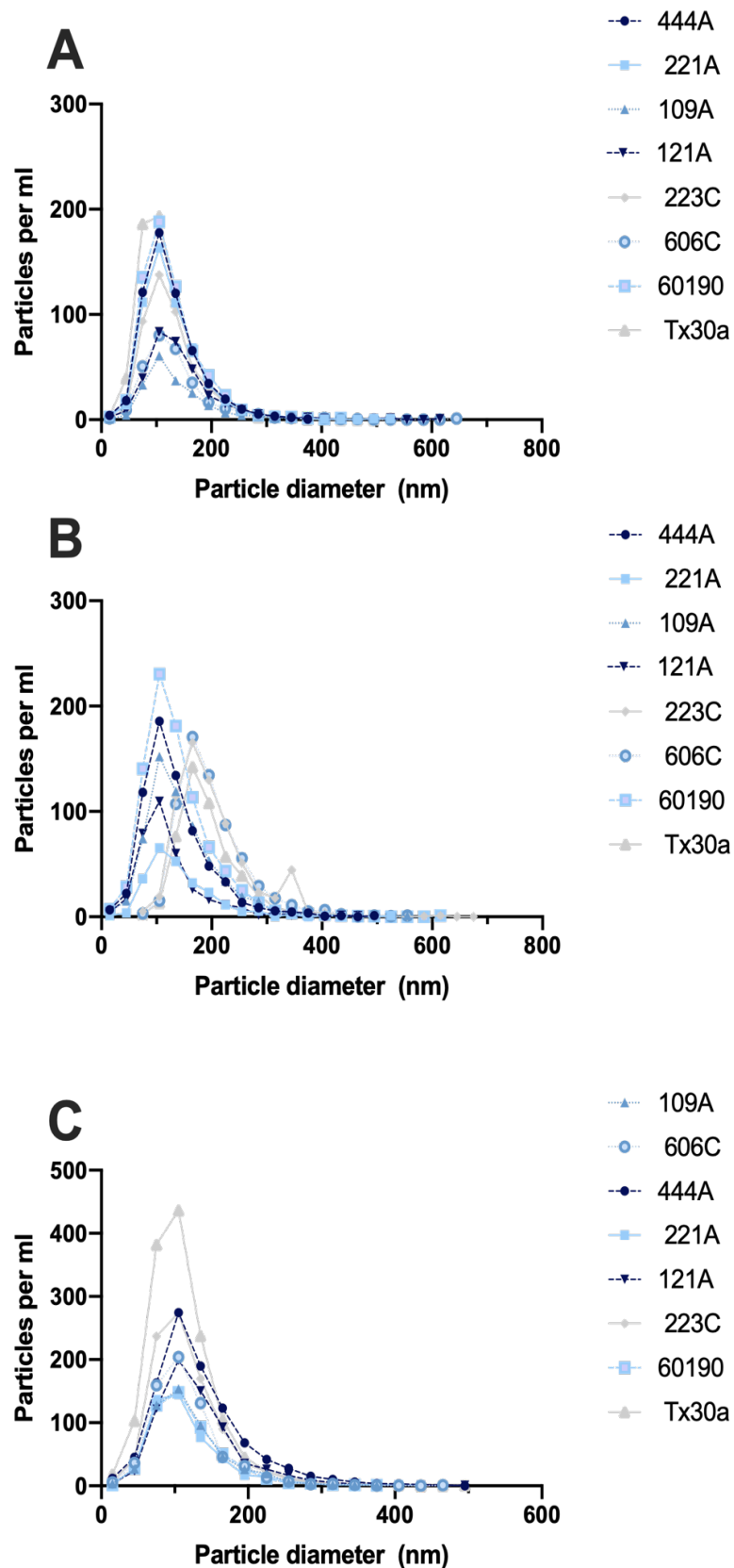


Figure 3.5: OMV size distribution. Isolated OMV from (A) early broth, (B) late broth and (C) plate cultures of 8 *H. pylori* strains were diluted to 1:10,000 dilution and analysed using Zetaview; nanoparticle tracking analysis. No statistical analysis was done on these curves but the mean/peak OMV diameter for each strain was compared by two-way ANOVA in Figure 3.5.

3.3.2. Correlation Between Pierce BCA- Protein Assay and Zetaview

Pierce BCA protein assay measures protein concentration in $\mu\text{g}/\text{ml}$ while the Zetaview counts the number of OMV per ml. The correlation between the two quantification methods was statistically analysed using simple linear regression to determine the agreement of both methods with each other (Figure 3.6). This analysis showed a weak correlation ($r = 0.3799$) between OMV quantity determined by Pierce BCA- protein assay and by Zetaview, and this correlation was not statistically significant ($p = 0.3532$) (Figure 3.6).

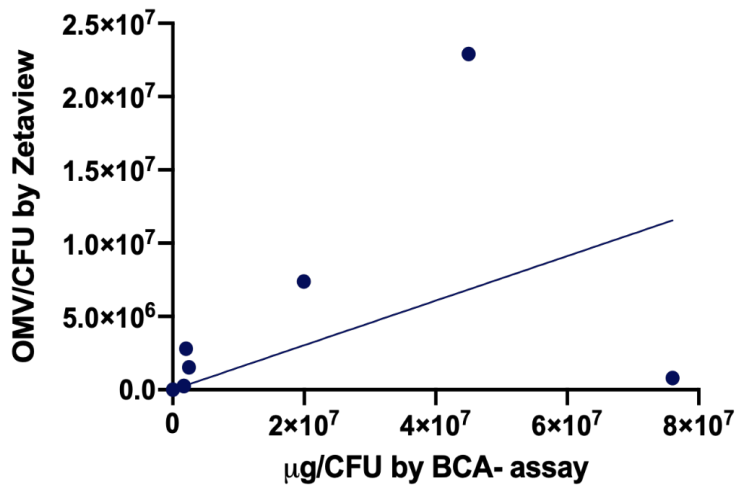


Figure 3.6: Correlation between Pierce BCA- protein assay and Zetaview. Isolated OMV of 8 *H. pylori* strains were quantified using Pierce BCA- protein assay and Zetaview. Simple linear regression ($Y = 0.1520 \cdot X + 0.000$) and two-tailed Pearson correlation coefficient analyses were performed to assess how well the Pierce BCA- protein assay and Zetaview correlated with each other. The mean of blank corrected values of three independent replicates is shown (+/-SD). $r = 0.3799$ and $p = 0.3532$.

3.3.3. Association Between the Quantity of OMV Produced and Bacterial Virulence

The association between the virulence of the *H. pylori* clinical isolates and the quantity of produced OMV was also analysed using unpaired t-test (Figures 3.7). Due to small studied group of strains and not having the Sydney score information for the clinical strain 223C, OMV production was not correlated to Sydney scores. Strain 444A, which is highly virulent, produced the most OMV both in broth and on plates. However, the analysis of all 8 strains together showed that there was no significant association between the quantity of OMV produced and the virulence of the producing strain ($p > 0.05$) (Figure 3.7).

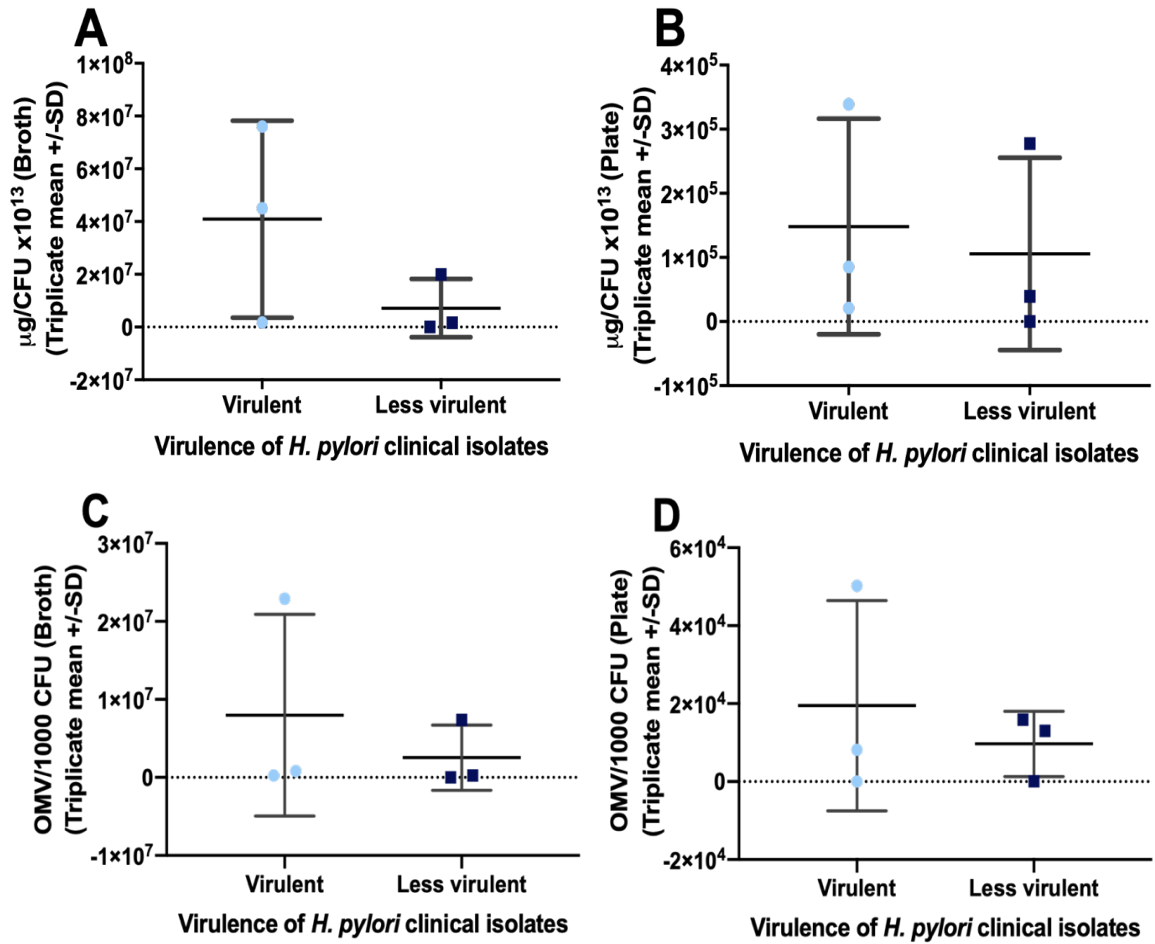


Figure 3.7: Association between OMV quantity and bacterial virulence. Isolated OMV of 6 *H. pylori* clinical strains from broth and plate cultures were quantified using (A and B) Pierce BCA- protein assay and (C and D) Zetaview. Unpaired t-test analysis was performed to look for an association between quantity of isolated OMV and virulence of *H. pylori* clinical strains. The mean of blank corrected values of three independent replicates is shown (\pm SD).

3.4. DISCUSSION

3.4.1. Characterisation of OMV from *H. pylori* Strains

H. pylori growth conditions affect the quantity and characteristics of the OMV produced. In the present study, OMV from the early broth, late broth, and plate cultures of 8 *H. pylori* strains (Table 2.1) were purified and quantified. All strains showed variation in the quantities of OMV produced between growth conditions; however, these differences were not statistically significant ($p > 0.05$) (Figures 3.1 and 3.2). Seven of the eight strains tested produced more OMV in broth cultures than on agar plates (Figure 3.1), though statistical significance was not reached. Strain 444A showed significantly higher OMV production in early broth culture than on plate cultures (p^{****}) (Figure 3.1 B).

Based on the strong correlation between the BacTiter-Glo assay and the Miles and Misra quantification method (Figure 3.3), it seems that the amount of OMV isolated from late broth cultures (Figure 3.2) was higher than those isolated from early broth and plate cultures (Figure 3.1). These differences could be directly compared; however, these could not be statistically analysed because of the different methods used to quantify bacteria in the late broth cultures. It was not possible to determine CFU/ml from late broth cultures because no colonies were recovered, but the presence and quantity of viable bacteria was instead confirmed using BacTiter-Glo assay. This is consistent with the findings of a recent study on *H. pylori* OMV, which showed a significantly higher production of OMV in late broth cultures than the early broth cultures (Zavan *et al.* 2018). In Zavan *et al.* (2018) study, they isolated OMV from broth cultures after 16, 48, and 72 hours and found that as the bacteria growing, they produce more OMV. In fact, this was expected because bacteria naturally produce OMV during their active growth (Kuehn 2005). Hence, late broth cultures contained more OMV than early broth cultures because the bacteria had been growing for longer and producing OMV during all of that time. However, in our study, we could not directly compare the production of late broth to early broth because of the need to determine CFU/ml of the bacteria.

Nevertheless, it is important to know whether late broth condition impacts OMV characterisation, components, or toxicity. Because as bacteria grow for a longer time

in broth, the nutrients will become limited, creating stress on the bacteria. That also reported to induce the production of bacterial OMV (Chatterjee and Chaudhuri 2012; McBroom and Kuehn 2007). Therefore, further studies and investigations were suggested to understand the mechanism of OMV formation. Also, OMV isolation and characterisation on a daily basis for 1 to 6 days growth in broth were suggested.

On the other hand, in the Zavan *et al.* (2018) study, *H. pylori* OMV were only isolated from broth cultures. However, in our study, we isolated OMV from broth and plate cultures, an entirely different environmental condition than the broth. In previous studies on *H. pylori* or other bacterial species, OMV were isolated from broth cultures with different conditions. No study compared the characteristics of OMV of *H. pylori* or other bacterial species isolated from agar plate cultures. Therefore, this aspect of our work is novel and has not yet been published elsewhere, to our knowledge. Thus, further investigations were needed to characterise differences between the isolated OMV, including cytotoxicity and proteomics analyses.

OMV isolated from different growth conditions were approximately similar in size, with mean diameters ranging from 100 to 130 nm (Figures 3.4 and 3.5). Although they were similar in size, OMV of strains 606C, 223C, and Tx30a isolated from late broth culture were significantly larger than those isolated from early broth and plate cultures (Figures 3.4 and 3.5 B). Interestingly, 444A OMV from the plate were larger in size than those from early and late broth (Figure 3.4). Also, 444A OMV from late broth were larger than those from early broth (Figure 3.4). That is consistent with previous studies' findings that not all growth conditions are favourable for the bacteria to produce OMV, and that might affect OMV characterisation (Chatterjee and Chaudhuri 2012). Also, it has been reported that the growth stage can affect OMV size and protein content (Zavan *et al.* 2018).

They found that OMV harvested at 48 and 72 hours (50 to 350 nm in size) were similar to smaller than those harvested at 16 hours (50 to 500 nm in size) (Zavan *et al.* 2018). That is in contrast to our study as we found that OMV from early (1 day of incubation) broth cultures showed larger size than those of late broth (6 days of incubation), except for *H. pylori* 444A strain (Figure 3.4). Also, OMV from plate cultures showed a different size of OMV to those from broth cultures, as evident in Figure 3.4. Hence,

the growth stage and the environmental conditions alter the formation of OMV and might affect their contents and composition. Another study reported that OMV size influences the protein content of *H. pylori* vesicles and determine their entry path into the host cells (Turner *et al.* 2018). It seems that the formation of bacterial vesicles and their characteristics are regulated by the bacterial growth environment and its condition.

Moreover, the OMV size in Zavan *et al.* and Turner *et al.* was measured using NanoSight 3.2; nanoparticle tracking analysis. Whereas, in our study, we used the Zetaview to measure OMV size, not the NanoSight. Differences between the two instruments, such as their software, might affect the measurements. A recent comparative study between the Zetaview and NanoSight showed that Zetaview is more precise in measuring the concentration (particle/ml) of extracellular vesicles of mammalian cells than the NanoSight (Bachurski *et al.* 2019). However, the Zetaview was not as precise as the NanoSight in measuring particles' size (Bachurski *et al.* 2019). Although both instruments and findings were different, still our study is consistent with the idea that the bacterial growth stage can affect OMV size. The Zetaview has not previously been used to characterise *H. pylori* OMV, to our knowledge; however, it has been used to measure the size distribution and concentration of the Uropathogenic *E. coli* (Svennerholm *et al.* 2017), *Campylobacter jejuni* (*C. jejuni*) (Davies *et al.* 2019), and *P. aeruginosa* (Zhang *et al.* 2020) OMVs. In *P. aeruginosa* study, OMV were isolated from the normal condition of broth cultures and from broth cultures exposed to x-rays. They measure the size of these OMVs using the Zetaview and did not find differences in size (Zhang *et al.* 2020). However, irradiation-induced OMV showed a significantly higher concentration than those from normal broth condition (Zhang *et al.* 2020). Thus, stressful conditions can alter the mechanism of OMV formation and might purposely induce their production.

Besides that, *H. pylori* can change its morphology to survive in stressful environments from a spiral into U-shaped and doughnut shape (Cammarota *et al.* 2012; Rudnicka *et al.* 2014) then finally into coccoid form, which is a non-culturable but viable shape (Cellini *et al.* 2008; Andersen and Rasmussen 2009). This transition likely explains why recovery of colonies from late broth cultures was not possible in the current study, despite the presence of viable bacteria being proven using the BacTiter Glo assay. *H.*

pylori also has the ability to revert to its spiral shape in mice (Cellini *et al.* 1994; Kusters *et al.* 1997; Rudnicka *et al.* 2014). This change in morphology might alter the physiology of *H. pylori* and its OMV-producing behaviour. It is well-known that *H. pylori* taken from the edge of the growth on agar plates is more suitable for onward culture than *H. pylori* at the centre of the patch of growth, and we previously observed the bacteria to be spiral-shaped at the edge of the agar plate, but U-shaped at the centre (AlSharaf and Winter, unpublished data). Furthermore, we previously observed that spiral-shaped *H. pylori* taken from the edge of agar plates produced more biofilm than U-shaped bacteria taken from the centre (AlSharaf and Winter, unpublished data). We also previously observed that old *H. pylori* that had grown on a blood agar plate for 6 days formed more biofilm than freshly passaged bacteria that had grown for only one day (AlSharaf and Winter, unpublished data).

In the current study, *H. pylori* had different morphology between early and late broth cultures, as shown in Figure 3.8 below. *H. pylori* in late broth culture (6 days of incubation) were mainly U-shaped, while those in early broth culture (1 day of incubation) were spiral-shaped (Figure 3.8). These morphological changes might affect the production of OMV and their characteristics. Interestingly, *H. pylori* 444A strain, which is a highly virulent strain, produced more OMV per CFU compared to the other strains (Figure 3.1 B). Also, the size of its OMV from plate culture was greater than those from broth cultures (Figure 3.4), and OMV from the late broth was larger than those from early broth (Figure 3.4). Additionally, among 6 patients, the patient that had been diagnosed with an intermediate precancerous condition (intestinal metaplasia) is the one that was infected with strain 444A (Table 2.1). This strain is also the best at forming biofilm (AlSharaf and Winter, unpublished data). It seems that infections with 444A strain would be more likely to result in severe disease (ulcers and gastric cancer) compared with less virulent *H. pylori* strains. Further investigations on this strain are suggested.

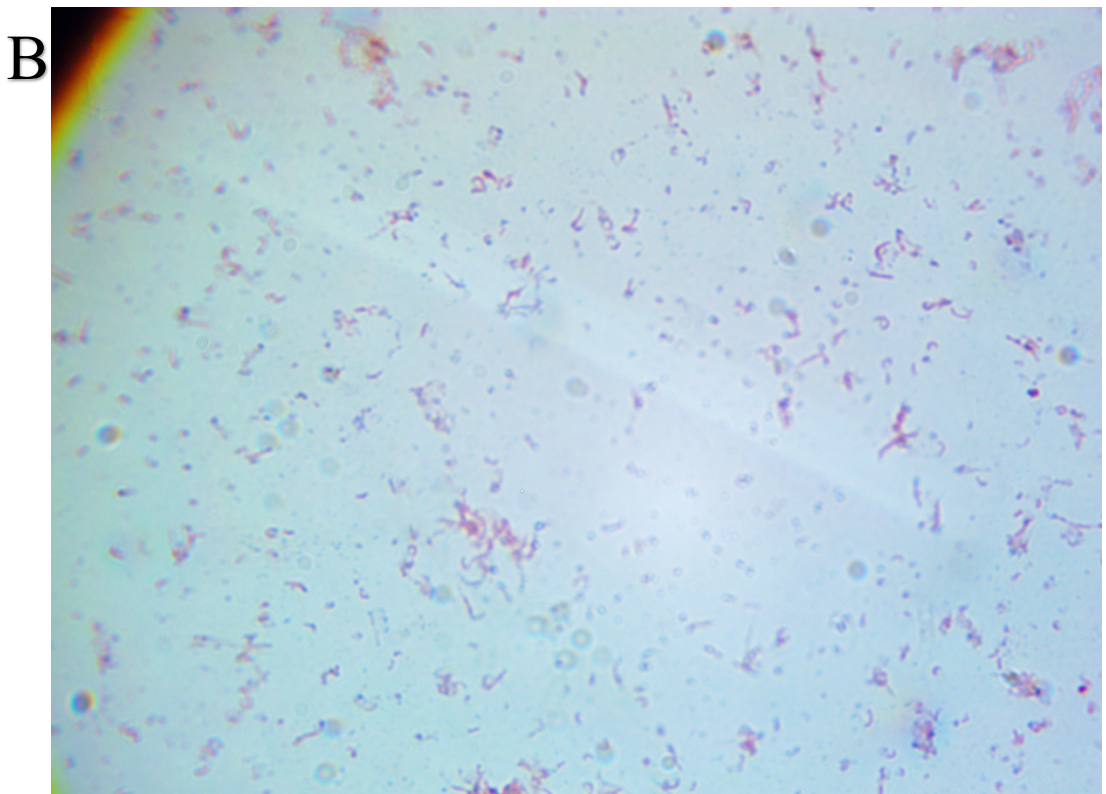
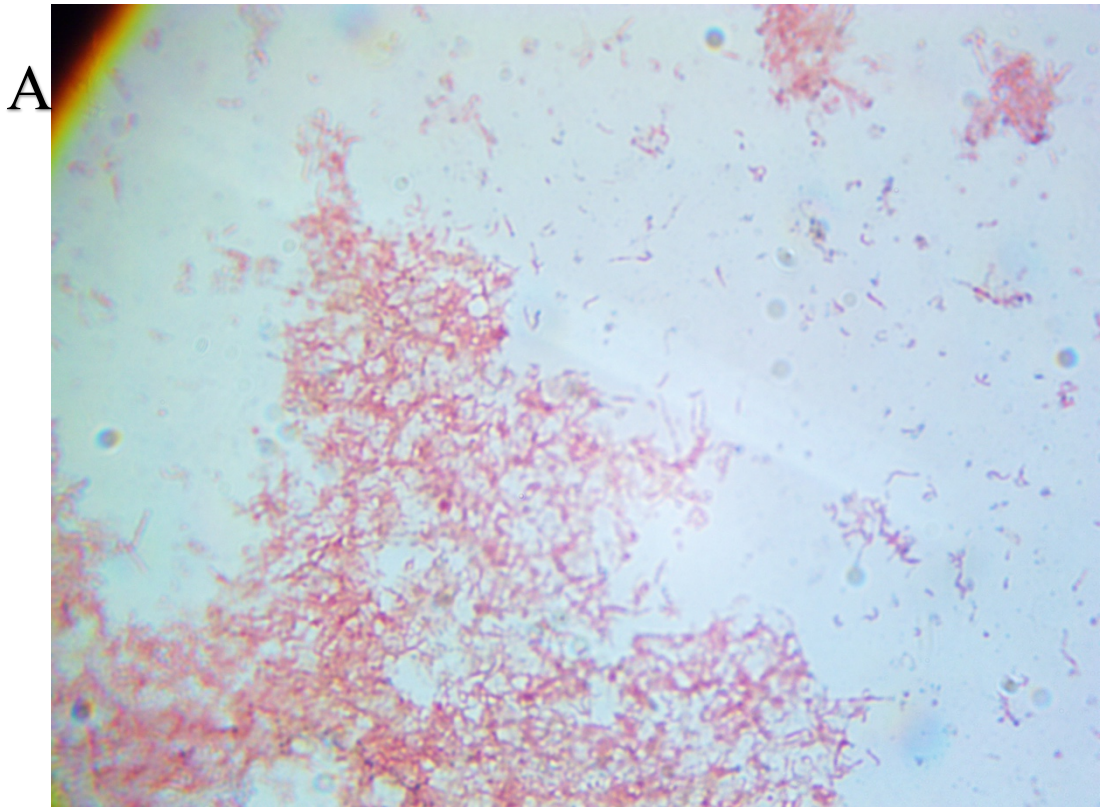


Figure 3.8: Gram stain of 60190 strain. (A) After 1 day of incubation in BHI broth supplemented with 0.2% of β -cyclodextrin and (B) After 6 days of incubation in BHI broth supplemented with 0.2% of β -cyclodextrin (Magnification: 100X).

3.4.2. Correlation Between Pierce BCA- Protein Assay and Zetaview

All OMV quantification data were analysed to look for a relationship between the Pierce BCA- protein assay and the Zetaview (Figure 3.6). Differences in data obtained between the two methods, reflect the limitations of each method for OMV quantification. Unfortunately, there is no single method that can perfectly quantify OMV. The Pierce BCA- protein assay measures the protein concentration within OMV, as illustrated earlier (see Section 2.4.3.). The BCA assay is sensitive to interference by some components from bacteriological broths and agar plate formulations, and the extent of this depends on the OMV washing process. Variations in BCA assay results could also be attributed to changes in the Protein to lipid ratio of OMV, which might vary due to different growth conditions and from strain to strain.

On the other hand, the Zetaview measures the number of particles (OMV) per unit volume. Due to the narrow measuring range of the instrument, samples have to be subjected to different dilutions (1:100 to 1:10,000) depending on their OMV concentrations, which might introduce variation in the results. Also, pipetting error could be a limitation for both methods. Although the analysis showed that both techniques were broadly in agreement with each other, they did not correlate closely. Therefore, the Zetaview is recommended for OMV quantification as it counts the actual number of particles. Whereas, the Pierce BCA- protein assay is recommended for proteomics study as the protein concentration within the OMV is essential for this type of analysis.

3.4.3. Association Between the Quantity of Isolated OMV and Bacterial Virulence

In this study, the quantification data of isolated OMV from broth and plate cultures were analysed to look for an association between OMV production and bacterial virulence. It has been shown that pathogenic strains can produce higher OMV than those non-pathogenic (Lai *et al.* 1981; Wai *et al.* 1995). However, the results showed no significant association between OMV production and bacterial virulence or pathogenicity ($p > 0.05$) (Figure 3.7). That might be due to the small number of strains/patients in the studied group. A larger group study is suggested for future

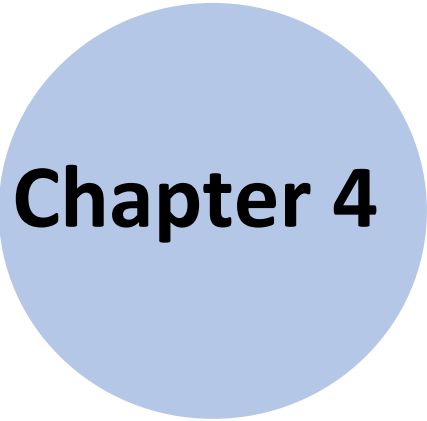
work to determine whether or not there is a significant association between OMV production and *H. pylori* virulence.

3.5. CHAPTER SUMMERY

Outer membrane vesicles (OMV) are naturally produced from pathogenic and non-pathogenic bacteria during growth. They contain virulence factors and other bacterial membrane structures. OMV have been reported to have different roles in pathogenesis including packing and delivery of virulence factors into host cells, alteration of host immune response, and protection of bacteria in stressful environments. Several variables affect the production and the structure of membrane vesicles. This study aimed to characterise *H. pylori* OMV and compare their production between pathogenic and non-pathogenic strains.

H. pylori strains from patients with and without gastric disease were grown in BHI broth with 0.2% β -cyclodextrin and on blood agar plates for 24 hours or in broth for 6 days. The OMV produced under each culture condition were purified by filtration and ultracentrifugation and characterised. OMV were quantified by Pierce BCA-protein assay and nanoparticle tracking analysis (ZetaView). The amount of OMV produced per bacterial cell was determined by Miles and Misra quantification of the bacteria and BacTiter-Glo assay (for late broth culture only).

There was no clear association between the quantity of OMV produced, and the virulence of the bacterial strain. However, the method of culturing *H. pylori* did affect OMV production and characteristics. *H. pylori* produced higher quantities of OMV in broth culture than on plates. Characteristics of *H. pylori* OMVs within a strain change depending on the environment in which the bacteria grow. This has potential consequences for the bacterial virulence, and this will be explored further in the next chapter.



Chapter 4

EFFECTS OF OMV ON MAMMALIAN CELLS

4. EFFECTS OF OMV ON MAMMALIAN CELLS

4.1. INTRODUCTION

H. pylori continuously releases outer membrane vesicles during active growth. These vesicles have several identified roles in cellular interactions and pathogenesis (see Section 1.5.1.). They function as a secretion system by packing and delivering their associated proteins to the target cells. They also support *H. pylori* survival within stressful environments such as bacterial biofilm and under antimicrobial treatment (Murray *et al.* 2020; Keenan 2000; Yonezawa *et al.* 2009). Outer membrane vesicles have different mechanisms to interact with and enter the target cells, delivering their virulence factors. OMV can cross the cellular membrane and enter into target cells via different routes (O'Donoghue and Krachler 2016) including membrane fusion. For instance, *P. aeruginosa* OMV membranes can fuse with those of the host epithelial cells (Bomberger *et al.* 2009; see O'Donoghue and Krachler 2016). This mechanism is still doubtful because of the differences between eukaryotic and prokaryotic membranes. However, this route might cause alteration to the host's cellular response.

Furthermore, OMV entry depends on their associated proteins and composition (Kaparakis-Liaskos and Ferrero 2015; Pathirana and Kaparakis-Liaskos 2016). For example, *Enterohemorrhagic E. coli* (EHEC) OMV containing hemolysin A (HlyA) can enter into host cells via the clathrin-mediated route (Bielaszewska *et al.* 2013; see O'Donoghue and Krachler 2016; Bielaszewska *et al.* 2017). This is initiated by HlyA binding to cell surface receptors, mediating OMV internalisation into host endothelial cells (Bielaszewska *et al.* 2013; see O'Donoghue and Krachler 2016; Bielaszewska *et al.* 2017). Similarly, *H. pylori* OMV containing VacA toxin can enter host gastric epithelial cells through endocytosis (Fiocca *et al.* 1999; Ricci *et al.* 2005; Parker *et al.* 2010). VacA facilitates OMV attachment to the cell surface as it is a membrane-associated protein, which triggers OMV uptake into the gastric epithelial cells (Fiocca *et al.* 1999; Ricci *et al.* 2005; Parker *et al.* 2010).

Besides that, *H. pylori* OMV are composed of LPS and lipids that can allow their entry into the gastric epithelial cells via lipid rafts (Olofsson *et al.* 2014; Kaparakis *et al.* 2010). Researchers reported a decrease in cellular uptake of OMV of *H. pylori* 60190

strain when cellular membrane lipids were disrupted by depletion of cholesterol (Olofsson *et al.* 2014; Kaparakis *et al.* 2010). The internalisation of OMV into host cells depends on the content and composition of OMV, but vesicle size can also affect and direct their entry pathway. OMV of Gram-negative bacteria are between 20 to 300 or 500 nm in diameter (Perez-Cruz *et al.* 2013; Zavan *et al.* 2018; Turner *et al.* 2015). Small vesicles enter mainly via clathrin- or caveolin-mediated and lipid rafts, as described above. Whereas vesicles sized more than 200 nm in diameter enter the cells via macropinocytosis (O'Donoghue and Krachler 2016). The size of *H. pylori* OMV in this study ranged between 100 and 120 nm (see Sections 3.4.1. and 3.5.1.). However, some strains produced larger OMV depending on their growth conditions (see Sections 3.4.1. and 3.5.1.). Endosomes containing OMV have previously been visualised in gastric cells suggesting that host cell endosomes facilitate OMV migration (Olofsson *et al.* 2014; Fiocca *et al.* 1999).

Outer membrane vesicles might be able to migrate from the infected site to another within the infected host. *H. pylori* OMV were observed in contact with the gastric epithelial cells of the infected host (Keenan *et al.* 2000; Fiocca *et al.* 1999). Also, a biopsy of an infected patient showed the attachment of vesicles onto the intestinal cells (Heczko *et al.* 2000). Therefore, migration of *H. pylori* OMV beyond gastric mucosa and the epithelial lining has been suggested. More importantly, CagA was detected in serum samples of patients infected with *H. pylori* and suffering gastric cancer (Shimoda *et al.* 2016). The CagA was found in serum-derived exosomes (Shimoda *et al.* 2016). It has been hypothesised that exosomes might serve as transporters that deliver CagA to different parts of the body and as CagA is an oncogenic protein that might cause extragastric disorders (Shimoda *et al.* 2016). Moreover, OMV migration beyond the infection site was also observed in *Neisseria meningitidis* as OMV were found in the blood and the cerebrospinal fluid of patients with meningitis (Namork and Brandtzage 2002; Bjerre *et al.* 2000).

Several *in vitro* and *in vivo* studies have been conducted on *H. pylori* OMV previously. It seems that OMV are cytotoxic to the gastric epithelial cells and might contribute to gastric diseases. *H. pylori* OMV contain lipids and different proteins, including toxins and virulence factors that are related to adherence, cytotoxicity, acid resistance, and others (see Section 1.5.2.). Two significant virulence factors found within *H. pylori*

OMV are CagA and VacA (Olofsson *et al.* 2010; Fiocca *et al.* 1999; Zavan *et al.* 2018; Choi *et al.* 2017; Mullaney *et al.* 2009). CagA is a cytotoxin injected into host cells via the type IV secretion system, mainly at the tight junction between epithelial cells (see Section 1.3.3.) (Turkina *et al.* 2015). CagA is associated with gastric cancer and ulcers because it damages the gastric mucosa, works on breaking the tight junctions and causing loss of cells polarity and integrity (Turkina *et al.* 2015). Consequently, the elongation of epithelial cells would occur (Parker *et al.* 2010). After decades of infection, this disruption can cause gastric or duodenal ulcers, and ultimately might progress to cancer. VacA is an exotoxin secreted in the growth environment that also causes gastric mucosal injury (Molinari *et al.* 1997). VacA also binds and enters into the cells and generates vacuoles. Furthermore, it might affect gastric epithelial cells' integrity and induce cellular apoptosis (see Section 1.3.4.) (Papini *et al.* 1998; Wang *et al.* 2009).

H. pylori is a polymorphic pathogen. It has very high recombination and mutation rates even within its virulence genes depending on various factors (see Section 1.3.). That results in a diversity of *H. pylori* strains and their virulence factors, for example, the *vacA* polymorphisms (see Section 1.3.4.). Therefore, infection severity and disease progression vary greatly among infected people. Polymorphisms of *H. pylori* also affect OMV characteristics and composition, which might affect their invasion into and effects on the gastric epithelial cells. Previous studies have showed that there is substantial variation in the protein contents within OMV of different *H. pylori* strains (reviewed by Parker and Keenan 2012). Thus, the effects of *H. pylori* OMV on gastric epithelial cells and their roles in pathogenesis might also be different, depending on the type and quantity of each OMV-associated protein.

4.2. AIM OF THIS STUDY

Although several studies have previously been conducted to identify the role of *H. pylori* OMV in pathogenesis, there are still controversies and gaps in our understanding. Therefore, further studies are needed to fully characterise the cytotoxic effects of *H. pylori* OMV and the impacts of *H. pylori* polymorphisms and strain variations on OMV cytotoxicity.

This chapter aimed to characterise the cytotoxic effects of OMV produced by *H. pylori* strains with high and low virulence, under different growth conditions, on human gastric epithelial cells. The research questions were:

- Are OMV produced by virulent *H. pylori* strains more toxic to human gastric epithelial cells than OMV produced by less virulent *H. pylori* strains?
- Do the bacterial growth conditions influence the cytotoxicity of the OMV produced by *H. pylori*?

4.3. MATERIAL AND METHODS

4.3.1. *H. pylori* OMV

Outer membrane vesicles of *H. pylori* 444A, 221A, Tx30a, and 60190 strains isolated from early broth (1 day), late broth (6 days), and plate (24 hours) cultures (see Section 2.4.2.) were used in this study.

4.3.2. Cell Culture

Human gastric adenocarcinoma (AGS) cells (ATCC CRL-1739) were used in this study. Cells were grown in F-12K media with 10% HI-FCS and maintained three times a week as described previously in Chapter 2 (see Section 2.5.1). The purity of AGS cells was confirmed using the *Mycoplasma* detection test (see Section 4.3.4.).

4.3.3. OMV cytotoxicity

Minimally passaged AGS cells were harvested, washed and added to the wells of 96-well plates at a concentration 1×10^5 cells/ml. After 24 hours incubation for growth and adherence, the cells were treated with a range of OMV concentrations (0-50 $\mu\text{g}/\text{ml}$). After a further 24 hours incubation, OMV cytotoxicity was determined by CellTiter 96 assay as an endpoint assay (see Section 2.5.2.1.). Cytotoxicity over the full 24 hours of OMV treatment was determined by RealTime-Glo MT cell viability assays (see Section 2.5.2.2.).

4.3.4. *Mycoplasma* Detection Test

Mycoplasma is a microscopic bacterium (~100 nm). These bacteria lack a cell wall. Therefore, they are resistant to beta-lactam antibiotics and other antibiotics that target cell wall synthesis (InvivoGen, 2016). *Mycoplasma* utilises the host cells to survive, causing damage to the host cells' genomic material (InvivoGen, 2016). AGS cells and other cell lines might become contaminated with *Mycoplasma* either due to using contaminated culture media or other reagents or from laboratory workers infected with *Mycoplasma fermentans* or *Mycoplasma orale* (InvivoGen, 2016). Also, cell lines might be received from another laboratory with *Mycoplasma* infection. Therefore, the AGS cells were purchased directly from ATCC, especially for this study, and were minimally passaged before use.

The purity of AGS cells was confirmed by the EZ-PCR *Mycoplasma* detection Kit (Biological Industries). One millilitre of cell culture supernatant was transferred into a 1.5 ml sterile Eppendorf centrifuge tube and centrifuged at 250 *xg* for 5 minutes to pellet down cellular debris. The supernatant was then transferred into a new sterile 1.5 ml tube and centrifuged at 15,000 *xg* for 10 minutes to pellet the *Mycoplasma*. The supernatant was discarded, and the pellet was re-suspended with 50 μ l of supplied buffer solution and mixed well. The sample was then heated to 95°C for 3 minutes and then stored at -20°C until used. The PCR amplification and gel electrophoresis were conducted by Grace Atobatele at Nottingham Trent University following the manufacturer's instructions.

4.3.5. Statistical Analysis

All data were analysed using GraphPad Prism software version 8 for Mac IOS. All differences between the percentage survival of treated human gastric epithelial cells with OMV of each strain isolated from different conditions were compared using two-way ANOVA of variance with multiple comparisons. Similarly, two-way ANOVA of variance with multiple comparisons was performed to compare differences between the Real-time OMV effect on AGS cells treated with OMV of each strain isolated from different conditions and untreated AGS cells. No statistical analysis was performed on differences in cell viability and cell death of treated AGS cells with OMV of each strain isolated from different conditions and untreated AGS cells. Probability (*p*) value < 0.05 (*), < 0.01 (**), < 0.001 (***), and < 0.0001 (****) were considered statistically significant. Error bars on the graphs show three individual repeats of experiments performed in triplicates with the standard deviations (SD) for replicates.

4.4. RESULTS

OMV of four *H. pylori* strains (444A, 221A, 60190, and Tx30a) were used in this study. *H. pylori* strain 444A (high virulence, *vacA* s1 i1 m1, *cagA*+, high biofilm former) was isolated from a patient suffering gastric ulceration disease with moderate Sydney scores including intestinal metaplasia. Whereas, strain 221A (low virulence, *vacA* s1 i2 m2, *cagA*-, low biofilm former) was isolated from a patient not suffering such ulcer disease, and with lower Sydney scores indicating little or no inflammation or metaplasia (Table 2.1). Strains 60190 and Tx30a are control strains with high and low virulence, respectively (Table 2.1). OMV produced by these four strains were isolated from different environments (early broth, late broth, and plate cultures). Differences in OMV toxicity on human gastric epithelial cells were determined using CellTiter 96 assay, an endpoint assay which measured cell viability after 24 hours, and Realtime-Glo MT cell viability assay, which was used to measure cell viability at regular timepoints over 10 hours with a final timepoint at 24 hours. In addition, live cell analysis was conducted using the IncuCyte instrument, which allowed visual monitoring of the cells and also measured cell viability over 24 hours.

4.4.1. *Mycoplasma* detection

AGS cells (ATCC CRL-1739) used in this study were tested for their purity from *Mycoplasma* contamination. AGS cells were analysed by 2% agarose gel electrophoresis. No *Mycoplasma* has detected in AGS cells samples compare to controls (Figure 4.1). Only one PCR product (357 bp) was detected in both screened samples (Figure 4.1). *Mycoplasma* negative control showed only one PCR product (357 bp), whereas positive control showed two PCR products (357 bp and 270 bp) (Figure 4.1).

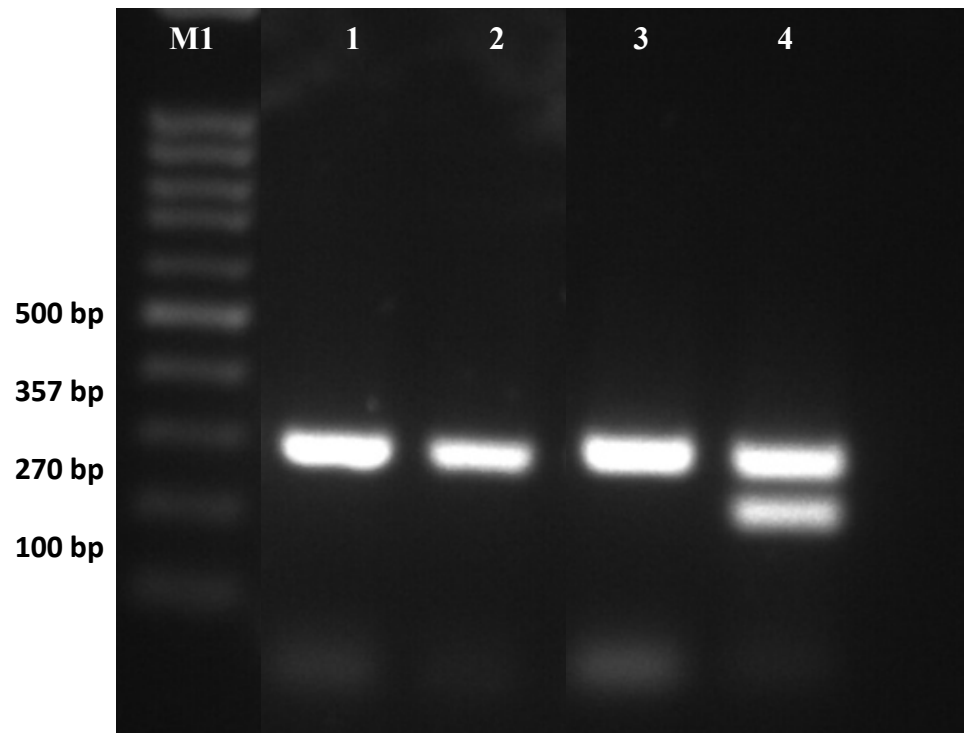


Figure 4.1: Detection of *Mycoplasma* in AGS cells. Agarose gel electrophoresis (2% agarose gel with 0.2 $\mu\text{g}/\text{ml}$ of ethidium bromide) of PCR amplified products using complimentary *Mycoplasma* template. Lanes 1 and 2 for AGS cells. Lane 3 for *Mycoplasma* negative control. Lane 4 for *Mycoplasma* positive control. M1= 100 bp DNA ladder (Biological Industries). PCR products (357 bp) were detected in both screened samples and negative control. Postive control showing the presence of 357 bp and 270 bp fragments in lane 4.

4.4.2. OMV cytotoxicity

4.4.2.1. Effect of OMV on AGS cells after 24 hours (CellTiter assay)

All isolated OMV of 4 *H. pylori* strains from three different growth conditions were analysed for their toxicity on the human gastric epithelial cells after 24 hours treatment. A high concentration (50 $\mu\text{g}/\text{ml}$) of OMV of strains 60190 and 444A isolated from plate cultures was significantly toxic to AGS cells compared to untreated cells ($***p < 0.001$ and $**p < 0.01$, respectively) (Figure 4.2). Similarly, 444A OMV isolated from late broth cultures were significantly toxic to AGS cells compared to untreated cells ($**p < 0.01$). However, although toxicity of 60190 OMV isolated from late broth cultures was evident, this did not reach statistical significance. (Figure 4.2). OMV of all four strains isolated from early broth cultures did not show a toxic effect on AGS compared to untreated cells (Figure 4.2). However,

early broth OMV from strain 221A significantly *increased* %survival of AGS cells compared to 221A OMV isolated from late broth cultures (** $p < 0.01$) (Figure 4.2).

Effects of OMV on cell viability were dose-dependent. Lower doses of OMV of 60190 and 444A strains isolated from early and late broth cultures slightly induced cells proliferation compared to those untreated cells. However, this was not statistically significant (Figure 4.3 A and C). Also, Tx30a OMV from plate cultures significant increased %survival of AGS cells at concentrations 50 $\mu\text{g}/\text{ml}$ and 12 $\mu\text{g}/\text{ml}$ compared to untreated cells (**** $p < 0.0001$ and *** $p < 0.001$) (Figure 4.3 D). OMV from strain 221A isolated from early broth, late broth, and plate cultures had no significant effects on cell viability in the dose-response CellTiter assay (Figure 4.3 B).

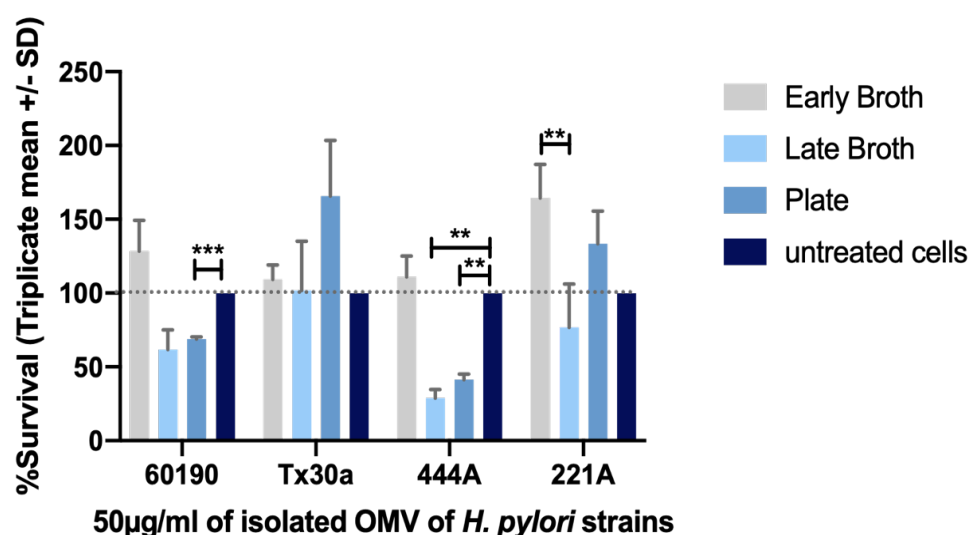


Figure 4.2: Effects of high dose of OMV on human gastric epithelial cells. AGS cells were treated with 50 $\mu\text{g}/\text{ml}$ of OMV of 4 *H. pylori* strains isolated from early, late broth and plate cultures in triplicate and incubated in 5% CO_2 for 24 hours at 37 $^\circ\text{C}$. Promega CellTiter 96 assay reagent was added, mixed well, and incubated for 1 hour at 37 $^\circ\text{C}$ before measuring the absorbance at 490 nm. Two-way ANOVA analysis was performed to test the significance of difference between the percentage survival of human gastric epithelial cells treated with OMV of each strain. The percentage survival of AGS cells compared against untreated control cells are shown. Error bars show the mean of blank corrected values of three independent replicates (+/- SD). *** and ** indicate $p < 0.001$ and < 0.01 , respectively.

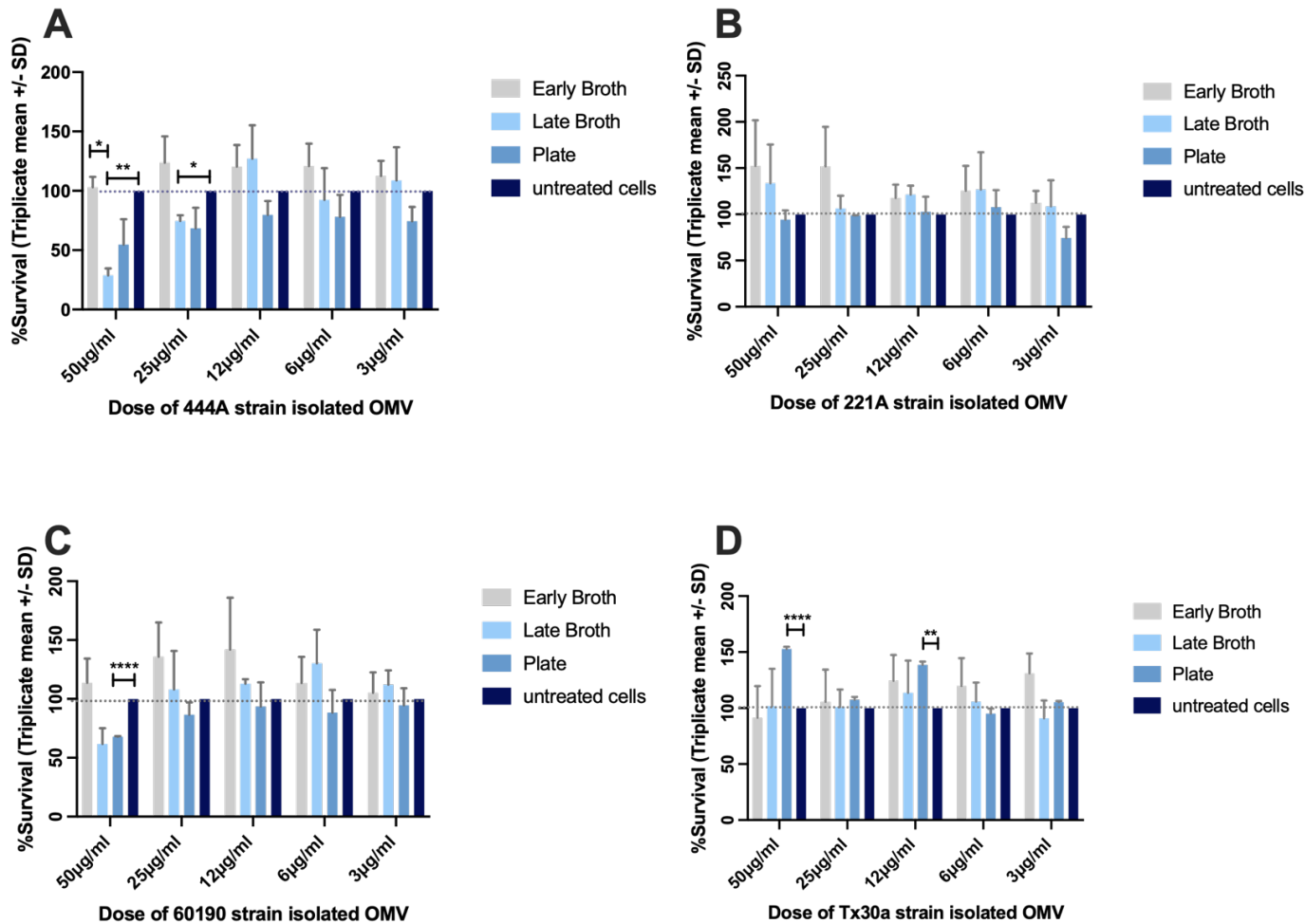


Figure 4.3: Effects of a range of doses of OMV on human gastric epithelial cells. AGS cells were treated with different doses (0-50 µg/ml) of of (A) 444A, (B) 221A, (C) 60190, and (D) Tx30a OMV from early and late broth and plate cultures in triplicate and incubated in 5% CO₂ for 24 hours at 37 °C. Promega CellTiter 96 assay reagent was added, mixed well, and incubated for 1 hour at 37 °C before measuring the absorbance at 490 nm. The percentage survival of OMV treated compared to untreated control cells are shown. Error bars show the mean of blank corrected values of three independent replicates (+/- SD). ****, **, and * indicate $p < 0.0001$, < 0.01 , and < 0.05 , respectively from two-way ANOVA with Tukey post-hoc tests.

4.4.2.2. Effects of OMV on AGS cell viability over 24 hours (Realtime Glo assay)

AGS cells were treated with 25 µg/ml of OMV of 4 *H. pylori* strains isolated from three different growth conditions. The viability of the AGS cells was measured using a Realtime Glo assay at regular time points over 10 hours, with a final reading at 24 hours. In this assay, OMV from strains 60190 and Tx30a had no significant effects on AGS cell viability compared to untreated cells ($p > 0.05$) (Figure 4.4 C and D). At 24 hours, AGS cells treated with 60190 OMV isolated from plate cultures had decreased cell viability compared to untreated cells (Figure 4.3 C), but this did not reach statistical significance ($p > 0.05$) (Figure 4.4 C).

OMV isolated from early broth cultures of all four *H. pylori* strains caused a decrease in treated AGS cells viability compared to untreated cells; however, not statistically significant ($p > 0.05$) (Figure 4.4).

444A OMV isolated from early broth cultures significantly decreased AGS cell viability at 8 and 10 hours compared to untreated cells ($*p < 0.05$) (Figure 4.4 A). Whereas 444A OMV isolated from late broth cultures significantly *increased* cell proliferation at 3 hours compared to untreated cells ($***p < 0.001$) (Figure 4.4 A) but this increase was not significant at the other time points and overall, little difference was seen between treated and untreated cells (Figure 4.4 A). 444A OMV isolated from plate cultures also had no effect on AGS cells in this assay. 221A OMV isolated from late broth cultures also caused a significant increase in AGS cell proliferation at 3 hours compared to untreated cells ($*p < 0.05$) (Figure 4.4 B) but again this increase was not significant at the other time points. Overall, 221A OMV from late broth and plate cultures had little effect on AGS cells in this assay.

Taken together, the results from all strains and growth conditions for this assay indicate that at a dose of 25 µg/ml, OMV isolated from early broth cultures of virulent strains somewhat reduce AGS cell viability but OMV isolated from late broth or plate cultures of virulent strains, or any of the tested growth conditions from less virulent strains, have little effect.

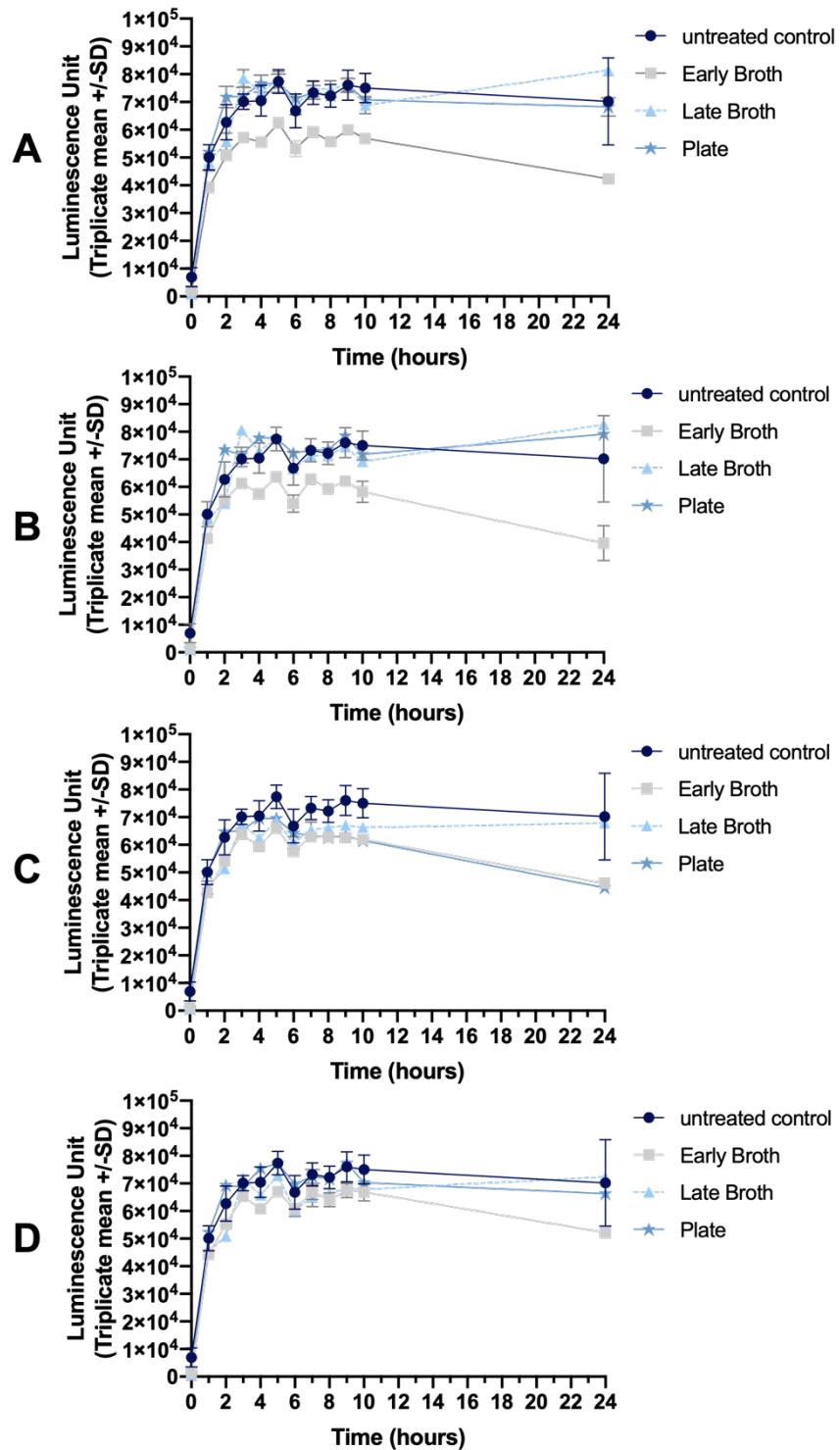


Figure 4.4: Real-time effects of OMV on human gastric epithelial cells. AGS cells were treated with 25 $\mu\text{g/ml}$ of OMV of (A) 444A, (B) 221A, (C) 60190, and (D) Tx30a *H. pylori* strains isolated from early and late broth and plate cultures in triplicate with 1X Promega Realtime-Glo substrate and enzyme. Treated cells were incubated in 5% CO_2 condition for 24 hours at 37 $^\circ\text{C}$. Luminescence was measured hourly. Two-way ANOVA analysis was performed and the results are summarised in the main text. Error bars show the mean of blank corrected values of three independent replicates (\pm SD).

4.4.3. Live OMV-AGS cells image-based (Incucyte) analysis

AGS cells were treated with 50 µg/ml of OMV of 4 *H. pylori* strains isolated from three different growth conditions. The effects of the OMV on the AGS cells were monitored over 24 hours by microscopy using an automated system to determine %confluence (label free) and cell death (red staining). Due to condensation on the lids of the 96-well plates, microscopy images were unclear at some timepoints, including 0, 3-5, 7-8, 10-12, 14, 16-17, 19-24 hours, especially in treated cells so measurements at these timepoints were excluded from the analysis. AGS cells treated with 221A OMV isolated from plate cultures were also excluded from the analysis due to condensation. No statistical analysis was performed for this study because of the missing data due to condensation which affected some measurements.

4.4.3.1. Cell viability (% confluence)

Untreated AGS cells steadily increased in confluence over time, with an overall increase of 23 percentage points over 18 hours (Figures 4.5 and 4.6). AGS cells treated with OMV of virulent *H. pylori* strains (444A and 60190) isolated from the early broth, late broth, and plate cultures induced some AGS cell proliferation at the first and second hours. But then the proliferation appeared to be inhibited because the %confluence of treated cells did not continue to increase over time, compared to untreated cells (Figure 4.5 A and C). OMV of 444A strain isolated from early broth cultures induced more cell proliferation than 444A OMV isolated from late broth and plate cultures (Figure 4.5 A). Also, 444A OMV isolated from early broth cultures inhibited AGS cells proliferation as the overall increase was zero percentage points over 18 hours, or on the other hand, this may indicate a balance between killed and growing cells (Figure 4.6 A). OMV of 60190 strain isolated from plate cultures induced more cell proliferation than those isolated from other growth conditions, with an overall increase of 20 percentage points over 18 hours (Figures 4.5 C and 4.6 C).

On the other hand, AGS cells treated with low virulence *H. pylori* strains (221A and Tx30a) isolated from early and late broth cultures had little to no proliferative response, with the %confluence of treated cells only slightly increasing over time. (Figure 4.6 B and D) (Figure 4.6 B and D). No cytotoxic or inhibitory effects were seen

over time on AGS cells treated with Tx30a OMV isolated from plate cultures (Figure 4.5 D).

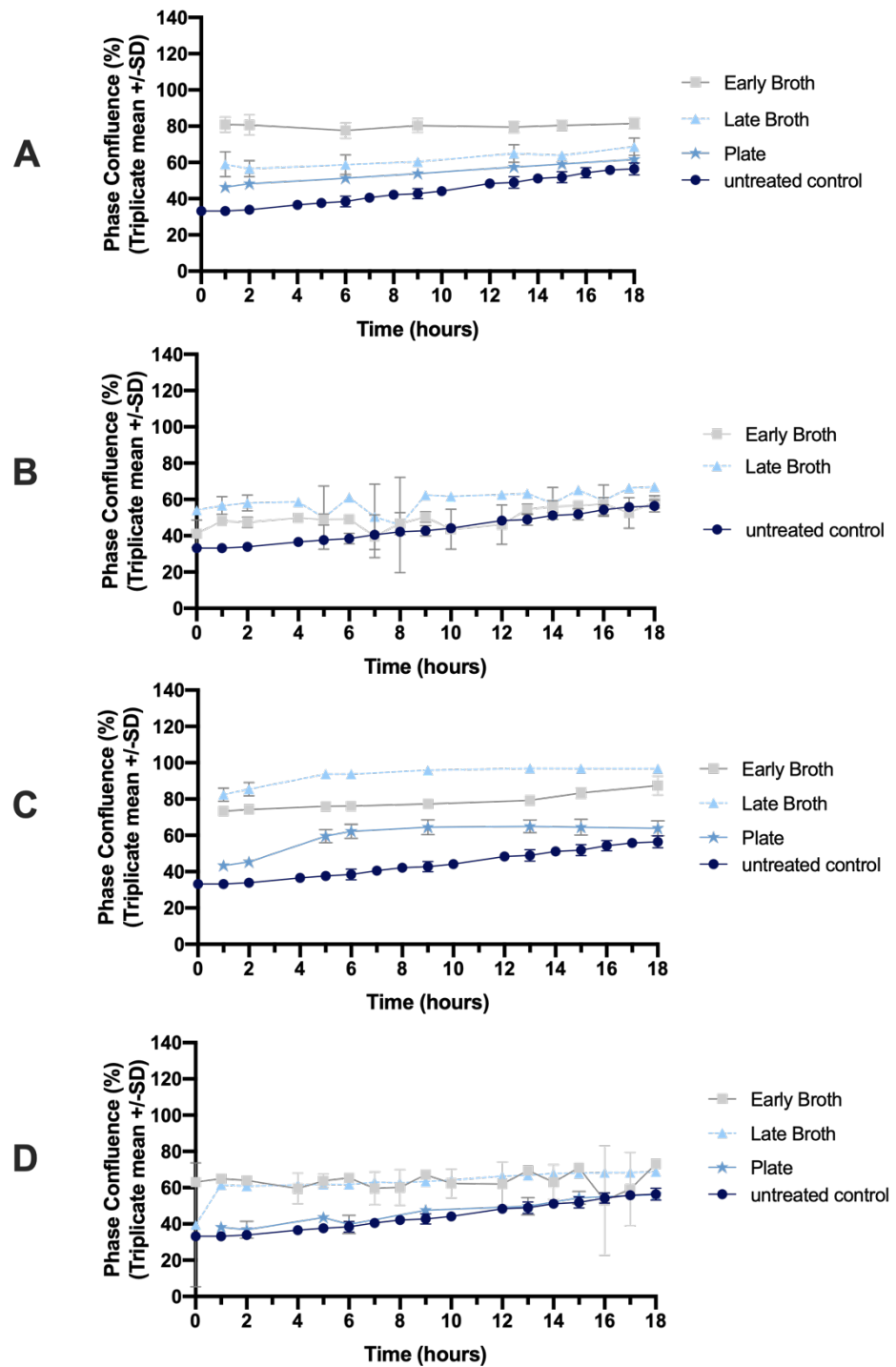


Figure 4.5: Confluence of human gastric epithelial cells treated with *H. pylori* OMV. AGS cells were treated with 50 μ g/ml of isolated OMV of (A) 444A, (B) 221A, (C) 60190, and (D) Tx30a *H. pylori* strains isolated from early and late broth and plate cultures in triplicate. Treated cells were incubated in 5% CO₂ condition for 18 hours at 37 °C and phase confluence (%) was measured. Error bars show the mean of blank corrected values of independent replicates (\pm SD).

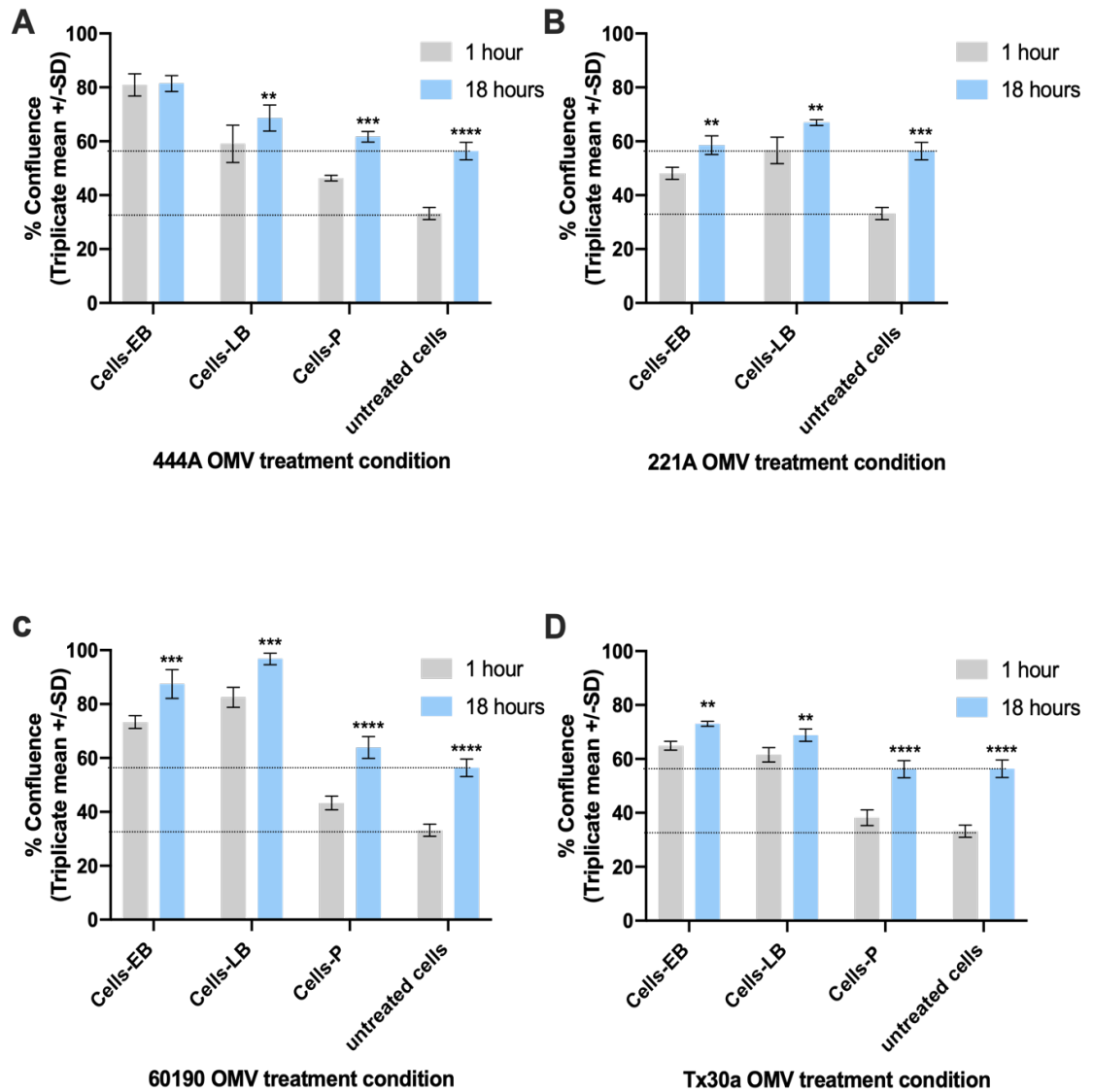


Figure 4.6: Effect of each OMV treatment on % confluence of human gastric epithelial cells. AGS cells were treated with 50 $\mu\text{g}/\text{ml}$ of isolated OMV of (A) 444A, (B) 221A, (C) 60190, and (D) Tx30a *H. pylori* strains isolated from early and late broth and plate cultures in triplicate. Treated cells were incubated in 5% CO_2 condition for 24 hours at 37 $^\circ\text{C}$ and phase confluence (%) was measured. The overall effect of each treatment on % confluence compared to untreated cells are shown. Comparison between 1 and 18 hours was performed using two-way ANOVA with Tukey post-hoc tests. Error bars show the mean of blank corrected values of independent replicates (+/- SD). ****, **, and * indicate $p < 0.0001$, < 0.01 , and < 0.05 , respectively from two-way ANOVA with Tukey post-hoc tests.

4.4.3.2. Cell death

Addition of the Incucyte Cytotox Red Dye allowed real time monitoring of cytotoxicity, measured by red fluorescence as the dye interacted with DNA released from dead/dying cells. No cell death was detected in the untreated control cells (Figure 4.7). Treatment with OMV of virulent *H. pylori* strains (444A and 60190) isolated from early broth and late broth cultures caused high dead cell readouts from this assay, which decreased slightly over time (Figure 4.7 A and C). However, 444A and 60190 OMV isolated from plate cultures appeared to be much less cytotoxic (Figure 4.7 A and C).

On the other hand, very little cell death was detected over time in AGS cells treated with OMV from low virulence *H. pylori* strains (221A and Tx30a), except for modest cytotoxic effects of 221A OMV from late broth cultures and Tx30a OMV from early broth cultures (Figure 4.7 B and D).

All the cell death data from the Incucyte had limited reliability because the images showed spots of red dye in some areas (see Section 4.4.3.3.), which interfere with dead cells measurements. Moreover, some red areas did not appear to co-localise with real dead cells, as shown on the images in Section 4.4.3.3, especially those of AGS cells treated with OMV of Tx30a strain isolated from early broth cultures (Table 4.7).

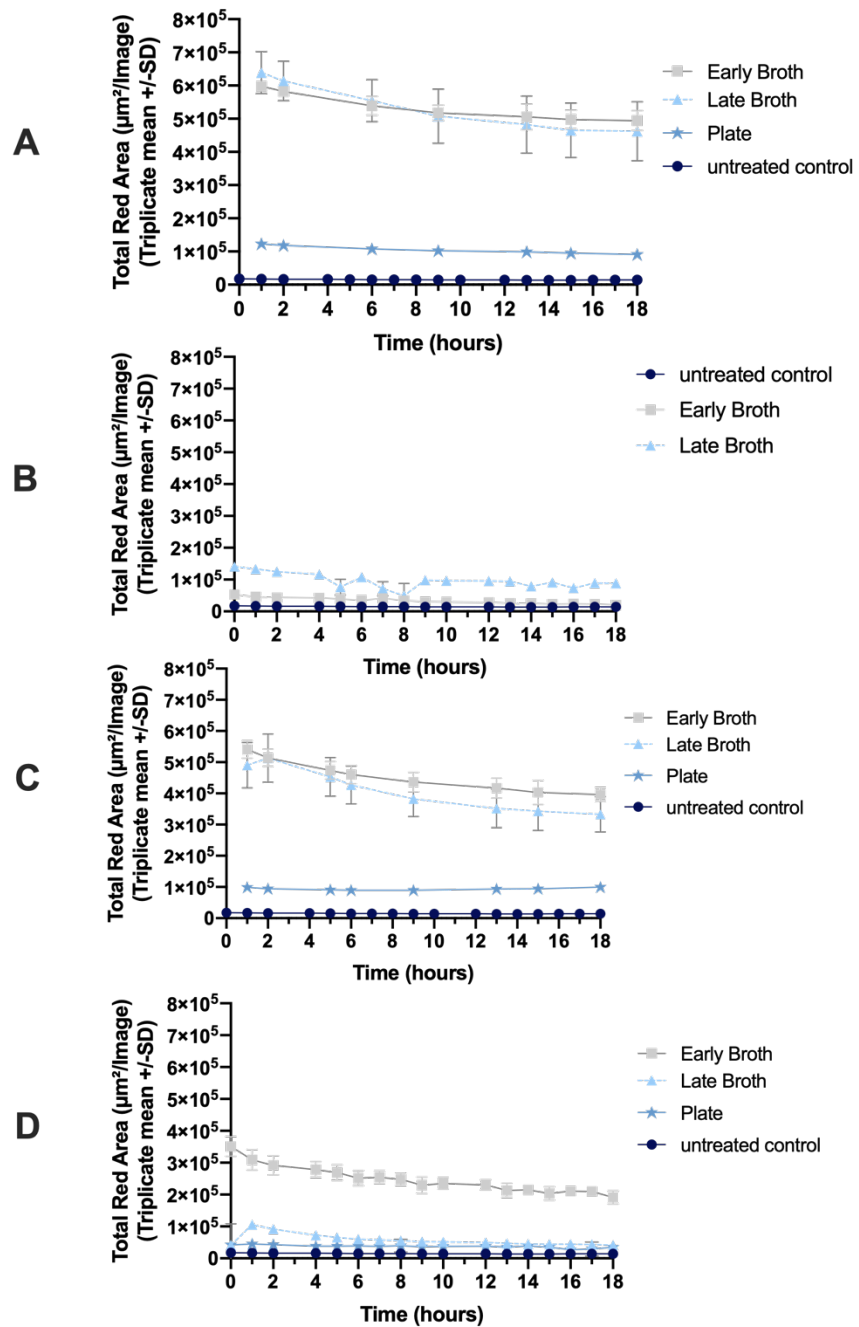


Figure 4.7: Cell death of human gastric epithelial cells treated with *H. pylori* OMV. AGS cells were treated with 50 µg/ml of isolated OMV of (A) 444A, (B) 221A, (C) 60190, and (D) Tx30a *H. pylori* strains isolated from early and late broth and plate cultures in triplicate with IncuCyte Cytotox Red Reagent. Treated cells were incubated in 5% CO₂ condition for 18 hours at 37 °C and cell death count was measured. Error bars show the mean of blank corrected values of independent replicates (\pm SD). Dead cells expressed as total red area.

4.4.3.3. Microscopy analysis of OMV treated cells

All images obscured by condensation were excluded from the analysis. The other images were categorised based on treatment conditions and exposure time points. Images were then numbered, and only one image was randomly selected out of around 12 images per treatment per time point, using Random Picker 2.1 software for IOS (Random Picker;URL). Images presented in this study show the effects of OMV on AGS cells at different time points. The IncuCyte Cytotox Red Dye was used in this study to detect dead cells. However, the red area per image did not seem to correlate well with cell death, and the red dye did not always co-localise well with dead or dying cells in the microscopy images inspected.

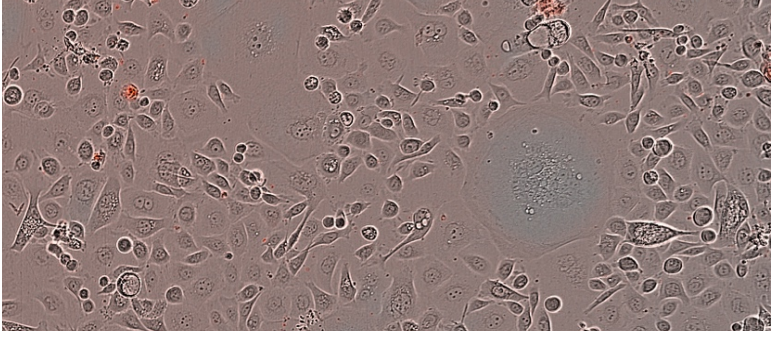
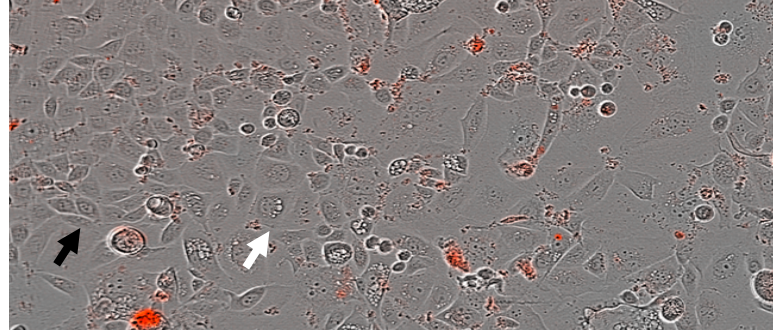
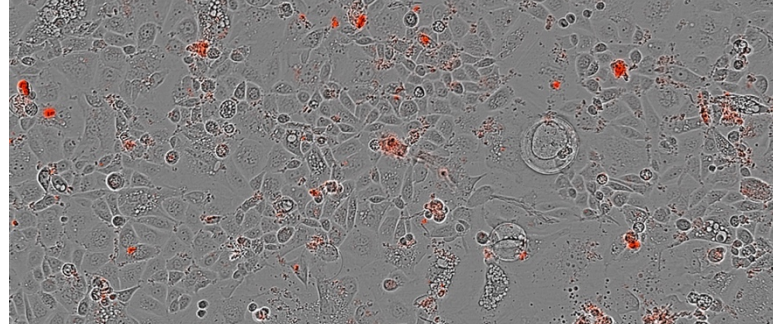
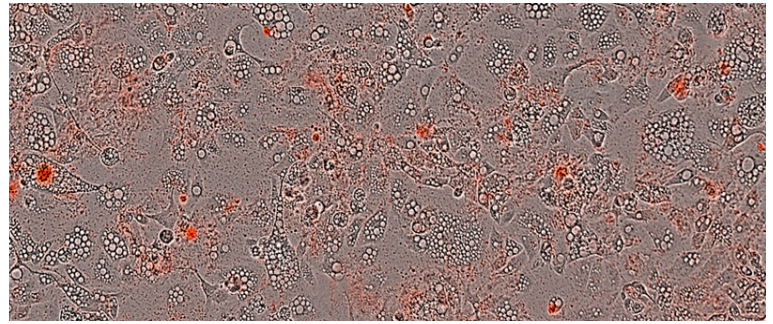
From inspection of the microscopy images, it was clear that some OMV-treated cells showed evidence of the vacuolating activity of the *H. pylori* toxin VacA. Therefore, to study this more quantitatively a four-tier grading score scheme was used to describe the presence and extent of vacuolation (Table 4.1).

Untreated cells at time points 0, 6, 12, and 18 hours appeared to be healthy and grew well over time (Table 4.2). AGS cells treated with *H. pylori* 444A OMV isolated from early broth cultures had grade 1 perinuclear vacuoles after 6 hours and grade 1 large vacuoles were visible after 18 hours (Table 4.3). Grade 2 perinuclear and large vacuoles were also observed in AGS cells treated with *H. pylori* 444A OMV isolated from plate cultures after 18 hours, though none were seen at the 6 hours time point (Table 4.3). On the other hand, no vacuoles (grade 0) were seen in AGS cells treated with *H. pylori* 444A OMV isolated from late broth cultures at either 6 or 18 hours (Table 4.3). Moreover, some elongated cells (hummingbird phenotype) (Figure 4.8) were seen 6 and 18 hours after treatment with *H. pylori* 444A OMV isolated from all growth cultures, indicating activity of the CagA toxin (Table 4.3).

Similarly, AGS cells treated with *H. pylori* 60190 OMV isolated from the early broth, late broth, and plate cultures showed grade 3 perinuclear and large vacuoles after 18 hours (Table 4.5). Grade 2 vacuoles were also seen in AGS cells treated with *H. pylori* 60190 OMV isolated from plate cultures after 6 hours (Table 4.5). In addition, there were some hummingbird cells (Figure 4.8) present after 6 and 18 hours incubation in the presence of 60190 OMV from all three growth conditions (Table 4.5). No vacuoles

(grade 0) were observed in AGS cells treated with any of the OMV preparations from the less virulent *H. pylori* strains 221A (Tables 4.4) or Tx30a (Tables 4.6). Effects of OMV on AGS cells were summarised in Table 4.7.

Table 4.1: Vacuolation grading score.

Grade	Indication	Example
0	No vacuoles	
1	Mild vacuoles	
2	Moderate vacuoles	
3	Severe vacuoles	

Black arrow = normal epithelial cells; white arrow = vacuoles epithelial cells

Table 4.2: Images of untreated AGS cells at time points 0, 6, 12, and 18 hours.

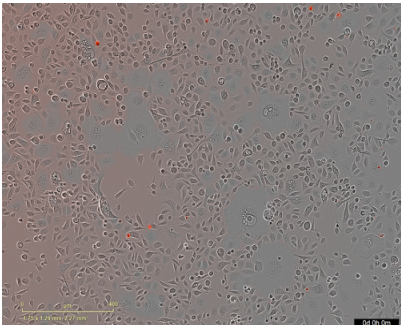
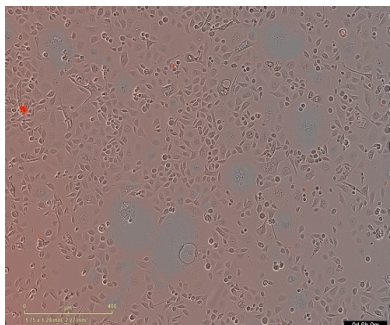
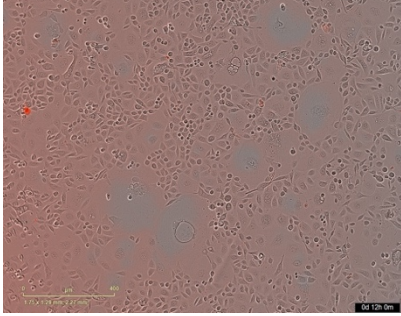
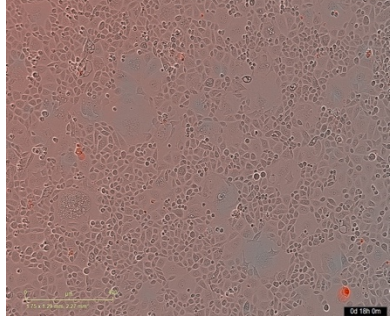
Timepoint	Untreated cells		Timepoint
0 hour			6 hours
12 hours			18 hours

Table 4.3: Images of AGS cells treated with OMV of *H. pylori* 444A strain at time points 6 and 18 hours.

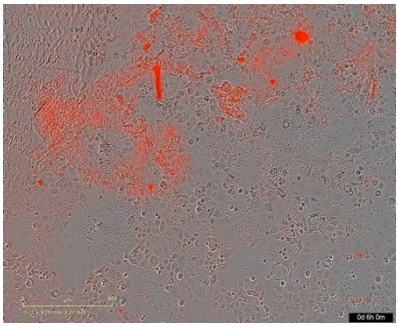
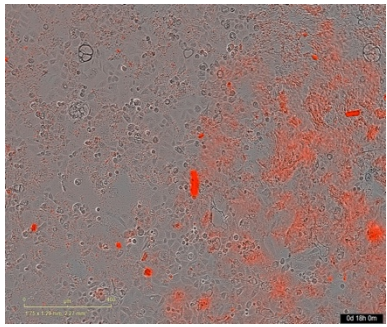
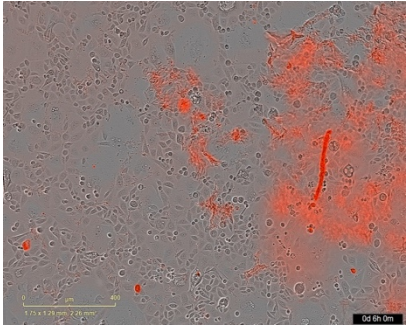
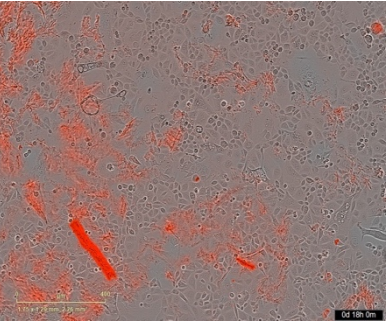
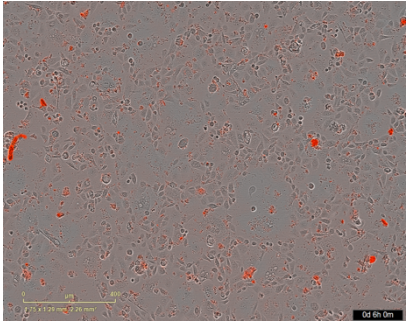
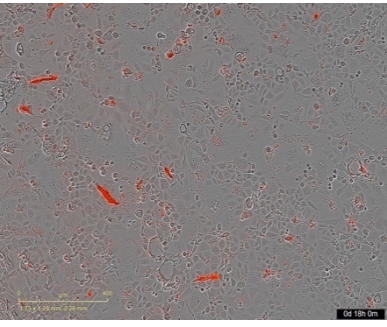
Timepoint	Treated cells with 444A OMV (Early broth)		Timepoint
6 hours			18 hours
Timepoint	Treated cells with 444A OMV (Late broth)		Timepoint
6 hours			18 hours
Timepoint	Treated cells with 444A OMV (Plate)		Timepoint
6 hours			18 hours

Table 4.4: Images of AGS cells treated with OMV of *H. pylori* 221A strain at time points 0, 6, 12, and 18 hours.

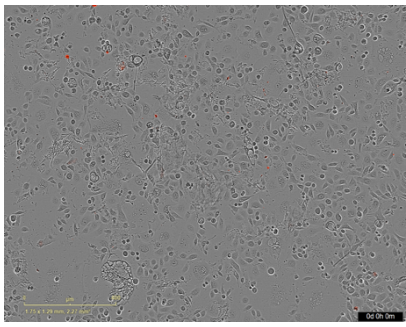
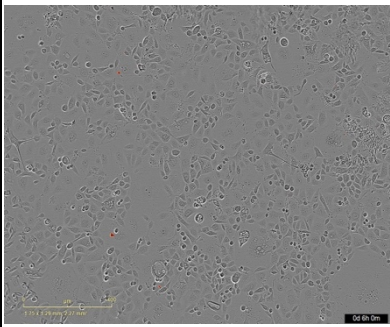
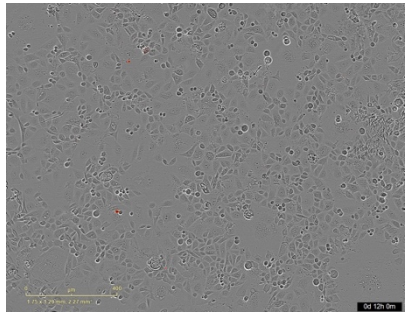
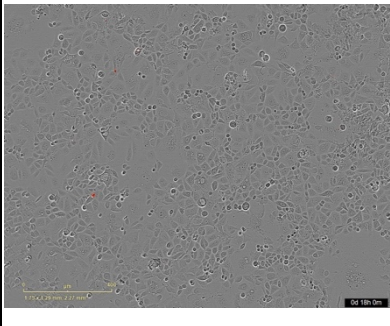
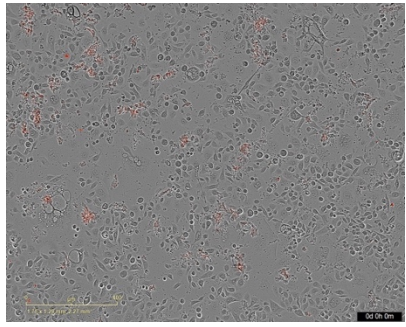
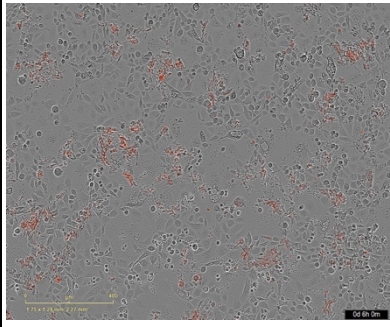
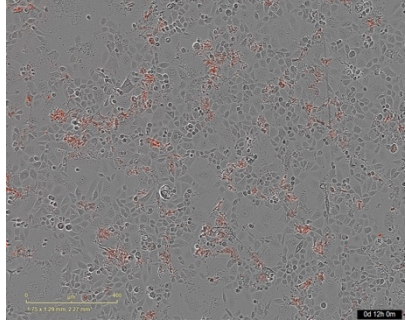
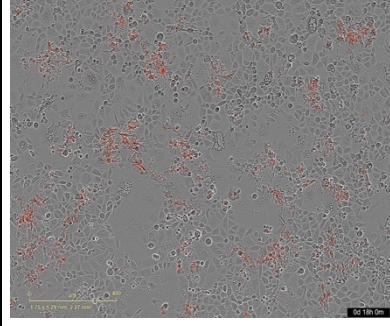
Timepoint	Treated cells with 221A OMV (Early broth)		Timepoint
0 hour			6 hours
12 hours			18 hours
Timepoint	Treated cells with 221A OMV (Late broth)		Timepoint
0 hour			6 hours
12 hours			18 hours

Table 4.5: Images of AGS cells treated with OMV of *H. pylori* 60190 strain at time points 6 and 18 hours.

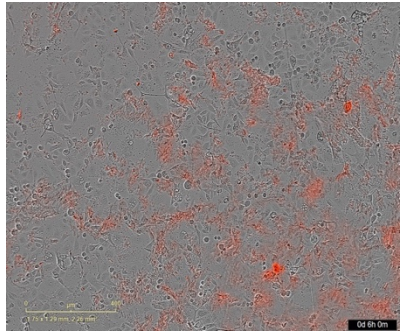
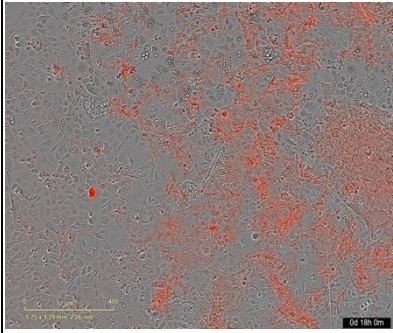
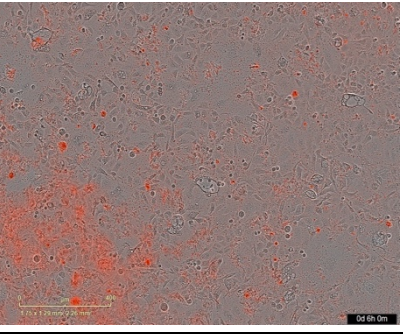
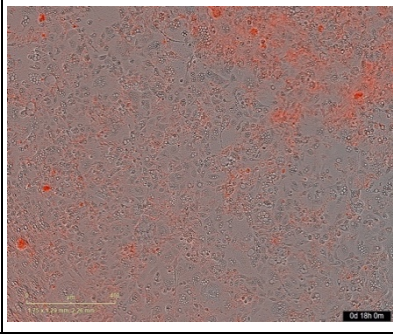
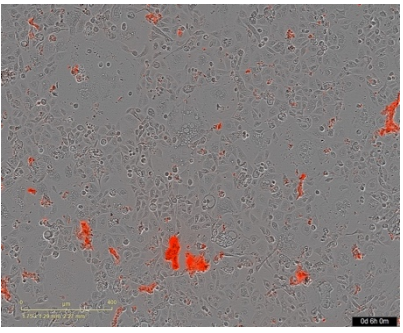
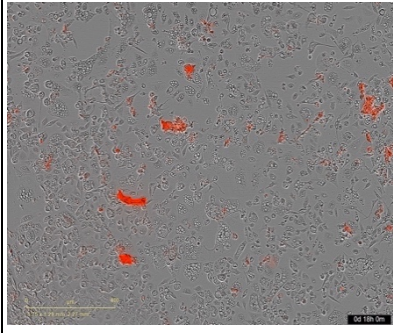
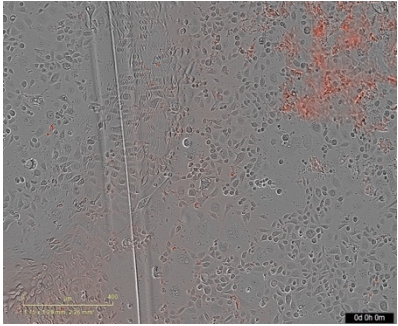
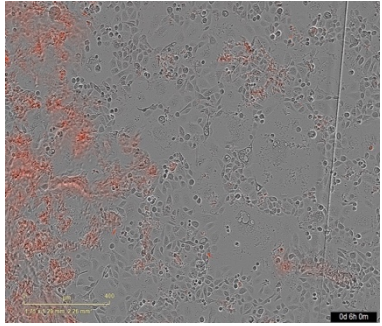
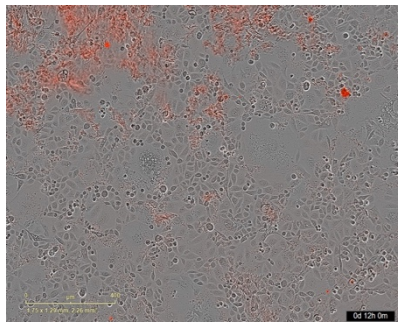
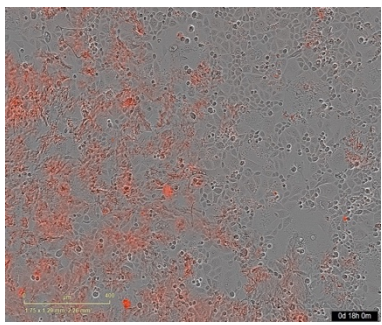
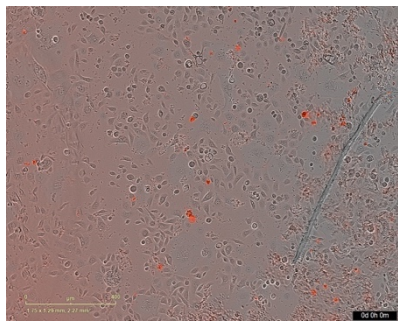
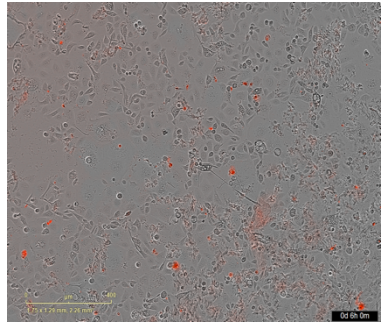
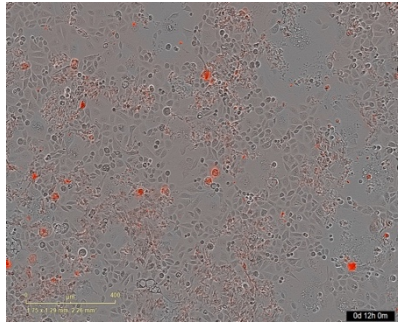
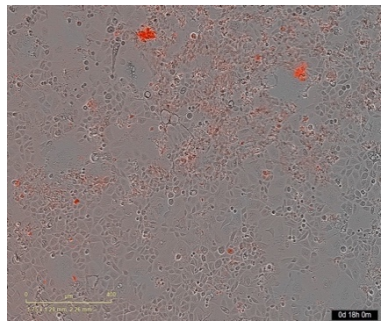
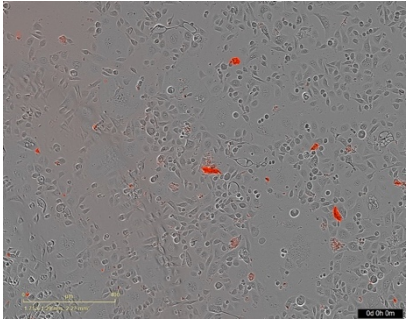
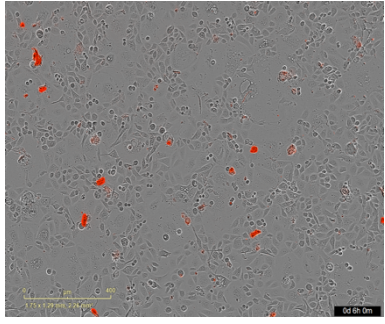
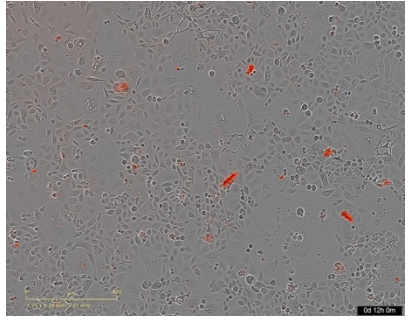
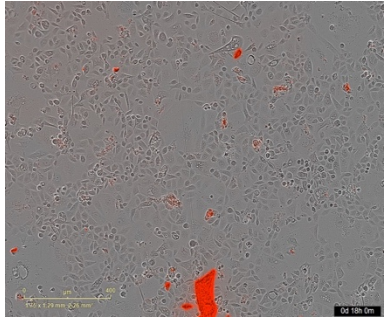
Timepoint	Treated cells with 60190 OMV (Early broth)		Timepoint
6 hours			18 hours
Timepoint	Treated cells with 60190 OMV (Late broth)		Timepoint
6 hours			18 hours
Timepoint	Treated cells with 60190 OMV (Plate)		Timepoint
6 hours			18 hours

Table 4.6: Images of AGS cells treated with OMV of *H. pylori* Tx30a strain at time points 0, 6, 12, and 18 hours.

Timepoint	Treated cells with Tx30a OMV (Early broth)		Timepoint
0 hour			6 hours
12 hours			18 hours
Timepoint	Treated cells with Tx30a OMV (Late broth)		Timepoint
0 hour			6 hours
12 hours			18 hours

Timepoint	Treated cells with Tx30a OMV (Plate)		Timepoint
0 hour			6 hours
12 hours			18 hours

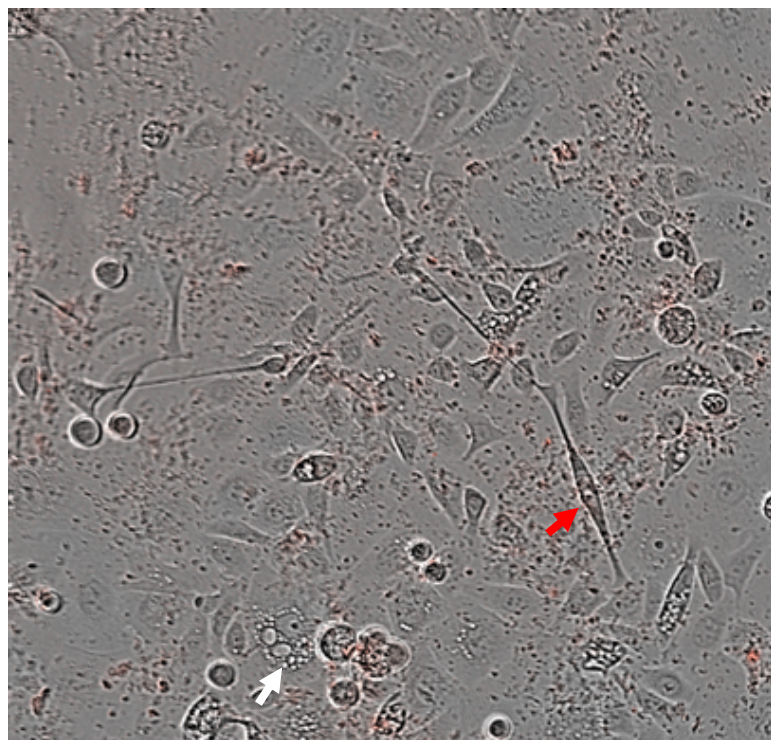


Figure 4.8: Hummingbird phenotype. Elongated AGS cells (red arrow), indicating CagA toxin activity on AGS cells treated with 60190 OMV from early broth cultures after 6 hours of treatment. White arrow = vacuolated cells

Table 4.7: Effects of OMV on AGS cells.

Strain	<i>vacA</i> type	<i>cagA</i> type	Growth condition	cytotoxicity (CellTiter 24 h)	cytotoxicity (RealTime 24 h)	cytotoxicity (Incucyte % confluence)	cytotoxicity (Incucyte red dye)	Vacuolation grade	Hummingbird phenotype
60190	s1 i1 m1	+	early broth	–	+	–	++	+++ ^L	++
			late broth	++	N	–	++	+++ ^L	++
			plate	+++***	+	–	+	++ ^E /+++ ^L	++
444A	s1 i1 m1	+	early broth	N	+	–	+++	+ ^{E,L}	+
			late broth	+++**	–	–	+++	N	+
			plate	+++**	N	–	+	++ ^L	+
Tx30a	s2 i2 m2	–	early broth	N	N	–	++ ^F	N	n/a
			late broth	N	N	–	N	N	n/a
			plate	–	N	+	N	N	n/a
221A	s1 i2 m2	–	early broth	–**	+	–	N	N	n/a
			late broth	+	–	–	+	N	n/a
			plate	–	–	n/d	n/d	N	n/a

+, ++, and +++ indicate mild, moderate, and severe toxicity effects; N = No effect; (–) indicates proliferation response observed instead of cytotoxicity; (^E) indicates early onset of vacuolation (after 6-hours); (^L) indicates late onset of vacuolation (after 18-hours); (^F) = false positive; n/a = not applicable; n/d = no data. Where the effects were statistically significant compared to untreated cells. this is indicating using * $p < 0.05$, ** $p < 0.01$, *** $p < 0.001$, **** $p < 0.0001$.

4.5. DISCUSSION

4.5.1. OMV cytotoxicity

Bacterial virulence and the growth environment of parental bacteria affect OMV toxicity. In this study, OMV toxicity to mammalian cells was examined. Variation in OMV toxicity to AGS cells was seen in different aspects. First, between OMV of different *H. pylori* strains with high and low virulence. Second, between OMVs of the same *H. pylori* strain, however, isolated from different growth environments. The dose and duration of OMV treatment also influenced the extent of cytotoxicity.

4.5.1.1. Effect of OMV on AGS cells after 24 hours (CellTiter assay)

The toxicity of *H. pylori* OMV after 24 hours of exposure was examined in this study by CellTiter 96 assay. It was evident in Figure 4.1 that OMVs of *H. pylori* strains with high virulence (444A and 60190) were more toxic to AGS cells than those of strains with low virulence (221A and Tx30a). In this study, our definition of strains as high or low virulence was based primarily on the *vacA* and *cagA* toxin genotypes. All *H. pylori* strains have the *vacA* gene. However, it varies in sequence type and activity between strains (see Section 1.3.4). In contrast, not all *H. pylori* strains have a *cagA* gene. Nevertheless, strains without *cagA* still can induce cell responses because they have other toxins. In Ismail *et al* they isolated OMV from 60190 (*cagA+*) and Tx30a (*cagA-*) strains and AGS cells were treated with these OMV in a dose-dependent manner. They found that OMV from both strains induced cell proliferation at lower doses OMV and in higher doses both showed inhibition response (Ismail *et al.* 2003). Likewise, in our study OMVs from strains with high and low virulence showed proliferation induction in lower doses and inhibition in higher doses (Figure 4.2). However, cell responses were dependent on the growth conditions where the OMVs isolated from (Figure 4.2). The VacA and CagA proteins have both previously been detected within *H. pylori* OMV (Zavan *et al.* 2018; Olofsson *et al.* 2010; Turner *et al.* 2015; Liu *et al.* 2019). As the quantity of each protein might differ in the OMV of each strain, that could influence the toxicity of the OMV.

In terms of the growth environment of the parental strain, OMVs of 444A and 60190 strains isolated from plate cultures caused a significant decrease in %survival of AGS

cells compared to untreated cells (p^{**} and p^{***} , respectively) (Figure 4.1). Furthermore, 444A and 60190 OMVs isolated from late broth cultures also decrease the %survival of AGS cells, in contrast to those isolated from early broth cultures, which showed slight induction of cell proliferation (Figure 4.1).

On the other hand, OMV isolated from the less virulent strains 221A and Tx30a did not have any toxic effects on AGS cells. Depending on the growth conditions, some minor stimulation of cell proliferation was seen but this was statistically significant only for 221A OMV from early broth cultures (p^{**}) (Figure 4.1).

These differences between OMVs within a strain isolated from different growth conditions were expected as other studies have also reported that growth conditions could affect OMV composition, characteristics, and components (Olofsson *et al.* 2010; Zavan *et al.* 2018). For instance, Olofsson *et al.* were isolating *H. pylori* OMV from plate cultures and from broth at some stages. The SDS-PAGE analysis showed noticeable differences between OMV from plate and broth in their protein profiles (Olofsson *et al.* 2010). However, they did not compare their toxicity effect on gastric cells. Also, they did not compare the protein contents quantitatively to identify proteomics differences between both conditions. While, Zavan *et al.* were comparing *H. pylori* OMV isolated from broth cultures at different time points. They reported variation in OMV characterisation between growth stages, which is consistent with our findings in the characterisation study, as previously discussed in Section 3.5. In addition to that they performed a quantitative proteomics analysis and found that protein contents are differ between growth stages as OMV from early growth stage contained higher amount of CagA and VacA and Urease compared to OMV from late stage (Zavan *et al.* 2018). In terms of toxicity, although early stage OMV (16 hour of incubation) contained more CagA, VacA, and Urease than late stage, they show less induction of IL-8 response from gastric epithelial cells (Zavan *et al.* 2018). However, they did not study OMV from plates and they did not compare OMV effects on cell proliferation or apoptosis. Thus, in our study, a proteomics analysis was suggested to understand the various toxicity effects of OMV between the three environmental conditions.

The growth environment on the agar plate is very different to that in broth. On a plate, the bacteria are nonmotile; however, they aggregate as they grow and generate a stressful environment with competition for limited nutrients. Also, a previous study showed that bacteria at the edge of the plate are spiral-shaped, whereas, at the centre of the plate, they were more U-shaped and transitioning towards a viable but non-culturable (VBNC) form (AlSharaf and Winter, unpublished data). All these variables can cause physiological changes in the bacteria, so the structure and contents of OMV would likely also change. Iron in the blood agar might also affect the expression of VacA, as stated by previous studies (Keenan *et al.* 2000; Keenan and Allardyce 2000; Fiocca *et al.* 1999). They found that high concentration of iron in the growth environment upregulates the expression of VacA toxin. That might explain the increased toxicity of OMV isolated from plate cultures of *H. pylori* 444A and 60190 strains as these strains have a more virulent type of VacA (s1 i1 m1) (Table 2.1).

Similarly, in late broth cultures, although bacteria are motile after 6 days, the bacterial population has increased substantially. That also increases the competition for nutrients within the environment, which puts the bacteria under stress. In contrast, *H. pylori* grown in broth for only 24 hours (early broth cultures) are less likely to have experienced stress and nutrient depletion. Additionally, the *H. pylori* 444A strain showed a change in morphology between 1 and 6 days (see Section 3.5.1.) indicative of environmental stress. As explained above, this might cause alteration to *H. pylori* physiological traits and gene expression levels, leading to changes in the production and characteristics of OMV (see Section 3.5.1.). It seems that this also might influence the toxicity of bacterial OMV. Thus, proteomic analysis would be a logical next step to identify and quantify the proteins within OMV produced under different environmental conditions.

4.5.1.2. Effect of OMV on AGS cells over 24 hours (Realtime Glo assay)

The toxicity of *H. pylori* OMV over time was examined in this study by RealTime-Glo MT assay. During the first 10 hours, the AGS cells grew normally and none of the OMV tested had any significant inhibitory effects (Figure 4.3). This was consistent with a previous study on *H. pylori* 60190, which showed minimal OMV effects on AGS cells

during the first 12 hours of exposure (Choi *et al.* 2017). Nonetheless, after 24 hours of exposure, OMVs isolated from early broth cultures of strains 444A, 221A, and 60190 had inhibited cellular proliferation (Figure 4.3 A, B, and C). OMV of 60190 isolated from plate cultures also inhibited cellular proliferation at 24 hours (Figure 4.3 C). One of this study's limitations is that no data was recorded for exposure times between 10 and 24 hours (see Section 4.6).

Additionally, no cytotoxic effect was seen on AGS cells treated with 60190 OMV isolated from late broth cultures (Figure 4.3 C). OMV of 444A strains isolated from late broth cultures induce the proliferation of AGS cells at 24 hours of exposure. In comparison, those isolated from plate cultures did not show any toxicity to the cells (Figure 4.3 A). On the other hand, both 221A OMVs isolated from late broth and plate cultures induce AGS cells proliferation (Figure 4.3 B). The growth of AGS cells treated with OMVs of Tx30a strain isolated from different growth condition was stable, and no toxicity effect was seen (Figure 4.3 D). Effects of OMV on AGS cells were summarised in Table 4.7.

The results from the CellTiter and RealTime-Glo assays did not always agree with each other in this study. Besides technical errors, each assay used in this study to determine OMV toxicity has different principles and measurements something different (see Sections 2.5.2.1. and 2.5.2.2.). The CellTiter 96 assay is a colorimetric endpoint assay based on the ability of viable cells to reduce an MTS tetrazolium compound to form a coloured dye with maximal absorbance at 490-500 nm (Promega; URL). However, the RealTime-Glo MT assay is based on a cell viability substrate that can freely enter viable cells, where it is then converted to a NanoLuc substrate that diffuses back out of the cells and interacts with luciferase in the media to generate light (Promega; URL). The luminescent signal is proportional to the number of viable cells. This assay allows repeated measurements of the same sample over time.

The two assays showed different cytotoxic effects of OMVs on AGS cells at the same time point and same concentration (25 µg/ml), especially for OMVs isolated from early broth cultures (Figures 4.2 and 4.3). However, both assays agreed that OMVs of Tx30a were not cytotoxic to AGS cells (Figures 4.2 and 4.3). The differences between

these assays should be taken into consideration and further studies might be required to determine the correlation between these assays. Another study to assess OMV toxicity in a dose-dependent manner using the RealTime-Glo MT assay is suggested.

4.5.2. Microscopy analysis of OMV treated cell

The interaction between *H. pylori* outer membrane vesicles and AGS cells was characterised by automated microscopy using an Incucyte system in this part of the study. The live-cell analysis illustrates the ability of *H. pylori* OMV to interact with the human AGS cells directly, *in vitro*, and deliver their virulence factor to the cells. Cell viability and death were also measured in this study; however, data at some time points and data for AGS cells treated with 221A OMV from plate cultures were not recorded due to condensation (see Section 4.6).

In terms of cell viability, AGS cells treated with OMVs of *H. pylori* 444A strain from early broth cultures showed a slight increase in proliferation at the first 2 hours (Figure 4.5 A). However, proliferation was then inhibited as the % of confluence did not increase over the 18 hours (0% of confluence) (Figure 4.6 A). In contrast, AGS cells treated with all other OMVs of *H. pylori* strains showed an increase in proliferation and increased % confluence over exposure time range between ~8% to ~20% (Figure 4.7).

All these results are not reliable as the 0-hour results were not recorded in this analysis, which is needed to confirm whether or not the % confluence of all samples were comparable at the start of the experiment, to confirm or refute the apparent rapid increases in proliferation during the first hour. It seems unlikely that AGS cells could increase from ~35% confluence to ~80% confluence within one hour since the doubling time of these cells is between 20 (ATCC; URL), 22 (Cowley *et al.* 2014), and 24 hours (Matozaki *et al.* 1992) and they normally take several days to reach ~80% confluence.

In addition to monitoring % confluence from microscopy images in a label-free manner, the Incucyte instrument can also measure cell death if the Cytotox Red Dye

is added to the wells. This dye can only enter dead or dying cells, once membrane permeability increases. After binding with DNA, a red fluorescent signal is emitted.

Using this assay, AGS cells treated with OMVs of *H. pylori* strains with high virulence isolated from early and late broth cultures had an increased cell death rate compared to untreated cells (Figure 4.7 A and C). However, cells treated with OMVs of *H. pylori* strains with high virulence isolated from plate cultures had a minimal cell death rate (Figure 4.7 A and C). In contrast, AGS cells treated with OMVs of *H. pylori* strains with low virulence showed little or no cell death (Figure 4.7 B and D). In this study, the cell death was measured based on the % red area. The reliability of this measure is relatively poor because there were some red dye spots that may have interfered with the assay, and also some red areas did not appear to co-localise well with dead cells, as shown in the images in Table 4.2, for example. That affects the red area measurements per image, which consequently affects the whole data set. This is particularly illustrated by the false apparent increase in cell death in AGS cells treated with low virulence Tx30a OMV isolated from early broth cultures (Table 4.6).

However, the Incucyte microscopy images were very useful for illustrating the effects of VacA and CagA toxins delivered by OMV into AGS cells (Tables 4.2 to 4.6). Cellular vacuolation from the activity of VacA toxin (Palframan *et al.* 2012) was evident in some cells, and the hummingbird phenotype which is a hallmark of CagA toxin activity was evident in others (Krisch *et al.* 2016; Kurashima *et al.* 2008).

444A OMV isolated from early broth and plate cultures induced grade 1 and 2, respectively, vacuolation after 18 hours of exposure, indicating VacA activity (Table 4.3). Also, grade 1 perinuclear vacuoles were seen at 6 hours in AGS cells treated with 444A OMV isolated from early broth cultures (Table 4.3). But no vacuoles were seen in cells treated with 444A OMV isolated from late broth cultures (Table 4.3). Zavan *et al.* found that the amount of VacA differ between early and late growth stage OMV (Zavan *et al.* 2018). That might explain the difference in vacuolation activity between early and late broth OMV. Hence, the amount of VacA expression might alter its toxic activities. Therefore, proteomics analysis was suggested to identify the OMV-associated proteins in each condition and determine their level of expression, which help in understanding their effects on gastric epithelial cells.

Similarly, 60190 OMV isolated from all three growth conditions induced grade 3 vacuolation after 18 hours and grade 2 at 6 hours, only in cells treated with 60190 OMV isolated from plate cultures (Table 4.5). Interestingly, these results contradict previous studies' results as the studies stated that *H. pylori* 60190 OMV are stable for the first 12 hours in AGS cells (Choi *et al.* 2017). Nonetheless, vacuolation activity of 60190 OMV has been evident in treated AGS cells after 4 hours of exposure (Chitocholtan *et al.* 2008). Furthermore, a few hummingbird cells were seen in AGS cells treated with OMV of *H. pylori* 444A and 60190 strains, indicating the toxicity of CagA (Tables 4.3 and 4.5). As expected, no vacuolation or hummingbirds were seen in AGS cells treated with 221A and Tx30a OMVs because these strains lack CagA and active VacA (Tables 4.4 and 4.6). It was evident that VacA mutant strains and strains with less active VacA did not show vacuolation activity; however, they can induce cell apoptosis (Ayala *et al.* 2006; Chitcholtan *et al.* 2008; Ismail *et al.* 2003) OMV of all *H. pylori* strains still have other virulence factors that might influence OMV cytotoxicity and contribute to disease. However, it seems that OMV from more virulent *H. pylori* strains (CagA+ and VacA s1 i1 m1) have more toxic effects on AGS cells than those of low virulence strains (CagA- and less active VacA types). Optimisation and replication of this analysis are suggested for future work to avoid condensation and red dye issues.

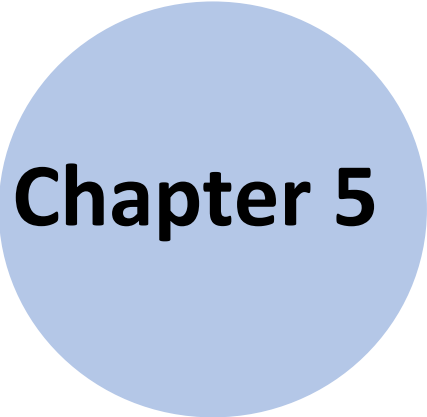
4.6. CHAPTER SUMMARY

Outer membrane vesicles are released constantly from *H. pylori* during growth. These vesicles contain virulence factors and are reported to contribute to *H. pylori* pathogenesis. OMV contents and properties can vary depending on bacterial virulence and environmental conditions. This study aimed to characterise the cytotoxicity of isolated OMV from *H. pylori* strains grown under different environmental conditions.

OMV were purified from different *H. pylori* strains cultured in BHI broth with 0.2% β -cyclodextrin after 1 and 6 days, or on blood agar plates after 24 hours. OMV toxicity on human gastric epithelial (AGS) cells was determined by CellTiter 96 assay, Realtime-Glo MT cell viability assay, and IncuCyte live cell analysis. The purity of AGS cells was confirmed by the *Mycoplasma* detection test.

OMV from *H. pylori* strains with high virulence were more toxic to AGS cells than those with low virulence. However, the growth conditions of the strains also influenced OMV toxicity. OMV toxicity also varied depending on the OMV concentration. Vacuoles were only seen in AGS cells treated with OMV from *H. pylori* strains with high virulence, indicating VacA activity.

Since strain polymorphisms and environmental conditions both influence the cytotoxicity of *H. pylori* OMV, this should be taken into account in the design of future studies. It is possible that changes in the properties of OMV in response to environmental changes could affect the outcome of gastric diseases.



Chapter 5

PROTEOMIC STUDY

5. PROTEOMIC STUDY

5.1. INTRODUCTION

Pathogenic and non-pathogenic Gram-negative bacteria produce outer membrane vesicles in all growth conditions. However, the growth conditions might affect OMV characteristics (Chatterjee and Chaudhuri 2012). These vesicles have several functions, such as facilitating interactions between bacteria and the host, providing protection against stressors and enhancing bacterial growth (Kuehn 2005; Chatterjee and Chaudhuri 2012; MacDonald and Beveridge 2002; Kulp and Kuehn 2010; Murray *et al.* 2020). In addition to that, OMV deliver their enclosed cargo to target cells and can induce host immune responses (Kuehn 2005; Winter *et al.* 2014).

OMV originate from the bacterial cell membrane, and they have some structures and compositions similar to their parental bacteria (Perez-Cruz *et al.* 2013; Kuehn 2005; Chatterjee and Chaudhuri 2012). They contain proteins, LPS, nucleic acids, peptidoglycan, and other bacterial virulence factors and toxins (Perez-Cruz *et al.* 2013; Kuehn 2005; Chatterjee and Chaudhuri 2012; Parker and Keenan 2012; Winter *et al.* 2014). There is growing evidence that bacteria selectively package some proteins into OMV while purposely excluding others. For example, *Porphyromonas gingivalis* OMV contain different proteins to the bacterial membrane (Haurat *et al.* 2011). Another study on *Myxococcus xanthus* strains found that OMV from ten strains isolated from the same growth environment significantly differed in total identified protein in each, and they shared only a few proteins (Zwarycz *et al.* 2020). Moreover, 7 out of 10 strains used in the study had similar genomes, but the protein contents of their OMV were not identical (Zwarycz *et al.* 2020). Packaging of proteins into OMV appeared to be driven by protein characteristics, including function.

Although different factors affect OMV production, including bacterial pathogenicity and the growth phases and environmental conditions (Chatterjee and Chaudhuri 2012) yet, the biogenesis of OMV is not fully understood. Further investigations and studies are needed to illustrate and understand the mechanism of OMV formation. Also, the process of bacterial selection and packing of cargo in the OMV is still controversial.

H. pylori OMV, like other bacterial OMV, contain many outer membrane proteins and proteins derived from elsewhere in the cell. They also contain peptidoglycans, LPS, and some OMV enclose nucleic acids, DNA and sRNA (Keenan *et al.* 2008; Koepfen *et al.* 2016; Zhang *et al.* 2020; Polakovicova *et al.* 2018). Hundreds of *H. pylori* OMV proteins have been identified to date in several proteomics studies. These include flagellin, urease, SabA and BabA, VacA, CagA and Type IV secretion system protein, NapA, and OipA. These proteins are, respectively, correlated to bacterial motility, acid resistance, adherence, virulence, and host immune response (Mullaney *et al.* 2009; Zavan *et al.* 2018; Turner *et al.* 2018; Olofsson *et al.* 2010 Turner *et al.* 2015; Lui *et al.* 2019; Winter *et al.* 2014; Ayala *et al.* 2006; Kaparakis *et al.* 2010; Choi *et al.* 2017). Besides these, numerous uncharacterised proteins have also been detected in *H. pylori* OMV (Zavan *et al.* 2018). Studies on *H. pylori* OMV have reported significant variation in OMV contents between *H. pylori* strains (Parker and Keenan 2012). Differences in OMV content between growth phases and growth environments have also been reported (Parker and Keenan 2012; Olofsson *et al.* 2010). Different factors can lead to OMV diversity, as mentioned above, in conjunction with *H. pylori* polymorphisms and strain variations. Together, these might affect the characteristics of OMV.

OMV size can also influence *H. pylori* OMV content, with larger OMV reported to contain more diverse proteins (Turner *et al.* 2018). OMV size also influences the path of vesicle internalisation into host cells, which also depends on OMV composition (Perez-Cruz *et al.* 2013; Zavan *et al.* 2018; Turner *et al.* 2015; O'Donoghue and Krachler 2016). The growth conditions may influence the virulence of *H. pylori* OMV. For example, *H. pylori* OMV isolated from high iron medium contained more VacA than those from low iron medium (Keenan *et al.* 2000; Keenan and Allardyce 2000; Fiocca *et al.* 1999). Thus, it seems that *H. pylori* and other bacteria might sense and respond to environmental conditions and may have evolved to select optimal proteins and virulence factors to pack in their OMV to function accordingly. For example, *H. pylori* OMV were observed within a biofilm (Yonezawa *et al.* 2016). These OMV contained some essential biofilm formation proteins, such as Alp (adherence-associated protein) (Yonezawa *et al.* 2016). This observation is consistent with the idea that bacteria might purposely package their OMV cargo to promote optimal

survival of different environmental conditions. Because as stated earlier *H. pylori* has different mechanism to survive within an environment and some mechanism might alter their genetics and physiological traits like in biofilm formation. That might also affect on the amount of produced virulence factors, which would promote their survival in the environment. Therefore, the idea of purposeful proteins packaging into OMVs was suggested.

In Chapters 3 and 4 of this study, we reported variation in OMV production between *H. pylori* strains with high and low virulence (see Section 3.5.). Also, within a strain, OMV characteristics varied depending on their parental bacteria's growth conditions (see Section 3.5.). OMV of *H. pylori* strains with high and low virulence varied in their cytotoxic effects on human gastric epithelial cells (see Section 4.5). Moreover, within a strain, OMV isolated from three different growth conditions also had different cytotoxic effects on the epithelial cells (see Section 4.5). Therefore, a proteomics study was conducted to identify the differences in the content of OMV isolated from the three different growth environments.

5.2. AIM OF THIS STUDY

Several previous studies on *H. pylori* outer membrane vesicles have revealed their components and characteristics. However, further work is needed to help understand how *H. pylori* can modulate OMV protein contents in response to different growth conditions, and what effects this might have on bacterial virulence.

This chapter aimed to identify and compare the protein contents of *H. pylori* OMV isolated from different conditions. The cellular responses of AGS cells to treatment with *H. pylori* OMV, in terms of protein expression, were also investigated. The research questions were:

- What are the protein contents of *H. pylori* OMV?
- How do the bacterial growth conditions influence protein contents and quantity within *H. pylori* OMV?
- Do OMV produced by virulent *H. pylori* strains have a similar protein profile compared with less virulent *H. pylori* strains?

- How does the protein expression of human gastric epithelial (AGS) cells change in response to treatment with *H. pylori* OMV?

5.3. RESULTS

OMV of four *H. pylori* strains (444A, 221A, 60190, and Tx30a) were used in this study. OMV were isolated from three growth conditions (early broth, late broth, and plate cultures). Differences in protein profile within OMV of *H. pylori* strains and those between OMV isolated from different growth conditions within each strain were determined using SDS-PAGE. Only OMV of *H. pylori* 444A strain isolated from the early broth, late broth, and plate cultures were used for more in-depth proteomics analysis by LC-MS/MS. *H. pylori* 444A strain is a high virulence strain based on the presence of the *cagA* gene and *vacA* s1 i1 m1 genotype (see Table 2.1). This strain was isolated from a patient suffering gastric ulceration disease with intermediate intestinal metaplasia (Table 2.1). The proteins expressed by untreated AGS cells and cells treated with OMV of *H. pylori* 444A strain were also identified using in-depth LC-MS/MS proteomic analysis. OMV proteins were clustered with confidence scores ≥ 0.75 . Kendall correlation was performed to test differences between conditions using R software. Bar graphs, heatmap with bidirectional clustering, Venn diagram, Sankey plot, and box plot were generated by Lesley Hoyles at the Department of Biosciences, Nottingham Trent University using R software.

5.3.1. OMV-associated protein analysis by SDS-PAGE

100 $\mu\text{g/ml}$ of OMV isolated from *H. pylori* 444A, 221A, Tx30a, and 60190 strains isolated from the early broth, late broth, and plate cultures were analysed for their proteomic profiles (see Section 2.6.1.). Proteins within OMV were separated using SDS-PAGE and visualised with PageBlue protein stain (see Section 2.6.1.). SDS-PAGE showed substantial variation in protein profiles between OMV of different *H. pylori* strains (Figures 5.1 and 5.2). It also showed that, within each strain, the protein band's concentration varied slightly between OMV isolated from the three different environments (Figures 5.1 and 5.2). No clear protein bands were seen in OMV of *H. pylori* 221A strain isolated from early broth cultures (Figure 5.1). One clear protein band and other few faint protein bands were shown in isolated OMV from early broth culture of *H. pylori* 444A strain (Figure 5.1). A faint protein band (~ 15 kDa) appeared

in OMV isolated from plate culture but this was not visible in OMV isolated from early and broth cultures (Figure 5.1).

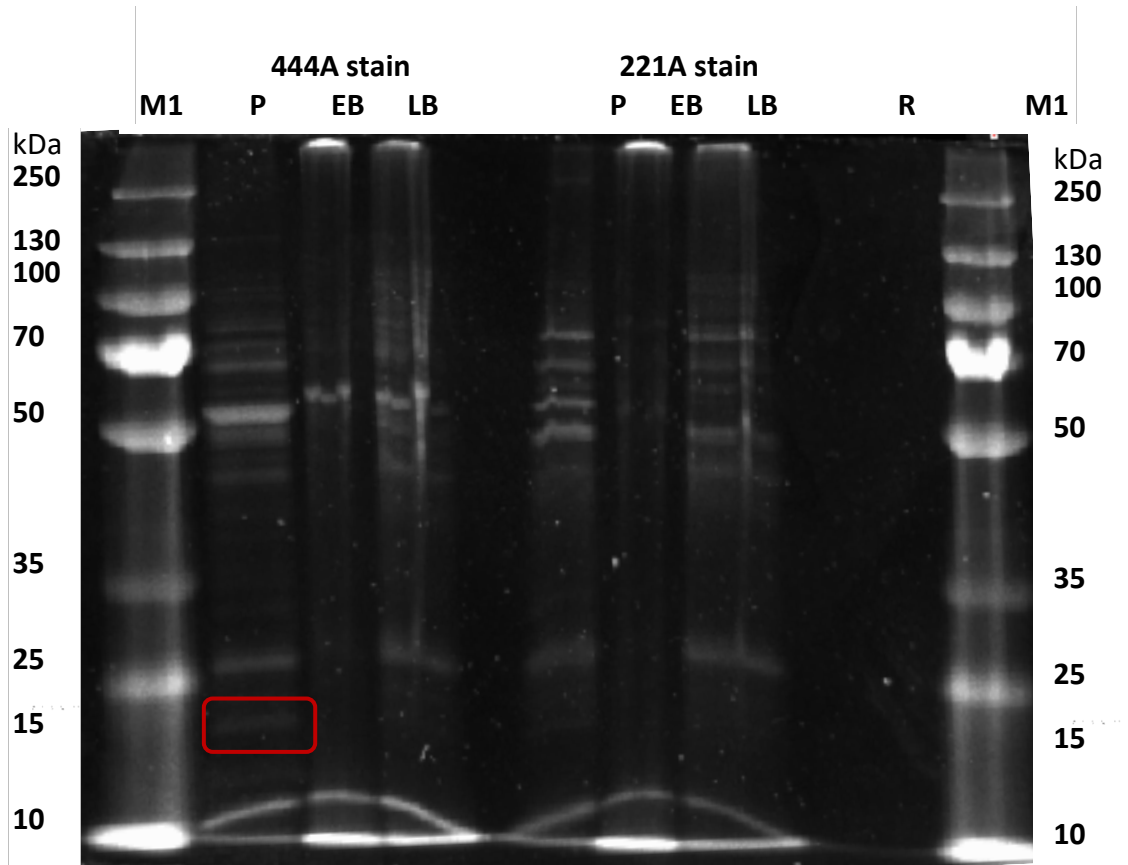


Figure 5.1: SDS-PAGE analysis of 444A and 221A OMV isolated from three growth conditions. OMV of *H. pylori* strains 444A and 221A harvested from early broth, late broth, and plate cultures were loaded in 12% Tri-Glycine gel and stained with PageBlue protein stain. P = OMV from plate cultures. EB = OMV from early broth cultures. LB = OMV from late broth cultures. Lane 7 for Resin. M1 = 250 kDa protein ladder.

No differences were seen in protein profiles between isolated OMV from the early broth, late broth, and plate cultures of *H. pylori* Tx30a strain (Figure 5.2). However, isolated OMV of *H. pylori* 60190 strain showed slight differences in protein profile between conditions as some faint protein bands (at 250 and 130 KDa) and a clear protein band (at ~50 KDa) were visible in OMV isolated from plate culture but not visible in those isolated from early and broth cultures (Figure 5.2).

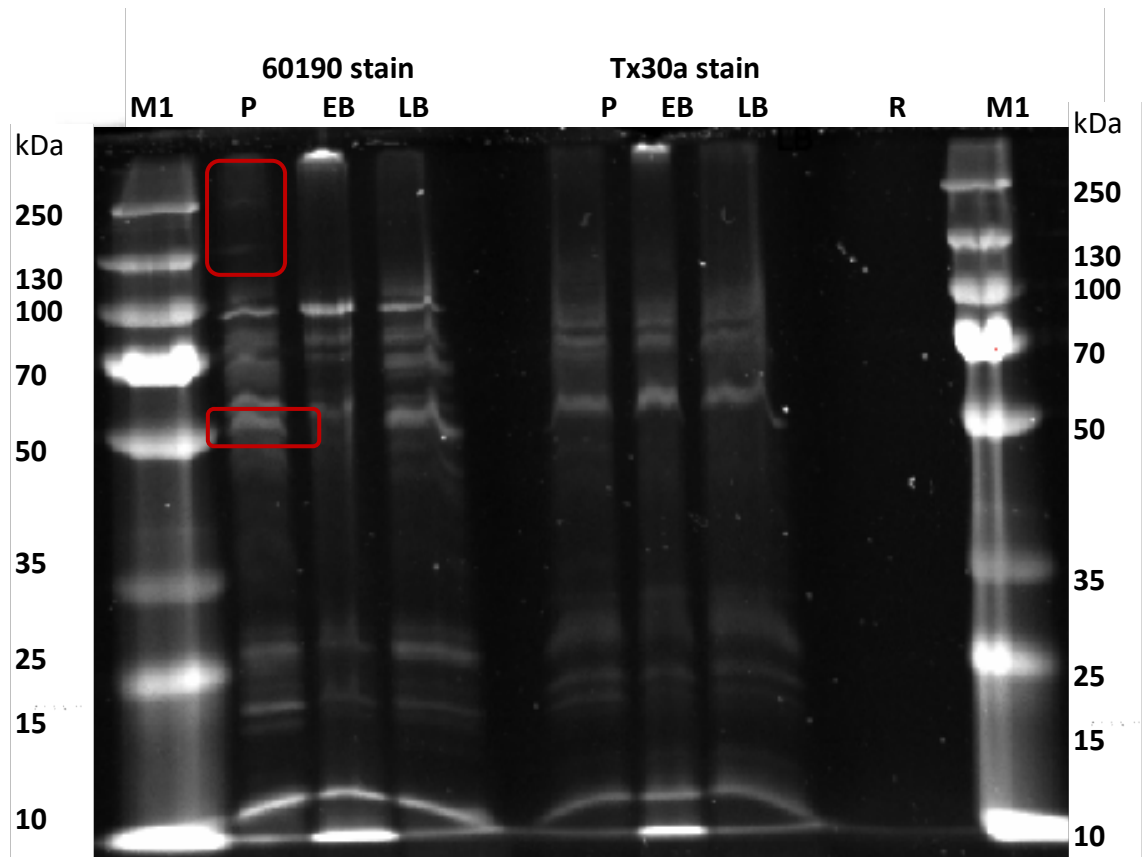


Figure 5.2: SDS-PAGE analysis of 60190 and Tx30a OMV isolated from three growth conditions. OMV of *H. pylori* strains 60190 and Tx30a harvested from early broth, late broth, and plate cultures were loaded in 12% Tri-Glycine gel and stained with PageBlue protein stain. P = OMV from plate cultures. EB = OMV from early broth cultures. LB = OMV from late broth cultures. Lane 7 for Resin. M1 = 250 kDa protein ladder.

5.3.2. OMV associated protein analysis by LC-MS/MS

Six independent replicate preparations per condition of OMV of *H. pylori* 444A strain isolated from early broth, late broth, and plate cultures were highly purified using density gradient centrifugation (see Section 2.6.2.). 50 µg OMV from each replicate of each condition was prepared and protein contents analysed LC-MS/MS and SWATH-MS (see Section 2.6.3.). The analysis showed differences in 444A OMV proteins between growth conditions. A total of 638 proteins were detected in OMV isolated from plate cultures, and 601 proteins in OMV isolated from late broth cultures. Fewer (431) proteins were detected in OMV isolated from the early broth cultures. Proteins of 444A OMV isolated from the early broth, late broth, and plate cultures were compared against each other, in pairs, by the Sciex OneOmics software to quantify differences in protein levels between conditions. The comparisons are early broth versus late broth, early broth versus plate, and late broth versus plate.

Proteins with confidence scores ≥ 0.75 were analysed using normalised protein count. Proteins from each condition were compared based on fold changes using Kendall correlation to identify differences in the quantity of each protein between conditions using R software. Bar graphs, heatmap with bidirectional clustering, Venn diagram, Sankey plot, and box plot were generated by Lesley Hoyles at the Department of Biosciences, Nottingham Trent University using R software.

Among the hundreds of proteins identified in *H. pylori* 444A OMV, the two major *H. pylori* toxins, VacA and CagA, were detected in *H. pylori* 444A OMV from all growth conditions. Many proteins were downregulated in early broth OMV compared to late broth, while only a few were upregulated (Figure 5.3). But among the upregulated proteins in early broth OMV compared to late broth OMV, were key virulence factors. For example, there was around 2-fold more VacA and CagA in OMV from early broth than those from late broth (Figure 5.3). CagA had the highest confidence score (0.97) for differential quantity from all of the proteins that were compared between early and late broth OMV. CagA protein was also upregulated around 1.5-fold in early broth OMV compared to plate OMV (Figure 5.4).

Also, the Type IV Secretion System was upregulated in early broth compared to plate OMV (Figure 5.4). However, VacA was not included in this analysis because its

confidence score in the early broth versus plate comparison was less than 75%. Late broth versus plate comparison showed that VacA was downregulated about 1.5-fold in late broth OMV compared to plate OMV (Figure 5.5). However, CagA is not included in this comparison because its confidence score in the late broth versus plate comparison was less than 75%.

Proteins were bidirectionally clustered in a heat map (Figure 5.6) to characterise the overall extent of protein differences between conditions. This analysis showed that 444A OMV isolated from plate cultures had completely different protein profiles to OMV from early and late broth cultures. Proteins in 444A OMV from plate cultures were clustered as separate groups from broth (Figure 5.6).

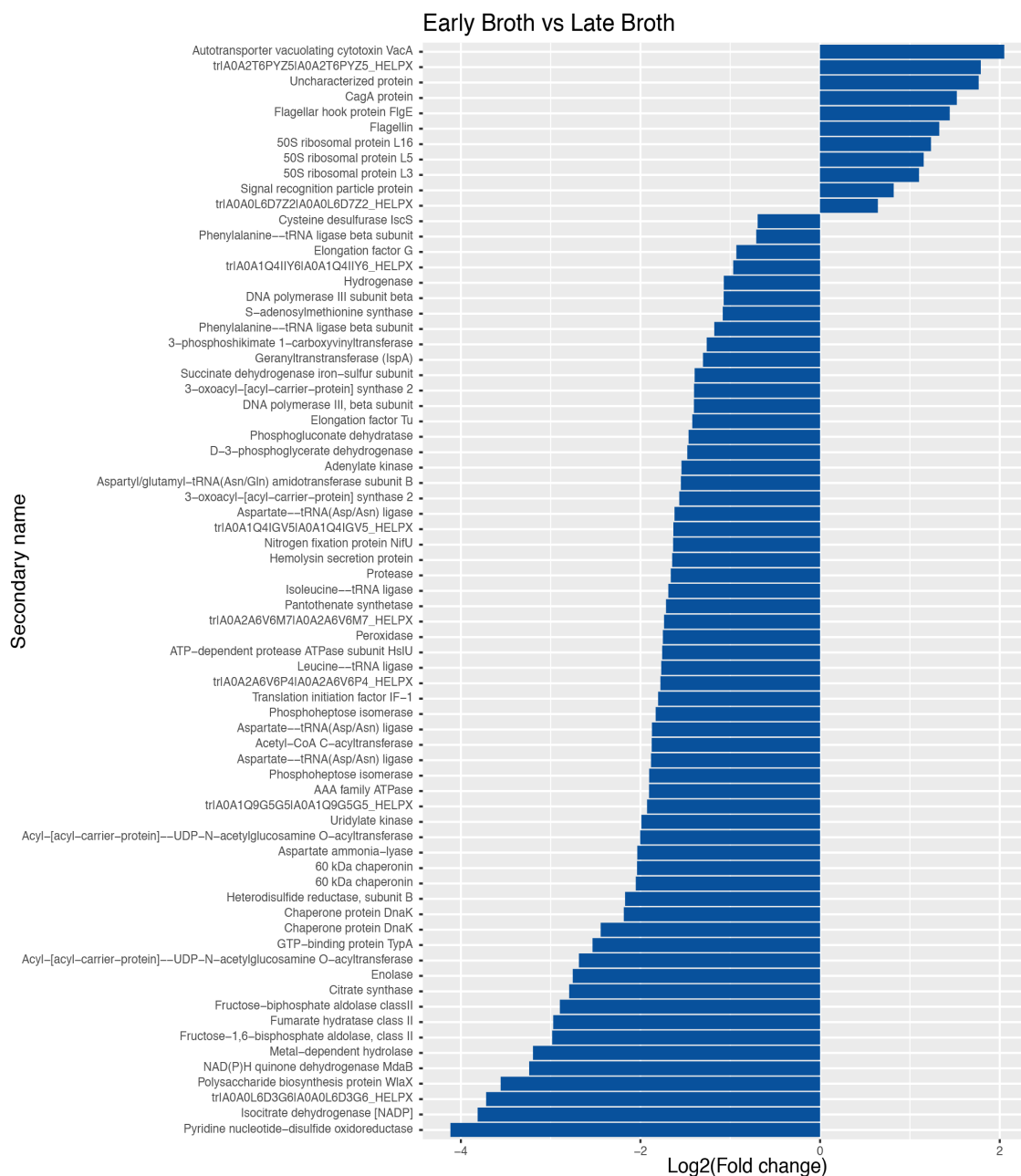


Figure 5.3: Comparison of early and late broth OMV proteins level. Identified proteins with $\geq 75\%$ confidence in OMV isolated from both early and late broth cultures were compared. The bar graph shows the mean log₂ (Fold change) of 6 independent replicates, x-axis, and detected proteins with confidence scores $\geq 75\%$, y-axis. Positive values indicate upregulation of proteins within OMV isolated from early broth cultures. Negative values indicate downregulation of proteins within OMV isolated from early broth cultures.

Early Broth vs Plate

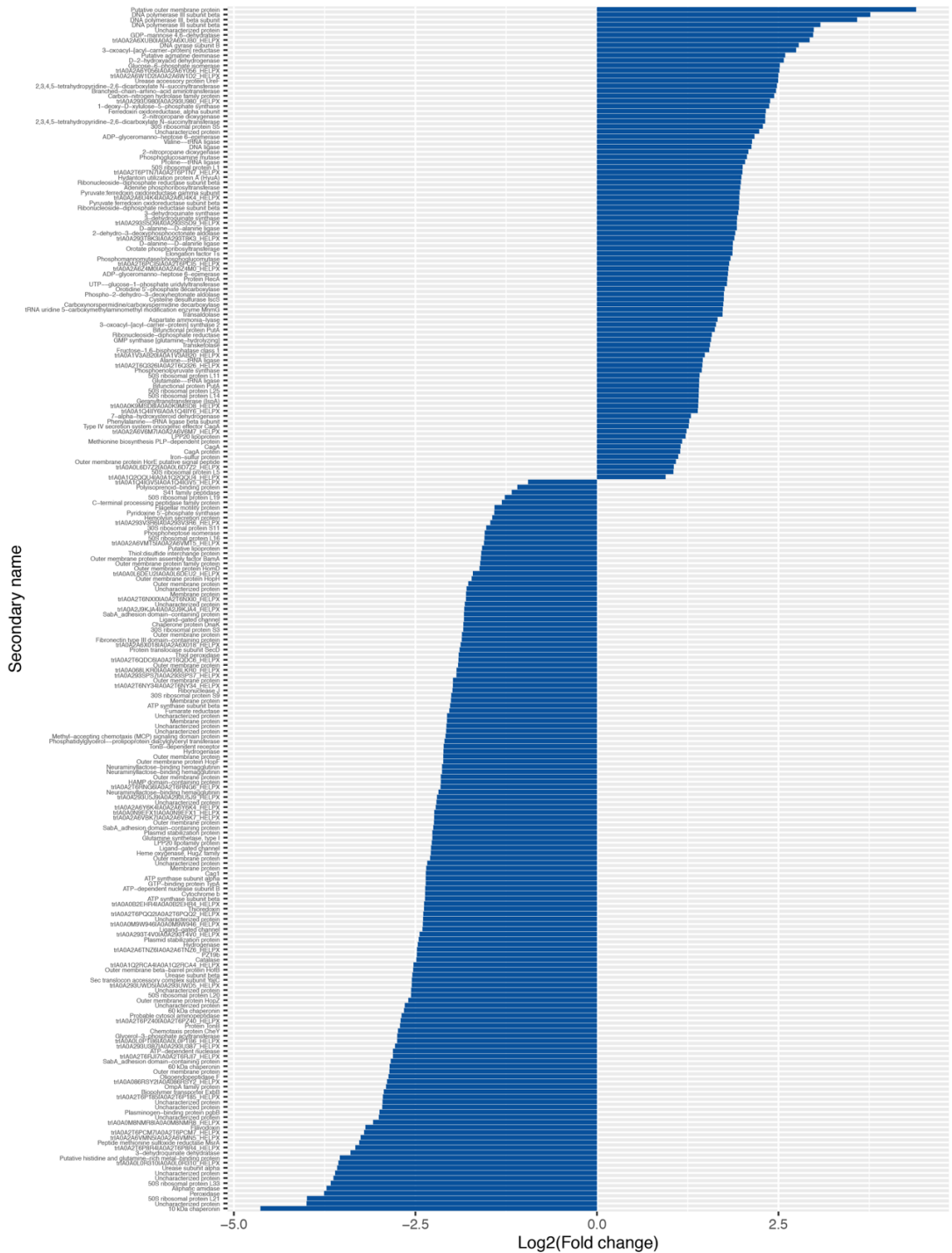


Figure 5.4: Comparison of early broth and plate OMV proteins level. Identified proteins with $\geq 75\%$ confidence in OMV isolated from both early broth and plate cultures were compared. The bar graph shows the mean log₂ (Fold change) of 6 independent replicates, x-axis, and detected proteins with confidence scores $\geq 75\%$, y-axis. Positive values indicate upregulation of proteins within OMV isolated from early broth cultures. Negative values indicate downregulation of proteins within OMV isolated from early broth cultures.

Late Broth vs Plate

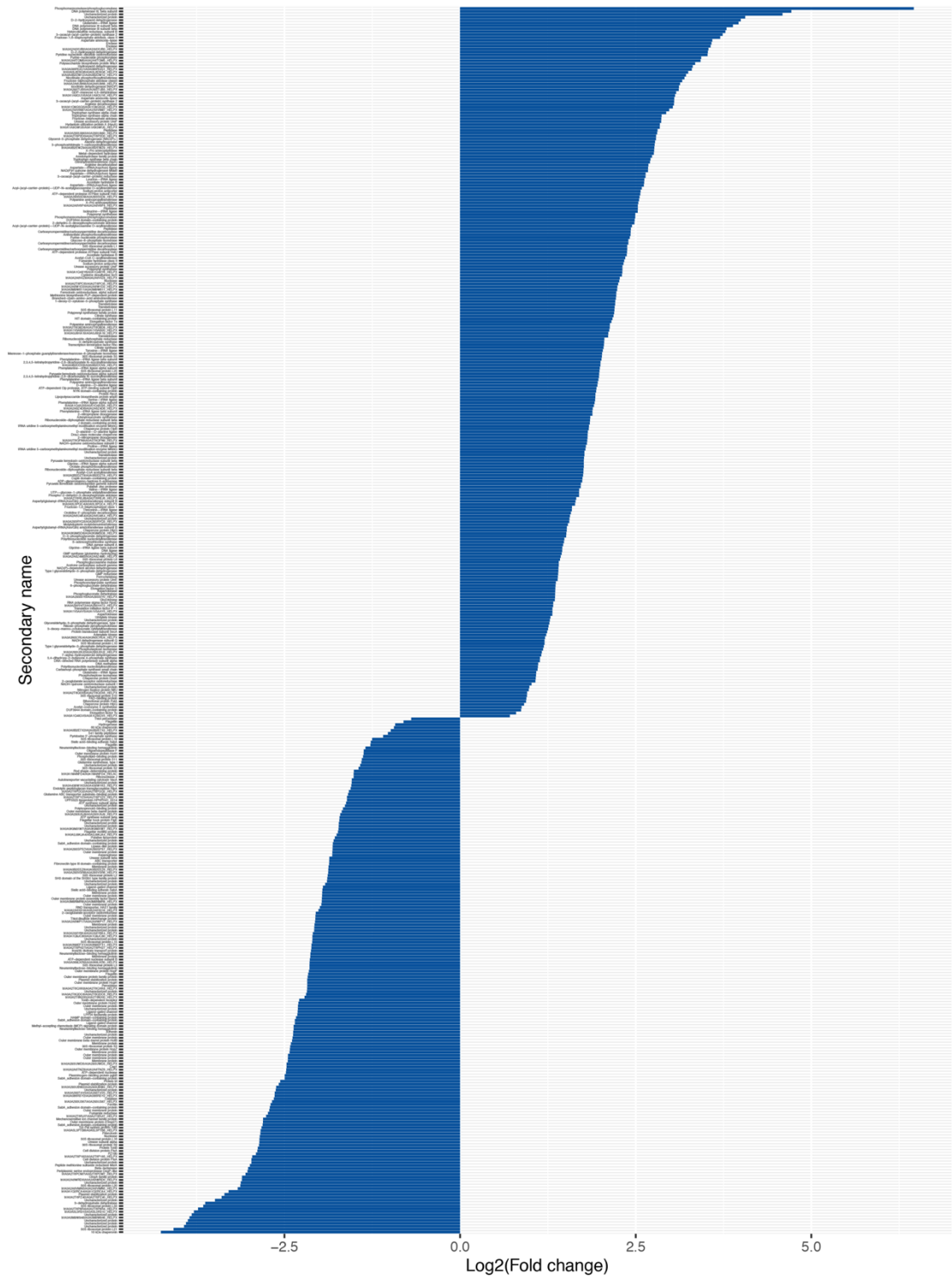


Figure 5.5: Comparison of late broth and plate OMV proteins level. Identified proteins with $\geq 75\%$ confidence in OMV isolated from both late broth and plate cultures were compared. The bar graph shows the mean log₂ (Fold change) of 6 independent replicates, x-axis, and detected proteins with confidence scores $\geq 75\%$, y-axis. Positive values indicate upregulation of proteins within OMV isolated from late broth cultures. Negative values indicate downregulation of proteins within OMV isolated from late broth cultures.

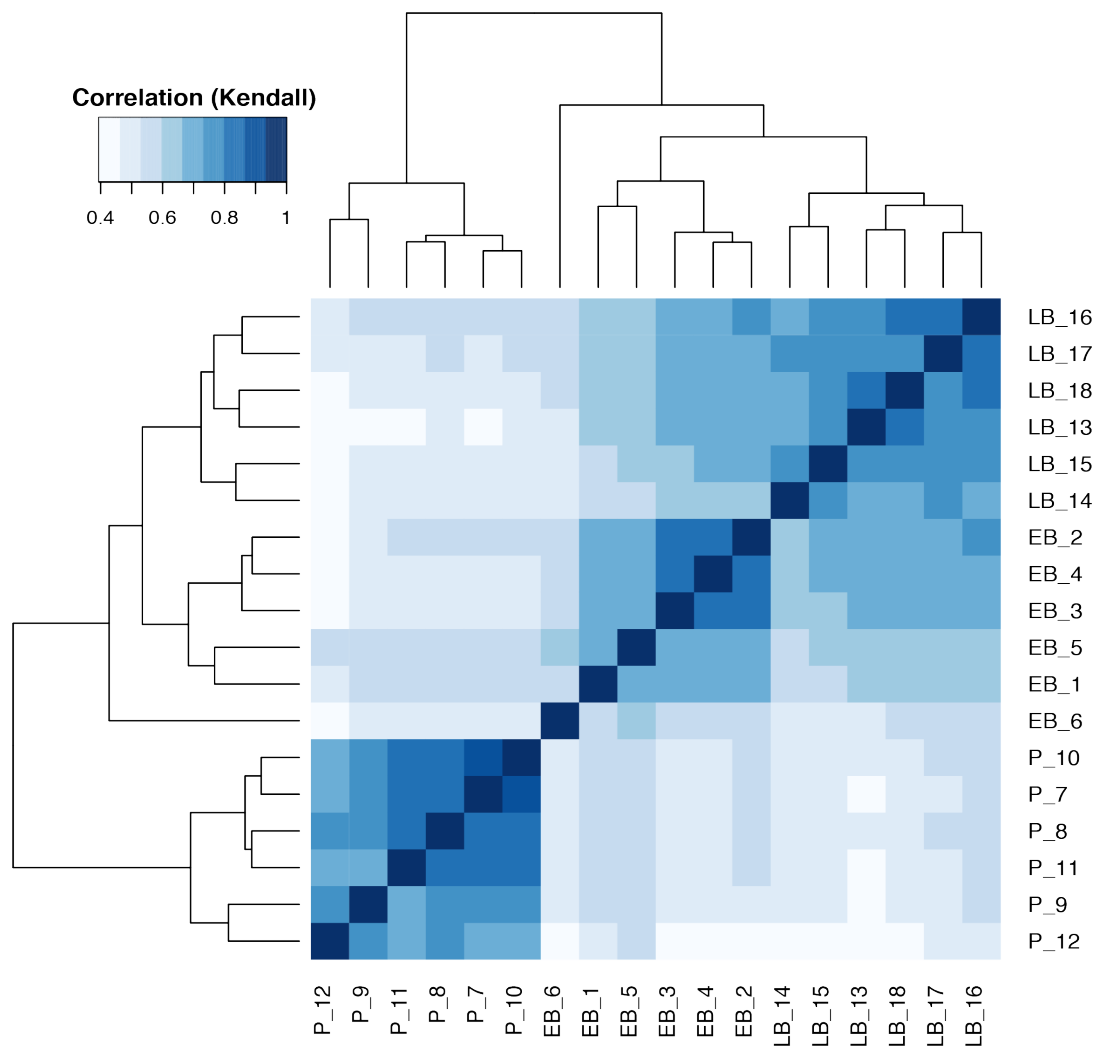


Figure 5.6: Correlation heatmap of proteins detected within *H. pylori* 444A OMV isolated from early broth (EB), late broth (LB), and plate (P) cultures. Heatmap with bidirectional clustering shows the normalised data clustering for proteins with confidence scores $\geq 75\%$ of 6 independent replicates. Annotations on top of the heatmap show clustering of the samples. Data was analysed by Kendall correlation. A higher value with darker colour represents a stronger correlation.

Of the 431 proteins that were detected in OMV from early broth cultures, 71 of these were detected in late broth OMV and 237 were detected in plate OMV. Of the 601 proteins that were detected in OMV from late broth cultures, 423 of these were detected in OMV from plate cultures. A Venn diagram was plotted to determine the relationship between proteins in each comparison. The Venn diagram showed that only 6 proteins were differentially packaged in early broth compared to late broth (Figure 5.7). 8 proteins were unique in early broth (Figure 5.7). Whereas, 43 proteins were unique in late broth (Figure 5.7). Furthermore, 42 proteins were differentially packaged in early broth compared to the plate, and 193 proteins in late broth compared to plate OMV. However, 173 proteins were unique in plate growth condition (Figure 5.7).

Interestingly, only 14 proteins were identified as differentially expressed between all three conditions (Figure 5.7). These proteins function in DNA replication, translation, ribosomal proteins synthesis and modification, fatty acid and phospholipids metabolism, and detoxification (Table 5.1). Further analysis was performed for these 14 proteins to identify the quantity of each protein in OMV from each condition (Figures 5.8 and 5.9). Sankey and box plots showed that the majority of peroxidase and 60-kDa chaperonin were found in plate OMV with much lower quantities of these two proteins detected in OMV isolated from early or late broth cultures (Figures 5.8 and 5.9). Both of these proteins were also found in a higher amount in late broth OMV compared to early broth (Figure 5.9). 9/14 of the proteins detected in OMV from all conditions were present in the highest quantities in late broth OMV (Figure 5.9). Only one protein was found in the largest amount in early broth OMV; however, it was an uncharacterised protein (Figure 5.9).

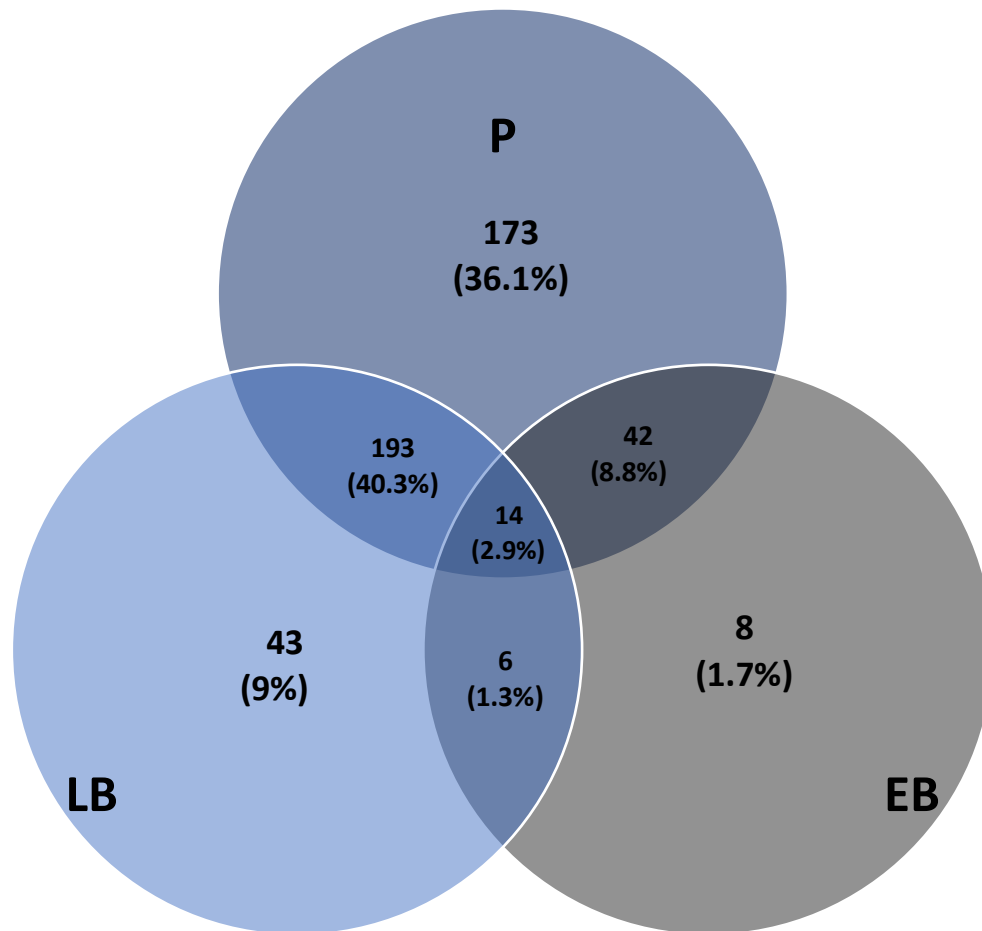


Figure 5.7: Venn diagram of detected differentially expressed *H. pylori* 444A OMV proteins. Comparisons were performed between proteins detected from each condition. The analysis includes proteins with $\geq 75\%$ confidence scores. A total of 71 proteins were detected as differentially expressed in EB vs LB, 423 proteins were detected as differentially expressed in LB vs P, and 237 proteins were detected as differentially expressed in EB vs P. 8 proteins were detected in EB population. 173 proteins were detected P population. 43 proteins were detected in LB population. 14 proteins were detected as differentially packaged in all comparisons. Only 6 proteins were detected as differentially packaged in EB vs LB, 42 proteins were detected in EB vs P, and 193 proteins were detected in LB vs P.

Table 5.1: Common identified proteins of *H. pylori* 444A OMV in all data sets.

NO.	ACCESSION ¹	PROTEIN NAME	SPECIES	PREDICTED FUNCTION
1	tr A0A1Q4IGV5 A0A1Q4IGV5_HELPX	tr A0A1Q4IGV5 A0A1Q4IGV5_HELPX	HELPX	Unknown
2	tr A0A1Q4IY6 A0A1Q4IY6_HELPX	tr A0A1Q4IY6 A0A1Q4IY6_HELPX	HELPX	Unknown
3	tr A0A2A6V6M7 A0A2A6V6M7_HELPX	tr A0A2A6V6M7 A0A2A6V6M7_HELPX	HELPX	Unknown
4	tr A0A438SNZ5 A0A438SNZ5_HELPX	Phenylalanine--tRNA ligase beta subunit	HELPX	ATP binding, magnesium ion binding, and Phenylalanine--tRNA ligase activity ²
5	tr A0A439ADA2 A0A439ADA2_HELPX	DNA polymerase III subunit beta	HELPX	Oxidoreductase activity and Ferric iron binding ³
6	tr B6JLE1 B6JLE1_HELP2	3-oxoacyl-[acyl-carrier-protein] synthase 2	HELP2	Fatty acid biosynthetic process and beta-ketoacyl-carrier-protein synthase II activity ⁴
7	tr M3L550 M3L550_HELPX	DNA polymerase III, beta subunit	HELPX	Oxidoreductase activity and Ferric iron binding ³
8	tr M3MSD9 M3MSD9_HELPX	60 kDa chaperonin	HELPX	Protein misfolding prevention, ATP binding, and refolding unfolded polypeptides in stress conditions ⁵
9	tr O24909 O24909_HELPY	Uncharacterised protein	HELPY	Unknown
10	tr O25583 O25583_HELPY	Geranyltranstransferase (IspA)	HELPY	Geranyltranstransferase activity ⁶
11	tr T5CUD7 T5CUD7_HELPX	Peroxidase	HELPX	Protection in oxidative stress ^{7,8}
12	tr V5NMT2 V5NMT2_HELPX	Cysteine desulfurase IscS	HELPX	Cysteine desulfurase activity and iron-sulfur cluster ⁹
13	tr V6L820 V6L820_HELPX	Aspartate ammonia-lyase	HELPX	Aspartate ammonia-lyase activity ¹¹
14	tr X2IGA8 X2IGA8_HELPX	50S ribosomal protein L16	HELPX	rRNA and tRNA binding, translation and ribosomal structure ¹⁰

¹The entry name of identified peptide for the protein (UniProt database; URL).

²(Lu *et al.* 2020), ³(Pandey *et al.* 2016), ⁴(Choi *et al.* 2000), ⁵(Maguire *et al.* 2002), ⁶(UniProtKB-EC; URL), ⁷(Wan *et al.* 1998),

⁸(Bhattacharjee *et al.* 2002), ⁹(Benoit *et al.* 2018), ¹⁰(Doig *et al.* 1999), ¹¹(Mobley *et al.* 2001).

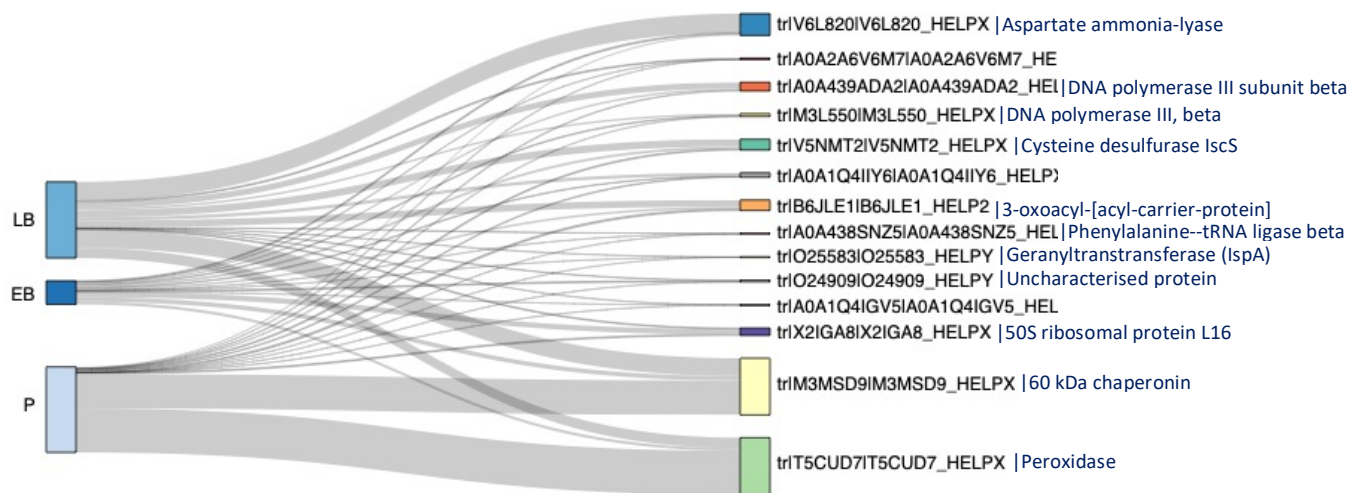


Figure 5.8: Relative quantities of *H. pylori* 444A proteins that were detected in OMV from all three growth conditions. Comparisons were performed between proteins detected from each condition. The analysis includes proteins with $\geq 75\%$ confidence scores. There were only 14 proteins that were found in OMV from all three growth conditions. Sankey plot showing the relative quantities of proteins detected within *H. pylori* OMV isolated from early broth (EB), late broth (LB), and plate (P) cultures.

Proteins found in all comparisons

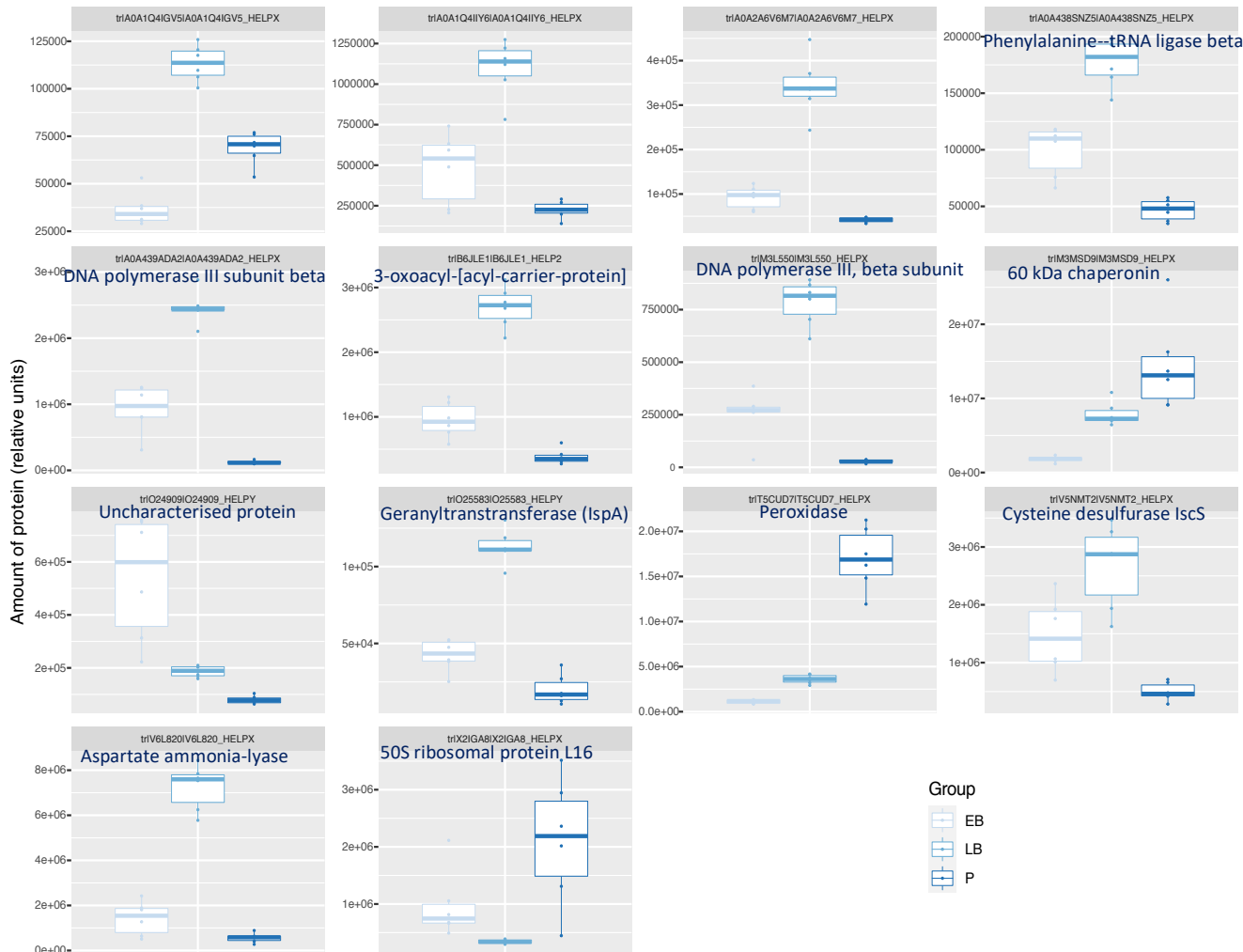


Figure 5.9: Relative quantities of *H. pylori* 444A proteins that were detected in OMV from all three growth conditions. Comparisons were performed between proteins detected from each condition. The analysis includes proteins with $\geq 75\%$ confidence scores. There were only 14 proteins that were found in OMV from all three growth conditions. Box plots showing the relative amounts of protein detected within *H. pylori* OMV isolated from early broth (EB), late broth (LB), and plate (P) cultures. The bars showed mean of normalised data of 6 independent replicates per condition. The boxes showed upper and lower quartiles data value. Whiskers showed the maximum and minimum data of 6 independent replicates per condition.

5.3.3. Analysis of proteins associated with AGS cell response to OMV treatment

AGS cells were treated with 6 µg/ml of OMV from *H. pylori* strain 444A for 24 hours to characterise the cellular response to treatment with a relatively low (non-cytotoxic) dose of OMV (see Section 2.6.4.). The dose of 6 µg/ml OMV was selected based on the cytotoxicity assays (see chapter 4) as a sub-lethal dose that might induce protein responses in the AGS cells without completely killing them. To reduce variability in results, six independent replicates were set up for each experimental condition – untreated cells, cells treated with OMV from early broth cultures, and cells treated with OMV from late broth cultures. 50 µg protein for each replicate sample was prepared and analysed by LC-MS/MS and SWATH-MS (see Section 2.6.3.). Identified proteins from OMV-treated AGS cells were compared with those from untreated (control) cells in pairs. A total of 295 proteins were detected in untreated AGS cells. A total of 291 proteins were detected in AGS cells treated with OMV isolated from early broth cultures, and 293 proteins in AGS cells treated with OMV isolated from late broth cultures. No proteomics data were obtained for AGS cells treated with OMV isolated from plate culture due to COVID-19 pandemic circumstances (laboratory closures).

Although almost 300 proteins were detected in each experimental condition, there were very few differences in protein expression between treated and untreated cells. The Venn diagram in Figure 5.10 shows that only 11 proteins were found to be differentially expressed in AGS cells treated with early broth OMV vs untreated cells, and 11 proteins in AGS cells treated with late broth OMV vs untreated cells. Almost all of these proteins were down-regulated in the OMV-treated cells compared to the untreated control cells (Table 5.2) and 6 proteins were downregulated in both datasets (Figure 5.10 and Tables 5.2 and 5.3, in blue text).

The differentially expressed proteins are listed in Tables 5.2 and 5.3. Due to few differentially expressed proteins were identified in response to OMV treatment, a confidence score cut-off of 50% was used in this analysis. All 11 proteins that were differentially expressed in cells treated with early broth OMV showed downregulation compared to untreated cells (Table 5.2). Similarly, in cells treated

with late broth OMV, all of the differentially expressed proteins were downregulated compared to untreated control cells, except for polypyrimidine tract-binding protein 1, which was upregulated approximately 2-fold by OMV treatment (Table 5.3). Polypyrimidine tract-binding protein 1 is an RNA binding protein. Besides its role in splicing regulation, it is reported as a multifunctional protein and can transport between the nucleus and cytoplasm (Romanelli *et al.* 2013).

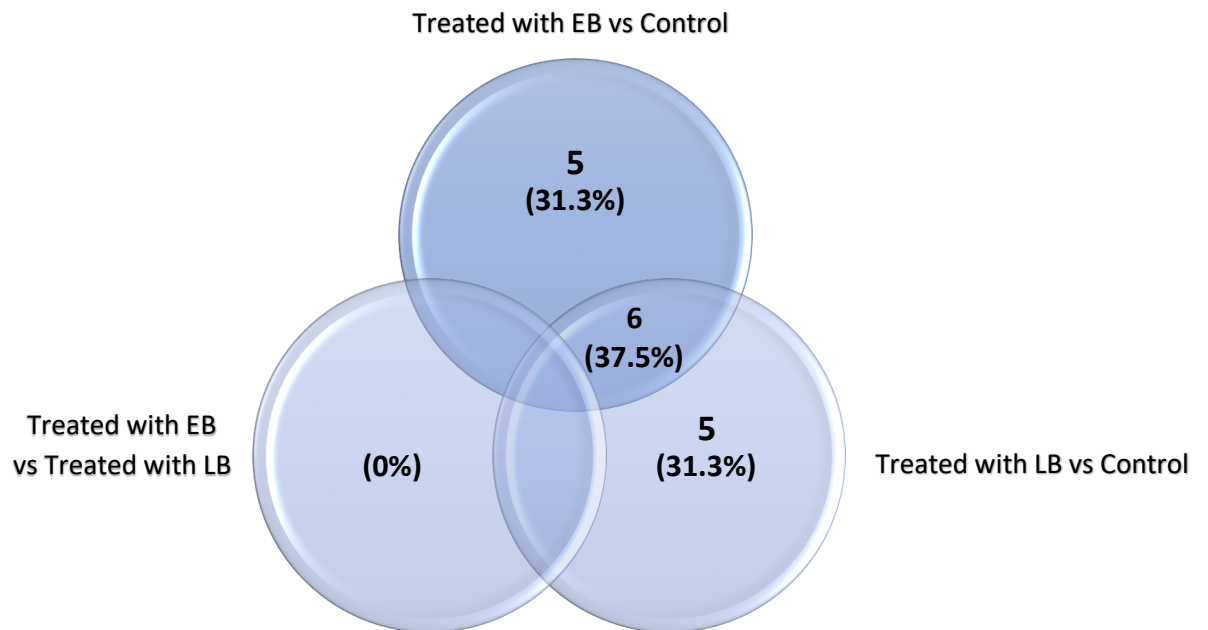


Figure 5.10: Venn diagram of treated and untreated AGS cells detected proteins. Comparisons were performed between proteins detected from each condition. The analysis includes proteins with $\geq 50\%$ confidence scores. A total of 11 proteins were detected in Treated cells with EB vs control, and 11 proteins were detected in Treated cells with LB vs control. There was 6 proteins were found in both Treated cells with EB vs control and Treated cells with LB vs control populations. No proteins were found in Treated cells with EB vs Treated cells with LB population.

Table 5.2: Differentially expressed proteins from AGS cells treated with *H. pylori* 444A OMV isolated from **early broth cultures compared to untreated control cells** identified by LC-MS/MS.

CONFIDENCE	FOLD CHANGES (log2)	ACCESSION	PROTEIN NAME	SPECIES
≥ 0.65	-0.658656681	sp P13693 TCTP_HUMAN	Translationally-controlled tumour protein	HUMAN
≥ 0.65	-0.682047002	sp P15880 RS2_HUMAN	40S ribosomal protein S2	HUMAN
>0.5	-0.545193697	sp P14618 KPYM_HUMAN	Pyruvate kinase PKM	HUMAN
>0.5	0.530118146	sp P53618 COPB_HUMAN	Coatomer subunit beta	HUMAN
>0.5	-0.567642302	sp Q8NC51 PAIRB_HUMAN	Plasminogen activator inhibitor 1 RNA-binding protein	HUMAN
>0.5	-0.80813732	sp P46781 RS9_HUMAN	40S ribosomal protein S9	HUMAN
>0.5	-0.534909522	sp P61513 RL37A_HUMAN	60S ribosomal protein L37a	HUMAN
>0.5	-0.466158934	sp P14923 PLAK_HUMAN	Junction plakoglobin	HUMAN
>0.5	-0.543839606	sp P61353 RL27_HUMAN	60S ribosomal protein L27	HUMAN
>0.5	-0.866984459	sp O00410 IPO5_HUMAN	Importin-5	HUMAN
>0.5	-0.708650114	sp Q02878 RL6_HUMAN	60S ribosomal protein L6	HUMAN

Minus symbol (-) = downregulation of protein in AGS cells treated with early broth 444A OMV

Table 5.3: Differentially expressed proteins from AGS cells treated with *H. pylori* 444A OMV isolated from **late broth cultures compared to control cells** identified by LC-MS/MS.

CONFIDENCE	FOLD CHANGES (log2)	ACCESSION	PROTEIN NAME	SPECIES
≥ 0.65	-0.766999564	sp P15880 RS2_HUMAN	40S ribosomal protein S2	HUMAN
≥ 0.65	-0.655543623	sp P14923 PLAK_HUMAN	Junction plakoglobin	HUMAN
>0.5	-0.869099245	sp P49368 TCPG_HUMAN	T-complex protein 1 subunit gamma	HUMAN
>0.5	-0.505506461	sp P83731 RL24_HUMAN	60S ribosomal protein L24	HUMAN
>0.5	-0.618220589	sp Q8NC51 PAIRB_HUMAN	Plasminogen activator inhibitor 1 RNA-binding protein	HUMAN
>0.5	-0.468749304	sp P14618 KPYM_HUMAN	Pyruvate kinase PKM	HUMAN
>0.5	-0.566865959	sp P61353 RL27_HUMAN	60S ribosomal protein L27	HUMAN
>0.5	0.702309668	sp O00151 PDLI1_HUMAN	PDZ and LIM domain protein 1	HUMAN
>0.5	-0.664731712	sp Q02878 RL6_HUMAN	60S ribosomal protein L6	HUMAN
>0.5	-0.770576813	sp P26641 EF1G_HUMAN	Elongation factor 1-gamma	HUMAN
>0.5	2.024509119	sp P26599 PTBP1_HUMAN	Polypyrimidine tract-binding protein 1	HUMAN

Minus symbol (-) = downregulation of protein in AGS cells treated with late broth 444A OMV

5.3.4. Correlation between VacA and CagA quantities and OMV cytotoxicity effect

The proteomics analysis reported in this study showed that *H. pylori* 444A OMV from all three growth conditions contained VacA and CagA; however, in different quantities (Table 5.4). OMV from early broth cultures had higher amounts of these toxins than OMV from late broth or plate cultures (Table 5.4). In the microscopic analysis of OMV treated cells (see Section 4.4.3.3.), vacuolation was observed in cells treated with OMV from early broth at 6 and 18 hours of treatment, indicating VacA toxin activity, in addition to a few hummingbird cells indicating CagA toxin activity (see Tables 5.4 and 4.3). A few hummingbird cells were also seen in cells treated with OMV from plate cultures at 6 and 18 hours of treatment. However, vacuolation was only seen after 18 hours of treatment with these OMV (see Tables 5.4 and 4.3). No vacuoles were seen in cells treated with OMV from late broth cultures, but again a few hummingbird cells were observed at 6 and 18 hours of treatment (see Tables 5.4 and 4.3).

Table 5.4: Quantity of toxins within *H. pylori* 444A OMV and their activities on OMV-treated AGS cells.

<i>H. pylori</i> OMV	Grading of vacuoles		Hummingbird cells		Protein count	
	6 hours	18 hours	6 hours	18 hours	VacA	CagA
From early broth	+	+	+	+	1,162,154	540,165
From late broth	-	-	+	+	317,686	155,682
From plate	-	++	+	+	898,831	245,934

5.4. DISCUSSION

5.4.1. SDS-PAGE

SDS-PAGE was performed in this study for a general comparison of OMV protein contents between *H. pylori* strains with low and high virulence. The analysis showed clear dissimilarities in protein profiles between *H. pylori* strains (Figures 5.1 and 5.2). This is unsurprising given the highly polymorphic nature of the *H. pylori* species, and is consistent with previous studies in *H. pylori* and other bacterial species showing that protein contents of OMV vary between strain (Zwarycz *et al.* 2020; Mullaney *et al.* 2009).

Additionally, within each strain, OMV were isolated from early broth (1 day), late broth (6 days), and plate (24 hours) cultures. The protein profiles within a strain seemed to be generally similar with slight differences, such as variations in bands' intensity (Figures 5.1 and 5.2). Some minor differences in banding patterns were seen between OMV of the same strain grown in different culture conditions. For example, OMV of 444A strain isolated from plate cultures had a 15 kDa band, which was absent from broth OMVs (Figure 5.1). Also, 130, 250, and ~50 kDa bands were present in 60190 OMV from the plate cultures but absent from broth OMVs (Figure 5.2). Due to the pandemic restrictions and lab closure these bands were not identified. However, these findings are consistent with previous studies that showed *H. pylori* strain type and growth environments can affect OMV content (Parker and Keenan 2012; Keenan *et al.* 1997; Olofsson *et al.* 2010). In the Olofsson *et al.* (2010) study, they were isolating *H. pylori* OMV from brucella blood agar plates and at some points they were isolating OMV from brucella broth. They analysed OMV-associated proteins in each condition by SDS-PAGE and they found that OMV from agar plates were significantly different from those from broth. Although they have identified this difference, they did not take the analysis further. However, in our study we have identified and compared OMV-associated proteins in each condition (see Section 5.5.2.). This aspect of our work is novel has not yet been published elsewhere, to our knowledge.

Interestingly, those different bands appear in the protein profiles of plate OMV of both the more virulent *H. pylori* strains (CagA+ and VacA s1 i1 m1). The environment between broth and agar plate cultures is entirely different. As previously explained

(see Section 4.5.1.1.), besides differences in medium components, bacteria on agar plates are growing in aggregation as they are non-motile, creating a stressful environment, especially to those grown at the centre of the plate. This environment causes a transformation of *H. pylori* from spiral to VBNC shape over time (AlSharaf and Winter, unpublished data). As a result, alterations in bacterial physiological traits might occur and might consequently alter the composition and contents of OMV. Bacteria may even respond to environmental conditions by selectively packaging or excluding some proteins from their OMV as an evolutionary adaptation to their own advantage, for example to support nutrient acquisition or stress survival (Orench-Rivera and Kuehn 2016). Therefore, an in-depth proteomic analysis was conducted to identify and quantitatively compare the protein contents of OMV produced by the high virulence strain 444A grown in three different conditions.

5.4.2. Analysis of OMV associated proteins

A liquid chromatography-tandem mass spectrometry was performed in this study to identify proteins of *H. pylori* 444A OMV isolated from three different environments; early (1 day) and late (6 days) broth and plate (24 hours) cultures. Proteins identified in 444A OMV in this study were related to the secretion system, motility, and immune evasion. Proteins associated with acid resistance, adherence, and toxins were also identified, along with many uncharacterised proteins. There were 638 proteins identified in plate OMV, 601 proteins in late broth OMV, and 431 proteins in early broth OMV. The total number of proteins identified in OMV from the plate was slightly higher than those from late broth and much higher than those from early broth. Since *H. pylori* 444A strain was the only strain that has larger OMV size than early and late broth OMVs, we hypothesised that these OMV might pack more proteins than the other. A previous study found that OMV-associated proteins are regulated by the size of the OMV (Turner *et al.* 2015).

In their study they separated isolated OMV based on their density using sucrose density gradient followed by nanoparticle tracking analysis to measure their actual size (Turner *et al.* 2015). They found that OMV separated from lower density fractions were smaller in size and those from higher density fractions were larger in size. This was then followed by proteomics analysis, which revealed that smaller OMV

contained a smaller number of proteins than the larger ones (Turner *et al.* 2015). This supports our hypothesis and findings. However, in our study once we carried out the density gradient all OMVs were isolated from the same high-density fraction (40%). OMV are also composed of lipids not only proteins, therefore, lower or higher density does not always represent the amount of proteins within OMV because the lipid:protein ratio might affect OMV density.

As previously discussed in Chapter 4, variation in *H. pylori* OMV protein contents between growth conditions was recently reported in the Zavan *et al* (2018) study, however they found that OMV from early growth stages contained higher numbers of protein than late growth stage (Zavan *et al.* 2018). This is in contradicted with our study as we found that OMV from early broth cultures contained fewer proteins than the late broth OMV.

Proteins from OMV produced in each condition were compared against each other quantitatively. Only proteins identified as differentially expressed between experimental conditions with $\geq 75\%$ confidence by the Sciex OneOmics software platform were included in the analysis. In this study, each condition was represented by a combination of data from 6 independent replicate samples into the Sciex OneOmics software to validate protein regulation in OMV from three different growth conditions. Data were searched using different libraries. Confidence score was calculated by analysing all fold changes (<fold change, 0, >fold change) then significant data validates protein regulation and confidence score.

The relative quantities of proteins in OMV from each condition were analysed based on fold changes. There were 71 proteins included in the comparison between early broth OMV-associated proteins and late broth. The comparison indicated that most of the proteins were downregulated in early broth OMV compared to late broth OMV (Figure 5.1). However, the two major toxins of *H. pylori* (VacA and CagA) were ~ 2 -fold upregulated in early broth OMV compared to late broth OMV (Figure 5.1). Flagellin was also present at ~ 2 -fold greater quantity in early broth compared to late broth OMV (Figure 5.1). This is consistent with Zavan *et al* (2018) as they harvested OMV of *H. pylori* 26695 strain from BHI broth supplemented with 0.2% β -cyclodextrin after 16 (early stage), 48, and 72 hours (late stage), and found more CagA and VacA in early

stage OMV than late stage. However, they did not compare OMV from plate cultures in their study.

Moreover, in this study, we interestingly found that as the environmental conditions became more challenging, the size of produced OMV increased. In the characterisation study (Chapter 3) 444A OMV from plate showed the largest size followed by late broth OMV and then early broth OMV were the smaller (Figures 3.5 and 3.7). Thus, packing more toxins in OMV isolated from early broth (non-challenging environment) means that while the bacteria are growing in a favourable condition, they pack high amounts of toxins. This suggests that cargo determination is regulated by the OMV assigned function. For example, at this stage the bacteria might release OMV as an adaptation mechanism and to interact with competing bacteria and with the host cells, establishing colonisation. In contrast, in more challenging environments such as the late broth and plate culture, bacteria tend to pack more proteins that support their survival in such environment. Because in this case, OMV may be released for the purpose of providing nutrient and support. Importantly, OMV isolated from plate cultures contained lots of peroxidase and 60-kDa DNA chaperones (Figures 5.8 and 5.9). These proteins might help the bacteria to survive in stressful environments. For instance, peroxidase protects bacteria under oxidative stress as it breaks down hydrogen peroxide (Murray *et al.* 2020; Wan *et al.* 1998; Bhattacharjee *et al.* 2002). Chaperones prevent protein misfolding and help to refold polypeptides in stressful environments (Table 5.1). (Maguire *et al.* 2002).

When comparing OMV from early broth cultures to plate cultures, 237 proteins were included in the analysis. The comparison indicated up- and downregulations in proteins between early broth and plate OMV (Figure 5.4) and overall, there were many more differentially expressed proteins between early broth and plate OMV (Figure 5.4), than between early broth and late broth OMV (Figure 5.3). This likely reflects the very different growth environment on agar plates compared to planktonic growth. CagA toxin and proteins of the associated Type IV secretion system were up-regulated ~1.5-fold in early broth OMV compared with plate OMV (Figure 5.4). VacA was excluded from this comparison because the confidence score was less than 75%. Once again, OMV isolated from the more stressful condition (growth on agar plates in close proximity to other bacteria, compared with early stage

culture in nutrient rich broth) contained more peroxidase and chaperonin, and less toxin.

Proteins of OMV from late broth were also compared to those from the plate. The analysis showed that VacA was downregulated ~1.5-fold in late broth OMV compared to plate OMV (Figure 5.5). CagA was excluded from this comparison because the confidence score was less than 75%.

Previous studies have also reported that different environmental conditions could alter the quantities of proteins in *H. pylori* OMV (Keenan *et al.* 2000; Keenan and Allardyce 2000; Fiocca *et al.* 1999). Keenan and Allardyce (2000) harvested *H. pylori* OMV from broth cultures with high and low iron concentrations. They found that culture under low iron conditions caused upregulation of protease in OMV, compared to OMV produced in high iron cultures. In contrast, VacA toxin appeared to be downregulated in OMV from low iron cultures compared with OMV from high iron cultures (Keenan *et al.* 2000; Keenan and Allardyce 2000; Fiocca *et al.* 1999). This is consistent with our finding in the current study that OMV produced under less stressful growth conditions contain more VacA toxin. Although we did not specifically manipulate iron availability in our cultures, iron availability was likely to decline over time as the bacteria were cultured in broth or on agar plates in close proximity to each other. Moreover, Keenan and Allardyce used enzyme-linked immunosorbent assay (ELISA), while Keenan *et al.* and Fiocca *et al.* used immunolocalization to identify and quantify the VacA. These are relatively old studies and the available technology for identification and quantification of proteins has since advanced dramatically, so these analyses are no longer considered sufficiently reliable or accurate. Additionally, these techniques can only be used to study one or a few proteins (in this case, the focus was solely on VacA). In the current study, samples were analysed using LC-MS/MS and SWATH for more accurate identification and quantitation of all of the proteins present in each sample.

As mentioned earlier, bacteria on an agar plate are creating a stressful environment as they grow. This is supported by our observation that bacteria at the centre of a plate tend to transform their shape from spiral to coccoid (viable but non-culturable form), presumably to cope and survive within the environment, while bacteria at the

edge of a plate close to unspent media remain spiral shaped for longer (AlSharaf and Winter, unpublished data). Also, bacteria in late broth cultures would experience a more stressful environment than bacteria in early broth cultures because nutrients will become limited over time. In this study, 60190 strain sampled at an early stage of broth culture was typically spiral shaped, while bacteria from late broth cultures showed a transformation from spiral to U-shaped (see Figure 3.10, Section 3.5.1.).

Several other studies have also reported *H. pylori* transformation from spiral to coccoid in stressful environments (Cammarota *et al.* 2012; Rudnicka *et al.* 2014; Cellini *et al.* 2008; Andersen and Rasmussen 2009). It has also been reported that OMV can help bacteria survival in stressful environments (Murray *et al.* 2020; Keenan 2000; Yonezawa *et al.* 2009). It is possible that due to transformation, and/or in response to stress, the determination of OMV cargo might be affected. The envelope stress response also alters the contents of OMV (Reviewed by Nagakubo *et al.* 2020; Olofsson *et al.* 2010). On balance, it is now well-established that growth conditions can influence the process of selection and packing proteins into bacterial vesicles.

A key finding from the proteomics analysis in this study was that OMV from plate cultures had completely different protein profiles compared to OMV from broth cultures. Although a few other studies have compared OMV harvested from different growth stages or conditions in broth, including for *H. pylori* (Zavan *et al.* 2018, Keenan & Allardyce 2000), we are not aware of any studies to date that have compared the protein contents of OMV from *H. pylori* grown on plates versus broth cultures.

There were 6 differentially expressed proteins unique to the early broth versus late broth OMV comparison, 42 differentially expressed proteins unique to the early broth versus plate OMV comparison, and 193 differentially expressed proteins unique to the late broth versus plate OMV comparison (Figure 5.7). Only 14 proteins were identified as differentially expressed across all of the pairwise comparisons between all three conditions (Figure 5.7) (Table 5.1).

These 14 proteins are associated with several functions, including DNA replication, detoxification, translation, fatty acid and phospholipids metabolism, and ribosomal protein synthesis and modification (Table 5.1). Proteins were distributed in different

quantities depending on the growth conditions (Figure 5.8 and 5.9). The highest amounts of peroxidase and 60-kDa chaperonin proteins were in OMV from plate cultures, as discussed above.

5.4.3. Analysis of proteins associated with cell response

In chapter 4, OMV from *H. pylori* strain 444A were shown to have cytotoxic effects on human gastric epithelial (AGS) cells, although this varied depending on the growth conditions, OMV dose and the type of cytotoxicity assay used. To further characterise the effects of OMV on AGS cells, a proteomics approach was used to determine which proteins were up- and down-regulated in cells exposed to a sub-lethal dose of OMV. AGS cells were subjected to a treatment with a low dose of *H. pylori* 444A OMV isolated from early (1 day) or late (6 days) broth cultures, or left untreated, and then the proteins from each cell population were analysed by LC-MS/MS. Unfortunately, no data could be collected for AGS cells treated with *H. pylori* 444A OMV isolated from plate cultures due to lab closures during the COVID-19 pandemic.

Although many proteins were identified (295 proteins in untreated AGS cells, 291 proteins in AGS cells treated with early broth OMV, and 293 proteins in AGS cells treated with late broth OMV, very few proteins could be confidently identified as differentially expressed in response to OMV treatment. Differentially expressed proteins with $\geq 50\%$ confidence were included in this analysis based on fold changes in protein quantity between untreated and OMV treated cells (Tables 5.2 and 5.3). There were 11 differentially expressed proteins between AGS cells treated with early broth OMV and untreated cells, and 11 differentially expressed proteins between AGS cells treated with late broth OMV and untreated cells (Tables 5.2 and 5.3) (Figure 5.10). Of these, there were 6 proteins in common between the two comparisons (Figure 5.10). 40S ribosomal protein S2, pyruvate kinase PKM, plasminogen activator inhibitor 1 RNA-binding protein, junction plakoglobin, 60S ribosomal protein L27 and 60S ribosomal protein L6 were down-regulated in both AGS cells treated with early broth OMV and AGS cells treated with late broth OMV (Table 5.3, in blue).

All of the proteins that changed in relative quantity in response to OMV treatment were downregulated, with the exception of polypyrimidine tract-binding protein 1 (PTBP1) which was up-regulated ~ 2 -fold in response to treatment with late broth

OMV (Table 5.3). PTBP1 has roles in pre-mRNA processing and regulation of alternative mRNA splicing (Uniprot), and is upregulated in some cancers (Zhu *et al.* 2020), but the reason for its upregulation in response to OMV treatment is unclear without further study.

A confidence score cut-off of 50% was used in this analysis because so few differentially expressed proteins were identified in response to OMV treatment. Only three proteins were identified as differentially expressed in response to OMV treatment with a higher confidence score ($\geq 65\%$). These were translationally-controlled tumour protein (down-regulated in response to early broth OMV), junction plakoglobin (down-regulated in response to both types of OMV, but with higher confidence score in the late broth OMV analysis), and 40S ribosomal protein S2 which was identified as down-regulated in response to both types of OMV with confidence score $\geq 65\%$ (Table 5.2). Translationally-controlled tumour protein is a ubiquitous protein with roles in cell proliferation and apoptosis (Bommer and Thieke 2004; Böhm *et al.* 1989). 40S ribosomal protein has a role in ribosomal structure and translation (UniProt; URL). Junction plakoglobin has roles in cell-cell adherence and tumour suppression (Reviewed by Aktary *et al.* 2017). Downregulation of junction plakoglobin might affect cellular morphology, and a low level of junction plakoglobin was detected in carcinomas (Reviewed by Aktary *et al.* 2017).

We selected a dose of 6 $\mu\text{g}/\text{ml}$ OMV based on the cytotoxicity assays (see chapter 4) as a sub-lethal dose that might induce protein responses in the AGS cells without completely killing them. However, overall, the protein responses of AGS cells to this OMV treatment were very modest in this study and further investigations, ideally using a range of OMV doses and time points, and including OMV from plate cultures, are needed for a better understanding of the effects of *H. pylori* OMV on host cell protein expression.

5.4.4. Correlation between VacA and CagA quantities and OMV cytotoxicity effect

H. pylori 444A strain (high virulence, *vacA* s1 i1 m1, *cagA*+, high biofilm former) was isolated from a patient suffering gastric ulceration disease with moderate Sydney scores, including intestinal metaplasia. In the cytotoxicity study (Chapter 4), AGS cells

were treated with 444A OMV for 24 hours. The microscopic analysis (Section 4.4.3.3.) showed vacuolation in AGS cells treated with 444A OMV from early broth at 6 and 18 hours and in AGS cells treated with 444A OMV from early broth at 18 hours (see Section 4.4.3.3., Table 4.3). This indicated that VacA was present in the OMV and capable of inducing vacuolation in the OMV-treated cells. However, no vacuolation activity was seen in AGS cells treated with late broth OMV (see Section 4.4.3.3., Table 4.3). On the other hand, hummingbird cells, which indicate the activity of CagA, were presented in small numbers in AGS cell populations treated with all three types of OMV (see Section 4.4.3.3., Table 4.3).

In this chapter, OMV proteomics analysis revealed that 444A OMV isolated from the three culture conditions all contained VacA and CagA. However, the protein quantities differed between the culture conditions (Table 5.4). OMV from early broth contained the highest amounts VacA and CagA, while OMV from late broth had the lowest concentration of both proteins (Table 5.4). The quantity of VacA within the OMV correlated with their capacity to induce vacuolation in human gastric epithelial cells.

5.5. CHAPTER SUMMARY

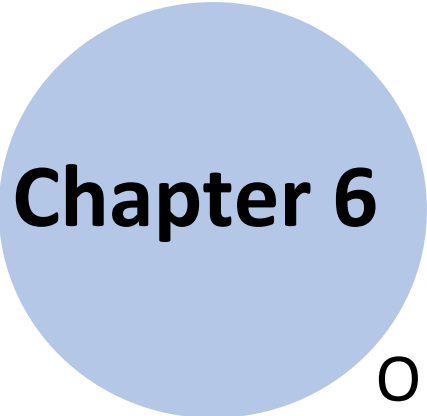
H. pylori OMV contain different virulence factors that can have toxic effects gastric epithelial cells, including VacA and CagA. However, the environmental conditions under which OMV are produced can influence the packaging of virulence factors into OMV and their subsequent effects on host cells. This study aimed to characterise the protein contents of OMV isolated from *H. pylori* grown under different environmental conditions and to determine the effects of these OMV on protein expression in OMV-treated AGS cells, using a proteomics approach.

To do this, OMV were purified from different *H. pylori* strains cultured in BHI broth with 0.2% β -cyclodextrin after 1 and 6 days, or on blood agar plates after 24 hours, and highly purified by OptiPrep density gradient centrifugation. OMV associated proteins from several *H. pylori* strains were initially analysed by SDS-PAGE and then strain 444A OMV associated proteins were characterised by LC-MS/MS and quantified by SWATH-MS (label-free) to determine relative protein concentrations (expressed as fold change) between OMV isolated from different culture conditions. In addition, AGS cells were treated with a low dose of 444A OMV for 24 hours and proteins associated with host cell response to OMV treatment were characterised by LC-MS/MS and quantified by SWATH-MS (label-free) to determine changes in protein expression.

The main results from this chapter are:

- Protein profiles of *H. pylori* OMV vary substantially between strains.
- OMV isolated from plate cultures had completely different protein profiles compared with OMV from broth cultures.
- OMV from early broth cultures contained more VacA and CagA toxins than OMV from late broth or plate cultures. This was consistent with the more extensive vacuolation seen in AGS cells treated with early broth OMV in the previous chapter.
- Very few changes in protein expression were seen in AGS cells in response to treatment with low (sub-lethal) doses of *H. pylori* OMV.

In conclusion, growth conditions can change *H. pylori* OMV protein contents, influencing their cytotoxicity.



Chapter 6

MUTAGENESIS OF KEY GENE

6. MUTAGENESIS OF KEY GENE

6.1. INTRODUCTION

H. pylori releases outer membrane vesicles as it is actively growing. These vesicles contain heterogeneous proteins including some that are implicated in virulence. Plenty of well-known virulence proteins of *H. pylori* have been identified in outer membrane vesicles in the current study (chapter 5) and in the published work of others. These include CagA toxin (Olofsson *et al.* 2010; Zavan *et al.* 2018; Mullaney *et al.* 2009; Turner *et al.* 2015; Liu *et al.* 2019) (see Section 5.5.2.). The expression of CagA toxin is strongly associated with ulcerations and carcinomas due to the damage it causes to the gastric mucosa and epithelial cells (Turkina *et al.* 2015) (see Section 1.3.3.). CagA is classified as an oncogenic protein (Ohnishi *et al.* 2008; Neal *et al.* 2013). Hence, patients infected with CagA positive strain are at higher risk for developing ulcers and gastric cancer (Atherton 2000; Hacker and Kaper 2000).

The CagA protein (130 to 145 kDa) is encoded by the *cagA* gene that is localised at the 3' end of the 40 kb *cag* pathogenicity island (PAI) (Censini *et al.* 1996; Atherton 2000). The *cag* PAI is a 40 kb stretch of genomic DNA (gDNA) that can be transferred horizontally between different bacteria. Hence, *H. pylori* *cag* PAI might be acquired from other bacterial species (Atherton 2000) The *cag* PAI also encodes other many other virulence-associated genes, for example, the proteins making up the Type IV Secretion System (T4SS), which is a syringe-like structure responsible for injecting CagA toxin directly into gastric epithelial cells (Kim *et al.* 2006; Censini *et al.* 1996). Before CagA can be injected, *H. pylori* must adhere to host cells and this adhesion is supported by adhesin proteins such as BabA and SabA (Jiménez-Soto *et al.* 2009; Kwok *et al.* 2007). Once CagA is injected, the tyrosine kinases (Src and Abl families) of the host cells phosphorylate the CagA at the EPIYA motif, stimulating cellular signalling (Khaledi *et al.* 2020; Krisch *et al.* 2016; Kurashima *et al.* 2008; Ren *et al.* 2006; Segal *et al.* 1999). Phosphorylation also induces the host cells' elongation, known as the hummingbird phenotype, and cell migration might occur (Krisch *et al.* 2016; Kurashima *et al.* 2008; Ren *et al.* 2006; Segal *et al.* 1999).

Since *H. pylori* has high mutation and recombination rates, the *cagA* gene has polymorphisms, especially in the EPIYA-repeat region. In this region, four segments

have been identified (Figure 6.1), and these have been denoted EPIYA-A, EPIYA-B, EPIYA-C, and EPIYA-D segments (Khaledi *et al.* 2020; Krisch *et al.* 2016; Hatakeyama 2017). Differences in the expression of these segments can influence the virulence of the *H. pylori* strain (Krisch *et al.* 2016; Hatakeyama 2017). This is thought to be one of the key oncogenic differences between East Asian strains (which are more likely to cause cancer) and other strains from the rest of the world (Western CagA strains). The EPIYA-repeat region of Western CagA strains typically includes EPIYA-A, EPIYA-B, and 1 to 5 EPIYA-C segments (Hatakeyama 2017; Jones *et al.* 2009). Whereas, East Asian CagA strain contains segments EPIYA-A, EPIYA-B, and EPIYA-D (Hatakeyama 2017).

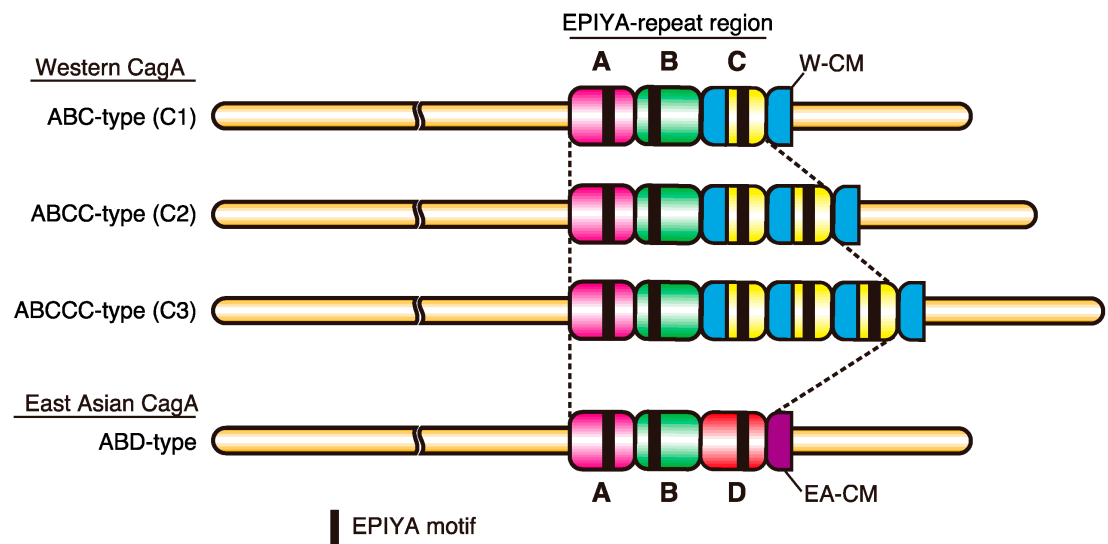


Figure 6.1: Polymorphism of *cagA* in EPIYA-repeated region. (Nishikawa and Hatakeyama 2017).

Tyrosine phosphorylation of the CagA protein mainly starts at motifs EPIYA-C and -D (Khaledi *et al.* 2020; Hatakeyama 2017). It has been reported that tyrosine phosphorylation also allows the formation of the CagA-SHP2 (Src homology 2-containing phosphatase 2) complex, which influences cellular signalling pathways (Krisch *et al.* 2016; Hatakeyama 2017; Atherton 2006; Jones *et al.* 2009). East Asian CagA strains were reported to have higher transformation activities than the Western CagA strains (Azuma *et al.* 2004; Argent *et al.* 2008). For instance, East Asian CagA strains induce more Interleukin 8 (IL-8) compared to the Western CagA strains. That might be due to the stronger binding of EPIYA-D to SHP2 inside host cells (Azuma *et al.* 2004). Moreover, as the CagA-SHP2 complex alters the signalling pathways, it can

induce the secretion of IL-8 (Brandt *et al.* 2005). It has been reported that high IL-8 expression stimulates the host immune response (Cammarota *et al.* 2012; Kim *et al.* 2006; Winter *et al.* 2014).

Although the number of EPIYA-C segments can vary among Western CagA strains, this does not seem to influence virulence (Argent *et al.* 2008; Khaledi *et al.* 2020). It is worth mentioning that non-phosphorylated CagA also affects cellular signalling and causes damage to the epithelial cells as it breaks the tight junctions between epithelial cells and causes defects in cells polarity and integrity (Turkina *et al.* 2015; Hatakeyama 2017). CagA is mainly injected at the tight junctions between epithelial cells (Turkina *et al.* 2015) and CagA+ OMV were localised at the junctions of epithelial cells, in contrast to the OMV of a CagA- mutant strain (Turkina *et al.* 2015). Non-phosphorylated CagA can also inhibit tumour suppressors (Hatakeyama 2017). Thus, CagA+ strains can induce carcinogenesis more readily.

6.2. AIM OF THE STUDY

CagA is an oncogenic protein and contributes to alteration cell morphology and proliferation, cell migration, and immune response alteration. Although CagA is well characterised, there are still gaps in our understanding of the toxicity of OMV-delivered CagA because different factors can alter the contents and characteristics of OMV. In chapter 5, CagA was one of the proteins identified with highest confidence as differentially expressed between OMV from early broth cultures and OMV produced in other growth conditions. In chapter 4, OMV produced under different growth conditions were found to have different cytotoxic effects on gastric epithelial cells.

in this chapter, the aim was to generate a *cagA* knock out *H. pylori* strain and then compare the effects of OMV from the wild type and mutant strains on gastric epithelial cells. The research questions were:

- Do *cagA* mutant *H. pylori* produce OMV that are less toxic to human gastric epithelial cells than OMV produced by wild type *H. pylori*?
- Do the bacterial growth conditions influence the cytotoxicity of the OMV produced by wild type and *cagA* mutant *H. pylori* strains?

The intention for this study was to generate a *cagA* knock out mutant in the strain 444A background and then test OMV from wild type 444A and *cagA* mutant 444A on AGS cells.

Due to pandemic-associated laboratory closures, it was not possible to complete all of the planned steps in time. This chapter describes progress towards generation of the Δ *cagA* mutant in the strain 444A background, and then testing of wild type and Δ *cagA* mutant OMV from the 60190 strain background. Wild type and Δ *cagA* mutant 60190 strains were kindly provided by Dr Karen Robinson and team at The University of Nottingham.

6.3. MATERIALS AND METHODS

6.3.1. *H. pylori* Strain

H. pylori 444A strain with high virulence (as determined by its genotype for the main virulence factors *vacA* and *cagA*) was used for the mutagenesis described in this study (sections 6.3.2 – 6.3.5) and strain 60190 (wild type and *cagA* mutant) were used for the cytotoxicity assays (sections 6.3.6 – 6.3.7). Strains were grown from the frozen stock onto blood agar and incubated in microaerophilic conditions for 24 to 72 hours at 37 °C with 80% humidity as described previously in Chapter 2 (see Section 2.3.1.). *H. pylori* was then passaged onto fresh blood agar plates and incubated for 48 hours in the microaerobic cabinet (see Section 2.3.1.).

6.3.2. Selection of Gene of Interest (GOI)

The *cagA* gene was selected as the gene of interest in this study, as outlined in the Introduction (see Section 6.4.1.).

6.3.3. Cloning Gene of Interest into pJET Cloning Vector

H. pylori genomic DNA was extracted and *cagA* gene was amplified, extracted and cloned into the pJET cloning vector (Figures 6.2 and 6.3) (see Sections 2.7.2.1. to 2.7.2.5.). Gene Cloning was confirmed using colony PCR (Figure 6.4) and *cagA*-pJET plasmid was purified using GeneJET plasmid miniprep kit following manufacturer's instructions (see Sections 2.7.2.6. and 2.7.2.7.). Sanger DNA sequencing was performed to confirm *cagA* cloning into the vector (see Section 2.7.2.8.).

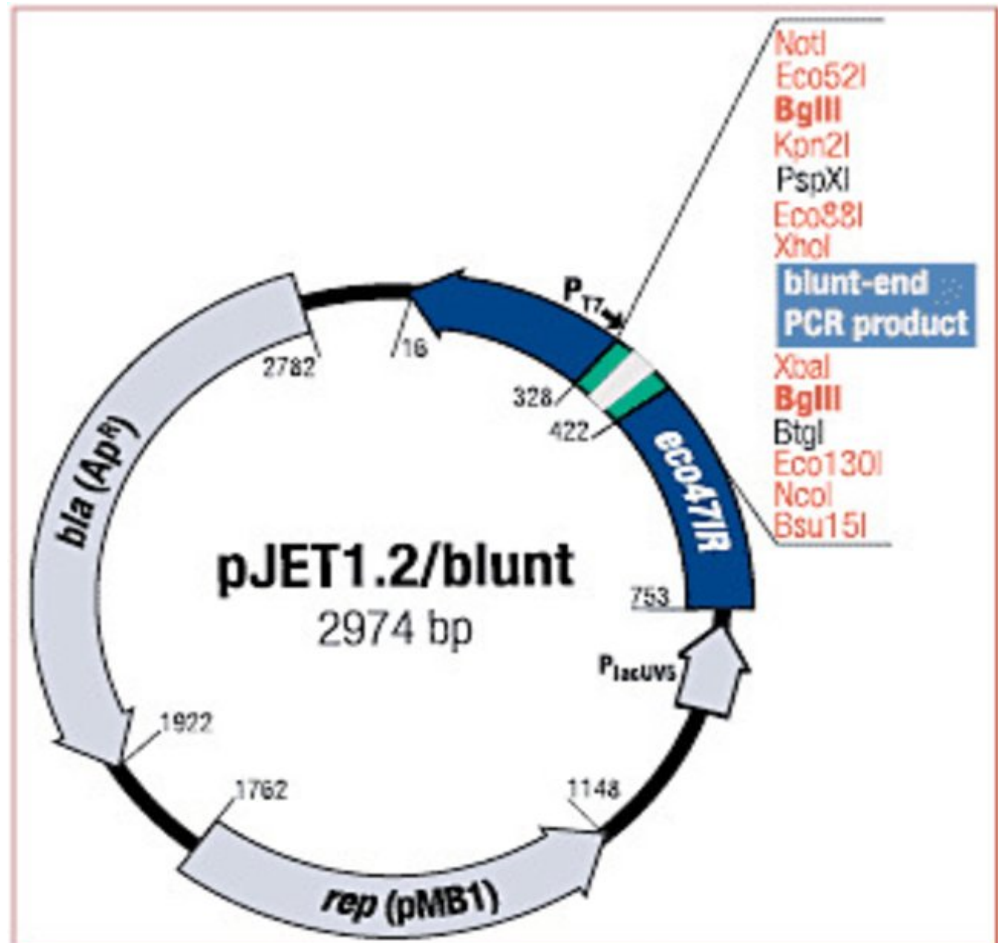


Figure 6.2: The map of pJET 1.2/blunt plasmid (ThermoFisher; URL).

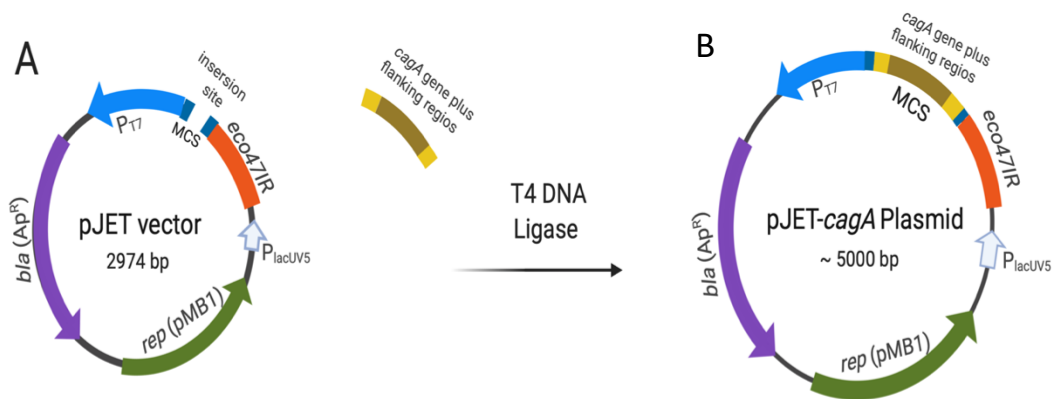


Figure 6.3: Ligation of *cagA* into pJET plasmid (Created with BioRender.com). (A) pJET vector and DNA fragment of *cagA*. (B) Constructed *cagA*-pJET plasmid.

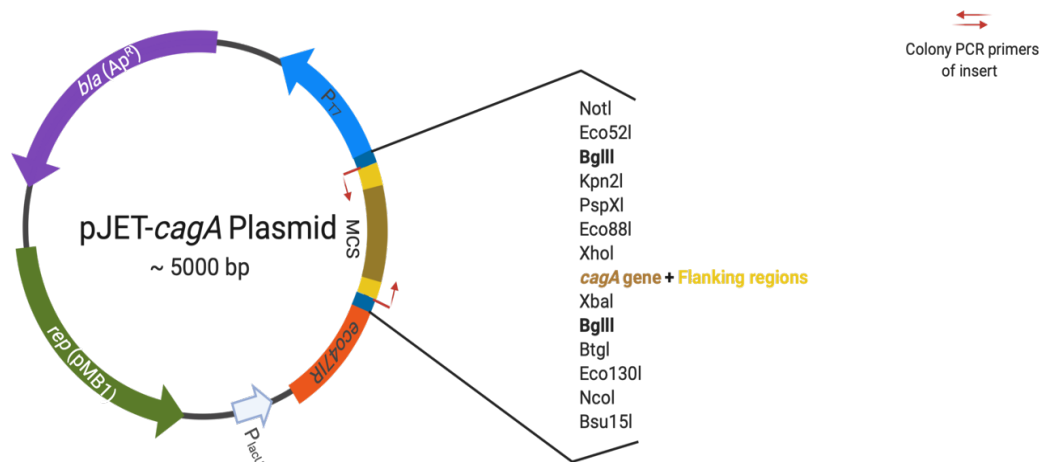


Figure 6.4: Colony PCR screening of *cagA* insert (Created with BioRender.com). *cagA*-pJET plasmid was used as a template. pJET forward and reverse primers were used for the PCR reaction. The reaction was then subjected to initial denaturation and enzyme activation cycle of 95 °C for 3 minutes followed by 25 cycles of denaturation at 94 °C for 30 seconds, annealing at 60 °C for 30 second and extension at 72 °C for 1 minute.

6.3.4. Inverse PCR and Construction of Mutation Plasmid

Inverse PCR was performed to amplify the pJET plasmid with *cagA* flanking regions (excluding the *cagA* gene) (Figure 6.5) and then purified using GeneJET plasmid miniprep kit (see Section 2.7.3.1.).

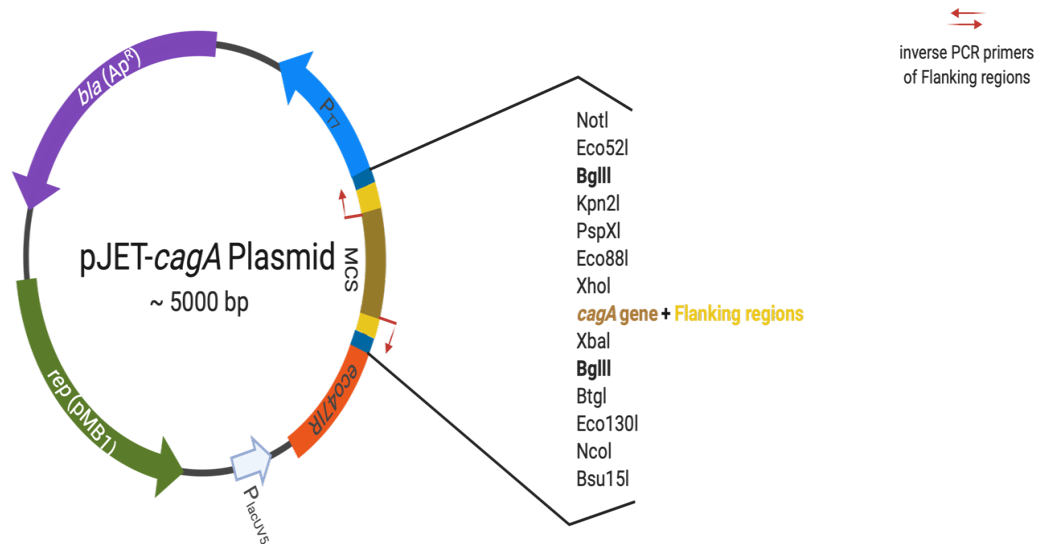


Figure 6.5: Inverse PCR of pJET-*cagA* plasmid (Created with BioRender.com). *cagA*-pJET plasmid was used as a template. Designed *cagINV* forward and reverse primers were used for the inverse PCR reaction. The reaction was then subjected to initial denaturation and enzyme activation cycle of 98 °C for 30 seconds followed by 30 cycles of denaturation at 98 °C for 10 seconds, gradient annealing temperature from 60 to 74 °C each for 30 second and extension at 72 °C for 1 minute followed by a final extension step at 72 °C for 10 minutes and hold at 4 °C.

The pBlueKm plasmid was purified from *E. coli* overnight culture using the GeneJET plasmid miniprep kit (Thermo Scientific), following the manufacturer's instructions (see Section 2.7.2.7.). The NovaBlue pBlueKm was provided by Darren Letley, University of Nottingham. This plasmid was used in this study as a source of the kanamycin resistance (KanR) cassette (Figure 6.6).

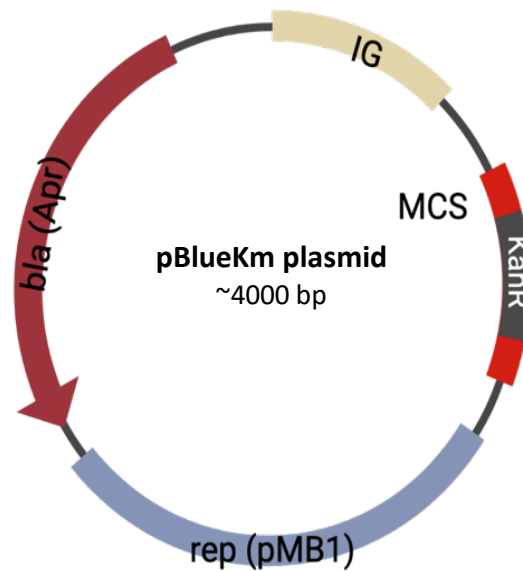


Figure 6.6: The extracted pBlueKm plasmid (Created with BioRender.com).

Purified pBlueKm plasmid and pJET-*cagA* flanks PCR product (Figures 6.7 and 6.8) were digested using the BamHI enzyme (see Section 2.7.3.3.). The digestion products were separated on a 1% agarose gel, and the appropriate sized bands for *KanR* cassette and pJET-*cagA* flanks were gel extracted and purified using the GeneJET gel extraction kit (see Section 2.7.2.4). The *KanR* was then cloned into the pJET-*cagA* flanking region plasmid (Figure 6.9) (see Section 2.7.3.4.) and purified using GeneJET plasmid miniprep kit (Thermo Scientific), following the manufacturer's instructions (see Section 2.7.2.7.).

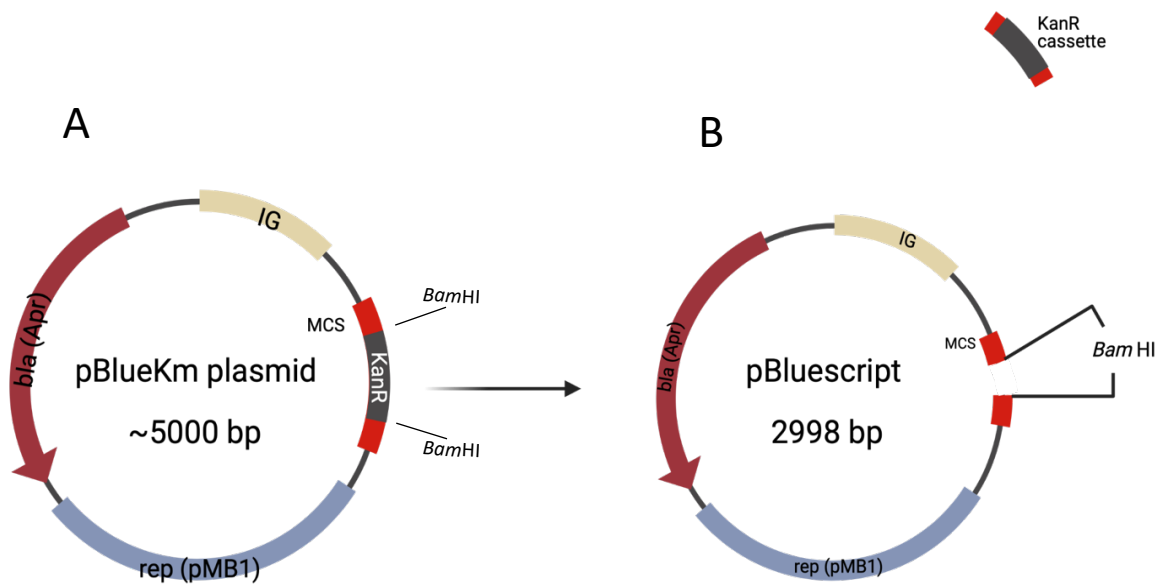


Figure 6.7: Digested pBlueKm plasmid (Created with BioRender.com). (A) pBlueKm plasmid (B) pBluescriptR plasmid and kanamycin resistance cassette (KanR) after BamHI digest.

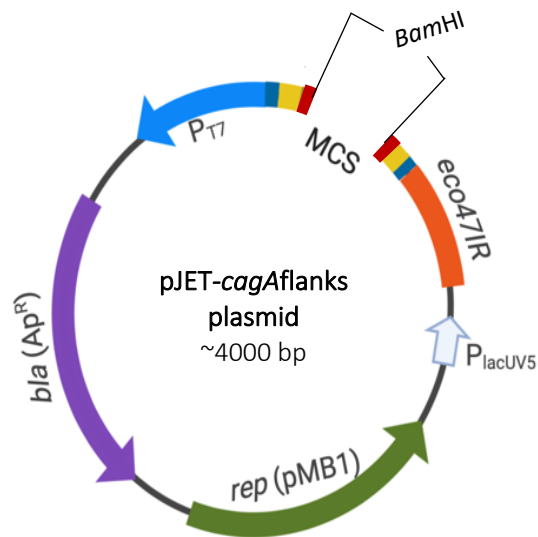


Figure 6.8: Digested pJET-cagA flanks plasmid (inverse PCR product) (Created with BioRender.com).

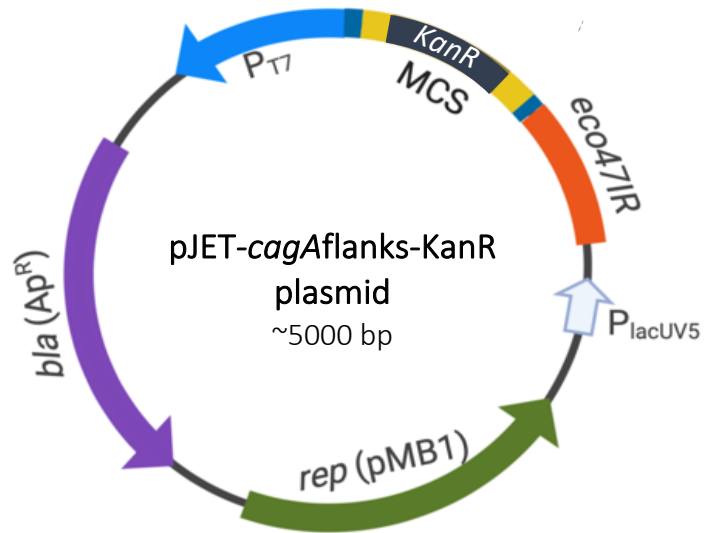


Figure 6.9: Constructed pJET-cagA flanks-KanR plasmid (Created with BioRender.com).

6.3.5. Transformation of *H. pylori*

H. pylori is a natural competent. In this study, a double recombination was needed for *H. pylori* transformation and knocking-out the *cagA* gene (Figure 6.10) (see Section 2.7.3.6.).

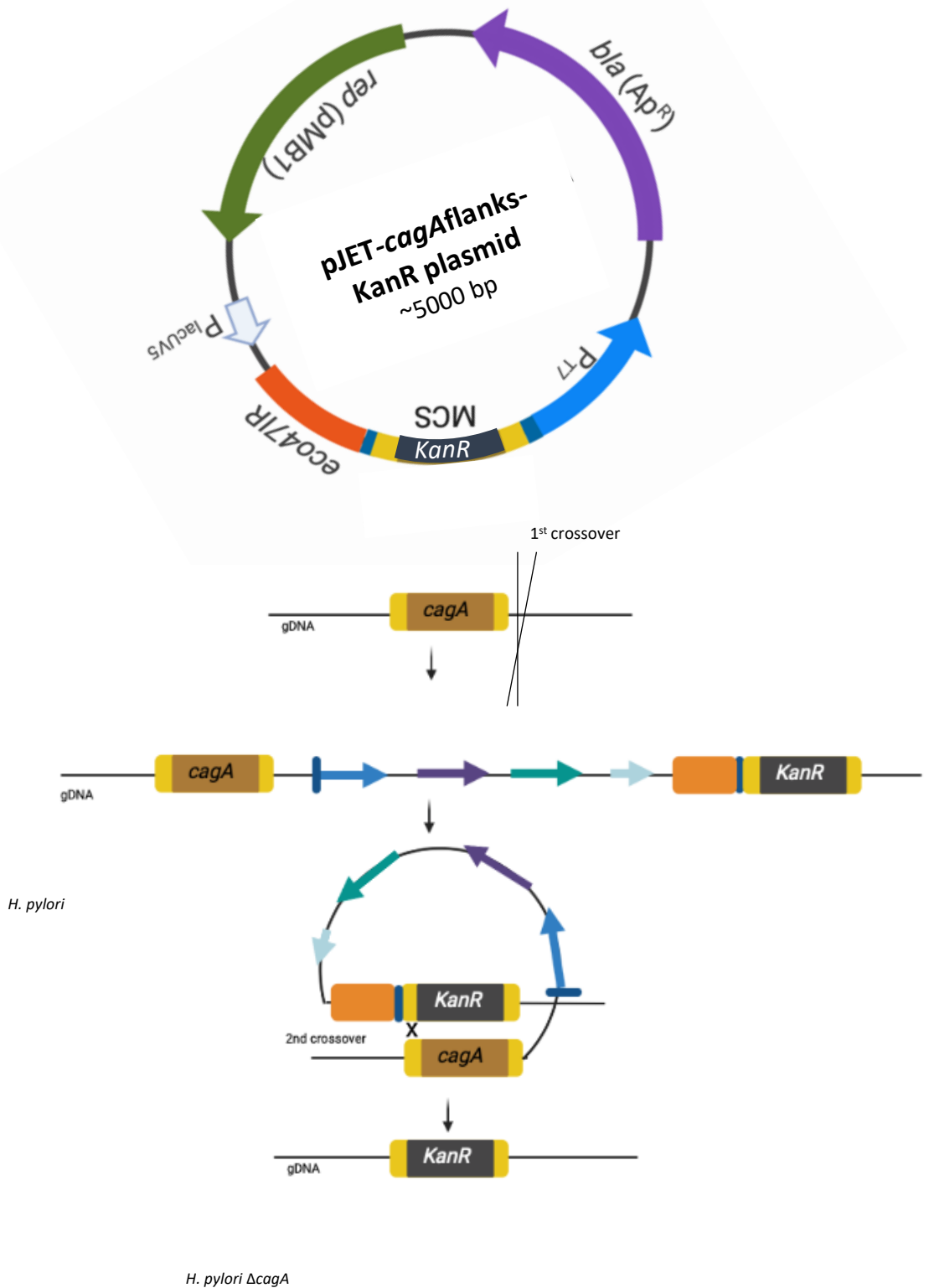


Figure 6.10: *H. pylori* DNA Recombination. KanR cassette double crossover into the genome to knock-out *cagA* (Created with BioRender.com).

6.3.6. Cytotoxicity of $\Delta cagA$ *H. pylori* 60190 OMV

6.3.6.1. Cell culture

Human gastric adenocarcinoma (AGS) cells (ATCC CRL-1739) were used in this study. Cells were grown in F-12K media with 10% HI-FCS and maintained three times a week as described previously in Chapter 2 (see Section 2.5.1). The purity of AGS cells was confirmed using the *Mycoplasma* detection test (see Section 4.3.4.).

6.3.6.2. *H. pylori* strain

H. pylori 60190 $\Delta cagA$ and wild type (WT) strains were used in this study. These lab strains were provided by Prof John Atherton and his team at The University of Nottingham. Both strains were grown in different *in vitro* environments and growth conditions as described previously in Chapter 2 (Sections 2.1. and 2.2.). Briefly, these conditions were liquid culture in broth for 24 hours (early broth OMV) or 6 days (late broth OMV) or on agar plates (plate OMV).

6.3.6.3. OMV isolation

H. pylori 60190 $\Delta cagA$ and WT strains were grown in BHI broth supplemented with 0.2% β -cyclodextrin and on blood agar plates for 24 hours as described previously (see Section 2.2.; 2.2.1. and 2.2.2.). The OMV were then purified by syringe filtration and ultracentrifugation as described previously (see Section 2.3.2.).

6.3.6.4. OMV cytotoxicity

Minimally passaged AGS cells were harvested, washed and added to the wells of 96-well plates at a concentration of 1×10^5 cells/ml. After 24 hours of incubation for growth and adherence, the cells were treated with 50 μ g/ml of OMV of $\Delta cagA$ 60190 and WT strains from different conditions. After a further 24 hours incubation, OMV cytotoxicity was determined by CellTiter 96 assay as an endpoint assay (see Section 2.5.2.1.).

6.3.7. Statistical Analysis

Cytotoxicity data were analysed using GraphPad Prism software version 8 for Mac IOS. Differences between the percentage survival of treated human gastric epithelial cells with OMV of $\Delta cagA$ 60190 and WT strains from different conditions were compared using two-way ANOVA of variance with multiple comparisons.

6.4.RESULTS

6.4.1. Selection of gene of interest

Gene of interest was selected based on different criteria. First, it should be expressed differently between OMV isolated from broth and plate cultures. Second, it should be a non-essential gene in *H. pylori* or one of a group of similar genes with similar sequences. Third, the flanking regions of the GOI should not be similar to other regions in the *H. pylori* genome, to minimise the risk of accidentally knocking out other genes. Also, the GOI should not have severe phenotypes when knocked out of different bacterial species. It is preferred that the GOI is not part of an operon. The *cagA* gene was selected as the gene of interest in this study.

cagA was selected as the gene of interest in this study because it is a key virulence gene in *H. pylori*. Also, it was expressed differently between OMV from early, late broth and plate cultures. The flanking regions of *cagA* are not similar to other genes. Therefore, the recombination of the mutagenesis construct into the *cagA* locus should be specific, and deletion of *cagA* might not induce any severe phenotypes.

6.4.2. Clone Gene of Interest into pJET Cloning Vector

The *cagA* amplification with gradient annealing temperature showed that the optimum annealing temperature was 57.9 °C (Figures 6.11) (Table 2.2). The *cagA* gene was detected at the expected size (~ 2000 bp) (Figures 6.11 and 6.12) and it was successfully extracted for ligation. The *cagA*-pJET plasmid transformation into the competent cells was confirmed by colony screening and colony PCR screening (Figures 6.13 and 6.14). The size of the *cagA*-pJET plasmid was about 5000 bp, as shown in Figure 6.13. The Sanger DNA sequencing showed that the *cagA* with the flanking regions were successfully cloned into the pJET vector. Due to COVID-19 pandemic circumstances, lockdowns and shortage of time, the mutagenesis process was continued while an alternative plan to instead compare cytotoxic effects of wild type and $\Delta cagA$ OMV in the 60190 strain background (where suitable wild type and mutant strains were already available) was simultaneously activated.

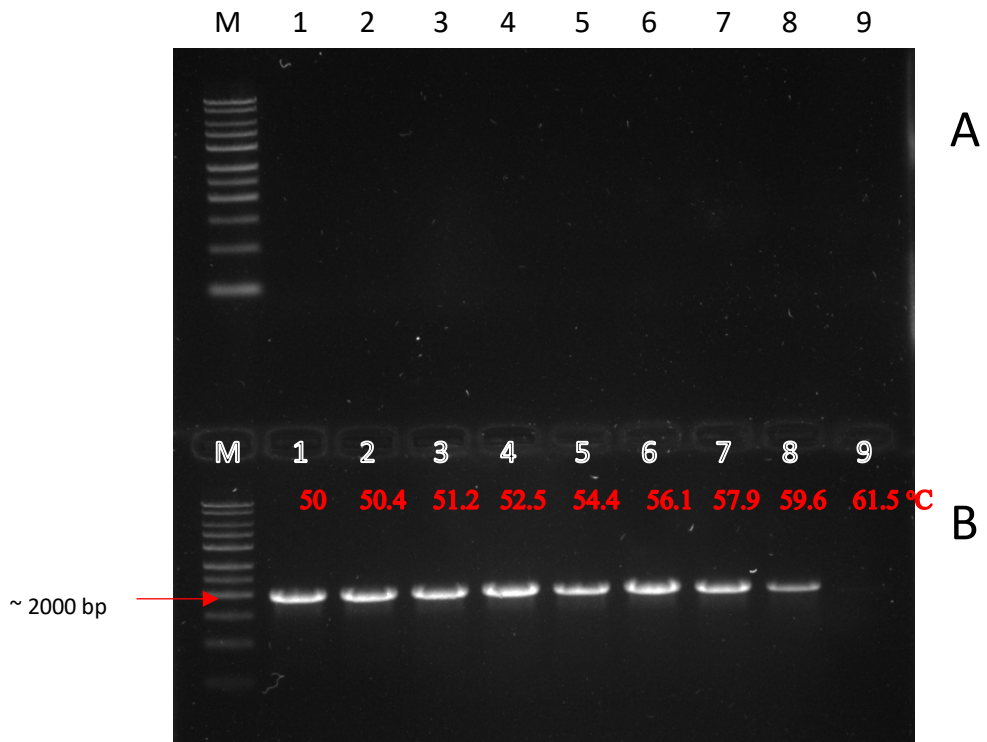


Figure 6.11: Gel electrophoresis of gradient PCR amplification of *cagA* gene. (A) Negative control. (B) Lanes from 1-9 are for *cagA* amplified at different annealing temperatures ranging from 50 to 64 °C. M= 1 kb DNA ladder. The optimum annealing temperature was 57.9 °C

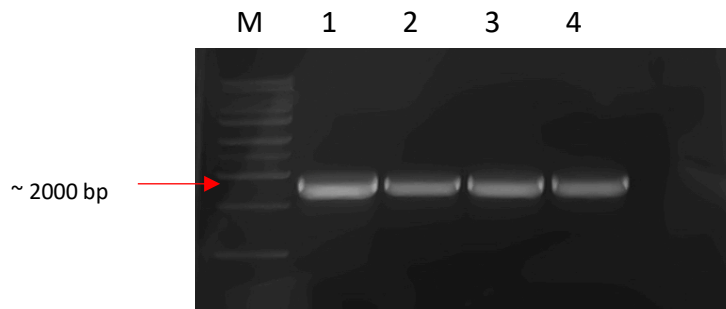


Figure 6.12: Gel electrophoresis of PCR amplification of *cagA* gene. Lanes from 1-4 are for amplified *cagA*. M= 1 kb DNA ladder. The reaction was subjected to initial denaturation and enzyme activation cycle of 95 °C for 30 seconds followed by 30 cycles of denaturation at 95 °C for 10 seconds, gradient annealing temperature from 50 to 64 °C each for 30 second and extension at 72 °C for 1 minute followed by a final extension step at 72 °C for 10 minutes and hold at 4 °C.

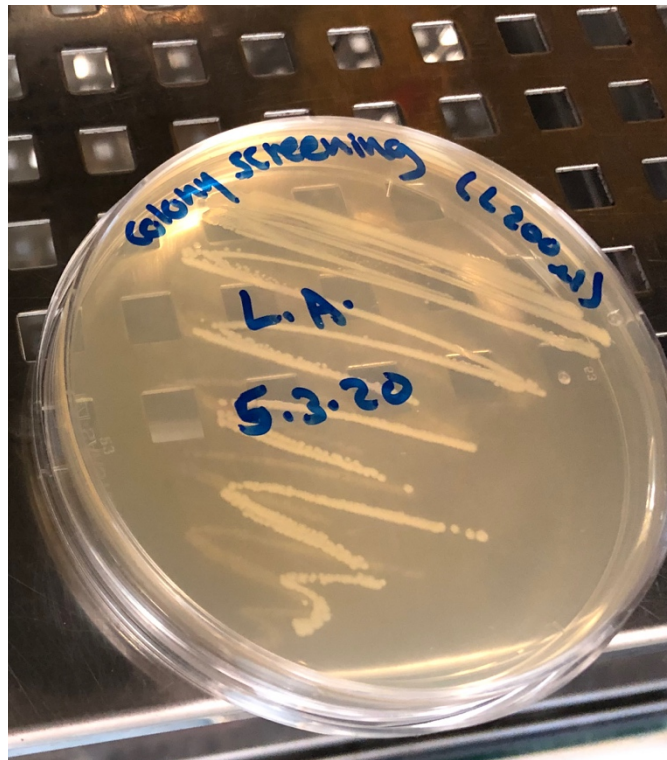


Figure 6.13: Colony screening of *E. coli* carrying *cagA*-pJET plasmid. Transformant NEB 5 alpha competent (*E. coli*) cells were cultured on LB broth agar plate and incubated for overnight at 37 °C.

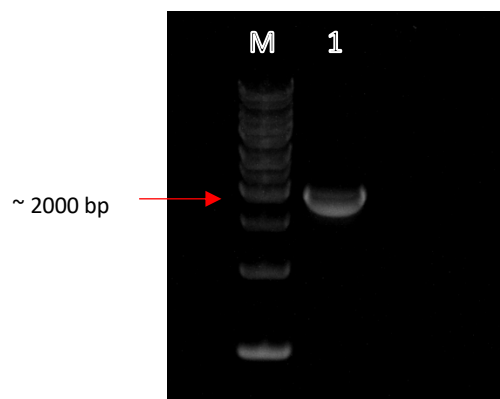


Figure 6.14: Gel electrophoresis of PCR colony screening of *cagA* insert. Lane 1 is the *cagA* gene. M= 1 kb DNA ladder. *cagA*-pJET plasmid was used as a template. pJET forward and reverse primers were used for the PCR reaction. The reaction was then subjected to initial denaturation and enzyme activation cycle of 95 °C for 3 minutes followed by 25 cycles of denaturation at 94 °C for 30 seconds, annealing at 60 °C for 30 second and extension at 72 °C for 1 minute.

6.4.3. Inverse PCR and Construction of Mutation Plasmid

The inverse PCR amplified the pJET plasmid and the flanking regions of the *cagA* gene while knocking out the *cagA*. The pJET-*cagA* flanks plasmid amplification with gradient annealing temperature showed that the optimum annealing temperature was 64.4 °C (Figures 6.15) (Table 2.2). The pJET-*cagA* flanks plasmid (without *cagA* gene, only including the flanking regions) was detected at the expected size (~ 4000 bp) (Figure 6.14) and successfully extracted. Restriction digest cut out the KanR cassette from the pBlueKm plasmid (Figure 6.15). The gel showed the digested pBluescript plasmid band sized ~ 3000 bp and KanR cassette sized ~ 1000 bp (Figure 6.16). The gel also showed the digested pJET-*cagA* flanks plasmid sized ~ 4000 bp. The KanR cassette was ligated into pJET-*cagA* flanks plasmid. The pJET-*cagA* flanks plasmid transformation into the competent cells was confirmed by colony screening (image not captured).

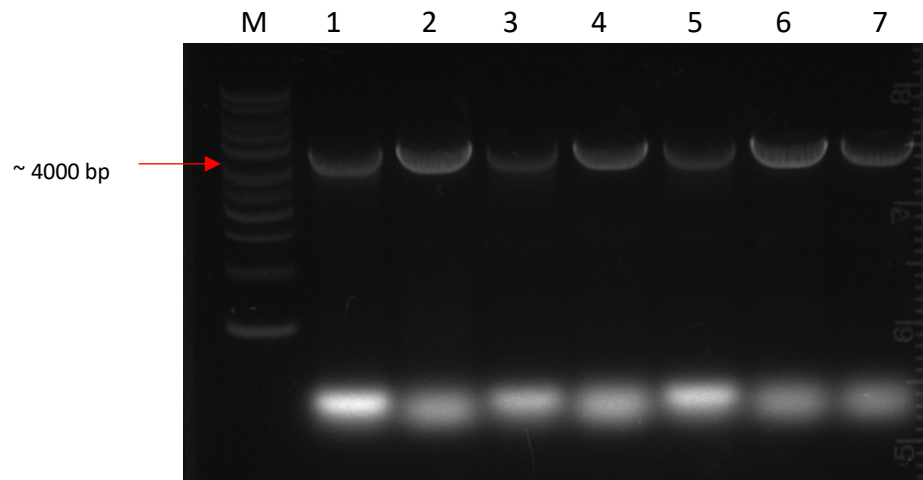


Figure 6.15: Gel electrophoresis of gradient inverse PCR of pJET-*cagA* plasmid. Lanes from 1-9 are for pJET-*cagA* flanks amplified at different annealing temperatures ranged from 60 to 74 °C. M= 1 kb DNA ladder. The optimum annealing temperature was 64.4 °C.

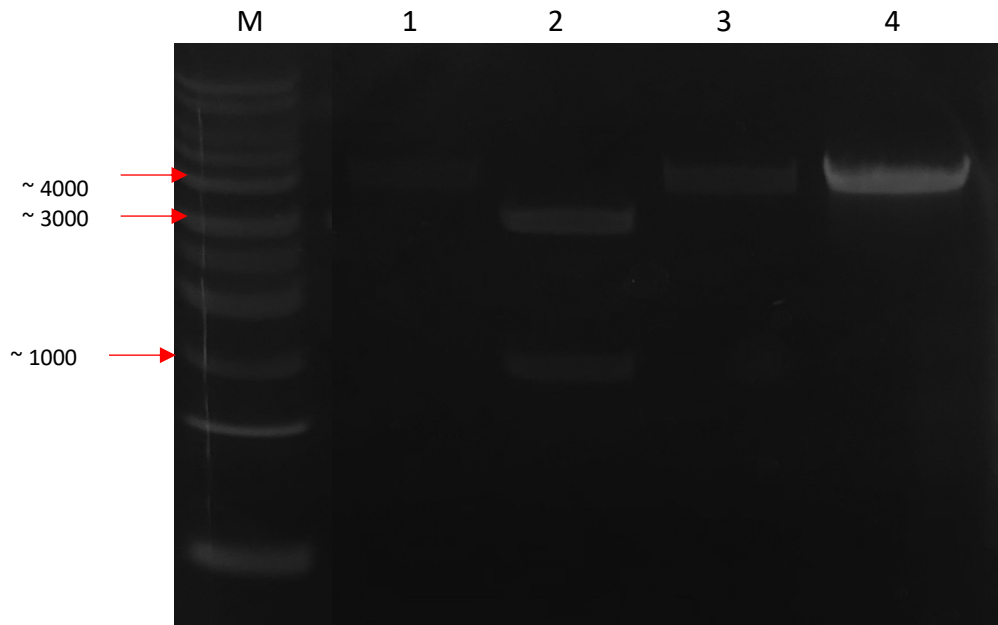


Figure 6.16: Gel electrophoresis of restriction digest. Lane 1= pBlueKm plasmid control (~4000 kb; light band). Lane 2= pBluescriptR plasmid (~3000 kb) and kanamycin resistance cassette (~1000 kb). Lane 3 = pJET-*cagA* flanks plasmid control (~4000 kb). Lane 4 = Digested pJET-*cagA* flanks plasmid (~4000 kb). M = 1 kb DNA ladder.

6.4.4. Transformation of *H. pylori*

H. pylori is a natural competent. Transformed *H. pylori* at the first recombination (Figure 6.10) will be able to grow on a kanamycin blood agar. However, in this study, it seems that the plasmid pJET-*cagA* flanks-KanR was not successfully transformed onto *H. pylori* as there was no *H. pylori* colonies grew in the presence of kanamycin. Therefore, second recombination was not performed.

6.4.5. Effect of WT and Δ *cagA* *H. pylori* 60190 OMV on AGS cells

All isolated OMV of *H. pylori* 60190 Δ *cagA* and WT strains from three different growth conditions were analysed for their toxicity on human gastric epithelial cells after 24 hours treatment. A high concentration (50 μ g/ml) of OMV of 60190 WT strain from all cultures was significantly more toxic to AGS cells compared to untreated cells (**** $p < 0.0001$ and * $p < 0.05$) (Figure 6.17). Similarly, OMV of 60190 Δ *cagA* isolated from early broth cultures were significantly more toxic to AGS cells compared to untreated cells (* $p < 0.05$). However, they were slightly less toxic than OMV from WT

60190. OMV of 60190 $\Delta cagA$ isolated from late broth cultures did not show a toxic effect on AGS compared to untreated cells (Figure 6.17). Also, OMV of 60190 $\Delta cagA$ isolated from plate cultures were more toxic to AGS cells compared to untreated cells; however, this difference was not statistically significant. It was evident that OMV from 60190 $\Delta cagA$, especially those isolated from late broth and plate cultures, were less toxic to AGS cells than OMV from 60190 WT (Figure 6.17). Comparing 60190 WT with 60190 $\Delta cagA$ showed that the OMV of 60190 WT isolated from late broth and plate were significantly more toxic to the untreated gastric epithelial cells than those of 60190 $\Delta cagA$ ($***p < 0.001$ and $**p < 0.01$, respectively) (Figure 6.17).

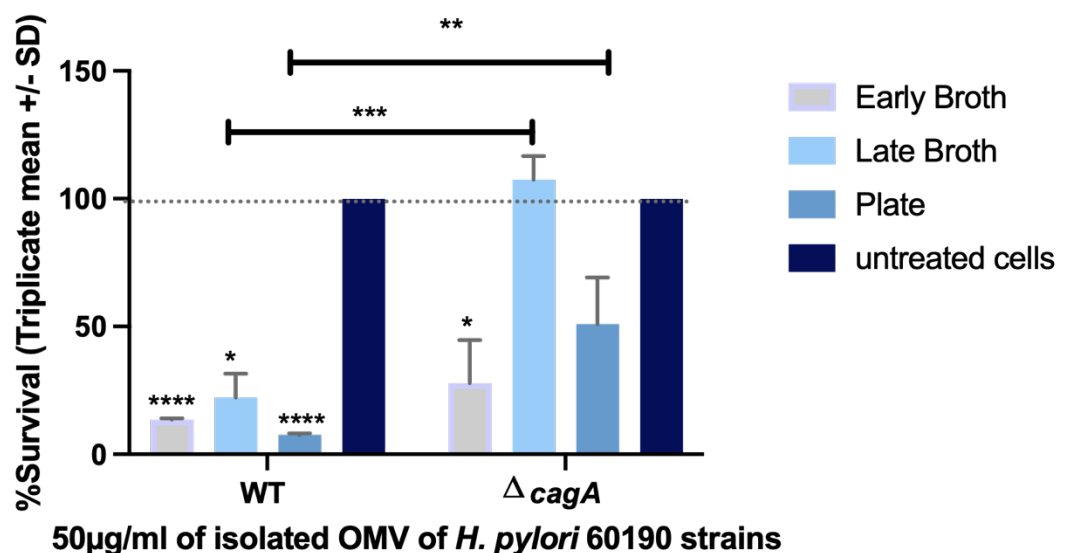


Figure 6.17: Effects of high dose of OMV on human gastric epithelial cells. AGS cells were treated with 50 µg/ml of OMV of *H. pylori* 60190 $\Delta cagA$ and wild type strains isolated from early, late broth and plate cultures in triplicate and incubated in 5% CO₂ for 24 hours at 37 °C. Promega CellTiter 96 assay reagent was added, mixed well, and incubated for 1 hour at 37 °C before measuring the absorbance at 490 nm. Two-way ANOVA analysis was performed to test the significance of difference between the percentage survival of human gastric epithelial cells treated with OMV of each strain. The percentage survival of AGS cells compared against untreated control cells are shown. Error bars show the mean of blank corrected values of three independent replicates (+/- SD). **** and * indicate $p < 0.0001$ and < 0.05 , respectively.

6.5. DISCUSSION

6.5.1. Mutagenesis of *cagA* gene

H. pylori 444A strain (high virulence, *cagA*⁺, *vacA* s1 i1 m1, high biofilm former) was isolated from a patient suffering gastric ulceration disease with moderate Sydney scores including intestinal metaplasia (Table 2.2). Both major virulence factors CagA and VacA were identified in *H. pylori* 444A OMV isolated from all three growth conditions but the toxins were packaged differently between conditions (Figures 5.3 and 5.4) (Table 5.6).

It has been reported that the amount of *cagA* expression can affect the virulence of *H. pylori* as high expression of *cagA* appears to induce carcinogenesis more readily (Jiménez-Soto and Haas 2016; Ohnishi *et al.* 2008; Neal *et al.* 2013). In this study, we found that CagA was detected in different quantities in OMV isolated from the three growth conditions. However, a few hummingbird cells were seen in all OMV treated cells at 6 and 18 hours, indicating CagA toxin activity (see Tables 4.3 and 5.6).

We aimed to construct an *H. pylori* 444A *cagA* mutant strain in this study to characterise the role of CagA in OMV pathogenesis in this strain background; however, although the mutagenesis plasmid was successfully constructed, the transformation of *H. pylori* was unsuccessful. That might be due to insufficient concentration of the constructed pJET-*cagA* flanks-KanR plasmid. Due to COVID-19 pandemic circumstances and lockdowns, the cloning could not be repeated. Mutating virulence genes of *H. pylori* in a range of strain backgrounds is suggested for future work to identify the role of each gene in OMV-mediated pathogenesis.

6.5.2. Effect of WT and Δ *cagA* *H. pylori* 60190 OMV on AGS cells

Since the Δ *cagA* mutant in the strain 444A background could not be generated in time, a comparison of the cytotoxicity of WT versus Δ *cagA* mutant OMV grown under different conditions was conducted in the 60190 strain background. Since this strain has been used extensively over the years for studies of CagA, isogenic 60190 wild type and mutant Δ *cagA* strains were readily available from our collaborators at the University of Nottingham.

The toxicity of OMV of *H. pylori* 60190 WT and $\Delta cagA$ strains was examined in this study by CellTiter 96 assay. It was evident in Figure 6.17 that OMV from *H. pylori* 60190 WT strain were more toxic to AGS cells than those from 60190 $\Delta cagA$ strain. This is consistent with previous studies, for example Turkina *et al.* 2015 added both types of OMV to monolayer epithelial cells, and only CagA OMV were localised at the tight junctions after 4 hours. Also, CagA OMV induced histone-ATP binding compared to $\Delta cagA$ mutant OMV (Turkina *et al.* 2015). Thus, CagA within OMV might promote OMV-cells interaction. However, further investigations are needed.

Regarding growth conditions, OMV from 60190 WT strain isolated from all three conditions significantly decreased the %survival of AGS cells compared to untreated cells (p^{****} and p^*) (Figure 6.17). OMV from the $\Delta cagA$ mutant strain isolated from early broth also decreased the %survival of AGS cells compared to untreated cells (Figure 6.17). That was statistically significant (p^*). Although OMV from the $\Delta cagA$ strain from plate cultures were toxic to AGS cells compared to untreated control cells, that was not significant statistically (Figure 6.17). Thus, *cagA* is not the only component of OMV that drives cytotoxicity. *H. pylori* have other toxins that can also induce cellular responses. OMV from strains without *cagA* can still cause inflammation. Interestingly, OMV from the $\Delta cagA$ strain from late broth cultures were not toxic to AGS cells compared to untreated cells, which was in contrast to those from the WT strain (Figure 6.17). It seems that CagA makes a significant difference in the OMV virulence for those isolated from a late broth culture. The growth conditions might also influence bacterial virulence and the determination of OMV contents. Moreover, OMV of 60190 WT isolated from late broth and plate showed a significant toxic effect on untreated gastric epithelial cells than those of 60190 $\Delta cagA$ ($***p < 0.001$ and $**p < 0.01$, respectively) (Figure 6.17).

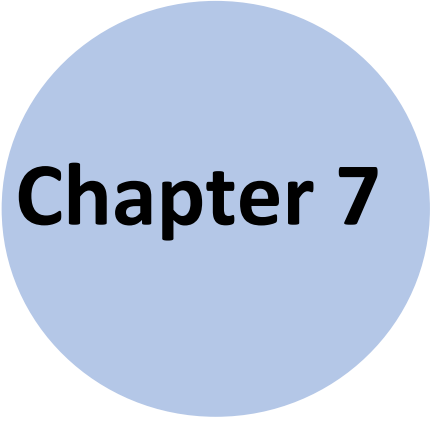
The proteomics study of 444A OMV-associated proteins showed that CagA was expressed differently between conditions (Table 5.6). In the mutagenesis study, the transformation of the *H. pylori* 444A strain was unsuccessful. Therefore, *H. pylori* 60190 WT and $\Delta cagA$ strains from the University of Nottingham were used instead. The *H. pylori* 60190 strain used for the cytotoxicity study (Chapter 4) was originally from The University of Nottingham but had been routinely stored and passaged at Nottingham Trent University for over 5 years. This strain had slightly different effects

on cells (chapter 4) compared with the 60190 WT strain more recently obtained from The University of Nottingham (chapter 6). *H. pylori* has a very high mutation rate and strains gradually change over time in labs based on the passaging process and the culturing techniques used in each lab. Therefore, differences in cytotoxicity between these two wild type 60190 strains were expected. It would be interesting to genome sequence the two strains to identify which genes have changed over time across the two labs, and it would also be interesting to compare the OMV proteomes of the two strains.

Constructing a *cagA* mutant of 444A strain is also recommended for future work to characterise the *cagA* gene's role in OMV pathogenesis because *H. pylori* 444A strain is a high virulence *cagA*+, *vacA* s1 i1 m1, and high biofilm forming strain. It was isolated from a patient suffering gastric ulceration disease with moderate Sydney scores, including intestinal metaplasia (Table 2.2).

6.6.CHAPTER SUMMARY

H. pylori OMV contain hundreds of different proteins. CagA protein was identified in *H. pylori* OMV by mass spectrometry. It is an oncogenic cytotoxin and its presence is associated with gastric cancer and peptic ulcers. This study aimed to characterise the toxicity of OMV-associated CagA under different environmental conditions. A *cagA* mutagenesis plasmid was constructed in the 444A background; however, the transformation into *H. pylori* 444A strain was not successful. Instead, OMV were purified from *H. pylori* 60190 WT and $\Delta cagA$ strains cultured in BHI broth with 0.2% β -cyclodextrin after 1 and 6 days or on blood agar plates after 24 hours. OMV toxicity on human gastric epithelial (AGS) cells was determined by CellTiter 96 assay. OMV from *H. pylori* 60190 WT strain were more toxic to AGS cells than those from the $\Delta cagA$ strain. Wild type OMV isolated from late broth cultures were toxic on AGS cells while $\Delta cagA$ OMV from late broth had no cytotoxic effect at all. On the other hand, OMV from early broth cultures were cytotoxic regardless of the presence/absence of CagA. CagA is not the only potentially cytotoxic protein present in *H. pylori* OMV and further studies will be needed to fully understand the reasons for differences in OMV cytotoxicity between growth conditions.



Chapter 7

DISCUSSION

7. DISCUSSION

H. pylori is the third leading cause of cancer-related deaths worldwide. It infects more than half of the world's population. *H. pylori* have several strategies for persisting in the human host and causing diseases, one of which is producing outer membrane vesicles. Several functions of these vesicles were identified to date; however, their role in pathogenesis still not fully understood. This study aimed to characterise OMV isolated from *H. pylori* strains with high and low virulence under different growth conditions to determine whether either of these variables (bacterial virulence and growth conditions) influence the characteristics of the vesicles. This study also aimed to determine whether or not they influence OMV toxicity on mammalian cells, and to identify and compare the OMV-associated proteins of a high virulence strain grown under three different conditions. For further understanding, this study aimed to mutate one of the critical OMV-associated virulence proteins to determine its impact on OMV cytotoxicity compared to the wild type.

To do this, OMV of 8 *H. pylori* strains with high and low virulence (Table 2.1) were isolated from broth cultures after 1 and 6 days and from agar plates after 24 hours. The broth and plate cultures are entirely different environment as they differ in their components, type of medium (liquid and solid), bacterial motility, availability of nutrients, and growth mode. Isolated OMV were quantified and characterised using Pierce BCA- protein assay and Zetaview nanoparticle tracking analysis. Although these methods employed different principles, they broadly agreed with each other (Figure 3.8). The analyses confirmed that all *H. pylori* strains could produce OMV in all three different growths conditions with variations in OMV characteristics between strains and, within each strain, between different growth conditions (Figures 3.1 – 3.3). Out of 8 tested strains, 7 strains showed higher OMV production in early broth than on plate (Figures 3.1 and 3.3). This was consistent with previously published findings that not all environmental conditions are equally favourable for bacteria to produce vesicles (Chatterjee and Chaudhuri 2012). The high virulence *H. pylori* strain 444A produced significantly more OMV in early broth than plate cultures (p^{****}) (Figure 3.1 B).

In this study, we detected the morphological transformation of *H. pylori* from spiral to coccoid shape after 6 days of incubation in broth cultures (Figure 3.10). Therefore, the bacteria were no longer culturable, so unfortunately, their CFU/ml could not be measured. However, bacterial viability was measured using the BacTiter-Glo assay instead. We found a good correlation between bacterial viabilities measured by the BacTiter-Glo and Miles and Misra quantification methods (Figure 3.4). It appeared that bacteria produced higher quantities of OMV in late broth cultures than in early broth or plate cultures (Figures 3.1 and 3.2). However, statistical analysis could not be performed to compare the production of OMV isolated from late broth cultures with those isolated from early broth and plate cultures due to the differences between methods used. It was expected that the longer the bacteria were growing, the more OMV would be produced. A recent study also showed that OMV were present in higher quantities in late broth cultures compared with early broth cultures (Zavan *et al.* 2018), but they did not include OMV from plate cultures in their analysis.

In terms of the OMV size, as measured by Zetaview, the OMV purified in this study were sized between 100 to 130 nm (Figure 3.5 and 3.6). OMV from early broth cultures were slightly larger than those from late broth and plate cultures, and OMV from plate cultures were smallest, except for the 444A strain (Figures 3.5 and 3.7). For strain 444A, OMV from plate cultures were larger than OMV from early and late broth cultures, and early broth OMV were the smallest in size (Figures 3.5 and 3.7). Zavan *et al.* (2018) also found that OMV from the early broth cultures were similar to or larger than OMV from late broth cultures, using the well-characterised laboratory strain 26695. Another study also found that the size of OMV influenced their protein contents and mode of cell entry (Turner *et al.* 2018). They reported that larger OMV contained a higher number of proteins than smaller OMV, and used a different pathway to enter host cells (Turner *et al.* 2018).

These studies carried out their OMV sizing using NanoSight, not the Zetaview (Zavan *et al.* 2018; Turner *et al.* 2018). The Zetaview has not been used previously for *H. pylori* OMV characterisation. Nonetheless, it has been used to measure the size distribution for other bacterial species such as uropathogenic *E. coli*, *P. aeruginosa*, and *C. jejuni* (Svennerholm *et al.* 2017; Zhang *et al.* 2020; Davies *et al.* 2019). None of these studies compared OMV from broth to OMV from agar plates. Also, in previous

studies, whether on *H. pylori* or other species, OMVs mainly were compared between different broth conditions. Therefore, this aspect of our work is novel and has not yet been published elsewhere, to our knowledge.

In *E. coli*, an enterotoxigenic strain has been shown to produce ten times more OMV than a commensal strain (Hostman and Kuehn 2002). We compared OMV production between high and low virulence *H. pylori* strains, but we found little variation in OMV production quantity and no significant association between OMV quantity and bacterial virulence (Figure 3.9). In this study, we used only 8 strains; however, a more extensive study with a larger number of strains is suggested for future work.

To determine OMV cytotoxicity, human gastric epithelial cells (AGS cells) were treated with a range of doses of OMV (0 – 50 µg/ml). OMV of 4 strains with high and low virulence isolated from the three different growth conditions were used in this study. In this study, the bacterial virulence was defined based on their *vacA* and *cagA* toxin genotypes, strains with *vacA* s1 i1 m1 and *cagA*⁺, considered high virulence strains (Table 2.1). OMV of high virulence strains (444A and 60190) were more cytotoxic to AGS cells than the less virulent strains 221A and Tx30a (Figure 4.1). However, OMV from less virulent strains were still capable of inducing cellular responses. In a dose-dependent manner, lower doses of OMVs from all of the strains tested induced cell proliferation while higher doses inhibited it; however, the extent of this varied with the bacterial growth conditions (Figure 4.2). Ismail *et al.* (2003) also reported inhibition of AGS cell proliferation in response to treatment with higher doses of *H. pylori* OMV, while lower doses of these OMV induced cell proliferation (Ismail *et al.* 2003).

In addition to varying OMV dose, we also examined OMV toxicity to AGS cells over a range of time points. Although the RealTime-Glo assay showed stability of cells over 10 hours of exposure to OMV (Figure 4.3), in live-cell microscopic analysis using Incucyte, we detected the toxic effects of OMV on AGS cells as early as 6 hours of exposure (Tables 4.2 – 4.6). This is similar to Chitocholtan *et al.* (2008) who reported cellular vacuolation after 4 hours of exposure to OMV. In the RealTime-Glo assay, OMVs of 60190, 444A, and 221A strains isolated from early broth cultures showed inhibition of proliferation after 24 hours of exposure (Figure 3.4 A, B, and C). Similarly,

60190 OMV from plate cultures inhibited cell proliferation after 24 hours (Figure 3.4 C). Whereas OMV from strain Tx30a did not have any toxic effects on AGS cells, regardless of the bacterial culture conditions used to generate the OMV (Figure 3.4 D). One of the limitations of this study is that time points between 10 - 24 hours were not recorded.

In the microscopy analysis, different degrees of vacuolating activity and hummingbird cells were detected in AGS cells treated with OMV from high virulence strains (444A and 60190) over the exposure time (Tables 4.1 – 4.6) (Figure 4.8). These toxic effects are the hallmarks of the VacA and CagA toxins' activities, respectively (Palframan *et al.* 2012; Krisch *et al.* 2016; Kurashima *et al.* 2008). These proteins have been previously detected within *H. pylori* OMV (Olofsson *et al.* 2010; Zavan *et al.* 2018). In this study, we noticed differential expressions of these proteins in OMV isolated from different bacterial culture conditions. For example, 444A OMV from early broth and plate cultures induced different grades of vacuolation (Table 4.3). However, no vacuoles were detected in AGS cells treated with 444A OMV from late broth cultures. The significance of this is that the environment in which the parental bacteria grew can affect the toxicity of the OMV that are produced, presumably by influencing the determination of OMV cargo.

Moreover, no vacuolation or hummingbirds were seen in AGS cells treated with OMV from the less virulent strains 221A and Tx30a, as expected (Tables 4.4 and 4.6). These strains lack CagA and active VacA (Ayala *et al.* 2006; Chitcholtan *et al.* 2008; Ismail *et al.* 2003). Based on Incucyte measurement of the % confluence of treated AGS cells, we also found that all types of OMVs tested in this study significantly induced a cellular proliferation response compared to untreated cells, except for 444A OMV from early broth cultures (Figures 4.5 and 4.6). They showed induction at the first 2 hours only, and then the proliferation was inhibited as the % confluence between 1 hour to 18 hours of exposure was 0% (Figures 4.5 A and 4.6 A). In addition to that, dead cells were also measured using the IncuCyte by adding the Cytotox Red Dye to each well. This dye specifically detects dead cells. Minimal dead cells were detected in AGS cells treated with OMV from the less virulent 221A and Tx30a strains (Figure 4.7 B and D), while AGS cells treated with 444A and 60190 OMV from early and late broth cultures had high cell death rates (Figure 4.7 A and C). However, OMV isolated

from plate cultures of these two virulent strains did not induce cell death (Figure 4.7 A and C).

Interestingly, also Tx30a OMV from early broth cultures initially appeared to induce an unexpectedly high rate of cell death, once we compared the microscopy images by eye we found that this was an artefact. The images contained spots of dye that were not representing real dead cells (Table 4.5). This was one of the limitations of this study that affected the reliability of these results. In addition to excluding some time points from the analysis due to condensation, which made some microscopy images unclear, especially at the 0 hour time point, it was important to compare the start points of each treatment and confirm these results' reliability. Therefore, repeating this analysis with further optimisations is suggested for future work. All of the cytotoxicity data were summarised in Table 4.7.

In this study, we found that *H. pylori* 444A strain produced higher quantities of OMV in broth cultures than on plates; however, their OMV size was larger from plates than from broth cultures. Also, OMV of strain 444A isolated from each condition had different cytotoxic effects on OMV-treated AGS cells, as explained above. *H. pylori* 444A is a high virulence strain with *vacA* s1 i2 m1 and *cagA*+. It is also a high biofilm forming strain. This strain was isolated from a patient with precancerous changes including intestinal metaplasia. Therefore, proteomics analysis was suggested for the OMV of this strain to identify and compare their associated proteins and understand and compare the effect of the growth conditions and measure their toxic effects on the mammalian cells.

At this stage of the study, isolated OMV from the 4 strains were run in 12% SDS-PAGE gels to identify differences between strains and conditions, in general. The gels showed clear differences between strains (Figures 5.1 and 5.2). Also, in OMV of strains 444A and 60190, there was a noticeable difference in protein profiles between plate and broth OMVs (Figures 5.1 and 5.2). This agreed with the findings of Olofsson *et al* (2010) as they also detected variations in protein profiles between OMV from broth and plate cultures using SDS-PAGE. However, they did not analyse these differences further. More recently, Zavan *et al.* (2018) reported differences in protein expression between OMV from early and late growth stages as they found

that early-stage OMV expressed more CagA and VacA than the late stage. However, they did not compare these OMVs with the plate OMVs. Therefore, in our study we conducted a comprehensive proteomics analysis to compare the protein profiles of OMV between growth conditions.

Quantitative proteomic analysis for 444A OMV was carried out by David Boocock and his team at John Van Geest Cancer Research Centre, Nottingham Trent University, using LC-MS/MS and following a method that previously described in Aldis *et al.* (2020). The analysis identified 638 proteins in plate OMV, 431 proteins in early broth OMV, and 601 proteins in late broth OMV. It has been reported previously that large OMV contained more proteins than small ones (Turner *et al.* 2018). In Zavan *et al.* (2018) they found more varied proteins in early stage OMV than in late stage. However, in our study, we found more proteins in late broth OMV than early OMV.

The proteins in our study were compared against each other, and the confidence score cut-off of ≥ 0.75 by the Sciex OneOmics software was used in this analysis. Based on fold changes, the analysis showed that early broth OMV contained ~2-fold more CagA and VacA than late broth and plate OMV (Figures 5.3 and 5.3). This is consistent with Zavan *et al.* (2018), as they found that OMV isolated from early broth cultures contained more CagA and VacA than OMV isolated from late broth cultures.

We also found that plate OMV contained a higher quantity of these two toxins than OMV from late broths (Figure 5.5). There was an association between *cagA* and *vacA* expression in each condition and variations in 444A OMV toxicity on AGS cells (Table 5.4). The protein contents of OMV can change depending on the environmental conditions, and this can influence the effects of the OMV on host cells.

Identified proteins in each condition were clustered, and the heatmap (Figure 5.6) showed that plate OMV had a completely different protein profile compared with the broth OMVs. A Venn Diagram (Figure 5.7) There were only 14 proteins identified that were differentially expressed between all three comparisons (Figures 5.7 – 5.9) (Table 5.1). These proteins were identified and quantified, and we found that plate OMV contained higher quantities of peroxidase and 60 kDa chaperone compared to broth OMV (Figures 5.8 and 5.9). These proteins may have a role to play in protecting the

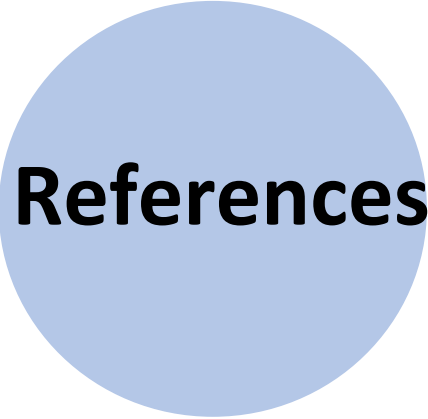
bacteria under stressful conditions, so it makes sense that their quantities in OMV broadly correlated with the stressfulness of the environment in which the OMV were produced. As mentioned earlier in this chapter, the protein profiles of OMV from plate and broth cultures were entirely different, and OMV from late broth cultures also differed somewhat from the early broth. In terms of the crude number of proteins identified, *H. pylori* under more stressful conditions appeared to package a higher number of proteins into OMV than in the more favourable environments (plate > late broth > early broth). This suggests that *H. pylori* forms and releases OMV for specific functions, and it can influence the protein contents of OMV to some extent accordingly to these functions. Zavan *et al.* (2018) and Keenan and Allardyce (2000) also studied the differences between OMV from different growth conditions, but did not characterised plate OMV and compared them to those from the broth. Therefore, this aspect of our work is novel.

In this study, we also treated AGS cells with a low dose of OMV from early and late broth cultures and identified proteins associated with cell response. Unfortunately, no proteomics data were obtained for AGS cells treated with OMV isolated from plate culture due to COVID-19 pandemic circumstances (laboratory closures). There were 295 proteins detected in untreated cells, 291 proteins detected in OMV from early broth, and 293 proteins were detected in OM from late broth. However, only 11 proteins were differentially expressed between treated and untreated cells (Figure 5.10) (Tables 5.2 and 5.3). All of these proteins were down-regulated in OMV treated cells. If this study were to be repeated, we suggest increasing the OMV dose to induce a more dramatic cellular response, in order to identify a larger number of differentially expressed host cell proteins.

At the final stage of this study, we aimed to construct a *cagA* mutant *H. pylori*. The *cagA* is highly associated with gastric cancers and ulcers, and it was expressed in 444A OMV from all three conditions and was identified as differentially expressed between growth conditions with a very high confidence score. The *cagA* mutagenesis plasmid was successfully constructed. However, *cagA* was, unfortunately, cloned in the wrong direction into the pJET plasmid and *H. pylori* transformation was not successful. Due to COVID-19 pandemic circumstances and lockdowns, the cloning could not be repeated. Instead, Δ *cagA* mutant and wild type strains of 60190 were

provided from our collaborators at the University of Nottingham. OMV were isolated from these strains under different growth conditions. AGS cells were treated with these OMV, and cytotoxicity was measured using a CellTiter assay. The analysis showed that WT OMV from late broth and plate cultures significantly decreased the % survival of AGS cells compared to $\Delta cagA$ OMV (p^{***} and p^{**}) (Figure 6.17). In WT OMV from all conditions significantly decreased the % survival of AGS cells (p^{****} and p^*) (Figure 6.17). In the $\Delta cagA$ mutant strain, OMV from early broth also significantly decreased the % survival of AGS cells compared to untreated cells (p^*) (Figure 6.17). Although $\Delta cagA$ OMV from plate cultures were also somewhat toxic to AGS cells compared to untreated control cells, this was not statistically significant (Figure 6.17). Thus, OMV from strains without *cagA* can still cause cytotoxicity because they still contain other virulence factors. However, the $\Delta cagA$ OMV were less cytotoxic than the OMV with CagA, across all three growth conditions, and $\Delta cagA$ 60190 OMV from late broth cultures were not toxic to AGS cells at all (Figure 6.17). It seems that CagA makes a significant difference to OMV virulence, especially for OMV isolated from a late broth culture.

In conclusion, the bacterial growth environment influences the characteristics of *H. pylori* OMVs within a strain as the OMV properties, and their associated proteins change according to the environmental conditions. This consequently affects the toxicity of OMV and their effects on host epithelial cells that could ultimately lead to different stomach disease outcomes.



References

- Aktary, Z., Alaei, M. and Pasdar, M., 2017. Beyond cell-cell adhesion: Plakoglobin and the regulation of tumorigenesis and metastasis. *Oncotarget*, 8(19), pp.32270-32291.
- Aldiss, P., Lewis, J., Lupini, I., Bloor, I., Chavoshinejad, R., Boocock, D., Miles, A., Ebling, F., Budge, H. and Symonds, M., 2020. Exercise Training in Obese Rats Does Not Induce Browning at Thermoneutrality and Induces a Muscle-Like Signature in Brown Adipose Tissue. *Frontiers in Endocrinology*, 11.
- Allan, N. and Beveridge, T., 2003. Gentamicin Delivery to *Burkholderia cepacia* Group IIIa Strains via Membrane Vesicles from *Pseudomonas aeruginosa* PAO1. *Antimicrobial Agents and Chemotherapy*, 47(9), pp.2962-2965.
- Allison, C.C., Kufer, T.A., Kremmer, E., Kaparakis, M., Ferrero, R.L., 2009. *Helicobacter pylori* induces MAPK phosphorylation and AP-1 activation via a NOD1-dependent mechanism. *J Immunol* 183(12):8099–8109. <https://doi.org/10.4049/jimmunol.0900664>.
- Alm RA, Bina J, Andrews BM, Doig P, Hancock RE (2000) Comparative genomics of *Helicobacter pylori*: analysis of the outer membrane protein families. *Infect Immun* 68(7):4155– 4168. <https://doi.org/10.1128/iai.68.7.4155-4168.2000>.
- AlSharaf, L. M. and Winter, J., unpublished data.
- Alting-Mees, M., Sorge, J. and Short, J., 1992. pBluescriptII: Multifunctional cloning and mapping vectors. *Methods in Enzymology*, pp.483-495.
- Amieva, M. and Peek, R., 2016. Pathobiology of *Helicobacter pylori*–Induced Gastric Cancer. *Gastroenterology*, 150(1), pp.64-78.
- Andersen, L., P., and Wadström, T., 2001. Bacteriology and culture. In *Helicobacter pylori: Physiology and Genetics*, edited by Mobley, H., L., T., Mendz, G., L., and Hazell, S., L., pp. 27-38. Washington, DC: ASM press.
- Andersen, L.P., and Rasmussen, L., 2009. *Helicobacter pylori* – Coccoid Forms and Biofilm Formation. *FEMS Immunol Med Microbiol*, 56: 112-115.
- Argent, R., Hale, J., El-Omar, E. and Atherton, J., 2008. Differences in *Helicobacter pylori* CagA tyrosine phosphorylation motif patterns between western and East Asian strains, and influences on interleukin-8 secretion. *Journal of Medical Microbiology*, 57(9), pp.1062-1067.
- Asaka, M., Takeda, H., Sugiyama, T. and Kato, M., 1997. What Role Does *Helicobacter pylori* Play in Gastric Cancer?. *Gastroenterology*, 113(6), pp. S56-S60.
- ATCC, 2021. AGS ATCC® CRL-1739™ *Homo sapiens* stomach gastric adenocarc. [online] [lgcstandards-atcc.org](https://www.lgcstandards-atcc.org). Available at: <https://www.lgcstandards-atcc.org/products/all/CRL-1739.aspx?geo_country=ro> [Accessed 15 February 2021].
- Atherton, J. and Blaser, M., 2009. Coadaptation of *Helicobacter pylori* and humans: ancient history, modern implications. *Journal of Clinical Investigation*, 119(9), pp.2475-2487.
- Atherton, J., 1998. *H. pylori* virulence factors. *British Medical Bulletin*, 54(1), pp.105-120.
- Atherton, J., 2000. CagA: a role at last. *Gut*, 47(3), pp.330-331.
- Atherton, J., 2006. The pathogenesis of *Helicobacter pylori*–induced gastro-duodenal DISEASES. *Annual Review of Pathology: Mechanisms of Disease*, 1(1), pp.63-96.
- Atherton, J., C., 1999. CagA, the cag pathogenicity island and *Helicobacter pylori* virulence. *Gut*, 44, 307-8.

- Attaran, B., Falsafi, F., and Moghaddam, A.N., 2016. Study of Biofilm Formation in C57BL/6J Mice by Clinical Isolates of *Helicobacter pylori*. *Saudi J Gastroenterol*, 22:161-8.
- Avakian, A., Sinel'nikova, M.P., Pereverzev, N.A., Gurskii, Iun., 1972. Electron microscopic study of biopsied sections of small intestine mucosa in patients with cholera and characteristics of the ultrastructure of causative agents of cholera in relation to toxinogenesis. *Zh Mikrobiol Epidemiol Immunobiol*. 49:86-92.
- Ayala, G., Torres, L., Espinosa, M., Fierros-Zarate, G., Maldonado, V. and Meléndez-Zajgla, J., 2006. External membrane vesicles from *Helicobacter pylori* induce apoptosis in gastric epithelial cells. *FEMS Microbiology Letters*, 260(2), pp.178-185.
- Azuma, T., Yamazaki, S., Yamakawa, A., Ohtani, M., Muramatsu, A., Suto, H., Ito, Y., Dojo, M., Yamazaki, Y., Kuriyama, M., Keida, Y., Higashi, H. and Hatakeyama, M., 2004. Association between Diversity in the Src Homology 2 Domain-Containing Tyrosine Phosphatase Binding Site of *Helicobacter pylori* CagA Protein and Gastric Atrophy and Cancer. *The Journal of Infectious Diseases*, 189(5), pp.820-827.
- Bachurski, D., Schuldner, M., Nguyen, P., Malz, A., Reiners, K., Grenzi, P., Babatz, F., Schauss, A., Hansen, H., Hallek, M. and Pogge von Strandmann, E., 2019. Extracellular vesicle measurements with nanoparticle tracking analysis – An accuracy and repeatability comparison between NanoSight NS300 and ZetaView. *Journal of Extracellular Vesicles*, 8(1), p.1596016.
- Backert, S., Tegtmeyer, N. and Selbach, M., 2010. The Versatility of *Helicobacter pylori* CagA Effector Protein Functions: The Master Key Hypothesis. *Helicobacter*, 15(3), pp.163-176.
- Backstrom, A., Lundberg, C., Kersulyte, D., Berg, D., Boren, T. and Arnqvist, A., 2004. From The Cover: Metastability of *Helicobacter pylori* bab adhesin genes and dynamics in Lewis b antigen binding. *Proceedings of the National Academy of Sciences*, 101(48), pp.16923-16928.
- Bauman, S. and Kuehn, M., 2006. Purification of outer membrane vesicles from *Pseudomonas aeruginosa* and their activation of an IL-8 response. *Microbes and Infection*, 8(9-10), pp.2400-2408.
- Baumgarten, T., Sperling, S., Seifert, J., von Bergen, M., Steiniger, F., Wick, L. and Heipieper, H., 2012. Membrane Vesicle Formation as a Multiple-Stress Response Mechanism Enhances *Pseudomonas putida* DOT-T1E Cell Surface Hydrophobicity and Biofilm Formation. *Applied and Environmental Microbiology*, 78(17), pp.6217-6224.
- Benoit, S., Holland, A., Johnson, M. and Maier, R., 2018. Iron-sulfur protein maturation in *Helicobacter pylori*: identifying a Nfu-type cluster carrier protein and its iron-sulfur protein targets. *Molecular Microbiology*, 108(4), pp.379-396.
- Bernadac, A., Gavioli, M., Lazzaroni, J.C., Raina, S., Lloubes, R., 1998. *Escherichia coli* tol-pal mutants form outer membrane vesicles. *J Bacteriol* 180(18):4872–4878.
- Bhattacharjee, M., Bhattacharjee, S., Gupta, A. and Banerjee, R., 2002. Critical role of an endogenous gastric peroxidase in controlling oxidative damage in *H. pylori*-mediated and nonmediated gastric ulcer. *Free Radical Biology and Medicine*, 32(8), pp.731-743.
- Bielaszewska, M., Rüter, C., Bauwens, A., Greune, L., Jarosch, K., Steil, D., Zhang, W., He, X., Lloubes, R., Fruth, A., Kim, K., Schmidt, M., Dobrindt, U., Mellmann, A. and Karch, H., 2017. Host cell interactions of outer membrane vesicle-associated virulence factors of enterohemorrhagic *Escherichia coli* O157: Intracellular delivery, trafficking and mechanisms of cell injury. *PLOS Pathogens*, 13(2), p.e1006159.
- BioRender. 2021. *BioRender*. [online] Available at: <<https://biorender.com/>> [Accessed 9 June 2020].

- Bitto, N.J., Chapman, R., Pidot, S., Costin, A., Lo, C., Choi, J., D’Cruze, T., Reynolds, E.C., Dashper, S.G., Turnbull, L., Whitchurch, C.B., Stinear, T.P., Stacey, K.J., Ferrero, R.L., 2017. Bacterial membrane vesicles transport their DNA cargo into host cells. *Sci Rep* 7(1):7072. <https://doi.org/10.1038/s41598-017-07288-4>
- Bjerre, A., Brusletto, B., Rosenqvist, E., Namork, E., Kierulf, P., Øvstebø, R., Joø, G. and Brandtzæg, P., 2000. Cellular activating properties and morphology of membrane-bound and purified meningococcal lipopolysaccharide. *Journal of Endotoxin Research*, 6(6), pp.437-445.
- Blaser, M. and Atherton, J., 2004. *Helicobacter pylori* persistence: biology and disease. *Journal of Clinical Investigation*, 113(3), pp.321-333.
- Blaser, M., Nomura, A., Lee, J., Stemmerman, G. and Perez-Perez, G., 2007. Correction: Early-Life Family Structure and Microbially Induced Cancer Risk. *PLoS Medicine*, 4(2), p.e100.
- Bohm, H., Gross, B., Benndorf, R., Strauss, M., Schunk, W., Kraft, R., Otto, A., Gaestel, M., Stahl, J., Drabsch, H. and Bielka, H., 1989. Molecular cloning, sequencing and expression in *Escherichia coli* of the 25-kDa growth-related protein of Ehrlich ascites tumor and its homology to mammalian stress proteins. *European Journal of Biochemistry*, 179(1), pp.209-213.
- Bommer, U. and Thiele, B., 2004. The translationally controlled tumour protein (TCTP). *The International Journal of Biochemistry & Cell Biology*, 36(3), pp.379-385.
- Boren, T., Falk, P., Roth, K., Larson, G. and Normark, S., 1993. Attachment of *Helicobacter pylori* to human gastric epithelium mediated by blood group antigens. *Science*, 262(5141), pp.1892-1895.
- Brandt, S., Kwok, T., Hartig, R., Konig, W. and Backert, S., 2005. NF- κ B activation and potentiation of proinflammatory responses by the *Helicobacter pylori* CagA protein. *Proceedings of the National Academy of Sciences*, 102(26), pp.9300-9305.
- Brown, L., 2000. *Helicobacter Pylori*: Epidemiology and Routes of Transmission. *Epidemiologic Reviews*, 22(2), pp.283-297.
- Cammarota, G., Branca, G., Ardito, F., Sanguinetti, M., Ianiro, G., Cianci, R., Torelli, R., Masala, G., Gasbarrini, A., Fadda, G., Landolfi, R., and Gasbarrini, G., 2010. Biofilm Demolition and Antibiotic Treatment to Eradicate Resistant *Helicobacter pylori*: A Clinical Trial. *Clinical Gastroenterology and Hepatology*, 8:817-820.
- Cammarota, G., Sanguinetti, M., Gallo, A., and Posteraro, B., 2012. Review article: biofilm formation by *Helicobacter pylori* as a target for eradication of resistant infection. *Aliment Pharmacol Ther*, 36: 222–230.
- Carvalho, A., Fonseca, S., Miquel-Clopés, A., Cross, K., Kok, K., Wegmann, U., Gil-Cardoso, K., Bentley, E., Al Katy, S., Coombes, J., Kipar, A., Stentz, R., Stewart, J. and Carding, S., 2019. Bioengineering commensal bacteria-derived outer membrane vesicles for delivery of biologics to the gastrointestinal and respiratory tract. *Journal of Extracellular Vesicles*, 8(1), p.1632100.
- Cellini, L., Allocati, N., Angelucci, D., Iezzi, T., Campli, E.D., Marzio, L., and Dainelli, B., 1994. Coccoid *Helicobacter pylori* Not Culturable *in Vitro* Reverts in Mice. *Microbiol. Immunol.*, 38 (11): 843-850.
- Cellini, L., Grande, R., Campli, E.D., Traini, T., Giulio, M.D., Lannutti, S.N., and Lattanzio, R., 2008. Dynamic Colonisation of *Helicobacter pylori* in Human Gastric Mucosa. *Scandinavian Journal of Gastroenterology*, 43: 178-185.
- Censini, S., Lange, C., Xiang, Z., Crabtree, J., Ghiara, P., Borodovsky, M., Rappuoli, R. and Covacci, A., 1996. cag, a pathogenicity island of *Helicobacter pylori*, encodes type I-specific

and disease-associated virulence factors. *Proceedings of the National Academy of Sciences*, 93(25), pp.14648-14653.

Chatterjee, S. and Chaudhuri, K., 2012. *Outer Membrane Vesicles of Bacteria*. Berlin, Heidelberg: Imprint: Springer.

Chatterjee, S. and Das, J., 1966. Secretory activity of *Vibrio cholerae* as evidenced by electron microscopy. In: Uyeda R (ed) *Electron Microscopy*. Maruzen Co Ltd, Tokyo.

Chatterjee, S. and Das, J., 1967. Electron Microscopic Observations on the Excretion of Cell-wall Material by *Vibrio cholerae*. *Journal of General Microbiology*, 49(1), pp.1-11.

Chen, Y., Mo, X., Huang, G., Huang, Y., Xiao, J., Zhao, L., Wei, H. and Liang, Q., 2016. Gene polymorphisms of pathogenic *Helicobacter pylori* in patients with different types of gastrointestinal diseases. *World Journal of Gastroenterology*, 22(44), p.9718.

Chitcholtan, K., Hampton, M. and Keenan, J., 2008. Outer membrane vesicles enhance the carcinogenic potential of *Helicobacter pylori*. *Carcinogenesis*, 29(12), pp.2400-2405.

Choi, J.W., Kim, S.C., Hong, S.H., Lee, H.J., 2017. Secretable small RNAs via outer membrane vesicles in periodontal pathogens. *J Dent Res* 96(4):458–466. <https://doi.org/10.1177/0022034516685071>.

Choi, K., Heath, R. and Rock, C., 2000. β -Ketoacyl-Acyl Carrier Protein Synthase III (FabH) Is a Determining Factor in Branched-Chain Fatty Acid Biosynthesis. *Journal of Bacteriology*, 182(2), pp.365-370.

Cole, S.P., Harwood, J., Lee, R., She, R., and Guiney, D.G., 2004. Characterisation of Monospecies Biofilm Formation by *Helicobacter pylori*. *Journal of Bacteriology*, 186 (10): 3124–3132.

Cook, K., Letley, D., Ingram, R., Staples, E., Skjoldmose, H., Atherton, J. and Robinson, K., 2014. CCL20/CCR6-mediated migration of regulatory T cells to the *Helicobacter pylori*-infected human gastric mucosa. *Gut*, 63(10), pp.1550-1559.

Correa, P., and Houghton, J., 2007. Carcinogenesis of *Helicobacter pylori*. *Gastroenterology*, 133: 659–672.

Covacci, A., Censini, S., Bugnoli, M., Petracca, R., Burroni, D., Macchia, G., Massone, A., Papini, E., Xiang, Z. and Figura, N., 1993. Molecular characterization of the 128-kDa immunodominant antigen of *Helicobacter pylori* associated with cytotoxicity and duodenal ulcer. *Proceedings of the National Academy of Sciences*, 90(12), pp.5791-5795.

Cover, T. L., Berg, D. E., Blaser, M. J. & Mobley, H. L. T. 2001. *Helicobacter pylori* pathogenesis. In *Principles of Bacterial Pathogenesis*, edited by Groisman, E. A., pp. 509-558. San Diego: Academic Press.

Cover, T., 2016. *Helicobacter pylori* Diversity and Gastric Cancer Risk. *mBio*, 7(1).

Cowley, G., Weir, B., Vazquez, F., Tamayo, P., Scott, J., Rusin, S., East-Seletsky, A., Ali, L., Gerath, W., Pantel, S., Lizotte, P., Jiang, G., Hsiao, J., Tsherniak, A., Dwinell, E., Aoyama, S., Okamoto, M., Harrington, W., Gelfand, E., Green, T., Tomko, M., Gopal, S., Wong, T., Li, H., Howell, S., Stransky, N., Liefeld, T., Jang, D., Bistline, J., Hill Meyers, B., Armstrong, S., Anderson, K., Stegmaier, K., Reich, M., Pellman, D., Boehm, J., Mesirov, J., Golub, T., Root, D. and Hahn, W., 2014. Parallel genome-scale loss of function screens in 216 cancer cell lines for the identification of context-specific genetic dependencies. *Scientific Data*, 1(1).

Crabtree, J., Covacci, A., Farmery, S., Xiang, Z., Tompkins, D., Perry, S., Lindley, I. and Rappuoli, R., 1995. *Helicobacter pylori* induced interleukin-8 expression in gastric epithelial cells is associated with CagA positive phenotype. *Journal of Clinical Pathology*, 48(1), pp.41-45.

- Crabtree, J., Shallcross, T., Heatley, R. and Wyatt, J., 1991. Mucosal tumour necrosis factor alpha and interleukin-6 in patients with *Helicobacter pylori* associated gastritis. *Gut*, 32(12), pp.1473-1477.
- Davies, C., Taylor, A., Elmi, A., Winter, J., Liaw, J., Grabowska, A., Gundogdu, O., Wren, B., Kelly, D. and Dorrell, N., 2019. Sodium Taurocholate Stimulates *Campylobacter jejuni* Outer Membrane Vesicle Production via Down-Regulation of the Maintenance of Lipid Asymmetry Pathway. *Frontiers in Cellular and Infection Microbiology*, 9.
- Deatherage, B.L., and Cookson, B.T., 2012. Membrane vesicle release in bacteria, eukaryotes, and archaea: a conserved yet underappreciated aspect of microbial life. *Infect Immun* 80(6):1948–1957. <https://doi.org/10.1128/IAI.06014-11>.
- Devoe, I. and Gilchrist, J., 1973. Release of Endotoxin in the Form of Cell Wall Blebs During in Vitro Growth of *Neisseria Meningitidis*. *Journal of Experimental Medicine*, 138(5), pp.1156-1167.
- DeVoe, I.W., and Gilchrist, J.E., 1975. Pili on *meningococci* from primary cultures of nasopharyngeal carriers and cerebrospinal fluid of patients with acute disease. *J Exp Med* 141:297. <https://doi.org/10.1084/jem.141.2.297>.
- Dixon, M., 2001. Pathology of Gastritis and Peptic Ulceration. In *Helicobacter pylori: Physiology and Genetics*, edited by Mobley, H. L. T., Mendz, G. L. & Hazell, S. L., pp. 459-469. Washington, DC: DC: ASM press.
- Dixon, M., Genta, R., Yardley, J. and Correa, P., 1996. Classification and Grading of Gastritis. *The American Journal of Surgical Pathology*, 20(10), pp.1161-1181.
- Dixon, M., Genta, R., Yardley, J. and Correa, P., 1996. Classification and Grading of Gastritis. *The American Journal of Surgical Pathology*, 20(10), pp.1161-1181.
- Doig, P., de Jonge, B., Alm, R., Brown, E., Uria-Nickelsen, M., Noonan, B., Mills, S., Tummino, P., Carmel, G., Guild, B., Moir, D., Vovis, G. and Trust, T., 1999. *Helicobacter pylori* Physiology Predicted from Genomic Comparison of Two Strains. *Microbiology and Molecular Biology Reviews*, 63(3), pp.675-707.
- Donlan, R.M. and Costerton, J.W., 2002. Biofilms: Survival Mechanisms of Clinically Relevant Microorganisms. *Clinical Microbiology Reviews*, 15 (2), 167–193.
- Dutta, S., Iida, K., Takade, A., Meno, Y., Nair, G. and Yoshida, S., 2004. Release of Shiga Toxin by Membrane Vesicles in *Shigella dysenteriae* Serotype 1 Strains and In Vitro Effects of Antimicrobials on Toxin Production and Release. *Microbiology and Immunology*, 48(12), pp.965-969.
- Eaton, K., Brooks, C., Morgan, D. and Krakowka, S., 1991. Essential role of urease in pathogenesis of gastritis induced by *Helicobacter pylori* in gnotobiotic piglets. *Infection and Immunity*, 59(7), pp.2470-2475.
- Eidt, S., Stolte, M., 1994. Antral intestinal metaplasia in *Helicobacter pylori* gastritis. *Digestion*. 1994;55:13–18.
- Ellis, T. and Kuehn, M., 2010. Virulence and Immunomodulatory Roles of Bacterial Outer Membrane Vesicles. *Microbiology and Molecular Biology Reviews*, 74(1), pp.81-94.
- Enno, A., O'Rourke, J., Howlett, C., Jack, A., Lee, A. and Dixon, M., 1995. MALToma-Like Lesions in the Murine Gastric Mucosa after Long-Term Infection with *Helicobacter felis* [online] [Ncbi.nlm.nih.gov](https://www.ncbi.nlm.nih.gov). Available at: <https://www.ncbi.nlm.nih.gov/pmc/articles/PMC1869885/pdf/amjpathol00043-0223.pdf> [Accessed 31 January 2020].

- Fang, X., Wei, J., He, X., An, P., Wang, H., Jiang, L., Shao, D., Liang, H., Li, Y., Wang, F. and Min, J., 2015. Landscape of dietary factors associated with risk of gastric cancer: A systematic review and dose-response meta-analysis of prospective cohort studies. *European Journal of Cancer*, 51(18), pp.2820-2832.
- Fikret, D., Kaya, Ö., Suna, E., Vahap, O., Mustafa, A., and Ebnem, A., 2001. Relationship between atrophic gastritis, intestinal metaplasia, dysplasia and *Helicobacter pylori* infection. *The Turkish J Gastro*, 12, 169-170.
- Fiocca, R., Necchi, V., Sommi, P., Ricci, V., Telford, J., Cover, T. and Solcia, E., 1999. Release of *Helicobacter pylori* vacuolating cytotoxin by both a specific secretion pathway and budding of outer membrane vesicles. Uptake of released toxin and vesicles by gastric epithelium. *The Journal of Pathology*, 188(2), pp.220-226.
- Galka, F., Wai, S., Kusch, H., Engelmann, S., Hecker, M., Schmeck, B., Hippenstiel, S., Uhlin, B. and Steinert, M., 2008. Proteomic Characterization of the Whole Secretome of *Legionella pneumophila* and Functional Analysis of Outer Membrane Vesicles. *Infection and Immunity*, 76(5), pp.1825-1836.
- Garcia, A., Salas-Jara, M.J., Herrera, C., Gonzalez, C., 2014. Biofilm and *Helicobacter pylori*: From Environment to Human Host. *World Journal of Gastroenterology*, 20 (19): 5632-5638.
- Genta, R., Hamner, H. and Graham, D., 1993. Gastric lymphoid follicles in *Helicobacter pylori* infection: Frequency, distribution, and response to triple therapy. *Human Pathology*, 24(6), pp.577-583.
- GLOBOCAN, 2021. *Global Cancer Observatory*. [online] Gco.iarc.fr. Available at: <<https://gco.iarc.fr>> [Accessed 16 March 2021].
- Grande, R., Campli, E., Bartolomeo, S., Verginelli, F., Giulio, M., Baffoni, M., Bessa, L.J., and Cellini, L., 2012. *Helicobacter pylori* biofilm: a protective environment for bacterial recombination. *Journal of Applied Microbiology* 113, 669–676.
- Gul, L., Modos, D., Fonseca, S., Madgwick, M., Thomas, J., Sudhakar, P., Stentz, R., Carding, S. and Korcsmaros, T., 2021. Extracellular vesicles produced by the human commensal gut bacterium *Bacteroides thetaiotaomicron* affect host immune pathways in a cell-type specific manner that are altered in inflammatory bowel disease. [This article is a preprint and has not been certified by peer review.](#)
- Hacker, J. and Kaper, J., 2000. Pathogenicity Islands and the Evolution of Microbes. *Annual Review of Microbiology*, 54(1), pp.641-679.
- Han, S., Zschausch, H., Meyer, H., Schneider, T., Loos, M., Bhakdi, S. and Maeurer, M., 2000. *Helicobacter pylori*: Clonal Population Structure and Restricted Transmission within Families Revealed by Molecular Typing. *Journal of Clinical Microbiology*, 38(10), pp.3646-3651.
- Harvey, V., Acio, C., Bredehoft, A., Zhu, L., Hallinger, D., Quinlivan-Repasi, V., Harvey, S. and Forsyth, M., 2014. Repetitive Sequence Variations in the Promoter Region of the Adhesin-Encoding Gene *sabA* of *Helicobacter pylori* Affect Transcription. *Journal of Bacteriology*, 196(19), pp.3421-3429.
- Hassan, T., Al-Najjar, S., Al-Zahrani, I., Alanazi, F. and Alotibi, M., 2016. *Helicobacter pylori* chronic gastritis updated Sydney grading in relation to endoscopic findings and *H. pylori* IgG antibody: diagnostic methods. *Journal of Microscopy and Ultrastructure*, 4(4), p.167.
- Hatakeyama, 2016. *Research | Hatakeyama Lab. [Department of Microbiology, Graduate School of Medicine and Faculty of Medicine, The University of Tokyo]*. [online] Microbiol.m.u-tokyo.ac.jp. Available at: <<http://www.microbiol.m.u-tokyo.ac.jp/research/eng.html>> [Accessed 14 March 2021].

HATAKEYAMA, M., 2017. Structure and function of *Helicobacter pylori* CagA, the first-identified bacterial protein involved in human cancer. *Proceedings of the Japan Academy, Series B*, 93(4), pp.196-219.

Haurat, M., Aduse-Opoku, J., Rangarajan, M., Dorobantu, L., Gray, M., Curtis, M. and Feldman, M., 2011. Selective Sorting of Cargo Proteins into Bacterial Membrane Vesicles. *Journal of Biological Chemistry*, 286(2), pp.1269-1276.

Hazlett, K.R.O., Caldon, S.D., McArthur, D.G., Cirillo, K.A., Kirimanjeswara, G.S., Magguilli M.L., *et al.*, 2008. Adaptation of *Francisella tularensis* to the mammalian environment is governed by cues which can be mimicked in vitro *Infect Immun*, 76, pp. [4479-4488](#).

Heczko, U., Smith, V., Mark Meloche, R., Buchan, A. and Finlay, B., 2000. Characteristics of *Helicobacter pylori* attachment to human primary antral epithelial cells. *Microbes and Infection*, 2(14), pp.1669-1676.

Herrero, R., Park, J. and Forman, D., 2014. The fight against gastric cancer – the IARC Working Group report. *Best Practice & Research Clinical Gastroenterology*, 28(6), pp.[1107-1114](#).

Hiippala, K., Barreto, G., Burrello, C., Diaz-Basabe, A., Suutarinen, M., Kainulainen, V., Bowers, J., Lemmer, D., Engelthaler, D., Eklund, K., Facciotti, F. and Satokari, R., 2020. Novel *Odoribacter splanchnicus* Strain and Its Outer Membrane Vesicles Exert Immunoregulatory Effects in vitro. *Frontiers in Microbiology*, 11.

Horstman, A. and Kuehn, M., 2002. Bacterial Surface Association of Heat-labile Enterotoxin through Lipopolysaccharide after Secretion via the General Secretory Pathway. *Journal of Biological Chemistry*, 277(36), pp.32538-32545.

IARC, 1994. Schistosomes, Liver Flukes and *Helicobacter pylori*. IARC Monogr Eval carcinog risks hum, 61: 1-241. PMID:7715068.

Ilver, D., Arnqvist, A., Ogren, J., Frick, I. M., Kersulyte, D., Incecik, E. T., Berg, D. E., Covacci, A., Engstrand, L., and Boren T., 1998. *Helicobacter pylori* Adhesin Binding Fucosylated Histo-Blood Group Antigens Revealed by Retagging. *Science*, 279(5349), pp.373-377.

Ilver, D., Arnqvist, A., Ogren, J., Frick, I., Kersulyte, D., Incecik, E., Berg, D., Covacci, A., Engstrand, L. and Boren, T., 1998. *Helicobacter pylori* Adhesin Binding Fucosylated Histo-Blood Group Antigens Revealed by Retagging. *Science*, 279(5349), pp.373-377.

InvivoGen, 2016. [online] [Invivogen.com](https://www.invivogen.com). Available at: <https://www.invivogen.com/sites/default/files/invivogen/resources/documents/reviews/review-mycoplasma-contamination-invivogen.pdf> [Accessed 9 April 2020].

Ishijima, N., Suzuki, M., Ashida, H., Ichikawa, Y., Kanegae, Y., Saito, I., Borén, T., Haas, R., Sasakawa, C. and Mimuro, H., 2011. BabA-mediated Adherence Is a Potentiator of the *Helicobacter pylori* Type IV Secretion System Activity. *Journal of Biological Chemistry*, 286(28), pp.25256-25264.

Ismail, S., Hampton, M. and Keenan, J., 2003. *Helicobacter pylori* Outer Membrane Vesicles Modulate Proliferation and Interleukin-8 Production by Gastric Epithelial Cells. *Infection and Immunity*, 71(10), pp.5670-5675.

Jiménez-Soto, L. and Haas, R., 2016. The CagA toxin of *Helicobacter pylori*: abundant production but relatively low amount translocated. *Scientific Reports*, 6(1).

Jiménez-Soto, L., Kutter, S., Sewald, X., Ertl, C., Weiss, E., Kapp, U., Rohde, M., Pirch, T., Jung, K., Retta, S., Terradot, L., Fischer, W. and Haas, R., 2009. *Helicobacter pylori* Type IV Secretion Apparatus Exploits β 1 Integrin in a Novel RGD-Independent Manner. *PLoS Pathogens*, 5(12), p.e1000684.

Jones, K., Joo, Y., Jang, S., Yoo, Y., Lee, H., Chung, I., Olsen, C., Whitmire, J., Merrell, D. and Cha, J., 2009. Polymorphism in the CagA EPIYA Motif Impacts Development of Gastric Cancer. *Journal of Clinical Microbiology*, 47(4), pp.959-968.

Kadurugamuwa, J. and Beveridge, T., 1995. Virulence factors are released from *Pseudomonas aeruginosa* in association with membrane vesicles during normal growth and exposure to gentamicin: a novel mechanism of enzyme secretion. *Journal of bacteriology*, 177(14), pp.3998-4008.

Kadurugamuwa, J. and Beveridge, T., 1998. Delivery of the Non-Membrane-Permeative Antibiotic Gentamicin into Mammalian Cells by Using *Shigella flexneri* Membrane Vesicles. *Antimicrobial Agents and Chemotherapy*, 42(6), pp.1476-1483.

Kaparakis-Liaskos, M., and Ferrero, R.L., 2015. Immune modulation by bacterial outer membrane vesicles. *Nat Rev Immunol* 15(6):375–387. <https://doi.org/10.1038/nri3837>.

Kaparakis, M., Turnbull, L., Carneiro, L., Firth, S., Coleman, H., Parkington, H., Le Bourhis, L., Karrar, A., Viala, J., Mak, J., Hutton, M., Davies, J., Crack, P., Hertzog, P., Philpott, D., Girardin, S., Whitchurch, C. and Ferrero, R., 2010. Bacterial membrane vesicles deliver peptidoglycan to NOD1 in epithelial cells. *Cellular Microbiology*, 12(3), pp.372-385.

Keenan, J. and Allardyce, R., 2000. Iron influences the expression of *Helicobacter pylori* outer membrane vesicle-associated virulence factors. *European Journal of Gastroenterology & Hepatology*, 12(12), pp.1267-1273.

Keenan, J., 2000. A role for the bacterial outer membrane in the pathogenesis of *Helicobacter pylori* infection. *Fems Microbiology Letters*, 182(2), pp.259-264.

Keenan, J., Davis, K., Beaugie, C., McGovern, J. and Moran, A., 2008. Alterations in *Helicobacter pylori* outer membrane and outer membrane vesicle-associated lipopolysaccharides under iron-limiting growth conditions*. *Innate Immunity*, 14(5), pp.279-290.

Keenan, J., Oliaro, J., Domigan, N., Potter, H., Aitken, G., Allardyce, R. and Roake, J., 2000. Immune Response to an 18-Kilodalton Outer Membrane Antigen Identifies Lipoprotein 20 as a *Helicobacter pylori* Vaccine Candidate. *Infection and Immunity*, 68(6), pp.3337-3343.

Ketley, J.M., 2007. *Campylobacter* and *Helicobacter*. In: Greenwood, D., Salck, R., Peutherer, J., and Barer, M., 2007. *Medical Microbiology*. 17th ed. Philadelphia: ELSEVIER, 2007, PP. 300-308.

Khaledi, M., Bagheri, N., Validi, M., Zamanzad, B., Afkhami, H., Fathi, J., Rahimian, G. and Gholipour, A., 2020. Determination of CagA EPIYA motif in *Helicobacter pylori* strains isolated from patients with digestive disorder. *Heliyon*, 6(9), p.e04971.

Khoder, G., Muhammad, J., Mahmoud, I., Soliman, S. and Burucoa, C., 2019. Prevalence of *Helicobacter pylori* and Its Associated Factors among Healthy Asymptomatic Residents in the United Arab Emirates. *Pathogens*, 8(2), p.44.

Kim, S., Lee, Y., Kim, H.K., and Blaser, M.J., 2006. *Helicobacter pylori* CagA Transfection of Gastric Epithelial Cells Induces Interleukin-8. *Cellular Microbiology*, 8 (1): 97–106.

Knox, K., Vesik, M. and Work, E., 1966. Relation Between Excreted Lipopolysaccharide Complexes and Surface Structures of a Lysine-Limited Culture of *Escherichia coli*. *Journal of Bacteriology*, 92(4), pp.1206-1217.

Koeppen, K., Hampton, T., Jarek, M., Scharfe, M., Gerber, S., Mielcarz, D., Demers, E., Dolben, E., Hammond, J., Hogan, D. and Stanton, B., 2016. A Novel Mechanism of Host-Pathogen

- Interaction through sRNA in Bacterial Outer Membrane Vesicles. *PLOS Pathogens*, 12(6), p.e1005672.
- Konturek, S., Konturek, P., Konturek, J., Plonka, M., Czesnikiewicz-Guzik, M., Brzozowski, T. and Bielanski, W., 2006. [online] jpp.krakow.pl. Available at: <http://jpp.krakow.pl/journal/archive/09_06_s3/pdf/29_09_06_s3_article.pdf> [Accessed 14 March 2021].
- Krisch, L., Posselt, G., Hammerl, P. and Wessler, S., 2016. CagA Phosphorylation in *Helicobacter pylori*-Infected B Cells Is Mediated by the Nonreceptor Tyrosine Kinases of the Src and Abl Families. *Infection and Immunity*, 84(9), pp.2671-2680.
- Kuehn, M., 2005. Bacterial outer membrane vesicles and the host-pathogen interaction. *Genes & Development*, 19(22), pp.2645-2655.
- Kulp, A. and Kuehn, M., 2010. Biological Functions and Biogenesis of Secreted Bacterial Outer Membrane Vesicles. *Annual Review of Microbiology*, 64(1), pp.163-184.
- Kurashima, Y., Murata-Kamiya, N., Kikuchi, K., Higashi, H., Azuma, T., Kondo, S. and Hatakeyama, M., 2007. Deregulation of β -catenin signal by *Helicobacter pylori* CagA requires the CagA-multimerization sequence. *International Journal of Cancer*, 122(4), pp.823-831.
- Kusters, J., G., Gerrits, M., M., Van Strijp, J., A., Vandenbroucke- Grauls, C., M., 1997. Coccoid forms of *Helicobacter pylori* are the morphologic manifestation of cell death. *Infect Immun*, 65: 3672–3679. PMID:9284136.
- Kwok, T., Zabler, D., Urman, S., Rohde, M., Hartig, R., Wessler, S., Misselwitz, R., Berger, J., Sewald, N., König, W. and Backert, S., 2007. *Helicobacter* exploits integrin for type IV secretion and kinase activation. *Nature*, 449(7164), pp.862-866.
- Lai, C., Listgarten, M. and Hammond, B., 1981. Comparative ultrastructure of leukotoxic and non-leukotoxic strains of *Actinobacillus actinomycetemcomitans*. *Journal of Periodontal Research*, 16(4), pp.379-389.
- Lehours, P. and Yilmaz, O., 2007. Epidemiology of *Helicobacter pylori* Infection. *Helicobacter*, 12(s1), pp.1-3.
- Leive, L., Shovlin, V.K., and Mergenhagen, S.E., 1968. Physical chemical and immunological properties of lipopolysaccharide released from *Escherichia coli* by Ethylenediaminetetraacetate. *J Biol Chem* 243(24):6384+
- Lekmeechai, S., Su, Y., Brant, M., Alvarado-Kristensson, M., Vallström, A., Obi, I., Arnqvist, A. and Riesbeck, K., 2018. *Helicobacter pylori* Outer Membrane Vesicles Protect the Pathogen from Reactive Oxygen Species of the Respiratory Burst. *Frontiers in Microbiology*, 9.
- Liu, Q., Li, X., Zhang, Y., Song, Z., Li, R., Ruan, H. and Huang, X., 2019. Orally-administered outer-membrane vesicles from *Helicobacter pylori* reduce *H. pylori* infection via Th2-biased immune responses in mice. *Pathogens and Disease*, 77(5).
- Loeb, M.R., 1974. Bacteriophage T4-mediated release of envelope components from *Escherichia coli*. *J Virol* 13:631–641.
- Loh, J., Gupta, S., Friedman, D., Krezel, A. and Cover, T., 2010. Analysis of Protein Expression Regulated by the *Helicobacter pylori* ArsRS Two-Component Signal Transduction System. *Journal of Bacteriology*, 192(8), pp.2034-2043.
- Loke, M.F., Ng, C.G., Vilashni, Y., Lim, J., and Ho, B., 2016. Understanding the Dimorphic Lifestyles of Human Gastric Pathogen *Helicobacter pylori* using the SWATH-based Proteomics Approach. *Scientific Reports*, 6:26784. Doi: 10.1038/srep26784.

- Lu, Y., Pang, J., Wang, G., Hu, X., Li, X., Li, G., Wang, X., Yang, X., Li, C. and You, X., 2020. Quantitative proteomics approach to investigate the antibacterial response of *Helicobacter pylori* to daphnetin, a traditional Chinese medicine monomer. *RSC Advances*, 11(4), pp.2185-2193.
- Macdonald, I.A., and Kuehn, M.J., 2013. Stress-induced outer membrane vesicle production by *Pseudomonas aeruginosa*. *J Bacteriol* 195(13):2971–2981. <https://doi.org/10.1128/JB.02267-12>.
- MacDonald, K.L., and Beveridge, T.J., 2002. Bactericidal effect of gentamicin-induced membrane vesicles derived from *Pseudomonas aeruginosa* PAO1 on Gram-positive bacteria. *Can J Microbiol* 48:810–820.
- Maguire, M., Coates, A. and Henderson, B., 2002. Chaperonin 60 unfolds its secrets of cellular communication. *Cell Stress & Chaperones*, 7(4), p.317.
- Mah, T.C., and O'Toole, G.A., 2001. Mechanisms of biofilm resistance to antimicrobial agents *TRENDS in Microbiology*, 9 (1), 34-39.
- Mahdavi, J., 2002. *Helicobacter pylori* SabA Adhesin in Persistent Infection and Chronic Inflammation. *Science*, 297(5581), pp.573-578.
- Marcos, N., Magalhães, A., Ferreira, B., Oliveira, M., Carvalho, A., Mendes, N., Gilmartin, T., Head, S., Figueiredo, C., David, L., Santos-Silva, F. and Reis, C., 2008. *Helicobacter pylori* induces β 3GnT5 in human gastric cell lines, modulating expression of the SabA ligand sialyl-Lewis x. *Journal of Clinical Investigation*.
- Marshall, B. J. & Warren, J. R. 2001. One hundred years of discovery and rediscovery of *Helicobacter pylori* and its association with peptic ulcer disease. In *Helicobacter pylori: Physiology and Genetics*, edited by Mobley, H. L. T., Mendz, G. L. & Hazell, S. L., pp. 19-24. Washington, DC: ASM press.
- Matozaki, T., Sakamoto, C., Matsuda, K., Suzuki, T., Konda, Y., Nakano, O., Wada, K., Uchida, T., Nishisaki, H., Nagao, M. and Kasuga, M., 1992. Missense mutations and a deletion of the p53 gene in human gastric cancer. *Biochemical and Biophysical Research Communications*, 182(1), pp.215-223.
- Mayrand, D. and Grenier, D., 1989. Biological activities of outer membrane vesicles. *Canadian Journal of Microbiology*, 35(6), pp.607-613.
- McBroom, A. and Kuehn, M., 2007. Release of outer membrane vesicles by Gram-negative bacteria is a novel envelope stress response. *Molecular Microbiology*, 63(2), pp.545-558.
- McBroom, A., Johnson, A., Vemulapalli, S. and Kuehn, M., 2006. Outer Membrane Vesicle Production by *Escherichia coli* Is Independent of Membrane Instability. *Journal of Bacteriology*, 188(15), pp.5385-5392.
- McCaig, W., Koller, A. and Thanassi, D., 2013. Production of Outer Membrane Vesicles and Outer Membrane Tubes by *Francisella novicida*. *Journal of Bacteriology*, 195(6), pp.1120-1132.
- Michael, P., Patricia, D., Jennifer, S., Beier, D., 2004. Genetic evidence for histidine kinase HP165 being an acid sensor of *Helicobacter pylori*. *Fems Microbiol*, 234(1):51–61.
- Miles, A., Misra, S. and Irwin, J., 1938. The estimation of the bactericidal power of the blood. *Epidemiology and Infection*, 38(6), pp.732-749.
- Mobley, H., Hu, L. and Foxall, P., 1991. *Helicobacter pylori* Urease: Properties and Role in Pathogenesis. *Scandinavian Journal of Gastroenterology*, 26(sup187), pp.39-46.

- Mobley, H.L.T., Mendz, G.L., Hazell, S.L., 2001. Urease. *Helicobacter pylori*: Physiology and Genetics. Washington (DC): [ASM Press](#).
- Molinari, M., Galli, C., Norais, N., Telford, J., Rappuoli, R., Luzio, J. and Montecucco, C., 1997. Vacuoles Induced by *Helicobacter pylori* Toxin Contain Both Late Endosomal and Lysosomal Markers. *Journal of Biological Chemistry*, 272(40), pp.25339-25344.
- Mukawa, K., Nakamura, T., Nakano, G. and Nagamachi, Y., 1987. Histopathogenesis of intestinal metaplasia: minute lesions of intestinal metaplasia in ulcerated stomachs. *Journal of Clinical Pathology*, 40(1), pp.13-18.
- Mullaney, E., Brown, P., Smith, S., Botting, C., Yamaoka, Y., Terres, A., Kelleher, D. and Windle, H., 2009. Proteomic and functional characterization of the outer membrane vesicles from the gastric pathogen *Helicobacter pylori*. *Proteomics - Clinical Applications*, 3(7), pp.785-796.
- Murray, B., Dawson, R., AlSharaf, L. and Anne Winter, J., 2020. Protective effects of *Helicobacter pylori* membrane vesicles against stress and antimicrobial agents. *Microbiology*, 166(8), pp.751-758.
- Muzahed, 2020. Helicobacter pylori Oncogenicity: Mechanism, Prevention, and Risk Factors. *The Scientific World Journal*, 2020, pp.1-10.
- Nagakubo, T., Nomura, N. and Toyofuku, M., 2020. Cracking Open Bacterial Membrane Vesicles. *Frontiers in Microbiology*, 10.
- Najm, W., 2011. Peptic Ulcer Disease. *Primary Care: Clinics in Office Practice*, 38(3), pp.383-394.
- Namork, E., and Brandtzaeg, P., 2002. Fatal meningococcal septicaemia with “blebbing” meningococcus. *Lancet* 360(9347):1741.
- Neal, J.T., Peterson, T.S., Kent, M.L., and Guillemin, K., 2013. *H. pylori* virulence factor CagA increases intestinal cell proliferation by Wnt pathway activation in a transgenic zebrafish model. *Dis. Model. Mech.* 6, 802–810.
- Nell, S., Kennemann, L., Schwarz, S., Josenhans, C., 2014. Dynamics of Lewis b binding and sequence variation of the babA adhesin gene during chronic *Helicobacter pylori* infection in humans. *mBio* 5(6):e02281–e02214.
- Nguyen, V., Nguyen, G., Phung, D., Okrainec, K., Raymond, J., Dupond, C., Kremp, O., Kalach, N. and Vidal-Trecan, G., 2006. Intra-familial Transmission of *Helicobacter pylori* Infection in Children of Households with Multiple Generations in Vietnam. *European Journal of Epidemiology*, 21(6), pp.459-463.
- NIDDK, 2013. *Gastritis & Gastropathy | NIDDK*. [online] National Institute of Diabetes and Digestive and Kidney Diseases. Available at: <<https://www.niddk.nih.gov/health-information/digestive-diseases/gastritis-gastropathy>> [Accessed 30 June 2018].
- Nishikawa, H. and Hatakeyama, M., 2017. Sequence Polymorphism and Intrinsic Structural Disorder as Related to Pathobiological Performance of the *Helicobacter pylori* CagA Oncoprotein. *Toxins*, 9(4), p.136.
- O'Donoghue, E. and Krachler, A., 2016. Mechanisms of outer membrane vesicle entry into host cells. *Cellular Microbiology*, 18(11), pp.1508-1517.
- Ogata, T., 1995. Electron microscopic study on the regenerating epithelium of the chronic gastric ulcer. *J. Submicroscop. Cytol. Pathol.* 1995;27:171–182.
- Ohnishi, N., Yuasa, H., Tanaka, S., Sawa, H., Miura, M., Matsui, A., Higashi, H., Musashi, M., Iwabuchi, K., Suzuki, M., Yamada, G., Azuma, T. and Hatakeyama, M., 2008. Transgenic

expression of *Helicobacter pylori* CagA induces gastrointestinal and hematopoietic neoplasms in mouse. *Proceedings of the National Academy of Sciences*, 105(3), pp.1003-1008.

Oleastro, M. and Ménard, A., 2013. The Role of *Helicobacter pylori* Outer Membrane Proteins in Adherence and Pathogenesis. *Biology*, 2(3), pp.1110-1134.

Olofsson, A., Nygård Skalmann, L., Obi, I., Lundmark, R. and Arnqvist, A., 2014. Uptake of *Helicobacter pylori* Vesicles Is Facilitated by Clathrin-Dependent and Clathrin-Independent Endocytic Pathways. *mBio*, 5(3).

Olofsson, A., Vallström, A., Petzold, K., Tegtmeyer, N., Schleucher, J., Carlsson, S., Haas, R., Backert, S., Wai, S., Gröbner, G. and Arnqvist, A., 2010. Biochemical and functional characterization of *Helicobacter pylori* vesicles. *Molecular Microbiology*, 77(6), pp.1539-1555.

Oohara T., Tohma H., Aono G., Ukawa S., Kondo Y., 1983. Intestinal metaplasia of the regenerative epithelia in 549 gastric ulcers. *Hum. Pathol.* 14:1066–1071.

Ordóñez-Mena, J., Schöttker, B., Mons, U., Jenab, M., Freisling, H., Bueno-de-Mesquita, B., O'Doherty, M., Scott, A., Kee, F., Stricker, B., Hofman, A., de Keyser, C., Ruiter, R., Söderberg, S., Jousilahti, P., Kuulasmaa, K., Freedman, N., Wilsgaard, T., de Groot, L., Kampman, E., Håkansson, N., Orsini, N., Wolk, A., Nilsson, L., Tjønneland, A., Pająk, A., Malyutina, S., Kubínová, R., Tamosiunas, A., Bobak, M., Katsoulis, M., Orfanos, P., Boffetta, P., Trichopoulou, A. and Brenner, H., 2016. Quantification of the smoking-associated cancer risk with rate advancement periods: meta-analysis of individual participant data from cohorts of the Chances consortium. *BMC Medicine*, 14(1).

Orench-Rivera, N. and Kuehn, M., 2016. Environmentally controlled bacterial vesicle-mediated export. *Cellular Microbiology*, 18(11), pp.1525-1536.

Owen, R., 1998. *Helicobacter* - species classification and identification. *British Medical Bulletin*, 54(1), pp.17-30.

Palframan, S., Kwok, T. and Gabriel, K., 2012. Vacuolating cytotoxin A (VacA), a key toxin for *Helicobacter pylori* pathogenesis. *Frontiers in Cellular and Infection Microbiology*, 2.

Pandey, P., Tarique, K., Mazumder, M., Rehman, S., Kumari, N. and Gourinath, S., 2016. Structural insight into β -Clamp and its interaction with DNA Ligase in *Helicobacter pylori*. *Scientific Reports*, 6(1).

Papini, E., Satin, B., Norais, N., de Bernard, M., Telford, J., Rappuoli, R. and Montecucco, C., 1998. Selective increase of the permeability of polarized epithelial cell monolayers by *Helicobacter pylori* vacuolating toxin. *Journal of Clinical Investigation*, 102(4), pp.813-820.

Park, Y. and Kim, N., 2015. Review of Atrophic Gastritis and Intestinal Metaplasia as a Premalignant Lesion of Gastric Cancer. *Journal of Cancer Prevention*, 20(1), pp.25-40.

Parker, H. and Keenan, J., 2012. Composition and function of *Helicobacter pylori* outer membrane vesicles. *Microbes and Infection*, 14(1), pp.9-16.

Parker, H., Chitcholtan, K., Hampton, M. and Keenan, J., 2010. Uptake of *Helicobacter pylori* Outer Membrane Vesicles by Gastric Epithelial Cells. *Infection and Immunity*, 78(12), pp.5054-5061.

Particle Metrix, 2020. *Introduction to Nanoparticle Tracking Analysis (NTA)*. [online] Particle-metrix.de. Available at: <<https://www.particle-metrix.de/en/technologies/nanoparticle-tracking/articles-nanoparticle-tracking/introduction-to-nanoparticle-tracking-analysis-nta>> [Accessed 1 June 2020].

- Pathirana, R. and Kaparakis-Liaskos, M., 2016. Bacterial membrane vesicles: Biogenesis, immune regulation and pathogenesis. *Cellular Microbiology*, 18(11), pp.1518-1524.
- Peek, R., Moss, S., Wang, S., Holt, P., Tham, K., Blaser, M., Perez-Perez, G., Miller, G. and Atherton, J., 1997. *Helicobacter pylori* cagA+ Strains and Dissociation of Gastric Epithelial Cell Proliferation from Apoptosis. *JNCI Journal of the National Cancer Institute*, 89(12), pp.863-868.
- Perez-Cruz, C., Carrion, O., Delgado, L., Martinez, G., Lopez-Iglesias, C. and Mercade, E., 2013. New Type of Outer Membrane Vesicle Produced by the Gram-Negative Bacterium *Shewanella vesiculosa* M7T: Implications for DNA Content. *Applied and Environmental Microbiology*, 79(6), pp.1874-1881.
- Pérez-Cruz, C., Delgado, L., López-Iglesias, C. and Mercade, E., 2015. Outer-Inner Membrane Vesicles Naturally Secreted by Gram-Negative Pathogenic Bacteria. *PLOS ONE*, 10(1), p.e0116896.
- Perry, S., De La Luz Sanchez, M., Yang, S., Haggerty, T. D., Hurst, P., Perez-Perez, G., and Parsonnet, J., 2006. Gastroenteritis and transmission of *Helicobacter pylori* infection in households. *Emerg Infect Dis*, 12, 1701-8.
- Pier, G., 2000. Peptides, *Pseudomonas aeruginosa*, polysaccharides and lipopolysaccharides – players in the predicament of cystic fibrosis patients. *Trends in Microbiology*, 8(6), pp.247-250.
- Plummer, M., Franceschi, S., Vignat, J., Forman, D. and de Martel, C., 2014. Global burden of gastric cancer attributable to *Helicobacter pylori*. *International Journal of Cancer*, 136(2), pp.487-490.
- Polakovicova, I., Jerez, S., Wichmann, I., Sandoval-Bórquez, A., Carrasco-Véliz, N. and Corvalán, A., 2018. Role of microRNAs and Exosomes in *Helicobacter pylori* and Epstein-Barr Virus Associated Gastric Cancers. *Frontiers in Microbiology*, 9.
- Promega, 2019. [online] Promega.com. Available at: <<https://www.promega.com/-/media/files/resources/protocols/technical-bulletins/0/celltiter-96-aqueous-one-solution-cell-proliferation-assay-system-protocol.pdf>> [Accessed 30 May 2019].
- Promega, 2019. [online] Promega.com. Available at: <<https://www.promega.com/-/media/files/resources/protocols/technical-manuals/101/realtimeloglo-mt-cell-viability-assay-protocol.pdf?la=en>> [Accessed 27 May 2019].
- Quintana-Hayashi, M., Rocha, R., Padra, M., Thorell, A., Jin, C., Karlsson, N., Roxo-Rosa, M., Oleastro, M. and Lindén, S., 2018. BabA-mediated adherence of pediatric ulcerogenic *H. pylori* strains to gastric mucins at neutral and acidic pH. *Virulence*, 9(1), pp.1699-1717.
- Rad, R., Gerhard, M., Lang, R., Schöniger, M., Rösch, T., Schepp, W., Becker, I., Wagner, H. and Prinz, C., 2002. The *Helicobacter pylori* Blood Group Antigen-Binding Adhesin Facilitates Bacterial Colonization and Augments a Nonspecific Immune Response. *The Journal of Immunology*, 168(6), pp.3033-3041.
- Random Picker. 2021. Random Picker. [online] Available at: <<https://www.randompicker.com>>.
- Rawla, P. and Barsouk, A., 2019. Epidemiology of gastric cancer: global trends, risk factors and prevention. *Gastroenterology Review*, 14(1), pp.26-38.
- Ren, S., Higashi, H., Lu, H., Azuma, T. and Hatakeyama, M., 2006. Structural Basis and Functional Consequence of *Helicobacter pylori* CagA Multimerization in Cells. *Journal of Biological Chemistry*, 281(43), pp.32344-32352.

Rhead, J., Letley, D., Mohammadi, M., Hussein, N., Mohagheghi, M., Eshagh Hosseini, M. and Atherton, J., 2007. A New *Helicobacter pylori* Vacuolating Cytotoxin Determinant, the Intermediate Region, is Associated with Gastric Cancer. *Gastroenterology*, 133(3), pp.926-936.

Ricci, V., Chiozzi, V., Necchi, V., Oldani, A., Romano, M., Solcia, E. and Ventura, U., 2005. Free-soluble and outer membrane vesicle-associated VacA from *Helicobacter pylori*: Two forms of release, a different activity. *Biochemical and Biophysical Research Communications*, 337(1), pp.173-178.

Rokkas, Liatsos, Petridou, Papatheodorou, Karameris, Ladas and Raptis, 1999. Relationship of *Helicobacter pylori* CagA(+) status to gastric juice vitamin C levels. *European Journal of Clinical Investigation*, 29(1), pp.56-62.

Romanelli, M., Diani, E. and Lievens, P., 2013. New Insights into Functional Roles of the Polypyrimidine Tract-Binding Protein. *International Journal of Molecular Sciences*, 14(11), pp.22906-22932.

Rothfield, L., and Pearlman-Kothencz, M., 1969. Synthesis and assembly of bacterial membrane components: a lipopolysaccharide-phospholipid-protein complex excreted by living bacteria. *J Mol Biol* 44:477.

Rudnicka, K., Graczykowski, M., Tenderenda, M., and Chmiela, M., 2014. *Helicobacter pylori* morphological forms and their potential role in the transmission of infection [online]. *Postepy Hig Med Dosw*, 68: 227-237. e-ISSN 1732-2693. Available at: www.phmd.pl [Accessed: 26th June 2017]. (Abstract – main article in Polish).

Saadat, I., Higashi, H., Obuse, C., Umeda, M., Murata-Kamiya, N., Saito, Y., Lu, H., Ohnishi, N., Azuma, T., Suzuki, A., Ohno, S. and Hatakeyama, M., 2007. *Helicobacter pylori* CagA targets PAR1/MARK kinase to disrupt epithelial cell polarity. *Nature*, 447(7142), pp.330-333.

Sakamoto, S., Watanabe, T., Tokumaru, T., Takagi, H., Nakazato, H., Lloyd, KO., 1989. Expression of Lewis a, Lewis b, Lewis x, Lewis y, sialyl-Lewis a, and sialyl-Lewis x blood group antigens in human gastric carcinoma and in normal gastric tissue. *Cancer Res.* 1989;49:745–752.

Schwechheimer, C. and Kuehn, M., 2015. Outer-membrane vesicles from Gram-negative bacteria: biogenesis and functions. *Nature Reviews Microbiology*, 13(10), pp.605-619.

Segal, E. D., Shon, J., Tompkins, L. S., 1992. Characterization of *Helicobacter pylori* urease mutants. *Infect. Immun.* 60:1883–1889.

Segal, E., Cha, J., Lo, J., Falkow, S. and Tompkins, L., 1999. Altered states: Involvement of phosphorylated CagA in the induction of host cellular growth changes by *Helicobacter pylori*. *Proceedings of the National Academy of Sciences*, 96(25), pp.14559-14564.

Shimoda, A., Ueda, K., Nishiumi, S., Murata-Kamiya, N., Mukai, S., Sawada, S., Azuma, T., Hatakeyama, M. and Akiyoshi, K., 2016. Exosomes as nanocarriers for systemic delivery of the *Helicobacter pylori* virulence factor CagA. *Scientific Reports*, 6(1).

Sjostrom, A.E., Sandblad, L., Uhlin, B.E., and Wai, S.N., 2015. Membrane vesicle-mediated release of bacterial RNA. *Sci Rep* 5:15329. <https://doi.org/10.1038/srep15329>.

Smit, J., Kamio, Y. and Nikaido, H., 1975. Outer membrane of *Salmonella typhimurium*: chemical analysis and freeze-fracture studies with lipopolysaccharide mutants. *Journal of Bacteriology*, 124(2), pp.942-958.

Sobala G. M., Crabtree J., Dixon M. F., Schorah C. J., Taylor J. D., Rathbone B. J., Heatley R. V., Axon A. T. R., 1991. Acute *Helicobacter pylori* infection: clinical features, local and systemic immune response, gastric mucosal histology and gastric juice ascorbic acid concentrations. *Gut*. 32:1415–1418.

Sobala G. M., Schorah C. J., Shires S., Lynch D. A. F., Gallacher B., Dixon M. F., Axon A. T. R., 1993. Effect of eradication of *Helicobacter pylori* on gastric juice ascorbic acid concentrations. *Gut*. 34:1038–1041.

Stark, R.M., Gerwig, G.J., et al., 1999. Biofilm Formation by *Helicobacter pylori*. *Letters in Applied Microbiology*, 28, 121-126.

Sundrud, M., Torres, V., Unutmaz, D. and Cover, T., 2004. Inhibition of primary human T cell proliferation by *Helicobacter pylori* vacuolating toxin (VacA) is independent of VacA effects on IL-2 secretion. *Proceedings of the National Academy of Sciences*, 101(20), pp.7727-7732.

Svennerholm, K., Park, K., Wikström, J., Lässer, C., Crescitelli, R., Shelke, G., Jang, S., Suzuki, S., Bandeira, E., Olofsson, C. and Lötvall, J., 2017. *Escherichia coli* outer membrane vesicles can contribute to sepsis induced cardiac dysfunction. *Scientific Reports*, 7(1).

Tashiro, Y., Ichikawa, S., Nakajima-Kambe, T., Uchiyama, H., Nomura, N., 2010. *Pseudomonas* quinolone signal affects membrane vesicle production in not only gram-negative but also gram-positive bacteria. *Microbes Environ* 25(2):120–125. <https://doi.org/10.1264/jsme2.me09182>.

Tham, K., Peek, R., Atherton, J., Cover, T., Perez-Perez, G., Shyr, Y. and Blaser, M., 2001. *Helicobacter pylori* genotypes, host factors, and gastric mucosal histopathology in peptic ulcer disease. *Human Pathology*, 32(3), pp.264-273.

ThermoFisher, 2021. [online] Available at: <<https://www.thermofisher.com/order/catalog/product/K1231#/K1231>> [Accessed 8 November 2020].

Thermofisher.com. 2019. Document Connect. [online] Available at: https://www.thermofisher.com/document-connect/document-connect.html?url=https%3A%2F%2Fassets.thermofisher.com%2FTFS-Assets%2FLSG%2Fmanuals%2FMAN0012707_CloneJET_PCR_Cloning_20rxn_UG.pdf [Accessed 8 November 2020].

Turkina, M., Olofsson, A., Magnusson, K., Arnqvist, A. and Vikström, E., 2015. *Helicobacter pylori* vesicles carrying CagA localize in the vicinity of cell–cell contacts and induce histone H1 binding to ATP in epithelial cells. *FEMS Microbiology Letters*, 362(11).

Turner, L., Bitto, N., Steer, D., Lo, C., D’Costa, K., Ramm, G., Shambrook, M., Hill, A., Ferrero, R. and Kaparakis-Liaskos, M., 2018. *Helicobacter pylori* Outer Membrane Vesicle Size Determines Their Mechanisms of Host Cell Entry and Protein Content. *Frontiers in Immunology*, 9.

Turner, L., Praszkiar, J., Hutton, M., Steer, D., Ramm, G., Kaparakis-Liaskos, M. and Ferrero, R., 2015. Increased Outer Membrane Vesicle Formation in a *Helicobacter pylori* tolB Mutant. *Helicobacter*, 20(4), pp.269-283.

Ubukata, H., Nagata, H., Tabuchi, T., Konishi, S., Kasuga, T. and Tabuchi, T., 2011. Why is the coexistence of gastric cancer and duodenal ulcer rare? Examination of factors related to both gastric cancer and duodenal ulcer. *Gastric Cancer*, 14(1), pp.4-12.

Ünal, C., Schaar, V. and Riesbeck, K., 2010. Bacterial outer membrane vesicles in disease and preventive medicine. *Seminars in Immunopathology*, 33(5), pp.395-408.

UniPort, 2021. *UniProt*. [online] Uniprot.org. Available at: <<https://www.uniprot.org/>> [Accessed 15 January 2021].

Wai, S., Takade, A. and Amako, K., 1995. The Release of Outer Membrane Vesicles from the Strains of Enterotoxigenic *Escherichia coli*. *Microbiology and Immunology*, 39(7), pp.451-456.

- Walker M. M., and Dixon M. F., 1996. Gastric metaplasia: its role in duodenal ulceration. *Aliment. Pharmacol. Ther.* 10(Suppl. 1):119–128.
- Wan, L., Twitchett, M., Eltis, L., Mauk, A. and Smith, M., 1998. In vitro evolution of horse heart myoglobin to increase peroxidase activity. *Proceedings of the National Academy of Sciences*, 95(22), pp.12825-12831.
- Wang F, Xia P, Wu F, Wang D, Wang W, Ward T, Liu Y, Aikhionbare F, Guo Z, Powell M, Liu B, Bi F, Shaw A, Zhu Z, Elmoselhi A, Fan D, Cover TL, Ding X, Yao X., 2008. *Helicobacter pylori* VacA disrupts apical membrane-cytoskeletal interactions in gastric parietal cells. *J Biol Chem.* 2008 Sep 26; 283(39):26714-25.
- Wang, Y., Wu, J. and Lei, H., 2009. *The Autophagic Induction in Helicobacter pylori-Infected Macrophage. Exp. Biol. Med.* 234, 171-180.
- Waters, K. and Voltaggio, L., 2017. Gastritis: a pattern-based approach. *Diagnostic Histopathology*, 23(12), pp.513-520.
- Winter, J., Letley, D., Rhead, J., Atherton, J. and Robinson, K., 2014. *Helicobacter pylori* Membrane Vesicles Stimulate Innate Pro- and Anti-Inflammatory Responses and Induce Apoptosis in Jurkat T Cells. *Infection and Immunity*, 82(4), pp.1372-1381.
- Wroblewski, L., Peek, R. and Wilson, K., 2010. *Helicobacter pylori* and Gastric Cancer: Factors That Modulate Disease Risk. *Clinical Microbiology Reviews*, 23(4), pp.713-739.
- Yamaoka, Y., 2008. Increasing evidence of the role of *Helicobacter pylori* SabA in the pathogenesis of gastroduodenal disease. *The Journal of Infection in Developing Countries*, 2(03).
- Yamaoka, Y., Ojo, O., Fujimoto, S., Odenbreit, S., Haas, R., Gutierrez, O., El-Zimaity, H., Reddy, R., Arnqvist, A. And Graham, D., 2006. *Helicobacter pylori* outer membrane proteins and gastroduodenal disease. *Gut*, 55(6), pp.775-781.
- Yanai, A., Maeda, S., Hikiba, Y., Shibata, W., Ohmae, T., Hirata, Y., Ogura, K., Yoshida, H., Omata, M., 2007. Clinical relevance of *Helicobacter pylori* sabA genotype in Japanese clinical isolates. *J Gastroenterol*, 22(12):2228–2232.
- Yonezawa H., Osaki T., Hanawa T., Kurata S., Ochiai K., et al., 2013. Impact of *Helicobacter pylori* Biofilm Formation on Clarithromycin Susceptibility and Generation of Resistance Mutations. *PLoS ONE* 8(9): e73301. doi:10.1371/journal.pone.0073301.
- Yonezawa, H., Osaki, T., and Kamiya, S., 2015. Biofilm Formation by *Helicobacter pylori* and Its Involvement for Antibiotic Resistance. *BioMed Research International*, 2015, 914791, 9 pages. doi.org/10.1155/2015/914791.
- Yonezawa, H., Osaki, T., Fukutomi, T., Hanawa, T., Kurata, S., Zaman, C., Hojo, F. and Kamiya, S., 2016. Diversification of the AlpB Outer Membrane Protein of *Helicobacter pylori* Affects Biofilm Formation and Cellular Adhesion. *Journal of Bacteriology*, 199(6).
- Yonezawa, H., Osaki, T., Kurata, S., Fukuda, M., Kawakami, H., Ochiai, K., Hanawa, T. and Kamiya, S., 2009. Outer Membrane Vesicles of *Helicobacter pylori* TK1402 are Involved in Biofilm Formation. *BMC Microbiology*, 9(1), p.197.
- Yonezawa, H., Osaki, T., Woo, T., Kurata, S., Zaman, C., Hojo, F., Hanawa, T., Kato, S., Kamiya, S., 2011. Analysis of outer membrane vesicle protein involved in biofilm formation of *Helicobacter pylori*. *Anaerobe*. Dec;17(6):388-90. doi: 10.1016/j.anaerobe.2011.03.020. Epub 2011 Apr 16. PMID: 21515394.

- Yu, J., Leung, W., Go, M., Chan, M., To, K., Ng, E., Chan, F., Ling, T., Chung, S. and Sung, J., 2002. Relationship between *Helicobacter pylori babA2* status with gastric epithelial cell turnover and premalignant gastric lesions. *Gut*, 51(4), pp.480-484.
- Zamani, M., Ebrahimitabar, F., Zamani, V., Miller, WH., Alizadeh-Navaei, R., Shokri-Shirvani, J., 2018. Systematic review with meta-analysis: the worldwide prevalence of *Helicobacter pylori* infection. *Aliment. Pharmacol Ther*, 47(7):868–876. <https://doi.org/10.1111/apt.14561>.
- Zarella, T.M., Singh, A., Bitsaktsis, C.T., Rahman, Sahay, B., Feustel, P.J., *et al.*, 2011. Host-adaptation of *Francisella tularensis* alters the bacterium's surface-carbohydrates to hinder effectors of innate and adaptive immunity. *PLoS ONE*, 6, p. e22335.
- Zavan, L., Bitto, N., Johnston, E., Greening, D. and Kaparakis-Liaskos, M., 2018. *Helicobacter pylori* Growth Stage Determines the Size, Protein Composition, and Preferential Cargo Packaging of Outer Membrane Vesicles. *PROTEOMICS*, p.1800209.
- Zhang, L., Zhao, S., Zhang, J., Sun, Y., Xie, Y., Liu, Y., Ma, C., Jiang, B., Liao, X., Li, W., Cheng, X. and Wang, Z., 2020. Proteomic Analysis of Vesicle-Producing *Pseudomonas aeruginosa* PAO1 Exposed to X-Ray Irradiation. *Frontiers in Microbiology*, 11.
- Zhu, W., Zhou, B., Rong, L., Ye, L., Xu, H., Zhou, Y., Yan, X., Liu, W., Zhu, B., Wang, L., Jiang, X. and Ren, C., 2020. Roles of PTBP1 in alternative splicing, glycolysis, and oncogenesis. *Journal of Zhejiang University-SCIENCE B*, 21(2), pp.122-136.
- Zwarycz, A., Livingstone, P. and Whitworth, D., 2020. Within-species variation in OMV cargo proteins: the *Myxococcus xanthus* OMV pan-proteome. *Molecular Omics*, 16(4), pp.387-397.